

**STUDIES ON THE SEPARATION AND RECOVERY OF  
RUTHENIUM**

*By*

**PRAVATI SWAIN**

Enrolment No: CHEM02200804005

**Indira Gandhi Centre for Atomic Research, Kalpakkam, India**

*A thesis submitted to the*

*Board of Studies in Chemical Sciences*

*In partial fulfillment of requirements*

*for the Degree of*

**DOCTOR OF PHILOSOPHY**

*of*

**HOMI BHABHA NATIONAL INSTITUTE**



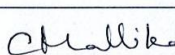
**August, 2013**

# Homi Bhabha National Institute

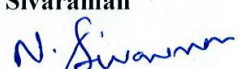
## Recommendations of the Viva voce Committee

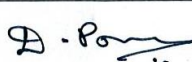
As member of Viva Voce Committee, we certify that we have read the dissertation prepared by Miss **Pravati Swain** entitled “**Studies on the Separation and Recovery of Ruthenium**” and recommend that it may be accepted as fulfilling the thesis requirement for the award of Degree of Doctor of Philosophy.

Chairman - **Dr. T. G. Srinivasan**  **Date:** 08.4.14

Guide / Convener – **Dr. C. Mallika**  **Date:** 08.04.14

External Examiner – **Prof. S. Sampath** **Date:**  
 8/4/14

Doctoral Committee Member 1 - **Dr. N. Sivaraman** **Date:**  
 8/4/2014

Doctoral Committee Member 2 - **Dr. D. Ponraju**  **Date:** 8/4/14

Technology Advisor- **Dr. R.V. Subbarao**  **Date:** 8/4/14

Final approval and acceptance of this dissertation is contingent upon the candidate's submission of the final copies of dissertation to HBNI.

I hereby certify that I have read this dissertation prepared under my direction and recommend that it may be accepted as fulfilling the dissertation requirement.

**Date:** 08.04.14

**Place:** IGCAR, Kalpakkam



**Guide/ Convener, Dr. C. Mallika**

### STATEMENT BY AUTHOR

This dissertation has been submitted in partial fulfillment of requirements for an advanced degree at Homi Bhabha National Institute (HBNI) and is deposited in the library to be made available to borrowers under rules of the HBNI.

Brief quotations from this dissertation are allowable without special permission, provided that accurate acknowledgement of source is made. Requests for permission for extended quotation from or reproduction of this manuscript in whole or in part may be granted by the Competent Authority of HBNI when in his or her judgment the proposed use of the material is in the interest of scholarship. In all other instances, however, permission must be obtained from the author.

Pravati Swain  
(Pravati Swain)

## DECLARATION

I, hereby declare that the investigation presented in the thesis has been carried out by me. The work is original and has not been submitted earlier as a whole or in part for a degree / diploma at this or any other Institution / University.

Pravati Swain  
(Pravati Swain)

## List of Publications arising from the thesis

### Journal

1. “Separation and recovery of ruthenium – A review”, **Pravati Swain**, C. Mallika, R. Srinivasan, U. Kamachi Mudali, R. Natarajan, *Journal of Radioanalytical and Nuclear Chemistry*, **2013**, 298, 781-796.
2. “Separation of ruthenium from simulated nuclear waste in nitric acid medium using n-Paraffin Hydrocarbon”, **Pravati Swain**, S. Annapoorani, R. Srinivasan, C. Mallika, U. Kamachi Mudali, R. Natarajan, *Separation Science and Technology*, **2014**, 49, 112-120.
3. “Separation and recovery of ruthenium from nitric acid medium by electro-oxidation”, **Pravati Swain**, S. Annapoorani, R. Srinivasan, C. Mallika, U. Kamachi Mudali, R. Natarajan, *Journal of Radioanalytical and Nuclear Chemistry* (Communicated).
4. “Studies on the Feasibility of Separation of Ruthenium from High Level Liquid Waste by constant potential electro-oxidation”, **Pravati Swain**, Dr. K. Sankaran, R. Srinivasan, C. Mallika, U. Kamachi Mudali, R. Natarajan, *Progress in Nuclear Energy* (Under revision)
5. “Electrochemical studies on the reduction behaviour of  $[RuNO]_{3+}$  in nitric acid medium”, **Pravati Swain**, C. Mallika, Ch. Jagadeeswara Rao, U. Kamachi Mudali and R. Natarajan, *Journal of Applied Electrochemistry* (Communicated).

### Conference Proceedings

1. **Pravati Swain**, R. Srinivasan, C. Mallika, U. Kamachi Mudali and R. Natarajan, Ruthenium Behavior on the Denitration of High Level Liquid Waste Generated in the Aqueous Reprocessing of Fast Reactor Fuels. 9th International Symposium on

Advances in Electrochemical Science and Technology (ISAEST-9), 2-4<sup>th</sup> Dec. 2010, Chennai, Tamil Nadu, India.

2. **Pravati Swain**, R. Srinivasan, C. Mallika, K.S. Viswanathan, U. Kamachi Mudali and R. Natarajan, Separation of Ruthenium during the Electrolytic Denitration of Simulated HLLW Solution. NUCAR-2011, 22-26<sup>th</sup> February 2011, Visakhapatnam, Andhra Pradesh, India.
3. S. Ramakrishna Reddy, **Pravati Swain**, S. Annapoorani, R. Srinivasan, C. Mallika, U. Kamachi Mudali and R. Natarajan, Influence of NaNO<sub>2</sub> on the Solvent Extraction of Ru into 30% TBP-NPH. International Conference on Vistas in Chemistry, (ICVC-2011), 11-13 October, 2011, IGCAR, Kalpakkam, India.
4. **Pravati Swain**, S. Annapoorani, R. Srinivasan, C. Mallika, U. Kamachi Mudali and R. Natarajan, Effect of Ceric Ions in the Extraction of Ruthenium into 30%TBP/NPH Systems. DAE – BRNS Biennial Symposium on Emerging Trends in Separation Science and Technology –SESTEC – 2012, February 27 - March 01, 2012, Mumbai, India. (Best Paper award).
5. **Pravati Swain**, S. Annapoorani, R. Srinivasan, C. Mallika, U. Kamachi Mudali and R. Natarajan, Separation of Ruthenium from a Simulated High Level Liquid Waste by Electro-Oxidation. ISAEST-10, 28-30<sup>th</sup> January, 2013, Chennai, India.

### **Conference Presentation**

1. **Pravati Swain**, S. Annapoorani, R. Srinivasan, C. Mallika, U. Kamachi Mudali and R. Natarajan, Extraction Behaviour of Ruthenium with Tributyl Phosphate and n-Paraffin Hydrocarbon. CRSM 2011, IGCAR, Kalpakkam, India.

# DEDICATIONS

*To*

*My Dear Parents*

*and*

*My Beloved Teacher: Sadasiba Biswal*

## ACKNOWLEDGEMENTS

First and foremost, I would like to express my deep sense of gratitude and indebtedness to my guide and supervisor **Dr. C. Mallika**, Head, PC&MS, RR&DD, Reprocessing Group, IGCAR for her constant encouragement, insightful guidance and excellent support all the way leading to completion of my PhD work. She taught me with extraordinary patience which gave me immense confidence to initiate my research work and to write the scientific articles. I specially thank her a lot, and place my admiration on record.

I am deeply indebted to **Dr. R. Srinivasan**, RR&DD, IGCAR, for his guidance, support and mentoring throughout my research work. He has pushed the limits of my thoughts and actions by throwing constant challenges and has made a noteworthy contribution to my research career.

I thank Director, IGCAR for providing me the opportunity to conduct the research work at IGCAR.

I thank **Dr. R. Natarajan**, Director, RpG for providing the facilities to carry out the research activities. I do appreciate the amenities and environment created by former Director **Dr. Baldev Raj**, for research scholars and for his encouragement in pursuing high-end research.

I am extremely thankful to **Dr. U. Kamachi Mudali**, Head, RR&DD, RpG, IGCAR for his help, useful discussions and support during the course of work.

I express my sincere thanks to my doctoral committee members **Dr. T.G. Srinivasan**, **Dr. N. Sivaraman**, **Dr. D. Ponraju** and **Dr. R.V. Subbarao** for their guidance, precious suggestions and constant support.

Words fail to express my indebtedness to **Ms. S. Annapoorani** for her patience, sincerity and kindheartedness to analyze my innumerable samples by ICP-OES techniques. I am very grateful to Dr. **K. S. Viswanathan**, **Dr. K. Sankaran**, **Mr. S. Sriram**, **Dr. Vijayalakshmi**, **Ms. R. Deivanayaki** and all other chemical lab members for valuable discussions.

I deeply thank **Dr. Ch. Jagadeeswar Rao** and **Dr. M. Jayakumar** for their valuable guidance and support in electrochemical experiments.

I want to register my thanks to **Mr. D. Nanda Gopal Krishna**, for characterizing and interpreting the XPS data. I would like to express my sincere thanks to **Dr. S. Amirthapandian**, for his valuable discussions and TEM study. I would like to thank **Dr. N. Ramanathan** for FTIR analysis. I would like to express my thanks to **Dr. G. Paneerselvam** for valuable discussion and XRD study.

I sincerely thank **Dr. N.K. Pandey** for his whole hearted support and valuable discussions. I especially thanks to **Dr. Falix Lawrence, Mr. G. Bharathi, Mr. Jayendra Kumar** for fruitful discussions and providing idea regarding the drawing of my experimental setup.

I deeply express my heart full thanks to all my colleagues, **Satyabrata, Sanat, Rahul, Ramakrishana, U. Veeramani, T. Selvan, Priyadarshini, Debasmita, Bijendra Kumar, Siba Kumar, Rama Kannan, R. Singaravel, C.V. Joyakin, S. Sundarmurthy** and all RR&DD members for sharing scientific adventures, help, caring and friendliness which have made my research life more smooth and enjoyable.

I owe my great pleasure to thank my beloved teachers **Sadasiba Biswal and Jamini Ranjan Mahanti**. I would not forget the love, care and inspiration that he bestowed upon me.

It is my great pleasure to keep a special line to my dear college friends, **Sweta, Shilpa, Ranjeeta, Pinky, Subhendu, Chandra, Siba, Gulu**. The moments I shared with my dear friends and batch mates, **Smiti, Maneesha, Sudeepta, Subhra, Sulata, Lucy, Madhusmita, Priyada, Juby, Anbu, Pranaya, Sudhansu, Pradeep, Prasan, Manas, Srimaha Vishnu, Ilayaraja, Ravi, Jagadish, Sharath, Herojit, Bubathi, Lakshmoji, Mariyappa, Srinivas, Naveen, Vijaya** shall linger in my memories forever. I would like to express my boundless gratitude to my roommate **Leona** and all other research scholar friends for making my life more amiable and charming during my stay at JRF Enclave, Kalpakkam.

I would like to express my heartiest gratitude and honor to my parents, **Rasik Ch. Swain** and **Basanta Manjari Swain** and all other family members, **Arabinda** and his family members for their love, compassion, caring nature, support and patience in the walkway of my life.

Above all, I bow my head humbly before the Almighty God for providing me this opportunity and granting me the capability to proceed successfully.

**(Pravati Swain)**

# CONTENTS

	<b>Page No.</b>
<b>Synopsis</b> .....	i
<b>List of Figures</b> .....	xv
<b>List of Tables</b> .....	xix
<b>List of Abbreviation</b> .....	xx
<b>CHAPTER 1. INTRODUCTION</b>	
1. 1 RUTHENIUM METAL .....	2
1.1.1 Characteristics of Ruthenium .....	2
1.1.2 Industrial Applications of Ruthenium .....	4
1.1.3 Occurrence and Production of Ruthenium .....	4
1.2 NUCLEAR FUEL CYCLE .....	5
1.2.1 Front End of Nuclear Fuel Cycle .....	5
1.2.2 Back End of Nuclear Fuel Cycle .....	7
1.3 ONCE THROUGH AND CLOSED NUCLEAR FUEL CYCLES .....	8
1.3.1 Non-aqueous Pyrochemical Reprocessing .....	10
1.3.2 PUREX Process .....	10
1.4 RUTHENIUM IN NUCLEAR REACTORS .....	11
1.4.1 Yield and Chemical State of Ruthenium .....	12
1.4.2 Paths Followed by Ruthenium in Nuclear Fuel Cycle .....	15
1.4.3 Problems Associated with Ru during Nuclear Fuel Reprocessing and Waste Management .....	16
1.5 CONCLUSIONS .....	18
1.6 REFERENCES .....	19
<b>CHAPTER 2. REVIEW OF LITERATURE ON THE SEPARATION AND RECOVERY OF RUTHNIUM</b>	
2.1 CHEMICAL METHODS .....	22
2.1.1 Volatilization .....	22
2.1.2 Precipitation .....	26
2.1.3 Pyrochemical Separation .....	27
2.2 SOLVENT EXTRACTION .....	29

2.2.1	Organic Solvents with Atoms Capable of Forming Coordinate Bonds .....	29
2.2.2	Extraction with Pyridine .....	30
2.2.3	Tertiary Amine and TBP Systems .....	30
2.2.4	Ruthenium Extraction with HDEHP in Hexane .....	31
2.2.5	Separation of Ru Using Halogen Substituted Alkanes .....	33
2.2.6	Extraction from Thiocyanate Complexes .....	33
2.2.7	Separation of Ru by Extraction with Novel Solvent Materials .....	34
2.3	CHROMATOGRAPHY .....	35
2.3.1	Ion Exchange Technique .....	35
2.3.2	Application of TLC and Sorbents .....	36
2.3.3	Alginate and Polymer Based Gels for Separation .....	37
2.4	SORPTION .....	38
2.5	ELECTROCHEMICAL METHOD .....	39
2.6	CONCLUSIONS .....	42
2.7	REFERENCES .....	44

### **CHAPTER 3. EXPERIMENTAL**

3.1	MATERIALS AND CHEMICALS .....	51
3.1.1	Chemicals .....	51
3.1.2	Materials .....	52
3.2	INSTRUMENTATION AND FACILITIES .....	52
3.2.1	Electrochemical System .....	52
3.2.2	UV-Visible Spectrophotometer .....	52
3.2.3	XRD .....	53
3.2.4	XPS .....	53
3.2.5	TEM .....	53
3.2.6	FTIR .....	54
3.2.7	ICP-OES .....	54
3.3	PREPARATION OF SOLUTIONS .....	57
3.3.1	Ruthenium Nitrosyl Solution .....	57
3.3.2	Simulated HLLW Solution .....	57
3.3.3	Ammonium Ceric Nitrate Solution .....	59
3.3.4	Nitric Acid Solutions .....	59
3.4	THEORY OF ELECTROANALYTICAL TECHNIQUES .....	59

3.4.1	Cyclic Voltammetry .....	60
3.4.2	Chronopotentiometry .....	64
3.4.3	Electro-oxidation .....	65
3.5	REFERENCES .....	66

## **CHAPTER 4. SEPARATION OF RUTHENIUM FROM SIMULATED NUCLEAR WASTE USING NORMAL PARAFFIN HYDROCARBON**

4.1	INTRODUCTION .....	68
4.2	EXPERIMENTAL .....	69
4.2.1	Chemicals .....	69
4.2.2	Equipment .....	70
4.2.3	Procedure for Separating Ru .....	71
4.2.3.1	Effect of the concentration of Ce(IV) .....	71
4.2.3.2	Effect of acid concentration, temperature and mixing time .....	78
4.2.3.3	Effect of ageing of ruthenium bearing solutions .....	78
4.3	RESULTS AND DISCUSSION .....	74
4.3.1	Separation of Ruthenium from $[\text{RuNO}]^{3+}$ Solution and SHLLW Containing $[\text{RuNO}]^{3+}$ Complexes .....	74
4.3.1.1	Effect of Ce(IV) concentration .....	74
4.3.1.2	Effect of nitric acid concentration and temperature on the separation of ruthenium .....	75
4.3.1.3	Ageing effect of ruthenium solution on its separation .....	77
4.3.2	Separation of Ruthenium from Nitrate Solutions .....	79
4.3.3	Characterisation of Black Ruthenium Suspension .....	81
4.3.4	Characterisation of NPH Before and After Ruthenium Separation .....	85
4.4	CONCLUSIONS .....	87
4.5	REFERENCES .....	88

## **CHAPTER 5. SEPARATION AND RECOVERY OF RUTHENIUM BY ELECTRO-OXIDATION**

5.1	INTRODUCTION .....	90
5.2	MATERIALS AND METHOD .....	91
5.2.1	Chemicals .....	91
5.2.2	Electrolytic Cell Assembly .....	92
5.2.2.1	Undivided cell .....	92
5.2.2.2	Divided cell with glass frit as diaphragm .....	93

5.2.3	Cyclic Voltammetric Measurements .....	94
5.3	RESULTS AND DISCUSSION .....	94
5.3.1	Separation of Ruthenium Using Undivided Cell .....	94
5.3.1.1	Effect of concentration of nitric acid .....	94
5.3.1.2	Effect of anodic current density, cerium concentration and temperature .....	97
5.3.1.3	Separation of Ru from simulated HLLW .....	98
5.3.2	Divided Cell with Glass Frit as Diaphragm .....	99
5.3.2.1	Effect of volume, concentration of redox catalyst and acid .....	99
5.3.2.2	Constant potential experiments .....	101
5.3.3	Cyclic Voltammetric Analysis .....	103
5.3.4	Recovery of Ruthenium .....	106
5.4	CONCLUSIONS.....	110
5.5	REFERENCES .....	111

## **CHAPTER 6. CONSTANT POTENTIAL ELECTRO-OXIDATION AND REDUCTION BEHAVIOUR OF $[\text{RuNO}]^{3+}$ IN NITRIC ACID**

6.1	INTRODUCTION .....	113
6.2	EXPERIMENTAL .....	115
6.2.1	Chemicals .....	115
6.2.2	Electro-volatilization Cell .....	116
6.2.3	Electrochemical Measurements .....	116
6.3	RESULTS AND DISCUSSION .....	118
6.3.1	Separation of Ruthenium by Constant Potential Electro-oxidation .....	118
6.3.1.1	Oxidation potential and cyclic voltammetry of ruthenium .....	118
6.3.1.2	Separation of Ru from $[\text{RuNO}]^{3+}$ solution by electro-oxidation .....	120
	i. Effect of applied potential and nitric acid concentration .....	120
	ii. Effect of temperature .....	121
	iii. Effect of redox mediator, cerium .....	123
6.3.1.3	Determination of kinetic parameters in the electrochemical oxidation of Ru... ..	127
	i. Effect of nitric acid concentration and applied potential on the rate of oxidation of Ru .....	127
	ii. Effect of temperature on the rate of oxidation of Ru .....	129
	iii. Effect of redox mediator Ce on the rate of oxidation of Ru .....	131
6.3.1.4.	Separation of Ru from SHLLW at various applied potential and in presence of Ce .....	132
6.3.2	Reduction Behaviour of $[\text{RuNO}]^{3+}$ in Nitric Acid Medium.....	134

6.3.2.1	Reduction potential and cyclic voltammograms of $[\text{RuNO}]^{3+}$ complex .....	134
6.3.2.2	Estimation of kinetic parameters for the reduction of ruthenium nitrosyl complexes .....	137
6.3.2.3	Chronopotentiometric study on the reduction of ruthenium .....	142
6.3.2.4	Reduction of $[\text{RuNO}]^{3+}$ moiety using glassy carbon (GC) electrode .....	143
6.3.2.5	Comparison of the kinetic parameters obtained with different working electrodes .....	145
6.3	CONCLUSIONS.....	146
6.4	REFERENCES .....	147

## CHAPTER 7. SUMMARY AND CONCLUSIONS

7.1	SUMMARY .....	150
7.1.1	Separation of ruthenium by n-paraffin hydrocarbon .....	151
7.1.2	Separation of ruthenium by electro-oxidation.....	151
7.1.3	Feasibility study on the separation of ruthenium by constant potential electro-oxidation.....	152
7.1.4	Electroanalytical studies on the reduction of $[\text{RuNO}]^{3+}$ in nitric acid.....	153
7.2	SCOPE FOR FUTURE STUDIES.....	153

## SYNOPSIS

The Department of Atomic Energy (DAE) in India has drawn a three stage nuclear power program for meeting the long term energy requirement in which reprocessing is the link between the three steps [1]. The first stage involves the setting up of pressurized heavy water reactors known as thermal reactors in which natural uranium is used as the fuel. The spent fuel discharged from the nuclear reactor is reprocessed to separate and recover (a) the unspent uranium and (b) the plutonium produced in the reactor. Plutonium thus produced is mixed with U and is utilized as the fuel in the form of either oxide or carbide in a fast breeder reactor (FBR), in the second stage program. A 40 MW<sub>th</sub> fast breeder test reactor (FBTR) is operating for nearly three decades at Indira Gandhi Centre for Atomic Research (IGCAR) at Kalpakkam and the unique and indigenously developed mixed carbide of U and Pu as the fuel in FBTR has already crossed a burn up of 165 GWd/t successfully. The large reserves of thorium present in monazite, available on the beach sand is utilised to produce the fissile element <sup>233</sup>U in FBRs, which is then reprocessed for considering as the fuel in the third stage. Closing the nuclear fuel cycle by reprocessing the spent fuel and recycling of uranium and plutonium back into reactor systems helps in exploiting the full potential of nuclear power and maximizes the resource utilization.

The nuclear fuel cycle is an industrial process involving various activities associated with the production of electricity from the fuel elements uranium and plutonium in nuclear reactors. The **front end** includes preparation of the fuel through different steps such as mining and milling, conversion, enrichment (if required), fuel fabrication to burning of fissile elements in nuclear reactors and **back end** activities include interim storage of the spent fuel, reprocessing and reuse before disposal as waste [2]. Reprocessing of the spent fuel is an important step of closed nuclear fuel cycle and the Plutonium Uranium Extraction (PUREX) process is the most commonly adopted aqueous method of reprocessing [3]. The PUREX

process is based on liquid–liquid extraction and the objective of this process is to recover the strategically important elements uranium and plutonium. In this process the spent nuclear fuel is mechanically decladded, chopped and dissolved in concentrated nitric acid. The resulting solution after dissolution, known as dissolver solution is subjected to conditioning, wherein the acidity of the solution is adjusted to 3-4 M, valency of U and Pu is conditioned to  $\text{UO}_2^{2+}$  and  $\text{Pu}^{4+}$  respectively, followed by adjusting the U to Pu ratio before extraction with the organic, 30 % TBP in n-dodecane. The U and Pu co-extracted by TBP are partitioned. The aqueous raffinate (containing all fission products, corrosion products and minor actinides in 3-4 M nitric acid) remained after the extraction of U and Pu into the organic phase (30% TBP) is referred to as high level liquid waste (HLLW). Like all other industries, nuclear reactor produces waste; however, much of the waste is radioactive and hence, it must be carefully managed and disposed as hazardous waste in order to safeguard human health and minimize its impact on the environment. The important nuclear waste management processes are denitration, evaporation and vitrification. The HLLW generated after fuel reprocessing needs to be stored in SS 304L waste tanks for sufficiently longer periods, until the beta and gamma radioactivity is reduced to levels at which handling the waste is feasible. To reduce the capacity of the waste storage tanks, the volume of HLLW requires to be reduced. For this purpose, the acidity in the waste solution must be destroyed by an economically viable process like chemical treatment with formaldehyde or formic acid, followed by evaporation of the denitrated waste solution. The HLLW concentrate thus obtained after evaporation is vitrified at high temperatures in a furnace with glass and the resulting solid melt which accommodates all the elements within its matrix is then encapsulated in canisters and disposed in geological repositories.

Ruthenium (Ru), a rare transition metal of platinum group in the periodic table is produced in significant quantity as a fission product in fast breeder reactors. The fission yield of

ruthenium varies according to type of the fuel and burn up, but as much as 10% in the case of  $^{235}\text{U}$  or even up to 40% in case of  $^{239}\text{Pu}$  [4]. Stable as well as radioactive isotopes of Ru are produced as fission product. The stable isotopes are  $^{99}\text{Ru}$ ,  $^{100}\text{Ru}$ ,  $^{101}\text{Ru}$ ,  $^{102}\text{Ru}$  and  $^{104}\text{Ru}$  [5]. Among the isotopes of Ru, the intrinsic radioactivity is caused by the isotopes  $^{103}\text{Ru}$  ( $t_{1/2} = 39$  days) and  $^{106}\text{Ru}$  ( $t_{1/2} = 373$  days).  $^{103}\text{Ru}$  undergoes beta decay with  $E_{\text{max}} = 0.76$  MeV and produces stable  $^{103}\text{Rh}$ .  $^{106}\text{Ru}$  is a soft beta emitter ( $E_{\text{max}} = 0.039$  MeV), which decays to  $^{106}\text{Rh}$  ( $t_{1/2} = 30$  s), a hard beta emitter ( $E_{\text{max}} = 3.54$  MeV) and also a gamma emitter of energy in the range 0.51-0.62 MeV [6-8]. In the irradiated  $\text{UO}_2$  and  $(\text{U}, \text{Pu})\text{O}_2$  fuels, ruthenium was observed to be present in the form of white metallic precipitate of Mo-Tc-Ru-Rh-Pd alloys [9, 10]. Based on the post irradiation examination of  $(\text{U}, \text{Pu})$  carbide fuel, ruthenium was reported to exist in the form of  $\text{CeRu}_2$  lanthanide-noble metal intermetallic compound and a dicarbide phase of the type  $(\text{U}, \text{Pu})_2\text{RuC}_2$ , regardless of the C/U ratio at all burn-ups [11]. Among the fission products, Ru is one of the most troublesome fission products during the aqueous reprocessing as well as in the waste management processes due to its large fission yield, relatively long half lives and its many oxidation states ranging from 0 to +8 [12].

The following problems have been encountered in the presence of ruthenium during nuclear fuel reprocessing and waste treatment:

- In the dissolution of irradiated nuclear fuel in concentrated nitric acid for reprocessing by the PUREX process, Ru passes into solution mainly in the form of various nitrate, nitro and nitrate-nitro complexes of trivalent ruthenium nitrosyl  $[\text{RuNO}]^{3+}$ , which further combine with hydroxo and aqua ligands to form the complex having the general formula as  $[\text{RuNO}(\text{NO}_3)_x(\text{NO}_2)_y(\text{OH})_z(\text{H}_2\text{O})_{5-x-y-z}]^{3-x-y-z}$  [13]. The trinitrate, tetranitrate, nitro-nitrate and nitro complexes formed by ruthenium exhibit complicated distribution behaviour between the aqueous and the organic phases and a few of them remain in TBP/Dodecane after stripping. Therefore, it is difficult to

completely separate ruthenium from uranium and plutonium which results in the possible release of radio-ruthenium in the environment [12].

- During the process of denitration and concentration of the highly radioactive aqueous waste containing nitrates of fission products in  $\text{HNO}_3$  medium, ruthenium is oxidized to volatile  $\text{RuO}_4$  and the oxide escapes to the vapour phase. Gaseous  $\text{RuO}_4$ , on contact with the cooler parts of the surface of stainless steel equipment decomposes to a non-volatile black deposit of  $\text{RuO}_2$ . As a result of contamination by the deposit, the radiation dose of the plant is increased and in extreme cases, pipes of the apparatus are plugged. The distilled nitric acid is also contaminated with the vapour of ruthenium oxide. The stability and decomposition of  $\text{RuO}_4$  to lower oxide have been discussed in the literature [14-16]. Sakurai et al., [14] investigated the interaction of  $\text{RuO}_4$  gas with stainless steel, Ni, Cu and Au and concluded that the black deposit produced consisted of a peroxy – bonded polymeric  $(\text{RuO}_4)_n$  species, whereas other researchers claimed that it is the oxyhydroxides of Ru(IV) and  $\text{RuO}(\text{OH})_2$  [15] and hydrous or anhydrous non-volatile  $\text{RuO}_2$  species [16].
- Ruthenium also poses problems in the vitrification process. During vitrification, when the dried waste and glass forming chemicals (borosilicate glasses) are heated to about 1273 K,  $^{106}\text{Ru}$  is oxidized to volatile  $\text{RuO}_4$  and deposits as insoluble black  $^{106}\text{RuO}_2$  on the walls of the vessel. Platinum Group Metals (PGM) are partially precipitated and accumulated at the bottom of the melter during the dissolution of HLLW into the molten glass, since their solubility is low in the molten glass. Sedimentation of PGMs leads to electric energy loss, local over-heating, high viscous glass formation and low rate of vitrification [17], which are mainly caused by the existence of needle like crystals of electrically conducting  $\text{RuO}_2$ . Thus, separation of Ru from HLLW is essential prior to waste fixing.

Ruthenium finds extensive applications in industries too, owing to its noble properties such as resistance to chemical attack, high catalytic activities and stable electrical properties. It is widely employed in electronics, electrical and electrochemical industries.

Ruthenium is scarce in nature and its natural abundance is about 0.001 ppm [18], whereas a significant quantity of ruthenium is produced as a fission product in nuclear reactors. The total estimated natural resources of Ru in the year 2000 was about 3090 ton and the projections indicate that by the year 2030, the global reserve will be limited to 2870 ton. However, about 1752 ton of Ru can be produced as fission product by the year 2030 [5]. If the worldwide development of nuclear power proceeds as currently envisaged, spent nuclear fuel can be recognized as an alternative resource for Ru by the year 2030 to meet the increasing need. Since Ru has unique chemical properties it can be separated from the rest of the fission products and cooled for 10 years to eliminate the radioactivity associated with it for further use in industry. Therefore, separation and recovery of ruthenium is a value added process since it not only can solve the problem of ruthenium interference in nuclear industry and but also can be used in other industries as an alternative source.

The main objective of the present study is to separate and recover ruthenium from high level liquid waste in order to solve the problems associated in the waste management processes. Ruthenium could be separated from simulated HLLW by chemical and electrochemical volatilization methods after oxidizing it to highly volatile  $\text{RuO}_4$ .

The thesis comprises seven Chapters and the abstract of each Chapter is given below.

## **Chapter 1**

In this Chapter, the physical and chemical properties of Ru have been briefly discussed. Closed and open nuclear fuel cycles are introduced with emphasis on the back end of closed fuel cycle such as reprocessing and waste management processes. The extraction behaviour

of Ru from nitric acid medium by TBP and the nuisance value of Ru in aqueous reprocessing and waste treatment steps have been elaborated.

Globally, there are two routes for managing nuclear fuel cycle: the 'open' or 'once through' fuel cycle, wherein the spent nuclear fuel discharged from the reactor is treated as waste and is disposed in repositories for indefinitely long time and, the 'closed' fuel cycle in which the spent nuclear fuel is reprocessed for the recovery of strategic metals uranium and plutonium. 'Once through' fuel cycle method has the advantage in terms of cost and proliferation resistance since there is no reprocessing and is favoured by the six countries: the United States of America, Canada, Sweden, Finland, Spain and South Africa. India has chosen to follow a closed fuel cycle policy to ensure long term energy security. With low reserves of uranium, this strategy of reprocessing and recycling of uranium and plutonium would lead to optimum resource utilization. Thus, in the Indian context spent fuel is a vital resource material and not a waste to be disposed off. In the widely adopted PUREX process for the aqueous reprocessing of spent fuels, ruthenium creates problems due to the extraction of some of the ruthenium nitrosyl complexes along with U and Pu into the organic phase and contaminating the product and in the waste management processes it forms highly volatile radiotoxic ruthenium tetroxide.

## **Chapter 2**

The various methods of separation of ruthenium from nuclear waste solutions as well as from minerals reported in literature and the drawback of each method in applying to the separation from nuclear waste are discussed in this Chapter. Separation of ruthenium can be accomplished by various methods like volatilization, precipitation, solvent extraction, ion exchange chromatography, sorption, electrochemical method etc. In the volatilization method of separation, Ru is oxidized to volatile  $\text{RuO}_4$  in the presence of a strong oxidizing agent and the gaseous  $\text{RuO}_4$  produced is removed from the reactor by driving it out and absorbed in a

suitable medium such as NaOH, HCl and HNO<sub>3</sub>. In the precipitation method, Ru is selectively separated out in the presence of selective precipitants. In La Hague reprocessing plant Ru was co-precipitated with ferrocyanide in an excess of Cu<sup>2+</sup> (as nitrate) from low level waste before their release to sea [19]. Pyrochemical method of separation of ruthenium with lead was reported for the separation of Ru from insoluble residue formed during the PUREX process. Solvent extraction method is one of the industrially applicable methods of separation; however, most of the extractants which successfully separate Ru from nitric acid medium are either sulphur or phosphorous based complexes which will not be suitable for nuclear industry due to corrosion related issues of the equipment. Many ion exchange techniques and sorbents have been tried for the separation of ruthenium, but most of them are applicable for pH level solutions and also most of the extractants and sorbents have very low radiation resistance. Among the sorbents used activated charcoal is found to be promising for the separation of ruthenium from radioactive waste solution. Electrochemical method is found to be applicable since this method does not require addition of external reagents which is highly desirable for the management of HLLW. Employing electrochemical method of separation Ru in one of its lowest oxidation states can either be deposited or oxidize it to RuO<sub>4</sub> which is the highest oxidation state.

### **Chapter 3**

The methods adopted for the separation of Ru, materials and other characterization techniques used throughout the thesis work are described. Experimental techniques such as Inductively Coupled Plasma Optical Emission Spectroscopy (ICP-OES) used for determining the concentration of ruthenium is discussed. Other experimental techniques used for speciation of powder Ru sample such as X-ray Diffraction method (XRD), X-ray Photoelectron Spectroscopy (XPS) and Transmission Electron Microscopy (TEM), and Fourier Transform Infrared Spectroscopy (FTIR) to investigate the structural modifications of

n-paraffin hydrocarbon (NPH) are briefly described in this Chapter. The UV-Visible spectroscopy for the determination of concentration of pure Ru as well as speciation of Ru complex in solution is mentioned. This Chapter also gives the theory behind the application of electroanalytical techniques such as cyclic voltammetry, chronoamperometry, chronocoulometry and chronopotentiometry for determining kinetic parameters involved in the electro-oxidation of Ru.

#### **Chapter 4**

The separation of Ru from pure  $\text{Ru}(\text{NO}_3)_3$ ,  $[\text{RuNO}]^{3+}$  and from simulated HLLW in nitric acid medium by volatilization method using ammonium ceric nitrate (ACN) as oxidizing agent in the presence of n-paraffin hydrocarbon (NPH, organic phase) is discussed in Chapter 4. In the presence of ACN, Ru in the aqueous phase was oxidized to volatile  $\text{RuO}_4$ . The  $\text{RuO}_4$  vapour evolved was trapped by paraffin oil (on the top of aqueous layer) and the black coloured precipitate of lower ruthenium oxide formed at the organic-aqueous interface was filtered off using cellulose fiber filter paper. The concentration of Ru in the aqueous phase before and after the separation was estimated by ICP-OES method. About 80 % of Ru could be separated from nitrosyl nitrate solutions, at low concentration of nitric acid in the range 0.5–1M using 0.02-0.04M Ce(IV) as the oxidizing agent and at ambient temperature. The optimum process parameters for separating 80-90 % Ru from ruthenium nitrate and a simulated waste solution (in the form of  $\text{Ru}(\text{NO}_3)_3$ ) were determined to be 0.04 M ACN in 4M nitric acid at ambient temperature. The black ruthenium oxide suspension at the interface between the organic and aqueous phases was characterized by XRD, TEM, EELS and XPS techniques. The XRD and TEM results revealed the Ru based powder to be amorphous phase and the presence of Ru and O in the powder was confirmed from EELS. The XPS results showed the Ru species present in the black suspension to be in +4 oxidation state corresponding to  $\text{RuO}_2$  and oxy-hydroxide species of Ru(IV) to some extent over the surface.

Separation of Ru was also carried out using n-dodecane instead of NPH and the efficiency of n-dodecane for the separation of Ru was observed to be marginally higher than that of NPH. The ketonic group formed in the used NPH was identified from IR spectra, which upheld the reduction of RuO<sub>4</sub> to RuO<sub>2</sub> by the alkane. As cerium is one of the fission products, its use as the oxidizing agent in the separation of Ru is not expected to increase the burden of waste fixing, because the amount of ACN to be added is about 70 % of the actual quantity required for the complete oxidation of Ru in the waste solution. As the procedure involved in the separation of Ru by volatilization after oxidation and absorption by NPH is simple and not time consuming and cost effective process, this method is suitable for deployment in the reprocessing plant for the separation and recovery of the troublesome fission product, ruthenium.

## **Chapter 5**

Separation of ruthenium from [RuNO]<sup>3+</sup> and from simulated HLLW in nitric acid medium by electro-oxidation method applying constant current in undivided and divided cells and with/without cerium redox mediator is discussed in Chapter 5. Ruthenium separation could be accomplished by electro-oxidation of Ru to volatile RuO<sub>4</sub> using cerium as the redox mediator in undivided cell configuration and the amount of RuO<sub>4</sub> collected in 8M nitric acid as well as in alkaline trap was compared under different experimental conditions. A divided cell fabricated using borosilicate glass frit as the separating membrane was employed for separating Ru from SHLLW without adding metal ions as the redox catalyst. The influence of experimental conditions like different concentrations of nitric acid, current density, temperature and concentration of cerium as the redox catalyst on the separation of Ru was investigated. Maximum separation of 95 % Ru could be achieved from ruthenium nitrosyl nitrate in 1M nitric acid using 20 mA/cm<sup>2</sup> as the anodic current density and with 0.02 M Ce at 318 K when electro-oxidation was performed in an undivided cell. The amount of Ru

separated from simulated waste was only 54 % under identical experimental conditions. To minimize the deleterious effect of nitrite ions produced at the cathode on the separation of Ru, the divided cell with glass frit as the diaphragm was engaged and about 74 and 80 % Ru were separated from  $[\text{RuNO}]^{3+}$  and simulated HLLW respectively in 4M  $\text{HNO}_3$  without any redox catalyst. Cyclic voltammetric study in nitric acid medium revealed that oxidation of Ru to  $\text{RuO}_4$  takes place on gold electrode in the potential range 1.28-1.49 V (vs Ag/AgCl). With Pt as working electrode there was a surge in anodic current from 1.2 V (vs Ag/AgCl) onwards corresponding to the oxidation of Ru along with water oxidation. The  $\text{RuO}_4$  formed during electro-oxidation was sucked via a vacuum pump and trapped either in alkaline (NaOH) or in nitric acid medium. A portion of  $\text{RuO}_4$  decomposed to lower oxide and got deposited on the inner wall of the electrolytic vessel. To prevent the deposition of  $\text{RuO}_2$  over the wall of the vessel, keeping a layer of NPH above the electrolyte was observed to serve as a better trap for gaseous  $\text{RuO}_4$ .

## **Chapter 6**

This Chapter deals with the separation of Ru from  $[\text{RuNO}]^{3+}$  and from simulated HLLW by electro-oxidation applying constant potential using a divided cell and study of the electroanalytical behaviour of  $[\text{RuNO}]^{3+}$  in nitric acid medium. Cyclic voltammetric experiments with  $[\text{RuNO}]^{3+}$  solution (containing 20 mM of Ru) using Pt as working and counter electrodes and Ag/AgCl reference electrode revealed that water oxidation and Ru to  $\text{RuO}_4$  oxidation occur together and from 1.2 V onwards there was a surge in anodic current and the current increased with increase in concentration of Ru, temperature and decrease in the concentration of nitric acid. The effect of these experimental parameters on the separation of Ru was investigated. Separation of Ru was carried out by chronoamperometric method using Pt mesh as working and counter electrodes and Ag/AgCl as reference electrode and by applying three different constant potentials 1.25, 1.45 and 1.65 V in a divided cell with glass

frit as diaphragm. When the applied potential was 1.25 V (vs Ag/AgCl), the separation of Ru increased from 17 to 23 and 35 % with decrease in acidity from 4 to 2 and 1 M respectively after electrolyzing for 10 h. Increasing the applied potential to 1.45 V (vs Ag/AgCl), the separation percentage was found to increase from 21 to 46 and 60 % and at the applied potential of 1.65 V the separation of Ru increased from 26 to 48 and 74 % with decrease in the concentration of nitric acid from 4 to 2 and 1M respectively after 10 h of electrolysis. Though separation percentage of Ru increased with increase in the applied potential, the current efficiency was found to decrease from 52 to 25 and 10 % when the applied potential was raised from 1.25 to 1.45 and 1.65 V (vs Ag/AgCl). In order to obtain better separation from 1M nitric acid solution at 1.25 V, experiments were carried out at a higher temperature and the percentage of Ru separated could increase from 35 to about 68 % by increasing the temperature from 300 to 333 K, for the same duration of 10 h of electrolysis. Separation of Ru was also carried out in the presence of 0.04M Ce from 1M nitric acid solution. Since the oxidation of Ce in 1M nitric acid occurs above 1.4 V [20], separation of Ru was investigated at the potentials 1.45 and 1.65 V (vs Ag/AgCl) and 89 and 97 % could be removed from 1M nitric acid solution after 10 h of electrolysis.

The redox behaviour of  $[\text{RuNO}]^{3+}$  to  $[\text{RuNO}]^{2+}$  was evaluated in nitric acid medium using the potentiostatic electrolysis techniques namely cyclic voltammetry (CV) and chronopotentiometry (CP) with Pt and Glassy carbon as the working electrodes. From the results of CV and CP measurements the diffusion coefficient ( $D_{\text{Ru}}$ ) values for  $[\text{RuNO}]^{3+}$  in 1M  $\text{HNO}_3$  was estimated. The reduction of  $[\text{RuNO}]^{3+}$  to  $[\text{RuNO}]^{2+}$  in 1M  $\text{HNO}_3$  was found to be quasi-reversible and the value of heterogeneous electron transfer rate constant ( $K_s$ ) was determined using Klingler and Kochi equation.

## Chapter 7

A summary of the investigations made for the separation and recovery of Ru from  $[\text{RuNO}]^{3+}$  and from simulated HLLW in nitric acid medium by chemical and electrochemical volatilization methods and the advantages and limitations of each of these methods are discussed in Chapter 7.

Removal of Ru by chemical volatilization method using ACN as the oxidizing agent was found to be quantitative, simple and cost effective method. This method of separation of Ru using ACN as oxidizing agent will not increase the waste volume and complicate the waste fixing as Ce is also one of the fission products. However, quantitative separation is possible from 1M nitric acid solution only. Hence, the HLLW in 4M nitric acid solution requires to be diluted. Separation of Ru from both pure  $[\text{RuNO}]^{3+}$  and from simulated HLLW could be accomplished efficiently by applying constant current/potential in undivided and divided cell with glass frit as diaphragm. Using undivided electrolytic cell, 95 % of Ru was separated from pure  $[\text{RuNO}]^{3+}$  solution prepared in 1M nitric acid, whereas only 54 % of Ru could be separated from SHLLW under similar experimental conditions. In the case of divided cell, quantitative separation was possible both from pure  $[\text{RuNO}]^{3+}$  and from simulated HLLW prepared in 4M  $\text{HNO}_3$  without any redox mediator by applying a constant current of 20  $\text{mA}/\text{cm}^2$ . However, the current efficiency in this method of separation by applying constant current was very low due to the simultaneous reaction of water oxidation. In order to obtain improved current efficiency, CV studies were carried out and electrolysis had been conducted by applying constant potentials in the divided cell. With 1.25 V as the applied potential, the current efficiency could be increased to only 52 % for pure  $[\text{RuNO}]^{3+}$  solution in 1M acid.

The parametric studies conducted for the separation of Ru can be implemented in the plant for the removal of Ru from the actual HLLW and also in continuous mode. Constant potential electrolysis using a redox mediator with lower oxidation potential requires to be carried out in

order to get good separation percentage as well as current efficiency. Designing suitable electrolytic cells and demonstrating the performance of these cells in separating Ru from simulated HLLW are also within the scope of future work.

## REFERENCES

1. Natarajan R., Baldev Raj, *J. Nucl. Sci. Tech.*, 44 (2007) 393
2. Baisden, P.A., Choppin, G.R., *Nuclear waste management and the nuclear fuel cycle*, In: Radiochemistry and Nuclear Chemistry, Nagy, S., (Ed.), Encyclopedia of Life Support Systems (EOLSS), EOLSS Publishers, Oxford, 2007
3. Swanson, J.L., PUREX flowsheets, In: Science & Technology of tributyl phosphate, vol. III, W. W. Schulz, L. L. Burger, J. D. Navratil, K. P. Bender, (Ed.), CRC Press, Boca Raton, 1984
4. Motojima, K., U.S. Patent No.4938895, 1990
5. Ache, H. J., Baestle, L. H., Bush, R. P., Nechaev, A. F., Popik, V. P., Ying, Y., Feasibility study of separation and utilization of Ru, Rh and Pd from high level waste. Technical Reports Series - No. 308, IAEA, Vienna, 1989
6. Kolarik, Z., Renard, E. V., *Platinum Metals Rev.*, 49 (2005) 79
7. Kolarik, Z., Renard, E. V., *Platinum Metals Rev.*, 47 (2003) 74
8. Martin, J. E., *A Hand Book of Physics for Radiation Protection, Second Edn*, (Wiley-VCH, Weinheim, Germany), p. 775, 2006
9. Kleykamp, H., *J. Nucl. Mater.*, 131 (1985) 221
10. Kurosaki, K., Tanaka, K., Osaka, M., Ohishi, Y., Muta, H., Uno M., Yamanaka, S., *Prog. Nucl. Sci. Technol.*, 2 (2011) 5
11. Agarwal, R., Venugopal, V., *J. Nucl. Mater.*, 359 (2006) 122

12. Motojima K., *J. Nucl. Sci. Technol.*, 26 (1989) 358
13. Scargill, D., Lyon, C.E., Large, N.R., Fletcher, J.M., *J. Inorg. Nucl. Chem.*, 27 (1965) 161
14. Sakurai, T., Hinatsu, Y., Takahusi, A., Fujisawa, G., *J. Phys. Chem.*, 89 (1985) 1892
15. Mun, C., Ehrhardt, J. J., Lambert, J., Madic, C., *Appl. Surface Sci.*, 253 (2007) 7613
16. Holm, J., Glanneskog, H., Ekberg, C., *J. Nucl. Mater.*, 392 (2009) 55
17. Krause, Ch., Luckscheiter, B., *J. Mater. Res.*, 6 (1991) 2535
18. Emsley, J., "Ruthenium". *Nature's Building Blocks: An A-Z Guide to the Elements*. Oxford, England, UK: Oxford University Press. pp. 368–370, 2003
19. Gandon, R., Boust, D., Bedue, O., *Radiochim. Acta.*, 61(1993) 41
20. Wei, Y., Fang, B., Arai, T., Kumagai, M., *J. Applied Electrochemistry*, 35 (2005) 561

## LIST OF FIGURES AND TABLES

Figure No.	Title of the Figure	Page No.
1.1	Fission of $^{235}\text{U}$ and nuclear chain reaction	6
1.2	Open fuel cycle: Once –through fuel	9
1.3	Closed fuel cycle	9
2.1	Variation of Ru decontamination factor with the concentration of hydrazine	25
2.2	Experimental apparatus for Ru separation system	28
2.3	Structures of extractants	32
2.4	Effect of pH on the $K_D$ value of Ru in NiS-PMMA composite material	37
2.5	Cylindrical glass cell for the electro-deposition of Ru	42
2.6	Structures of room temperature ionic liquids (RTILs)	42
3.1	Block diagram of a typical ICP – OES instrument	56
3.2	Calibration graph for Ruthenium	56
3.3	Cyclic voltammetry waveform and typical cyclic voltammograms	61
4.1	Black Ru suspension at the organic and aqueous interface: Before adding ACN and after adding ACN	72
4.2	Separation of Ru from $[\text{RuNO}]^{3+}$ and simulated HLLW solutions using Ce(IV) in 1 M nitric acid medium	75
4.3	Effect of temperature on the separation of Ru from $[\text{RuNO}]^{3+}$ solution in different concentrations of nitric acid	76
4.4	Separation of Ru from simulated HLLW at different temperatures and acid concentrations	77
4.5	Effect of ageing on the separation of Ru	78
4.6	The octahedral structure of ruthenium nitrosyl complex	78
4.7	XRD pattern of commercial (crystalline) $\text{RuO}_2$ and the black Ru suspension generated during the separation of Ru by NPH	83
4.8	TEM image and electron diffraction pattern of amorphous ruthenium oxide suspension	83
4.9	XPS spectra of Ru 3d core level lines on ruthenium species	84
4.10	XPS spectra of O 1s on ruthenium bearing species	84

4.11	IR spectra of NPH recorded before the separation experiment	86
4.12	IR Spectra of NPH recorded after Ru separation	86
5.1	Schematic diagram of the undivided electrolytic cell and divided electrolytic cell	96
5.2	Dependence of acidity on the separation of Ru	96
5.3	Variation in the separation of Ru with respect to anodic $J$ , temperature and [Ce]	97
5.4	Variation in the separation of Ru from pure $[\text{RuNO}]^{3+}$ solution and SHLLW during electrolysis in the cell with glass frit as diaphragm; Volume of anolyte: 440 ml; $J_a$ : 20 mA/cm <sup>2</sup> ; T: 313 K; $[\text{H}^+]$ : 4 M	101
5.5	Separation of Ru from $[\text{RuNO}]^{3+}$ solution and SHLLW in undivided cell (without glass frit); Volume of anolyte: 440 ml; $J_a$ : 20 mA/cm <sup>2</sup> ; T: 313 K; $[\text{H}^+]$ : 4 M	102
5.6	Comparison of separation yield of Ru from pure $[\text{RuNO}]^{3+}$ solution at 4 and 1 M acidity in the divided cell; Volume of anolyte: 440 ml; $J_a$ : 20 mA/cm <sup>2</sup> ; T: 313 K	102
5.7	Cyclic voltammogram of 5 mM $[\text{RuNO}]^{3+}$ solution ( $[\text{H}^+]$ : 0.15 M) recorded with Au working electrode; Counter electrode: Pt; Reference: Ag/AgCl; Scan rate: 100 mV/s; T: 298 K	104
5.8	Cyclic voltammograms of 5, 20 and 40 mM $[\text{RuNO}]^{3+}$ solutions ( $[\text{H}^+]$ : 1 M) recorded with Pt working electrode; CE: Pt; RE: Ag/AgCl; Scan Rate: 100 mV/s; T: 298 K	105
5.9	The UV-Visible spectra of $\text{RuO}_4$ formed during chronocoulometric study	105
5.10	Decomposition of $\text{RuO}_4$ and deposition as black lower oxide of Ru over the inner wall of electrolytic vessel	109
5.11	UV-Vis spectra of ruthenate and perruthenate in NaOH trap solution.	109
5.12	Trapping of $\text{RuO}_4$ by n- paraffin hydrocarbon	110
6.1	Cell assembly for electrochemical studies	117
6.2	Cyclic voltammetric studies with $[\text{RuNO}]^{3+}$ solution: <b>A.</b> In 1 M nitric acid with different Ru content; <b>B.</b> 20 mM of Ru in different acid concentrations and <b>C.</b> At different temperatures; CVs were recorded at Pt WE, Pt plate CE and Ag/AgCl RE; Scan rate: 50 mV/s	119

6.3	Plot of coulombic charge passed into the solution against time for the electro-oxidation of Ru from $[\text{RuNO}]^{3+}$ solution in 1M nitric acid at different applied potentials	121
6.4	Plot of coulombic charge passed into the solution against time for the electro-oxidation of Ru from $[\text{RuNO}]^{3+}$ solution at three different $[\text{HNO}_3]$ and at the fixed potential of 1.65 V	121
6.5	Variation in the separation of Ru from $[\text{RuNO}]^{3+}$ solution in 1 M nitric acid during electrolysis at different temperatures with the applied potential of 1.25 V	122
6.6	Plot of coulombic charge passed into the solution against time in the electro-oxidation of Ru from $[\text{RuNO}]^{3+}$ solution in 1 M nitric acid at different temperatures with 1.25 V as the applied potential	123
6.7	Plot of coulombic charge passed into the solution against time for the electro-oxidation of Ru from $[\text{RuNO}]^{3+}$ solution in the presence of 0.04 M Ce at various acidities and at 1.45 V (vs Ag/AgCl) as the applied potential	125
6.8	Plot of coulombic charge passed into the solution against time for the electro-oxidation of Ru from $[\text{RuNO}]^{3+}$ solution prepared in 1 M nitric acid in the presence of 0.04 M Ce at the applied potentials of 1.45 and 1.65 V	126
6.9	Variation of $[\text{Ru}]$ in the anolyte against time during the electrolysis of $[\text{RuNO}]^{3+}$ solution in 1 M nitric acid in the presence of 0.04 M Ce at the applied potentials 1.45 and 1.65 V	126
6.10	Variation in the ratio of Ru concentration in anolyte ( $[\text{Ru}]_t/[\text{Ru}]_0$ ) with time during the electrolysis of $[\text{RuNO}]^{3+}$ solution prepared in 4 M nitric acid at various applied potentials	128
6.11	Variation in the ratio of Ru concentration in anolyte ( $[\text{Ru}]_t/[\text{Ru}]_0$ ) with time during the electrolysis of $[\text{RuNO}]^{3+}$ solution prepared in 2 M nitric acid at various applied potentials	128
6.12	Ratio of Ru concentration in anolyte ( $[\text{Ru}]_t/[\text{Ru}]_0$ ) with time during the electrolysis of $[\text{RuNO}]^{3+}$ solution prepared in 1 M nitric acid at various applied potentials	129
6.13	Ratio of Ru concentration in the anolyte ( $[\text{Ru}]_t/[\text{Ru}]_0$ ) with time during the electrolysis of $[\text{RuNO}]^{3+}$ solution prepared in 1 M nitric acid at the applied potential of 1.25 V and different temperatures	130

6.14	Rate constant against inverse temperature for the oxidation of ruthenium	130
6.15	Variation of [Ru] in the anolyte against time during the electrolysis of SHLLW in 1 M nitric acid (with and without 0.04 M Ce) at different applied potentials	133
6.16	Cyclic voltammogram of 40 mM ruthenium nitrosyl ( $[\text{RuNO}]^{3+}$ ) solution in 1 M $\text{HNO}_3$ recorded with 0.05 V/s scan rate at platinum working electrode and at 298 K	135
6.17	Cyclic voltammograms of 5, 20 and 40 mM $[\text{RuNO}]^{3+}$ solution in 1 M $\text{HNO}_3$ recorded at 0.05 V/s scan rate at Pt working electrode at 298 K	135
6.18	Current vs time plot for the electrolysis of 160 ppm of ruthenium nitrosyl solution in 1 M $\text{HNO}_3$ ; WE: Pt mesh, CE: Pt mesh, RE: Ag/AgCl	138
6.19	UV-Visible spectra of $[\text{RuNO}]^{3+}$ solution in 1 M $\text{HNO}_3$ before and after electrolysis	139
6.20	Cyclic voltammograms of 40 mM of ruthenium nitrosyl solution in 1 M $\text{HNO}_3$ recorded at Pt electrode with different scan rates; T: 298 K	139
6.21	Plot of peak current vs square root of scan rate for the reduction of 40 mM of $[\text{RuNO}]^{3+}$ in 1 M $\text{HNO}_3$	141
6.22	Chronopotentiograms of 40 mM of $[\text{RuNO}]^{3+}$ in 1 M $\text{HNO}_3$ recorded with Pt electrode at different applied currents; WE: Pt, CE: Pt, RE: Ag/AgCl	142
6.23	Cyclic voltammograms of 40 mM $[\text{RuNO}]^{3+}$ solution in 1 M nitric acid recorded using glassy carbon electrode with different scan rates at 298 K; CE: Pt, RE: Ag/AgCl	143
6.24	Chronopotentiogram of 40 mM $[\text{RuNO}]^{3+}$ solution in 1 M $\text{HNO}_3$ recorded at GC electrode with different applied currents	145

<b>Table No.</b>	<b>Title of the Tables</b>	<b>Page No.</b>
1.1	Content of Ru isotopes in a spent fuel of PWR (3.2 % $^{235}\text{U}$ as $\text{UO}_2$ , 880 days irradiation, burn-up: $32.3 \text{ GWd.t}^{-1}$ ) at different cooling periods	13
3.1	Operating conditions and description of ICP-OES instrument	57
3.2	The chemical composition of fission and corrosion product elements in simulated waste solution in 4 M $\text{HNO}_3$	58
4.1	Separation of Ru using the organic phases NPH and n-dodecane at different ageing periods; $[\text{Ce(IV)}]: 0.025 \text{ M}$ ; Mixing time: 5 min; Temperature: 300 K; $[\text{HNO}_3]: 1 \text{ M}$	79
4.2	Separation of Ru from ruthenium nitrate solutions; $[\text{HNO}_3]: 4 \text{ M}$ and $[\text{Ce(IV)}]: 0.04 \text{ M}$	81
5.1	The separation percentage of ruthenium from $[\text{RuNO}]^{3+}$ solution of acidity 1 M	98
5.2	The separation percentage of Ru from simulated HLLW	99
5.3	Percentage separation of Ru from $[\text{RuNO}]^{3+}$ solution of acidity 4 M in the divided cell by constant potential electrolysis; Volume of anolyte: 440 ml; Anode: Pt mesh of surface area $84 \text{ cm}^2$ ; Cathode: Pt wire of surface area $9 \text{ cm}^2$	103
6.1	Comparison of separation percentage of Ru and Faradaic efficiency after 10 h of electrolysis at various applied potentials and concentration of nitric acid, with and without cerium	125
6.2	Reaction rate constant, $k_1$ for the electrochemical oxidation of Ru at different nitric acid concentrations and applied potentials	127
6.3	Reaction rate constant ' $k_1$ ' for the electro-oxidation of Ru from $[\text{RuNO}]^{3+}$ solution prepared in 1 M nitric acid at different temperatures; applied potential: 1.25 V	131
6.4	Rate constants $k$ and $k_1$ for the electrochemical oxidation of Ru from $[\text{RuNO}]^{3+}$ solution in the presence of 0.04 M Ce at various nitric acid concentration and applied potentials	132
6.5	Comparison of separation percentage of Ru and Faradaic efficiency during the electrolysis of SHLLW	134
6.6	Peak parameters obtained from the CVs for 40 mM $[\text{RuNO}]^{3+}$ solution in 1	140

	M HNO <sub>3</sub> recorded with Pt working electrode	
6.7	Peak parameters obtained for 40 mM [RuNO] <sup>3+</sup> solution in 1 M HNO <sub>3</sub> from the CVs recorded with GC working electrode	144
6.8	Comparison of kinetic parameters derived for the reduction of [RuNO] <sup>3+</sup> species in 1 M HNO <sub>3</sub> at different working electrodes	145

## ABBREVIATIONS USED IN THIS THESIS

FBRs	Fast Breeder Reactors
PUREX	Plutonium Uranium Extraction
SHLLW	Simulated High Level Liquid Waste
PGMs	Platinum Group Metals
HLW	High Level Waste
MWe	Mega Watt (electrical)
MOX	Mixed Oxide
HLLW	High Level Liquid Waste
TBP	Tri butyl phosphate
PWR	Pressurized Water Reactor
DBP	Di Butyl Phosphate
DF	Decontamination Efficiency
ICP-OES	Inductively Coupled Plasma – Optical Emission Spectroscopy
XPS	X-Ray Photoelectron Spectroscopy
XRD	X-Ray Diffraction
FTIR	Fourier Transform Infrared Spectroscopy
TEM	Transmission Electron Microscopy
EELS	Electron Energy Loss Spectra
PMT	Photo Multiplier Tube
FBTR	Fast Breeder Test Reactor
CV	Cyclic Voltammetry
CP	Chronopotentiometry
GC	Glassy Carbon

ACN	Ammonium Ceric Nitrate
NPH	Normal Paraffin Hydrocarbon
MW d/tonne	Mega Watt day per tonne
IR	Infrared Spectroscopy
mM	milli moles per dm <sup>3</sup>
mA	milli Ampere
V	Volts
Fig.	Figure
T	Temperature in Kelvin
E <sub>p,c</sub>	Cathodic Peak Potential, in V
I <sub>p,c</sub>	Cathodic Peak Current, in mA/A
E <sub>p,a</sub>	Anodic Peak Potential, in V
I <sub>p,a</sub>	Anodic Peak Current, in mA/A

---

# 1. INTRODUCTION

---

Ruthenium (Ru) is a rare transition metal element belonging to the platinum group in the periodic table. It is produced as a fission product in nuclear reactors in large quantities, particularly in the fission of the fissile elements uranium or plutonium in fast breeder reactors (FBRs). The yield of ruthenium in the reactor varies according to the type of fuel, burn up and cooling time after the fission, but as much as 10% in the case of  $^{235}\text{U}$  or even up to 40% in the fission of  $^{239}\text{Pu}$  in FBRs [1]. Reprocessing of the spent nuclear fuel is an important step in the closing of fuel cycle, to recover U and Pu which can be reused as fuel. The most commonly adopted aqueous method for nuclear fuel reprocessing is the PUREX (Plutonium Uranium Extraction) process. Among the fission products, Ru is one of the nuclides with nuisance value during the reprocessing of spent nuclear fuels because of its large fission yield, relatively long half lives ( $^{103}\text{Ru}$ : 39.26 days;  $^{106}\text{Ru}$ : 373.59 d) and its many oxidation states ranging from 0 to +8. It creates problem in the nuclear waste management processes due to the formation of highly volatile and radio-toxic  $\text{RuO}_4$ . Hence, separation of Ru is an essential step in reprocessing as well as in waste management of spent nuclear fuels. Ru is scarce in nature and the limited source is continuously dwindled due to its wide ranging applications in industries. Since significant quantity of Ru is produced as a fission product in the nuclear reactors, attempts can be made to separate and recover Ru, after eliminating the radioactivity associated with it, which could be done by cooling the burnt fuel for sufficiently longer period of time and the recovered Ru will be an alternative resource to meet its increasing demand. Therefore, separation and recovery of Ru from spent nuclear fuels is a value added process in addition to solving the problem in the waste management in nuclear industry. Ruthenium has extremely complex chemical properties. Owing to the existence of many oxidation states in addition to forming a large number of co-ordination complexes,

slow rate of reactions and numerous interfering effect from other PGMs (Platinum Group Metals) and the radioactivity associated with Ru, it is a serious challenge to separate and recover it from high level nuclear waste. In the present study efforts have been undertaken for the quantitative separation as well as recovery of Ru from simulated high level liquid waste (SHLLW).

## 1.1 RUTHENIUM METAL

Ruthenium (Ru) having atomic number 44 (atomic weight: 101.07) is a d-block element in the Period 5 and Group 8 of the periodic table. The electronic configuration of Ru is  $[\text{Kr}] 4d^7 5s^1$ . It is the first member of lighter triad (i.e. ruthenium, rhodium and palladium) of PGM. The metal was discovered in 1844 by Karl Karovich Klaus, Professor of Chemistry at the University of Kazan, Russia, while examining the residue after treatment of its ore with aqua regia.

### 1.1.1 Characteristics of Ruthenium

Ruthenium is a dark-grey metal, occurring in four crystal modifications:  $\alpha$ ,  $\beta$ ,  $\gamma$  and  $\delta$ . It is hexagonal in the crystalline state. High melting point (2607 K) and hardness (6.5 in Mho's scale) are the remarkable properties of the metal. Ruthenium has seven naturally occurring isotopes:  $^{96}\text{Ru}$ ,  $^{98}\text{Ru}$ ,  $^{99}\text{Ru}$ ,  $^{100}\text{Ru}$ ,  $^{101}\text{Ru}$ ,  $^{102}\text{Ru}$  and  $^{104}\text{Ru}$  with the relative abundance of 5.5, 1.9, 12.7, 12.6, 17.0, 31.6 and 18.7% respectively [2]. Additionally, 34 radioactive isotopes have been discovered. Of these radioisotopes, the most stable ones are  $^{106}\text{Ru}$ ,  $^{103}\text{Ru}$  and  $^{97}\text{Ru}$  with half-lives of 373.6, 39.3 and 2.9 days respectively [3]. Both  $^{103}\text{Ru}$  and  $^{106}\text{Ru}$  are beta ( $\beta$ ) emitters and  $^{106}\text{Ru}$  possessing beta energy of 39 keV ( $E_{\beta\text{max}} = 39 \text{ keV}$ ) is used for the treatment of eye cancer [4].

The chemistry of Ru is extremely complex because of its many oxidation states which range from +1 to +8 and -2 is also known in the complex  $\text{Ru}(\text{CO})_4^{2-}$ . Ru(III) is the most

stable oxidation state of the element. The four main ruthenium oxides are RuO, RuO<sub>2</sub>, RuO<sub>3</sub> and RuO<sub>4</sub> [5]. Volatile RuO<sub>4</sub> is the best known ruthenium oxide formed under the action of strong oxidizing agents like HClO<sub>4</sub>, HIO<sub>4</sub>, KMnO<sub>4</sub> and Ce(IV) or electrolytic oxidation. Ruthenium tetroxide is a powerful oxidizing agent, but it is less stable at room temperature and decomposes to lower ruthenium oxide mainly RuO<sub>2</sub>. RuO<sub>4</sub> forms pale yellow crystals with a high vapour pressure at room temperature. It melts at 298.5 K. RuO<sub>4</sub> is moderately soluble in water (2.03 g per 100 g of H<sub>2</sub>O at 293 K) and highly soluble in CCl<sub>4</sub> giving rise to a red orange colored solution. In alkaline solution RuO<sub>4</sub> is reduced to perruthenate (RuO<sub>4</sub><sup>-</sup>) and ruthenate (RuO<sub>4</sub><sup>2-</sup>) ions [6]. A great care with its handling is required due to its high volatility (B.P.: 313 K), toxicity and irritant effect on the eyes. RuO<sub>4</sub> is explosive above 453 K. Metallic Ru is insoluble in cold and hot mineral acids, including aqua regia. Addition of KClO<sub>4</sub> to an acid in contact with the metal results in an explosive mixture. Transfer of Ru into gaseous phase can be accomplished by three different methods. (a) Oxidation of Ru in acidified solution to volatile RuO<sub>4</sub> by oxidizing agents like HClO<sub>4</sub>, KMnO<sub>4</sub>, Ce(IV) etc., (b) Heating of metallic Ru or RuO<sub>2</sub> in air or in oxygen atmosphere at high temperatures and (c) Heating the residue after evaporation of a solution containing a soluble salt of Ru with sodium phosphate, nitrate and nitric acid to 773 K, results in the quantitative volatilization of Ru within a few minutes [7]. Ruthenium in HCl can exist in VI, IV, III and II oxidation states. Hydrochloric acid is a very good absorption medium for volatile tetroxide, and is mostly involved in separation procedures. Ru(VIII) is easily reduced in HCl to lower oxidation states. The reduction rate and the type of complexes formed depend on the concentration of HCl, temperature and reaction time [8].

In nitric acid solutions Ru can exist in various nitroso nitrate complexes of Ru(III) such as [RuNO(NO<sub>3</sub>)<sub>n</sub>(H<sub>2</sub>O)<sub>5-n</sub>]<sup>3-n</sup> and [RuNO(NO<sub>3</sub>)<sub>5-n-m</sub>OH<sub>m</sub>(H<sub>2</sub>O)<sub>n</sub>]<sup>p-</sup> or polymeric hydroxo nitrates of Ru(IV) like [Ru(OH)<sub>x</sub>(H<sub>2</sub>O)<sub>6-x</sub>](NO<sub>3</sub>)<sub>4-x</sub> [9].

### 1.1.2 Industrial Applications of Ruthenium

Resistance to chemical attack, high catalytic activity and stable electrical properties dictate the wide ranging applications of ruthenium. The major uses of ruthenium are in electronics, electrical and electrochemical industries. The largest application of Ru is in the electrolytic production of chlorine and sodium hydroxide where ruthenium dioxide coated anodes are used. Chip resistors, resistor networks containing ruthenium thick film pastes and electrodes coated with ruthenium dioxide provide the main industrial applications. Ruthenium is a very effective hardener of Pt and Pd. Alloys of high ruthenium content with other platinum metals or some base metals are used for severe wear and corrosion resistance applications. The corrosion resistance of titanium is increased markedly by the addition of a small amount of ruthenium. Elemental ruthenium as well as a large number of its complexes are widely employed as specific catalysts in chemical, petroleum and pharmaceutical industries. Recent investigations of ruthenium complexes as potential anti cancer drugs are of special interest.

### 1.1.3 Occurrence and Production of Ruthenium

Ruthenium occurs in earth's crust with the average abundance of 0.001 ppm. It is the 74<sup>th</sup> most abundant element i.e. exceedingly rare in the earth [10]. The common minerals of ruthenium are Laurite (Ru,Os) $S_2$  (65 to 67% Ru), Iridosmium (7 to 15% Ru), Osmiridium (9 to 14% Ru), ruarsite (ruthenium arsenic sulfide) and ruthenarsenite (ruthenium-nickel arsenide); however, none acts as a commercial source of Ru [9]. The natural resources of Ru are geographically limited to countries like South Africa, Russia and Canada [11]. Ruthenium is produced as a fission product in significant quantity in fast breeder nuclear reactors. The total estimated natural resources of Ru in the year 2000 was about 3090 tonnes and it was projected that by the year 2030 the global reserve would be limited to 2870 tonnes; nevertheless, about 1752 tonnes of Ru can be produced as fission product by the year 2030 [12]. If the worldwide development of nuclear power proceeds as currently envisaged, spent

nuclear fuels discharged from FBRs can be recognized as a potential resource for Ru in another two decades. Since Ru has unique chemical properties, it can be separated from rest of the fission products present in HLW and stored for 30-50 year period for eliminating the associated radioactivity. An approach for avoiding the cooling for longer time is to selectively separate the long-lived radioactive isotopes of Ru i.e.  $^{106}\text{Ru}$  and  $^{103}\text{Ru}$ , either by current methods of isotope separation or by special methods such as atomic vapour laser, plasma separation, laser separation and electromagnetic separation. However, high cost of recovery, decontamination and storage for longer duration make this source of ruthenium unattractive and rigorous R&D effort is required prior to initiating large scale separation [12-14].

## **1.2 NUCLEAR FUEL CYCLE**

It is essential to understand the nuclear fuel cycle before discussing in detail the behaviour of the fission product Ru in reprocessing the spent fuel. The fuel cycle is an industrial process involving various activities to generate electricity from uranium and plutonium in nuclear power reactors. The nuclear fuel cycle includes the ‘front end activities’, i.e. mining, milling, conversion, enrichment, fuel fabrication and up to burning of the fuel in a nuclear reactor, and the ‘back end’, i.e. the safe management of spent nuclear fuel comprising reprocessing and reuse and disposal [15].

### **1.2.1 Front End of Nuclear Fuel Cycle**

Uranium is one of the heaviest of all the naturally-occurring elements and is slightly radioactive. Uraninite ( $\text{UO}_2$ ) or pitchblende ( $\text{UO}_3$ ,  $\text{U}_2\text{O}_5$ ) collectively referred as  $\text{U}_3\text{O}_8$  is the primary ore of uranium. Natural uranium is a mixture of three isotopes: uranium-238 ( $^{238}\text{U}$ ), accounting for 99.275%;  $^{235}\text{U}$ – 0.72%; and traces of  $^{234}\text{U}$ – 0.005%.  $^{235}\text{U}$  isotope is important because it is a fissile material and it undergoes fission when bombarded with a neutron to

yield fission products, energy in the form of heat and two or three additional neutrons to sustain the fission reaction in the nuclear reactor (Fig. 1.1).

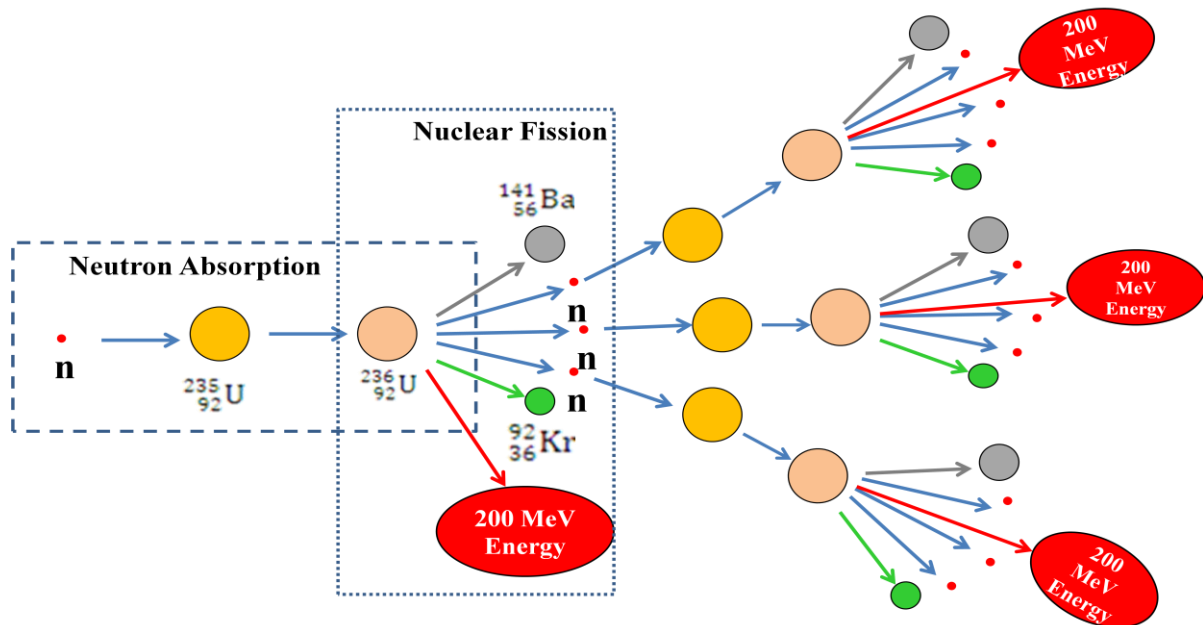


**Fig. 1.1** Fission of  $^{235}\text{U}$  and nuclear chain reaction

The heat energy created by splitting  $^{235}\text{U}$  atoms is utilized to produce steam which spins a turbine to drive a generator, producing electricity. The  $^{238}\text{U}$  isotope which is the most abundant in natural uranium is fertile and in the nuclear reactor it captures neutron and becomes fissile  $^{239}\text{Pu}$ . Uranium ore can be mined by open pit, underground and in situ leaching methods depending on its depth. Mined uranium ore is sent for milling to extract the uranium from the ore. In milling, the ore is crushed and ground to a fine slurry, which is subsequently leached in sulfuric acid or sometimes in strong alkaline solution to separate and recover uranium as uranium oxide ( $\text{U}_3\text{O}_8$ ) precipitate consisting of more than 80% of U, while the original ore may contain 0.1% or even less U. Enrichment of fuel to increase the fissile atom content is not required in the case of heavy water reactor and hence, at the conversion facility the uranium is refined to uranium dioxide and directly used as fuel. However, in the case of light water reactor (LWR), the concentration of the fissile  $^{235}\text{U}$  isotope needs to be increased from 0.7% typically to between 3.5 and 5%. The enrichment

process requires the uranium to be in a gaseous form. Uranium oxide concentrate is therefore, first converted to uranium hexafluoride, which is a gas at relatively low temperatures. The main enrichment process in commercial plants uses centrifuges. After enrichment,  $UF_6$  is reconverted to enriched uranium oxide ( $UO_2$ ) powder which is then pelletised and sintered at high temperatures. The pellets are encased in metal/alloy tubes to form fuel rods, which are arranged into a fuel assembly ready for introduction into a reactor. Several hundred fuel assemblies make up the core of a reactor. For a reactor with an output of 1000 megawatt (electrical) (MWe), the core would contain about 75 tonnes of low-enriched uranium. In the reactor core,  $^{235}U$  isotope undergoes controlled fission chain reaction, producing tremendous energy in the form of heat. The process depends on the presence of a moderator such as light/heavy water or graphite, and is fully controlled. Some of the  $^{238}U$  in the reactor core is turned into plutonium and about half of this also undergo fission, providing about one third of the reactor's energy output. With time, the concentration of fission fragments and heavy elements formed in the fuel will increase to the point where it is no longer practical to continue to use the fuel. So after about 18-36 months, the used fuel is removed from the reactor. The abovementioned details give a glimpse of the front end activities of nuclear fuel cycle.

### **1.2.2 Back End of Nuclear Fuel Cycle**

The fuel after irradiation in the nuclear reactor is no longer useful for sustaining a chain reaction and it is called as spent fuel which contains 96% uranium (most of the fertile  $^{238}U$  and little  $^{235}U$ ), 1%  $^{239}Pu$ , about 3% of fission products and traces of minor actinides. The back end activities of nuclear fuel cycle include reprocessing and waste management of spent nuclear fuel. When the spent fuel is removed from the reactor, it will be emitting radiation and heat; hence, it is stored in water filled spent fuel pool for years in order to dissipate heat and provide shield from radiation. After cooling, the fuel is reprocessed to chemically

separate and recover U and Pu from rest of the fission products, which can be reused in fast breeder reactor as mixed oxide (MOX) fuel. The high level liquid waste (HLLW) generated after reprocessing of the fuel is subjected to calcination to reduce the volume of waste by evaporating the water. The 'calcine' generated is vitrified, where it is heated at very high temperatures in a furnace with glass and the solid melt is encapsulated in stainless steel canisters and stored in geological repository and immobilized for thousands of years.

### **1.3 ONCE THROUGH AND CLOSED NUCLEAR FUEL CYCLES**

Globally, there are two routes for managing nuclear fuel cycle: the 'open' or 'once through' fuel cycle (Fig.1.2) where the spent nuclear fuel discharged from the nuclear reactor is treated as waste and is disposed in repositories for indefinitely long time and in the 'closed' fuel cycle (Fig.1.3), the spent nuclear fuel is reprocessed for the recovery of strategic metals like uranium and plutonium. The recovered U and Pu are re-fabricated into oxide or mixed oxide fuel and recycled back into the reactor. The high level waste comprising fission products in acid medium is subjected to various waste management treatment and then disposed. The advantage of nuclear fuel reprocessing is to recover valuable actinides such as U and Pu and thus, the need to mine new supply of U is eliminated, the life time of resources is extended and the waste volume is also reduced. The closed fuel cycle also has the advantage for long-term waste disposal, since long-lived actinides can be separated from the fission products and transmuted in a reactor. Once through fuel cycle method has the advantage in terms of cost and proliferation resistance since there is no reprocessing and is favoured by six countries: the United States, Canada, Sweden, Finland, Spain and South Africa. India has chosen to follow the closed fuel cycle policy to ensure long term energy security. Having low reserves of uranium, this strategy of reprocessing and recycling of uranium and plutonium would lead to optimum resource utilization. Thus, in the Indian context, spent fuel is a vital resource material and not a waste to be disposed off.

In closed fuel cycle, aqueous and non-aqueous processes are the two approaches available for reprocessing of the spent fuel.

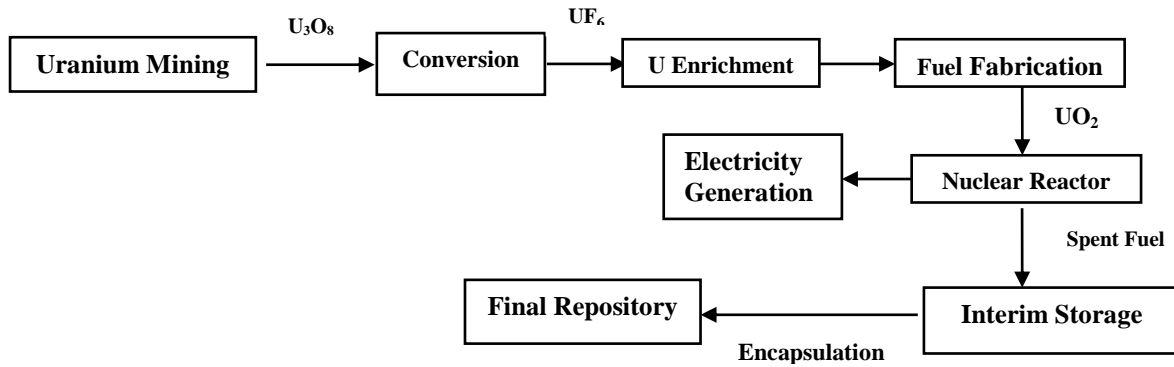


**Fig. 1.2** Open fuel cycle: Once –through fuel

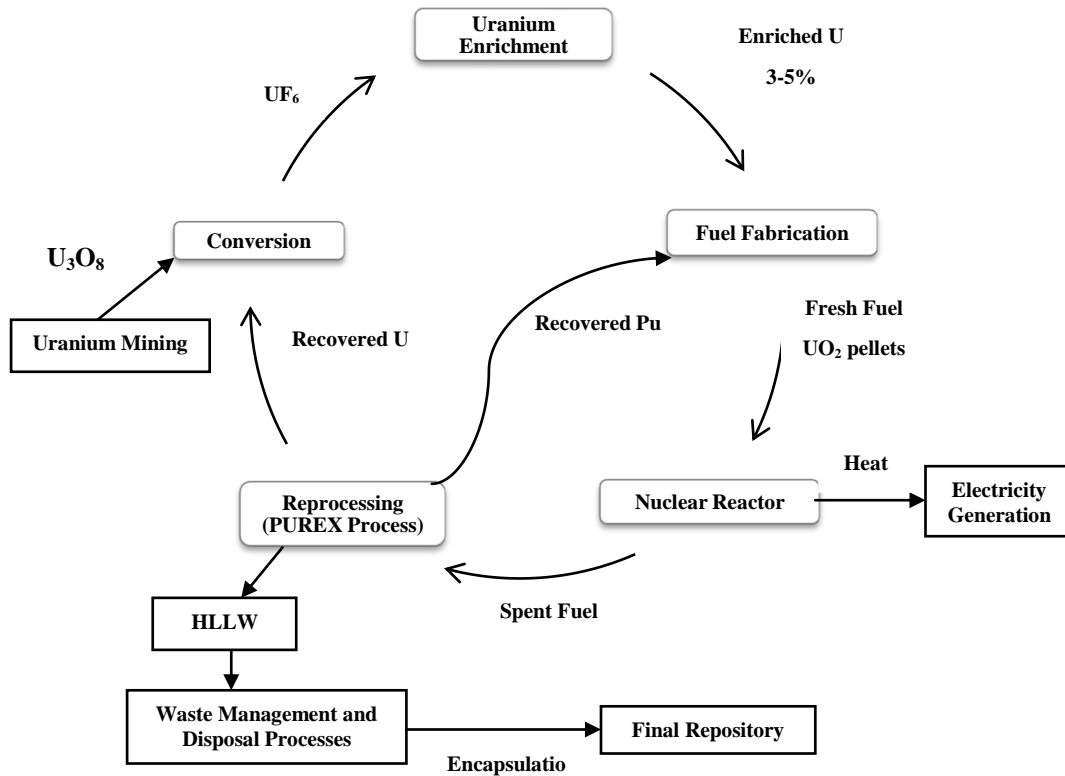


**Fig. 1.3** Closed fuel cycle

### 1.3.1 Non-aqueous Pyrochemical Reprocessing

Non-aqueous pyrochemical reprocessing has been developed at Argonne National Laboratory (ANL) in USA and elsewhere, but it is not significantly in use worldwide, as on today. This method of reprocessing has inherent advantages such as the ability to handle high burn-up spent fuel and hence, requires less cooling time, reduced criticality accidents since it does not use solvents containing H<sub>2</sub> and C, generation of minimum aqueous waste, feasibility of on-site reprocessing due to compact size and hence, avoids the transportation of spent fuel and its security issue. In pyrochemical reprocessing approach, the spent fuel after dismantling is treated by the following two routes: (i) by electrorefining, which was developed for the reprocessing of metallic fuel at Argonne National Laboratory as a part of Integral Fast Reactor (IFR) program [16] and (ii) by electrowinning which was developed at Research Institute of Atomic Reactors (RIAR, Russia) to process the spent MOX fuels of Fast Breeder Reactors [17]. In the case of electrorefining, the spent fuel is dissolved anodically and uranium and transuranium elements are deposited at the cathode in a condition of greater purity by electrotransport through a suitable electrolyte by means of an applied current [16], whereas in electrowinning, the spent fuel is dissolved into molten salt eutectic by chlorination and uranium is electrowon while plutonium is precipitated as PuO<sub>2</sub> from the melt [17]. The high temperature operation of the process, however, introduces problems in terms of plant design and corrosion from the use of highly reactive gases.

### 1.3.2 PUREX Process

The PUREX (Plutonium Uranium Extraction) process is the most widely adopted aqueous method for reprocessing. The PUREX process, which is based on liquid-liquid extraction was invented by Herbert H. Anderson and Larned B. Asprey in the Metallurgical Laboratory at the University of Chicago, USA and was first used at US Atomic Energy Commission's Savannah River Site in 1954. In this process the spent nuclear fuel is mechanically decladded

and chopped followed by dissolution in concentrated nitric acid. The resulting solution after dissolution is called as dissolver solution. The dissolver solution undergoes conditioning process in which the acidity of solution is adjusted to 3-4 M, valency of U and Pu are changed to only  $U^{6+}$  and  $Pu^{4+}$  followed by adjustment of U to Pu ratio before extraction with 30 % Tri butyl phosphate (TBP)-n-dodecane. The U and Pu co-extracted by TBP are partitioned. The aqueous raffinate (containing all fission products and minor actinides in 3-4 M nitric acid) remained after the extraction of U and Pu to the organic phase (i.e. 30% TBP in n-dodecane) is known as high level liquid waste. Although PUREX process is the widely adopted method of reprocessing, it has some limitations such as the chemical and radiolytic degradation of the solvents employed and generation of large volume of secondary liquid waste. In the late 1970s, U.S. government has decided to forego reprocessing based on the perception that the process contributed to the threat of proliferation of nuclear weapons by virtue of its ability to produce separated plutonium; however, the PUREX process has subsequently been used commercially by India, France, U.K. and Japan.

#### **1.4 RUTHENIUM IN NUCLEAR REACTORS**

The growth in the generation of electrical power from nuclear fission gives rise to platinum group elements in significant quantities. Of the platinum group metals only ruthenium, palladium and rhodium are produced in significant amount during the nuclear fission of uranium and plutonium. Among all the three fission platinoids, ruthenium generated is more and its metal fraction is about 56 % [18]. Since the price of platinoids is increasing steeply and those available in the earth's crust are about to be exhausted in another few decades, there is an increased interest in the recovery of these man-made platinoids from spent nuclear fuels. Even though Ru has huge industrial applications, its recovery from spent fuel is not yet attractive on industrial scale because of the long-lived and high radioactive isotopes and complicated chemistry of ruthenium. An important requirement for the separation of

ruthenium in nuclear industry is to minimize the problems created by the different species of ruthenium during reprocessing as well as in waste management processes.

#### 1.4.1 Yield and Chemical State of Ruthenium

Several stable and radioactive isotopes of Ru are formed as fission product in nuclear reactors and the fission yield (i.e. the fraction of a fission product produced per fission) of ruthenium varies according to the type of reactor system and burn-up (the thermal energy generated per unit mass of fuel) to which the fuel is taken. The fission yield increases with fuel burn-up, with fuel enrichment in  $^{235}\text{U}$  and the yield is more in MOX fuel than in  $\text{UO}_2$  fuel [19]. In a commercial light water reactor at a burn-up of 33 GWd/te about 4 kg of platinum group metals (i.e. Ru, Rh and Pd) are produced per tonne of heavy metal in the fuel. In a fast breeder reactor, because of the higher burn-up (about 100 GWd/te) and with different neutron spectrum for Pu fission, about 19 kg of platinum group metals per tonne are produced. For light water reactor fuel, the approximate composition of the platinum group metals is 56, 33 and 11 % for Ru, Pd and Rh respectively [18]. The amount of PGMs present in the spent fuel of pressurized water reactor, PWR (4.5% enrichment, burn-up: 45000 MWd/t, cooling period: 4 years) is ~ 1.7 kg of Pd, 2.9 kg of Ru and 0.57 kg of Rh [20]. The fission yield of ruthenium per tonne of FBTR fuel for the burn-up of 150 GWd/t was reported to be 122.41 mole by Agarwal and Venugopal [21]. Platinum group metals in the spent fuel contain both stable and radioactive isotopes, generated either by the fission process or by  $\beta$  decay of adjacent species that are produced during fission. Content of different isotopes of Ru in the spent nuclear fuel of a PWR (3.2 %  $^{235}\text{U}$  as  $\text{UO}_2$ , 880 days irradiation, burn-up: 32.3 GWd.t<sup>-1</sup>) is listed in Table 1.1 [12]. Among the PGMs, the fission produced Pd contains stable isotopes with masses 104, 105, 106, 108 and 110, and only one radioactive isotope, namely  $^{107}\text{Pd}$  ( $t_{1/2}$ :  $6.5 \times 10^6$  years) which is a soft  $\beta$ - emitter with maximum energy as 0.035 MeV. The fission product Rh consists almost exclusively of the stable isotope  $^{103}\text{Rh}$  and trace mass fractions of

the isotopes  $^{102}\text{Rh}$  ( $t_{1/2}$ : 2.9 years) and  $^{102\text{m}}\text{Rh}$  ( $t_{1/2}$ : 207 days). Electron capture is the exclusive decay mode of  $^{102}\text{Rh}$  and it is the main decay mode of  $^{102\text{m}}\text{Rh}$ , which also is a beta and positron emitter and undergoes an internal transition. The gamma radiation of the isotopes is rather energetic (0.47 to 1.1 MeV). Among all the three fission produced platinoids, Ru exhibits higher intrinsic radioactivity, caused by the isotopes  $^{103}\text{Ru}$  (0.0036 wt. %;  $t_{1/2}$ : 39 days) and  $^{106}\text{Ru}$  (3.8 wt. %;  $t_{1/2}$ : 1.02 years).  $^{103}\text{Ru}$  emits beta particles with  $E_{\text{max}} = 0.76$  MeV and little gamma radiation (0.05, 0.61 MeV), and decays to stable  $^{103}\text{Rh}$ .  $^{106}\text{Ru}$  is a soft beta emitter ( $E_{\text{max}} = 0.039$  MeV), which decays to  $^{106}\text{Rh}$  ( $t_{1/2}$ : 30 second), a hard beta emitter ( $E_{\text{max}} = 3.54$  MeV) and also a gamma emitter of energy in the range 0.51-0.62 MeV. The stable isotopes are  $^{99}\text{Ru}$  ( $2.4 \times 10^{-4}$  wt. %),  $^{100}\text{Ru}$  (4.2 wt. %),  $^{101}\text{Ru}$  and  $^{102}\text{Ru}$  (both 34 wt. %), and  $^{104}\text{Ru}$  (24 wt. %). The specific radioactivity of isolated Ru after 5 and 20 year storage has been compiled as  $3 \times 10^{11}$  and  $1 \times 10^7$  Bq  $\text{g}^{-1}$ , respectively [13, 14, 22].

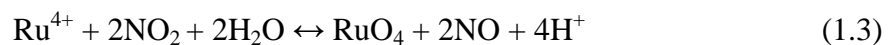
**Table 1.1** Content of Ru isotopes in a spent fuel of PWR (3.2 %  $^{235}\text{U}$  as  $\text{UO}_2$ , 880 days irradiation, burn-up: 32.3 GWd. $\text{t}^{-1}$ ) at different cooling periods [12]

Isotopes of Ru	Half life	Content in spent fuel after discharge (wt. %)	
		1 year	30 years
$^{99}\text{Ru}$	Stable	$2.4 \times 10^{-4}$	$3.6 \times 10^{-3}$
$^{100}\text{Ru}$	Stable	4.2	4.37
$^{101}\text{Ru}$	Stable	34.1	35.42
$^{102}\text{Ru}$	Stable	34.0	35.31
$^{103}\text{Ru}$	39.3 d	$3.6 \times 10^{-3}$	Nil
$^{104}\text{Ru}$	Stable	23.9	24.9
$^{105}\text{Ru}$	4.4 h	Trace	Trace
$^{106}\text{Ru}$	373.6 d	3.8	$8.5 \times 10^{-11}$

In the irradiated  $\text{UO}_2$  and  $(\text{U,Pu})\text{O}_2$  fuels, ruthenium is present in the form of white metallic inclusions of Mo-Tc-Ru-Rh-Pd alloys. The composition of the five component inclusion varies considerably and depends on the fission yield, the initial  $\text{O}/(\text{U} + \text{Pu})$  ratio of the fuel, i.e. the oxygen potential, the temperature gradients in the pin, and the burn-up. The metallic phases are mostly hexagonal and form a broad homogeneity range and cover mainly the quasi-binary section  $\text{Mo}-(\text{Tc,Ru})_{0.7}(\text{Rh,Pd})_{0.3}$  in the corresponding quinary system. Molybdenum and ruthenium are the main components of the metallic phases within the fuel [23, 24]. The post irradiation examination of  $(\text{U,Pu})$  carbide fuel revealed that ruthenium is present in the form of  $\text{CeRu}_2$  (lanthanide-noble metal intermetallic compound) and a dicarbide phase of the type  $(\text{U,Pu})_2\text{RuC}_2$ , regardless of the C/U ratio, at all burn-ups [21].

In the commercially used PUREX process for the reprocessing of spent fuel, Ru mainly passes into solution in the form of various nitrate, nitro and nitrate-nitro complexes of trivalent ruthenium nitrosyl  $[\text{RuNO}^{3+}]$  during the dissolution of irradiated fuel in nitric acid. These are complexed with hydroxo and aqua ligands and are of the general formula  $[\text{RuNO}(\text{NO}_3)_x(\text{NO}_2)_y(\text{OH})_z(\text{H}_2\text{O})_{5-x-y-z}]^{3-x-y-z}$ . Ru(IV) species formed in nitric acid undergoes hydrolysis to form  $(\text{RuO}_{\text{aq}})^{2+}$ . Ru(IV) nitrates of prominent brown colour are practically non extractable by TBP. The distribution ratio,  $D_{\text{Ru(IV)}}$  for 30% TBP is  $\leq 10^{-3}$ . Thus, their presence reduces the total amount of Ru extracted. They are extractable to a higher degree by di butyl phosphate (DBP), the primary hydrolysis product of TBP. High acid conditions oppose the formation of a Ru(IV) - DBP complex. Extractability of different nitrate or nitro complexes of ruthenium nitrosyl varies; therefore, the equilibrium between the species is critical for the decontamination of U and Pu from Ru. It was observed that nitrate complexes are generally about twice as extractable as nitro complexes and that among the ruthenium complexes, the trinitrate complexes are the most extractable in TBP [25]. Under the typical plant conditions of 2– 4 M  $\text{HNO}_3$  and  $10^{-2}$  to  $10^{-3}$  M  $\text{HNO}_2$ , 30 to 70% of the total Ru in the solution used as

feed to the first extraction cycle would be in the form of nitro complex rather than nitrate complexes. Thus, some of the ruthenium extracted into TBP might be in the form of nitrate or mixed nitrate-nitro complexes. On the other hand, Sczek and Steindler [26] attributed the extractability and retention of ruthenium in TBP mainly to dimers of the general composition  $[\text{RuNO}(\text{H}_2\text{O})(\text{NO}_2)(\text{NO}_3)]_2\text{OH}^-$  and  $[\text{RuNO}(\text{NO}_2)(\text{NO}_3)_2(\text{OH})]_2$ . Among the nitrate complexes of RuNO, trinitrate and tetranitrate complexes were found to be the most extractable, whereas dinitrate and mononitrate complexes are poorly extractable. In the case of the nitro complexes of RuNO, the dinitro complex is more extractable than higher nitro complexes, but its extraction coefficient is rather low. Mixed nitrate nitro species are more extractable than nitro compounds. The extent of extractability of some of these Ru species, primarily trinitrate complexes from nitric acid solutions is responsible for the complications in the PUREX process. The overall behaviour of the fission product ruthenium in the PUREX process is largely controlled by ruthenium nitrosyl nitrates [26]. High nitric acid concentration, high temperature and prolonged hold up time of the solution appear to enhance the volatilization of Ru [27] in the form of  $\text{RuO}_4$ . The following reactions were proposed for the oxidation of Ru by  $\text{HNO}_3$  [28].



The induction period (the period after which the volatilization of ruthenium occurs) is shorter at higher ruthenium concentrations than that at lower ruthenium concentrations. The induction period appears to shorten linearly with increasing nitric acid concentration.

#### 1.4.2 Paths Followed by Ruthenium in Nuclear Fuel Cycle

Nearly 30 % of platinoids remain as undissolved solid residue and the remaining 70 % dissolve into several nitrosyl and nitrate complexes, in the dissolution of spent fuel in 11 M  $\text{HNO}_3$  [12, 29]. The wastes generated from the hydrometallurgical solvent extraction based PUREX process are the main source of fission-platinoids. According to Ozawa et al. [20], about 85 % of Pd and 80 % of Ru get dissolved in warm concentrated nitric acid during the dissolution of standard light water reactor spent fuel and thus, exist in HLLW as complex ions. After conditioning, the dissolver solution is subjected to solvent extraction for the purpose of separating U and Pu and the resulting aqueous raffinate (called as HLLW) contains the main fraction of ruthenium as ruthenium nitrosyl complexes. Therefore, the undissolved solid residue, dissolver solution and HLLW are the main sources of ruthenium. Pyrochemical and chemical processes are ideal for the separation of ruthenium from the insoluble solid residue and the dissolver solution respectively. It is, however, not advantageous to separate Ru from dissolver solution due to the possible interference of U and Pu with Ru and also the interference of added chemicals in subsequent PUREX process. Further, the fraction of Ru accompanying uranium and plutonium may be so large that the final products are contaminated with  $^{106}\text{Ru}$  to a higher level than allowed by existing specifications; this can be avoided by selectively oxidizing ruthenium to volatile ruthenium tetroxide.

#### **1.4.3 Problems Associated with Ru during Nuclear Fuel Reprocessing and Waste Management**

The problems encountered in aqueous reprocessing of spent fuels and subsequent waste management processes by ruthenium are the following:

- During the dissolution of the spent fuel in nitric acid, ruthenium forms about hundreds of ruthenium nitrosyl complexes which have been discussed in detail in the Section 1.4.1. Various complexes formed by ruthenium, primarily trinitrato, tetranitrato,

nitronitrato and nitro complexes exhibit complicated distribution behaviour between the aqueous phase and the extract (organic) phase and a few of them remain in TBP/dodecane after stripping. Therefore, it is difficult to completely separate ruthenium from uranium and plutonium, which results in the possible release of radio-ruthenium in the environment.

- For long term storage, the radioactive waste is vitrified with glass materials and converted to a relatively insoluble and compact solid which will neither react nor degrade for extended periods of time [30]. As a solid, the waste becomes easy to store and handle; a small volume of the waste is desired because of the lower space requirement for long-term storage and keeping the solubility as low as possible reduces the chance of groundwater contamination. Prior to the solidification of HLLW by vitrification, the liquid waste is calcined to reduce the volume by evaporating the water followed by denitration to assist the stability of glass produced. In the process of concentration and denitration of highly radioactive aqueous waste containing many nitrates of fission products and  $\text{HNO}_3$ , ruthenium is oxidized to volatile  $\text{RuO}_4$  by  $\text{HNO}_3$  and the oxide escapes to the vapour phase. Gaseous  $\text{RuO}_4$ , on contact with the cooler parts of the surface of the stainless steel equipment decomposes to a non-volatile black deposit of  $\text{RuO}_2$ . As a result of contamination by the deposit, the radiation dose of the plant is increased and in extreme cases, pipes of the apparatus are plugged. The stability and decomposition of  $\text{RuO}_4$  to lower oxides have been discussed in literature reports [31-33]. Sakurai et al. [31] reported that combination of stainless steel surface and water vapour causes  $\text{RuO}_4$  to decompose; in the absence of light and water vapour,  $\text{RuO}_4$  is stable. However, there are claims by other researchers that the decomposition of  $\text{RuO}_4$  to  $\text{RuO}_2$  takes place even without light and water vapour and  $\text{RuO}_4$  can immediately be deposited over the wall of a

clean dry glass vessel located in the enclosure at 403 K. It is also reported that  $\text{RuO}_4$  is stable enough to exist at temperatures higher than 773 K. Sakurai et al. [31] studied the interaction of  $\text{RuO}_4$  gas with stainless steel, Ni, Cu and Au and concluded that the black deposit produced consisted of a peroxy-bonded polymeric  $(\text{RuO}_4)_n$ , whereas other researchers claimed that it is oxyhydroxides of Ru(IV) and  $\text{RuO}(\text{OH})_2$  [32] and hydrous or anhydrous non-volatile  $\text{RuO}_2$  species [33].

- Ruthenium creates problems in the vitrification process also, in addition to concentration and denitration processes. During vitrification, when the dried waste and glass forming chemicals (borosilicate glasses) are heated to about 1273 K,  $^{106}\text{Ru}$  is oxidized to volatile  $\text{RuO}_4$  and deposits as insoluble black  $^{106}\text{RuO}_2$  on the walls of the vessel. Platinum group metals are partially precipitated and accumulated at the bottom of the melter during vitrification of HLLW into the molten glass, since their solubility is low in the molten glass. Sedimentation of PGMs leads to electric energy loss, local over-heating, high viscous glass formation and low rate of vitrification [34], which is mainly caused by the existence of needle like crystals of electrically conducting  $\text{RuO}_2$ .

## 1.5 CONCLUSIONS

The noble metal ruthenium having wide industrial applications is scarce in nature whereas a significant quantity of ruthenium is produced as a fission product in nuclear reactors. The spent nuclear fuel can be recognized as an alternate resource of Ru, if the worldwide development of nuclear power proceeds as currently envisaged. However, high cost of recovery and storage of highly radioactive ruthenium makes this source unattractive. Separation of ruthenium is warranted during the aqueous reprocessing and waste fixing processes in closing the nuclear fuel cycle due to the severe problems created by Ru in the calcination, denitration and vitrification steps. Three reliable sources for the separation of

ruthenium are undissolved solid residue in the spent fuel, dissolver solution and HLLW. Separation of ruthenium from undissolved residue can be done by pyrochemical method whereas separation from dissolver solution is not advantageous due to the interference of added chemicals and Ru in the separation of U and Pu. Separation of ruthenium from HLLW eliminates the problems envisaged during the waste management processes. In the present study, separation and recovery of ruthenium could be accomplished from simulated high level liquid waste by oxidizing it to  $\text{RuO}_4$  using chemical and electrochemical methods.

## 1.6 REFERENCES

1. Motojima, K., U. S. Patent, No.4938895, **1990**
2. De Laeter, J. R., Bohlke, J. K., De Bièvre, P., Hidaka, H., Peiser, H. S., Rosman, K. J. R., Taylor, P. D. P., 'Atomic weights of the elements. Review 2000' (IUPAC Technical Report)". *Pure Appl. Chem.*, 75 (**2003**) 683
3. Audi, G., Bersillon, O., Blachot, J., Wapstra, A.H., *Nucl. Phys. A*, 729 (**2003**) 3
4. Lommatzsch, P.K., Transactions of the Ophthalmological Societies of the United Kingdom, 93 (**1973**) 119
5. Eichler, B., Zude, F., Fan, W., Trautmann, N., Herrmann, G., *Radiochim. Acta*, 56 (**1992**) 133
6. Seddon, E.A., Seddon, K.R., The chemistry of ruthenium, Monograph 19, Elsevier, Amsterdam, pp. 51, **1984**
7. Holgye, Z., *J. Radioanal. Nucl. Chem. Letters*, 117 (**1987**) 353
8. Balcerzak, M., Swiecicka, E., *Talanta*, 43 (**1996**) 471
9. Balcerzak, M., *Crit. Rev. Anal. Chem.*, 32 (**2002**) 181
10. Emsley, J. 'Ruthenium'. Nature's Building Blocks: An A-Z Guide to the Elements. Oxford, England, UK, Oxford University Press, pp. 368, **2003**

11. Hartman, H.L., Britton, S.G., <sup>2nd</sup> Edition, SME Mining Engineering Handbook. Littleton, Colo., Society for Mining, Metallurgy and Exploration. pp. 69, **1992**
12. Ache, H.J., Baestle, L.H., Bush, R.P., Nechaev, A.F., Popik, V.P., Ying, Y., Feasibility study of separation and utilization of Ru, Rh and Pd from high level waste. Technical Reports Series - No. 308, IAEA, Vienna, **1989**
13. Kolarik, Z., Renard, E.V., *Platinum Metals Rev.*, 49 (**2005**) 79
14. Kolarik, Z., Renard, E.V., *Platinum Metals Rev.*, 47 (**2003**) 74
15. Baisden, P.A., Choppin, G.R., Nuclear waste management and the nuclear fuel cycle, In: Radiochemistry and Nuclear Chemistry, Nagy, S., (Ed.), Encyclopedia of Life Support Systems (EOLSS), EOLSS Publishers, Oxford, **2007**
16. Laidler, J.J., Battles, J.E., Miller, W.E., Ackerman, J.P., Carls, E.L., *Prog. Nucl. Energ.*, 31 (**1997**)131
17. Vavilov, S., Kobayashi, T., Myochin, M., *J. Nucl. Sci. Technol.*, 41 (**2004**) 1018
18. Bush, R.P., *Platinum Metals Rev.*, 35 (**1991**) 202
19. Mun, C., Cantrel, L., Madic, C., *Nucl. Technol.*, 156 (**2006**) 332
20. Ozawa, M., Sano, Y., Ohara, C., Kasi, T., *Nucl. Technol.*, 130 (**2000**) 196
21. Agarwal, R., Venugopal, V., *J. Nucl. Mater.*, 359 (**2006**) 122
22. Martin, J.E., A Hand Book of Physics for Radiation Protection, Second Edn, (Wiley-VCH, Weinheim, Germany, pp. 775, **2006**
23. Kleykamp, H., *J. Nucl. Mater.*, 131 (**1985**) 221.
24. Kurosaki, K., Tanaka, K., Osaka, M., Ohishi, Y., Muta, H., Uno M., Yamanaka, S., *Prog. Nucl. Sci. Technol.*, 2 (**2011**) 5
25. Scargill, D., Lyon, C.E., Large, N.R., Fletcher, J.M., *J. Inorg. Nucl. Chem.*, 27 (**1965**) 161
26. Sczek, A.A., Steindler, M.J., *Atomic Energy Rev.*, 16 (**1978**) 4

27. Wilson, A. S., *J. Chem. Eng. Data*, 5 (1960) 521
28. Sato, T., *J. Radioanal. Nucl. Chem.*, 129 (1989) 77
29. Belyaev, A.V., *J. Struct. Chem.*, 44 (2003) 26
30. Dlouhy, Z., *Studies in Environ. Sci.*, 15 (1982) 155
31. Sakurai, T., Hinatsu, Y., Takahusi, A., Fujisawa, G., *J. Phys. Chem.*, 89 (1985) 1892
32. Mun, C., Ehrhardt, J.J., Lambert, J., Madic, C., *Appl. Surface Sci.*, 253 (2007) 7613
33. Holm, J., Glanneskog, H., Ekberg, C., *J. Nucl. Mater.*, 392 (2009) 55
34. Krause, Ch. Luckscheiter, B., *J. Mater. Res.*, 6 (1991) 2535

---

## **2. REVIEW OF LITERATURE ON THE SEPARATION AND RECOVERY OF RUTHENIUM**

---

The concept of removal of fission-produced platinoids from spent nuclear fuel was initiated in the late 1950s; however, the research interest in this field was subdued till 1990s [1]. Owing to the rapid increase in industrial applications and surge in the international prices of platinoids through 1990s, the curiosity of removal of them was renewed. Among the platinoids, ruthenium has comparatively less industrial applications and its separation from spent nuclear fuel is not much attractive due to the high cost of recovery of highly radioactive  $^{106}\text{Ru}$  and its long term storage which needs to be taken care. The major reason for its separation is to avoid the ensuing problems due to the complex chemistry during reprocessing and waste management of spent fuels. In this Chapter, the separation of ruthenium by various methods such as volatilization, precipitation, solvent extraction, chromatography and electrochemical methods reported in the literature, with emphasis on the methods suitable for adopting in nuclear fuel reprocessing plants is discussed.

### **METHODS OF SEPARATION OF RUTHENIUM**

#### **2.1 CHEMICAL METHODS**

##### **2.1.1 Volatilization**

In this method, ruthenium is oxidized to volatile  $\text{RuO}_4$  in the presence of strong oxidants such as  $\text{AgO}$ ,  $\text{Ce(IV)}$ ,  $\text{HClO}_4$ ,  $\text{H}_2\text{SO}_4$ ,  $\text{NaBiO}_3$ ,  $\text{K}_2\text{Cr}_2\text{O}_7$ ,  $\text{Cl}_2$  (in alkaline media) and  $\text{KMnO}_4$  and removed from multi-components by distillation of  $\text{RuO}_4$ . According to Holgye [2, 3], calcium/ sodium phosphate and sodium nitrate enhance the volatility of ruthenium and he exploited this volatilization behavior in the separation of  $^{103}\text{Ru}$  and  $^{106}\text{Ru}$  from other fission products [4]. Ruthenium from radio-active waste can also be separated by oxidizing with  $\text{O}_3$

or  $\text{KMnO}_4$  to  $\text{RuO}_4$  and subsequently treating with formic acid, hydrazine or  $\text{SO}_2$  gas to reduce  $\text{RuO}_4$  to  $\text{RuO}_2$  or Ru; otherwise  $\text{RuO}_4$  can be absorbed as ruthenate or perruthenate by contacting with an absorbent like NaOH [5, 6].  $\text{RuO}_4$  can also be absorbed into a melting vessel fed with saccharides or  $\text{CH}_4$  as well as Zn or Pb [7]. According to Motojima [8], Ru in  $\text{HNO}_3$  solution after oxidation to  $\text{RuO}_4$  by the addition of ceric nitrate (about 1.5 times the ruthenium equivalent) is immediately reduced to black  $\text{RuO}_2$  when contacted with n-paraffin oil. The black suspension formed at the organic-aqueous interface could be readily filtered off through a filter paper made of cellulose.  $\text{RuO}_2$  particle is hydrophobic and does not disperse in the aqueous phase. Ceric nitrate is the most favourable oxidizing agent because Ce is already contained as a fission product in the high level liquid waste (HLLW) and its addition does not complicate the waste treatment process. Grehl et al. [9] separated Ru by heating a solution containing noble metals to the temperature of 323–338 K with HCl (concentration [1 mol/l]) and adding sodium chlorate subsequently to the solution/suspension. The suspension/solution was heated to 353–363 K and  $\text{RuO}_4$  produced was captured by HCl. Hass et al. [10] recovered Ru in the form of ruthenium halide from catalyst materials. This method comprises chemical decomposition of the catalyst material producing raw Ru salt solution which is then treated with oxidizing agents like nitrates, chlorates, perchlorates, peroxydisulphate, permanganates, peroxide, chromates and dichromate of alkali or alkaline earth metals.  $\text{RuO}_4$  produced is collected as  $\text{RuCl}_3$  in HCl. Mayer et al. [11] had separated Ru from ruthenium oxides and noble metal ore concentrates, by introducing the material into highly alkaline alkali hydroxide melt in the presence of  $\text{NaNO}_3$  as oxidizing agent. The oxidized melt residue contains water soluble ruthenate ( $\text{RuO}_4^{2-}$ ) and by the addition of reducing agents like ethanol, methanol and glucose Ru was precipitated and filtered off. Isa and Takahashi [12] had recovered Ru from ruthenium containing acidic or a basic solution by adopting different chemical steps like dissolution of the substance by alkaline fusion mixture

of inorganic peroxide and alkaline hydroxide, oxidation by  $\text{KMnO}_4$  or  $\text{K}_2\text{Cr}_2\text{O}_7$ , collection of  $\text{RuO}_4$  in aqueous solution of  $\text{HCl}/\text{NaOH}$ , precipitation of the absorbed  $\text{RuO}_4$  by aqueous ammonia and recovery of solid Ru. According to DePablo et al. [13], Ru can be recovered from catalysts or electrode substrate materials by immersing them in a HF based stripping solution which comprises a mixture of  $\text{H}_2\text{O}_2$  and fluoroboric acid ( $\text{HBF}_4$ ) and the precipitate formed is oxidized to  $\text{RuO}_4$  by alkaline hypochlorite solution and then distilled and passed into concentrated HCl. A more recent work [14] involves the development of a process for the separation of Ru from HLW stream by volatilization using  $\text{KMnO}_4$  or  $\text{O}_3$  and trapping on PEEK pellet (adsorbent). Increasing the temperature and Ru content and decreasing the acidity were found to favour the volatilization of Ru using  $\text{KMnO}_4$ ; however,  $\text{KMnO}_4$  introduces corrosive potassium and manganese ions in the waste stream. Bogl et al. [15, 16] investigated the fast separation of the recoil product of  $^{252}\text{Cf}$  source in the gas phase using  $\text{Cl}_2$ ,  $\text{HCl}$  and  $\text{H}_2\text{O}_2$  as reactive gases. The recoil products were stopped, thermalized in  $\text{N}_2$  gas flow and carried to a gas inlet where chemical compounds were formed with reactive gases. The volatile compounds were separated partly by adsorption chromatography and the nuclides adsorbed in a trap were identified by gamma spectroscopy. The separation yield of Ru with  $\text{Cl}_2$  was 65 % when the temperature of the transfer tube was kept at 673 K. The Ru/Cl species transported were  $\text{RuCl}_3$  and  $\text{RuCl}_4$ . Selective separation of Ru and Tc using online gas phase separation method in about one second was reported by Matschob and Bachmann [17].

In nuclear industry volatilization method is applicable for the separation of ruthenium either from dissolver solution or from HLLW before subjecting the waste to treatment processes such as evaporation, calcination and vitrification. The major difficulties encountered in these waste management processes are due to volatilization of Ru to highly volatile radiotoxic  $\text{RuO}_4$ . In the absence of control measures, Ru is volatilized to the extent of

20–60 % while calcining at temperatures above 1123 K, required for producing a glassy solid. Clark and Godbee [18] suppressed the volatilization of Ru during evaporation and calcination of fission products by providing about 0.1 M phosphite or hypophosphite ion in the solution. This method is not effective for Zr bearing solutions, as Zr (about 0.3 M) reacts with phosphite or hypophosphite to form a precipitate and handling of the precipitate containing solutions is then required. Sato [19] added ferric nitrate to suppress the volatilization of Ru from boiling HNO<sub>3</sub> effectively. Addition of 0.1 M ferric ion retarded the volatilization rate of Ru to one twentieth under boiling conditions. Kubota et al. [20] suppressed the evaporation of Ru during HNO<sub>3</sub> recovery by adding 20–5000 mg/l hydrazine, thereby increasing the Ru decontamination efficiency in the nitric acid evaporator. Hydrazine reacts with HNO<sub>2</sub> at high temperatures in the following manner:



Reductive reaction takes place between hydrazine or reaction intermediates such as azides and the reaction intermediates of RuO<sub>4</sub>, and thus, inhibit the oxidation of Ru. Figure 2.1 shows the variation of ruthenium decontamination factor with the concentration of added hydrazine per liter of nitric acid solution.

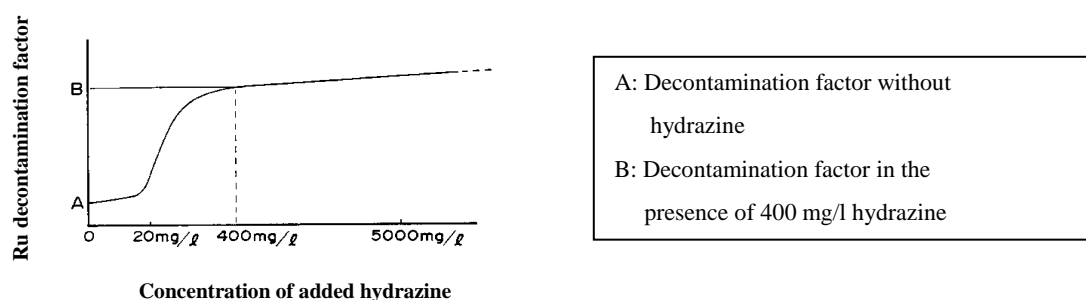


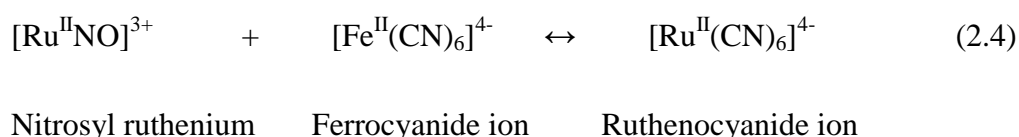
**Fig. 2.1** Variation of Ru decontamination factor with the concentration of hydrazine [20]

$$\text{Decontamination Efficiency (DF)} = \frac{\text{Amount of ruthenium in solution fed into evaporator}}{\text{Amount of Ru in the vapour from evaporator}}$$

Extraction of Ru into TBP along with U and Pu in the PUREX process could be suppressed by the addition of barbituric acid [21]. Decontamination of U and Pu from Ru was achieved by adding more than one mole of barbituric acid (C<sub>4</sub>H<sub>4</sub>O<sub>3</sub>N<sub>2</sub>) per mole of Ru to the aqueous solution of the spent fuel and digesting at 363–373 K for one hour. Addition of 0.05 M barbituric acid was found to reduce the amount of Ru extracted into the organic phase by a factor greater than 1000 as compared to a factor of 25 with the addition of hydrazine, when the concentration of HNO<sub>3</sub> was in the range 0.1–0.5 M.

### 2.1.2 Precipitation

Precipitation methods are rarely used to isolate Ru from multi-component mixtures due to lack of selective precipitants. Thio-organic compounds such as thiourea, thioacetamide, thiophenol, b-thiopropionic acid and 2, 3-dithiopropanol have been employed to pre-concentrate Ru using copper sulphide as a carrier [22]. Ruthenium was effectively precipitated from nitric acid solutions in the presence of U, Pu and other fission products by b-thiopropionic acid and 2,3-dithiopropanol by Moore [23]. Gandon et al. [24] reported that the complex Ru species formed during the nitric acid dissolution stage of the PUREX process can be eliminated by coprecipitation with ferrocyanide in an excess of Cu<sup>2+</sup> (as nitrate). The reaction involves the transfer of Ru from a nitrosyl complex to a soluble ruthenocyanide structure. The ruthenocyanide ion is subsequently co-precipitated as copper ruthenocyanide at the pH 5 ± 1.



Use of Na<sub>4</sub>[Fe(CN)<sub>6</sub>] is recommended to obtain higher Ru yields with lower quantities of reagents. This method allowed the removal of up to 98 % of <sup>106</sup>Ru contained in effluent

samples from the La Hague reprocessing plant before their controlled release into the sea. A decontamination factor of 7–8 was obtained in the removal of Ru from nuclear waste solutions using precipitating agents like ferrous/ferric hydroxide in the presence of  $\text{Na}_2\text{SO}_3$  as the reducing agent [25]. Ruthenium along with Cs and Sr were recovered by Kore et al. [26] from Low level liquid waste (LLW) by coprecipitating with chemicals like  $\text{CuSO}_4$ ,  $\text{K}_4\text{Fe}(\text{CN})_6$ ,  $\text{BaCl}_2$ ,  $\text{Na}_2\text{SO}_4$  and  $\text{Fe}(\text{NO}_3)_3$ . This method is used for the plant scale treatment of Cs, Sr and Ru. Sonar et al. [27] had investigated a chemical treatment method for the removal of  $^{106}\text{Ru}$  in the effluent using sulphides of Co and Ni. A DF value of 250 with respect to  $^{106}\text{Ru}$  and about 34 with respect to  $^{137}\text{Cs}$  could be achieved in two steps using 2500 ppm of  $\text{Ni}^{2+}$  and 1326 ppm of  $\text{S}^{2-}$ .

### 2.1.3 Pyrochemical Separation

Quantitative separation of Ru and Os by lead button, followed by recovery after dissolution with  $\text{HClO}_4$  in the presence of acetic acid was carried out by many researchers [28-30]. Ru, Pd and Mo were recovered by Naito et al. [31] from a simulated insoluble residue produced in the dissolver solution of spent nuclear fuel by means of Pb extraction and recovery was found to be more than 80 % for Ru and Pd. The insoluble residue was mixed with Pb metal (scavenger) and glass forming materials such as  $\text{Na}_2\text{B}_4\text{O}_7$  and  $\text{B}_2\text{O}_3$  to fix the constituents other than noble metals in the residue and then melted at high temperatures in the range  $823 \leq T/\text{K} \leq 1173$  in a stream of air or inert gas. The fused mixture splits into two phases based on the difference in the density; one was a Pb button phase containing noble metals and the other was a glass phase containing actinide oxides and crud components. The principle of the recovery process reported by Naito et al. was similar to the method developed for the recovery of noble metals from HLLW by Jensen [32] at Pacific North West Lab, but differs in some process conditions like operating temperature, chemical form and decontamination of Pu. Separation of Mo and/or Ru from ternary Mo–Ru–Pd alloy in the simulated insoluble

residue could be accomplished by the preferential vaporization during oxidation by Naito and co-workers [33, 34]. Naito et al. [35] also investigated the recovery and mutual separation of noble metals from the quaternary Mo–Ru–Rh–Pd alloy and the recovery yield was more than 90 % for Ru, Rh and Pd. Arai et al. [36] recovered noble metals from simulated insoluble residue like Mo–Ru–Rh–Pd alloy using Pb-extraction similar to the procedure used by Naito et al. Separation of Ru from the undissolved powder and dissolution fraction was done by passing O<sub>3</sub> in N<sub>2</sub> carrier for converting Ru to RuO<sub>4</sub>.



The schematic of the experimental set up used in this separation process is given in Fig. 2.2. The total recovery efficiency of Ru from the undissolved powder was more than 99.8 % and from the dissolution fraction was more than 93 % through the ozone oxidation process coupled with re-Pb extraction.

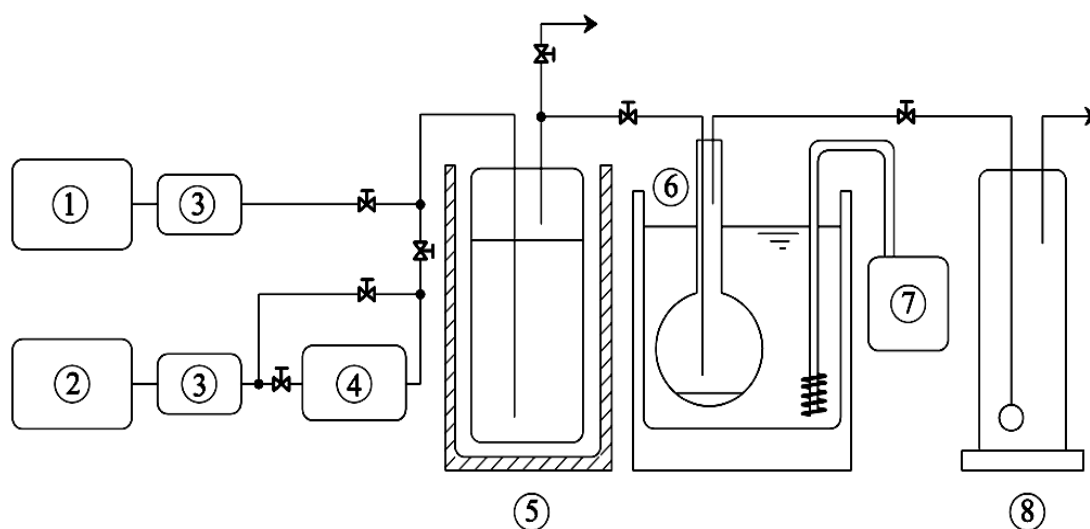


**Fig.2.2** Experimental apparatus for Ru separation system [36]

(1: Nitrogen source; 2: Oxygen source; 3: Mass flow controller; 4: Ozonizer; 5: Ozone reservoir with cold bath; 6: Oxidation reactor; 7. Thermocontroller and 8: Absorbing bottle)

## 2.2 SOLVENT EXTRACTION

Solvent extraction is widely employed in the separation of noble metals from their multi-component mixtures as well as from the associated base metals. The platinum group metal (PGM) species undergo extraction from aqueous solutions via non-coordinating outer sphere mechanism under the action of neutral solvating agents (e.g. oxygen containing solvents, organo-phosphorous and neutral sulphur containing compounds) as well as in the form of ion-pairs (e.g. with high molecular weight amines,  $R_4N^+$ ).

### 2.2.1 Organic Solvents with Atoms Capable of Forming Coordinate Bonds

Ruthenium could be separated from an aqueous solution by solvent extraction [37] using organic solvents such as ethers, esters, ketones and alcohol with a common structural property of having an atom capable of donating an electron pair to a coordination bond (e.g. ethyl ether, ethyl acetate, acetophenone, ethyl sulphide etc.) in the presence of nitrite anions such as  $NaNO_2$ . In the presence of nitrite anions, the distribution ratio (organic/aqueous) of Ru had considerably increased probably due to the formation of ruthenium–nitrite complex. An increase in nitrite quantity brought about a considerable improvement of ruthenium extraction and those ratios above 10:1 yielded optimal results. According to the invention of Fitoussi et al. [38], Ru from  $HNO_3$  can be extracted with an organic phase comprising an organo phosphorous compound having at least one electron donor sulphur atom i.e. di-(2-ethyl-hexyl)dithiophosphoric acid (DEHDTP) in the presence of compounds like sulphamic acid or hydrazine capable of displacing  $NO^+$  ions of the Ru complexes present in  $HNO_3$  at 343 K. These authors had also extracted Ru using DEHDTP in the presence of a quaternary ammonium salt like tricapryl methyl ammonium chloride and reported that the partition coefficient of Ru increased when compared to the extraction involving DEHDTP alone as the organic phase. As U(VI) and Pu are not practically extracted in this organic solvent, it was possible to recover ruthenium in satisfactory yield. The structure of DEHDTP along with the

structures available for other extractants (including TBP), which have been discussed in subsequent Sections are shown in Fig. 2.3 [39, 40].

### 2.2.2 Extraction with Pyridine

Kiba et al. [41] described a method of separating radioactive Ru from fission products and Tc by liquid–liquid extraction with pyridine. In this process, Ru in various ionic forms and oxidation states was oxidized by sodium hypochlorite to perruthenate, which was then transferred into pyridine from the aqueous solution. Solvent extraction investigation revealed that the extraction percentage of perruthenate in pyridine was higher at 3–4 M NaOH and 3 M sodium hypochlorite. Using this method, radioactive ruthenium had been separated from other fission products such as  $^{95}\text{Zr}$ ,  $^{95}\text{Nb}$ ,  $^{144}\text{Ce}$ ,  $^{144}\text{Pr}$ ,  $^{147}\text{Pm}$ ,  $^{90}\text{Sr}$ ,  $^{90}\text{Y}$ ,  $^{137}\text{Cs}$ ,  $^{137\text{m}}\text{Ba}$ ,  $^{89}\text{Sr}$  and  $^{91}\text{Y}$ .

### 2.2.3 Tertiary Amine and TBP Systems

Fieberg and Edwards [42] had separated and purified Ru from aqueous HCl using liquid anion exchanger. Ru is converted to nitrosyl ruthenium(II) complex using HCOOH or HCHO as reducing agent; nitrosyl ruthenium complex is converted to a nitrosyl ruthenium chloro complex  $[\text{RuNOCl}_5^{2-}]$  and any other Pt-group metals to chlorocomplexes by the addition of 6 M HCl. Two solvent extraction systems for the separation of Ru are tertiary amine and TBP systems. In tertiary amine system, the solvent extractant Alamine 310, diluted 20 % V/V or less in Solvesso 150 has a high capacity for nitrosyl ruthenium chloride. Alkali solutions like NaOH are employed as strippants. The hot strip solution was treated with sodium bromate to convert the nitrosyl complex to the soluble ruthenate anion  $\text{RuO}_4^{2-}$  and other insoluble base metals and PGMs were removed by filtration. Purified solution was treated with alcohol to reduce ruthenate to insoluble  $\text{RuO}_2$ . In TBP system, a 50 % solution of TBP in Solvesso 150 was the solvent extractant. Strippant was weak hydrochloric acid (0.5–0.1 M).

Separation and purification of Ru from HCl solution containing Rh, Pt, Pd and Ir by two stage solvent extraction with the tertiary amine (C<sub>7</sub>–C<sub>9</sub>)N235 in kerosene was achieved by Lingen et al. [43]. In the first stage Ru was separated from Pt and Pd, by reducing Ru(IV) to Ru(III) by hydroquinone; Pt and Pd in the form of  $\text{MCl}_6^{2-}$  and  $\text{MCl}_6^{4-}$  were extracted by N235 tertiary amine leaving behind  $\text{MCl}_6^{3-}$  (M = Ru, Rh and Ir).



In the second stage, Ru was first converted to  $\text{Ru}(\text{NO})^{3+}$ , subsequently to  $\text{Ru}(\text{NO})\text{Cl}_5^{2-}$  in the presence of excess of HCOOH and dilute  $\text{HNO}_3$  after acidifying the solution with 6 M HCl and extracted by tertiary amine leaving  $\text{IrCl}_6^{3-}$  and  $\text{RhCl}_6^{3-}$ . Ru of purity 99.9 % could be produced with more than 90 % recovery. Separation and purification of Ru using solvent extraction and extraction chromatography from an active effluent feed solution was achieved by Dhimi et al. [44]. These authors had contacted the feed solution with 30 % TBP in n-dodecane twice and the raffinate was passed through an extraction chromatographic column packed with KSM-17 impregnated on XAD-4 to bring down the activity of the feed from 100 to 70 mCi/l. Gaikwad et al. [45] adopted liquid–liquid extraction using 0.1 mol/dm<sup>3</sup> n-octylaniline in xylene through 0.05 mol/dm<sup>3</sup> sodium malonate solution for separating Ru(III) from Pd(II) and Rh(III).

#### 2.2.4 Ruthenium Extraction with HDEHP in Hexane

Healey [46] invented a solvent extraction method for the separation of fission products Ru, Cs, Rb, Ba, Sr, Ce, Zr, Nb and rare earths in 0.01 M HCl. In step-1, Ru, Cs, Sr and Ba were separated from the rest of the fission products by treating with the organic phase consisting of 1.5 M di(2-ethyl hexyl)phosphoric acid (HDEHP) in hexane. In step-2 the aqueous phase containing Ru, Cs, Sr and Ba was made alkaline and Cs was extracted with 0.01 M

dipicrylamine in nitrobenzene. Finally Sr and Ba were separated from Ru by extraction with 0.4 M HDEHP in hexane from a weak acid (pH 4–5).

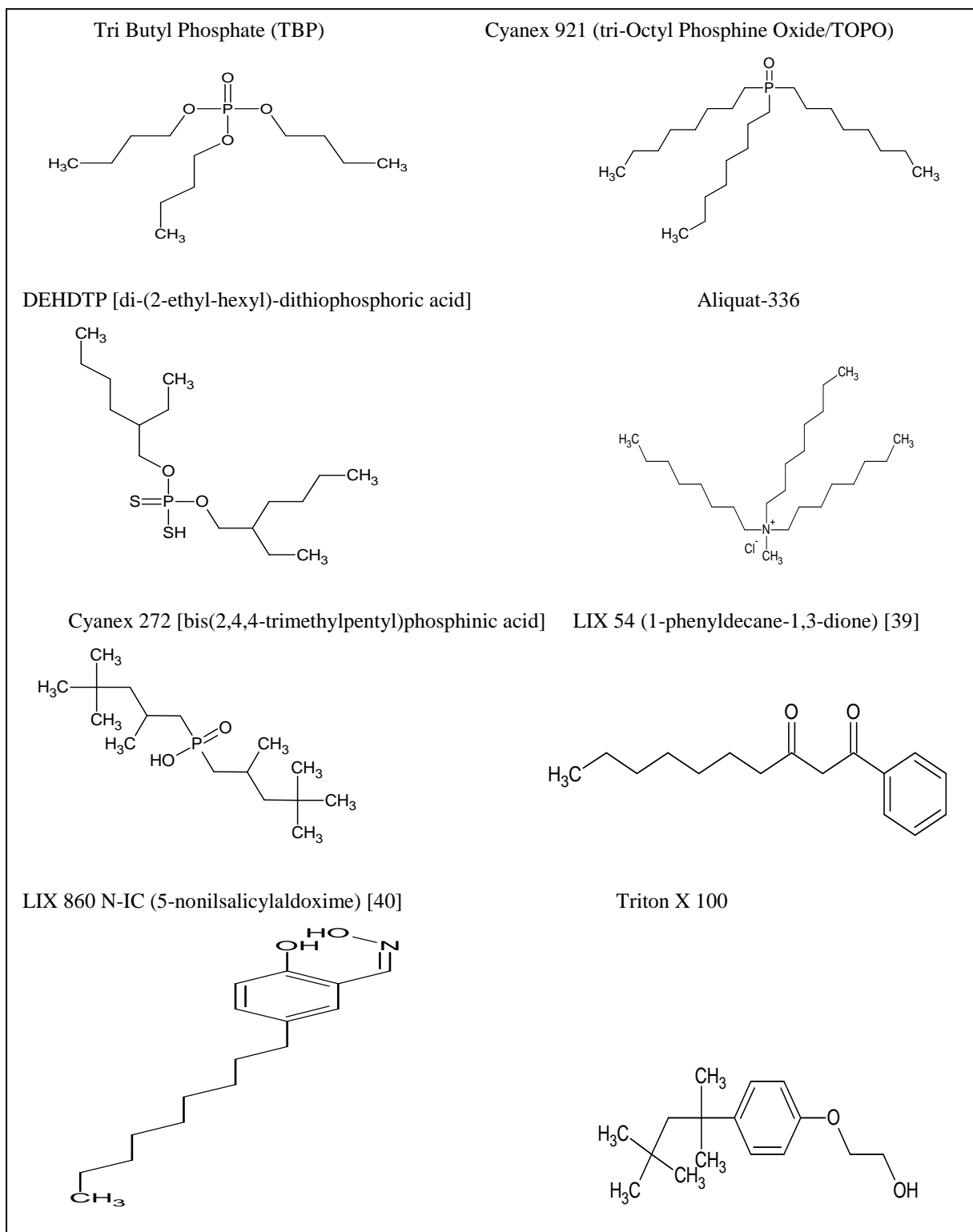


Fig. 2.3 Structures of extractants

### 2.2.5 Separation of Ru Using Halogen Substituted Alkanes

One way of recovering Ru ( $^{103}\text{Ru}$  and  $^{106}\text{Ru}$ ) from the residual aqueous nitrate solutions after uranium extraction is by oxidizing Ru to  $\text{RuO}_4$  using oxidizing agents like ammonium ceric nitrate (ACN) and subsequently extracting into halogen substituted liquid paraffin. The liquid paraffin can be from one of the groups consisting of  $\text{C}_2\text{H}_2\text{Cl}_4$ ,  $\text{C}_2\text{H}_2\text{Br}_4$ ,  $\text{CCl}_4$  and mixtures of these solvents [47]. About 90 % of Ru could be recovered into tetrachloroethane phase in two similar successive extraction treatments. Ru in the non-aqueous phase was stripped back with dilute HCl as  $\text{RuCl}_3$ . Epperson et al. [48] separated  $^{103}\text{Ru}$  and  $^{103}\text{mRh}$  from each other by adding ceric sulphate in  $\text{H}_2\text{SO}_4$  to oxidize  $^{103}\text{Ru}$  sulphate to  $^{103}\text{RuO}_4$ .  $\text{RuO}_4$  formed was extracted with  $\text{CCl}_4$  and recovered using an aqueous reducing agent.

### 2.2.6 Extraction from Thiocyanate Complexes

Ruthenium can be separated from Os and Rh after conversion into a thiocyanate complex and can be extracted from thiocyanate media into a variety of solvents. Marczenko and Balcerzak [49] reported the extractive separation of Ru from Os by extracting Ru complex from 1 M HCl solution with methyl isobutyl ketone. Jaya and Ramakrishna [50] separated Os and Ru from thiocyanate media by extraction into mesityl oxide and cyclohexanone respectively. Al-Bazi and Chow [51, 52] studied the separation of Os(IV), Rh(III) and Ru(III) from thiocyanate solutions using polyether type polyurethane foam. Surfactant extraction of Ru from thiocyanate media into Triton X-100 phase in the presence of zephiramine was also investigated [53]. Separation of Ru(III) from other elements with 2-mercaptobenzothiozole (2-HMBT) into chloroform was reported by Shetty and Turel [54]. Bahrainwala and Turel [55] separated Ru(III) with 2-mercaptobenzimidazole into butanol. The experimental details were the same as those used by Shetty and Turel, but the solvent used for extraction was different.

### 2.2.7 Separation of Ru by Extraction with Novel Solvent Materials

Mhaske and Dhadke [56] separated Os(VIII), Ru(IV) and Ir(III) metal ions from their mixture in aqueous HCl medium by taking advantage of the difference in their extraction and stripping conditions towards Cyanex 921 (tri-octyl phosphine oxide, TOPO), which is a solid with 99.9 % active component. Only Ir(III) was extracted from the mixture of Ru(IV) and Ir(III) when heated to 363 K for 15 min. and equilibrated for 1 min. at the aqueous acidity of 1 M HCl in the presence of 100 mmol/l tin(II) chloride using 25 mmol/l Cyanex 921. Separation of Ru(III) from large amounts of Pd(II) and Rh(III) in HCl medium was done by extracting the chelate complex of Ru(III) with 3-hydroxy-2methyl-1-phenyl-4-pyridone (HX) in dichloromethane or chloroform [57]. Kedari et al. [58] extracted Ir, Ru and Rh from their chloride solutions using different commercially available solvent extraction reagents such as Alamine 300, Alamine 336, Aliquat 336, Cyanex 272, LIX 54, LIX 860N-IC and TBP. Mixtures of extractants like Alamine + LIX 54, Aliquat 336 + LIX 54 and Cyanex 921 + TBP were found to be more effective for extraction, as well as for better stripping of Ru loaded in such organic phases. Solvent extraction of Ru from a dilute HCl solution with Aliquat 336 and Alamine 336 in kerosene was carried out by Panigrahi et al. [59]. Kedari et al. subsequently used Cyanex 923 dissolved in kerosene, a commercial extractant containing trialkyl phosphine oxide for extracting Ir(IV) and Ru(III) from aqueous hydrochloric acid medium [60]. Owing to the difference in extraction and stripping behaviour of Ir and Ru, they were separated from each other using multistep extraction process. Ir(IV) was extracted from aqueous solutions containing a low concentration of HCl by C923. The extraction increases with increase in concentration of HCl, whereas Ru(III) was best extracted from aqueous phase containing more than 1 M HCl. The extraction behaviour of Ir(IV), Ru(III) and Rh(III) with different commercially available extractants was reported by Kedari et al. [58, 60]. Based on the previous results, these authors used Alamine 336, an anion exchange extractant,

for selective separation of Ir, Ru and Rh from a chloride solution, varying the composition of aqueous and organic phases [61]. The difference in the extraction behaviour of individual metals at different concentrations of A336 and HCl in the organic and aqueous phases respectively, was used to mutually separate the three metals. A two step extraction scheme was proposed. In the first step, Ir(IV) was selectively extracted using a solvent comprising 0.1% A336 and 10% TBP in kerosene. In the second step, Ru(III) was quantitatively extracted using the solvent 5% A336 and 10% TBP in kerosene (all % V/V). Rh was selectively left behind in the raffinate.

Ru can be separated from Mo, Zr and Nd after oxidizing to  $\text{RuO}_4$  by 0.2 M  $\text{NaIO}_4$  and  $\text{K}_2\text{S}_2\text{O}_8$  in  $\geq 1.5$  M NaOH and extracting with  $\text{CCl}_4$  [62]. Re-extraction was accomplished by 5 M HCl containing 1 %  $\text{H}_2\text{O}_2$ . Solid phase extraction of Ru with 9,10-phenanthrene quinone monoxime into molten naphthalene [63], 3-hydroxy-2-methyl-1,4-naphthaquinone-4-oxime into microcrystalline p-dichlorobenzene [64] and by polyurethane foam [65] have also been reported.

## **2.3 CHROMATOGRAPHY**

Chromatographic methods are well established technique for the separation of noble metals from associated base metals as well as for their mutual separation. Ion-exchange chromatography provides the major contribution in the field of separation of noble metals. Both cation and anion exchangers can be used in separation procedures.

### **2.3.1 Ion Exchange Technique**

Polak [66] used ion exchange technique for isolation and identification as well as for the determination of the charge of Ru species. More than 95 % Ru could be separated from a complex mixture of the fission products Zr, Nb, Sn and Sb by adsorbing the sample solution on a Dowex 1X8 resin and eluting the complex with 3 M HCl at 352 K for about 2.5 h. The

separation of Pd(II) and Ru(III) using several anion exchangers was investigated by Lee and Chung [67]. Strong basic anion exchanger, Amberlite IR 400 was chosen to separate and preconcentrate Ru and other noble metals from silicate rock samples. Conversion of Ru into a complex with 2-(6-methyl-2-benzothiazolylazo)-5-diethylaminephenol allowed its separation from other noble metals and from mixtures with the transition metals Co, Ni and Cu [68]. Separation of Ru from Rh, Co and Cu was also possible on a Nucleosil C18 column using 1-(2-pyridylazo)-2-naphthol-6-sulphonic acid as a pre-column derivatization agent [69].

### **2.3.2 Application of TLC and Sorbents**

Thin layer chromatography (TLC), based on the difference in the extractability of the metal chelates formed under the action of chromatographic chelating agents was described by Singh et al. [70] for the separation of the noble metal multicomponent mixtures. Phenyl hydrazine-N-dithiocarbamates of Ru(III), Rh(III) and Pd(II) were separated from each other and from the complexes of other Group VIII metals (except Co) on silica gel G with  $\text{CHCl}_3$ , benzene, acetonitrile- $\text{CCl}_4$  (1:4) or ethyl acetate- $\text{CCl}_4$  (1:4). Samanta and Theyyuni [25] conducted several experiments with real nuclear waste and also with simulated test solution for the removal of radioactive Ru from intermediate level alkaline waste solutions using a number of sorbents, ion-exchangers and also by chemical precipitation method. The sorbents and ion exchangers used were coconut shell activated carbon before and after surface oxidation with nitric acid, hydrous ferric oxide loaded on macro porous strong base anion exchange resin and on Hychar SCG7 grade active carbon, cadmium sulphide loaded macro porous strong base, thiourea, urea-formaldehyde resin, macro porous chelating resin with iminodiacetate groups, molecular sieve zeolite etc., The only promising candidate for the actual waste solution was a mixture of activated carbon and zinc powder. About 96.6 % ruthenium could be removed and this method can be considered for plant scale. For the removal of ruthenium from uranyl nitrate containing solution, adding nitrite and passing over a quaternary

ammonium or tertiary amine resin and then eluting with a strong acid was proposed by Floreancig and Nicolas [71].

### 2.3.3 Alginate and Polymer Based Gels for Separation

Mimura et al. [72, 73] tried chromatographic separation of PGMs in  $\text{HNO}_3$  by employing columns packed with Cyanex 302-alginate microcapsules and barium alginate gel polymer was used for selective separation of  $\text{Ru}(\text{NO})^{3+}$  and also for the effective separation of  $\text{Ru}(\text{NO})^{3+}$  from  $\text{Rh}^{3+}$  ions. The inter separation of PGMs from halide solution using polysaccharide gel or a poly acryl amide gel was reported by Schmuckler [74]. Grant [75] attempted the separation of PGMs by passing  $[\text{Ru}(\text{NO})\text{Cl}_5]^{2-}/[\text{Ru}(\text{NO})\text{Cl}_4(\text{H}_2\text{O})]^-$  species in  $\text{HCl}$  through Toyopearl HW-40C or Sephadex G-10 resin and eluting with 1 M  $\text{HCl}$  either in the oxidizing eluent  $\text{NaClO}_3$  or reducing

eluent ascorbic acid. Sonar et al. [76] removed  $^{106}\text{Ru}$  from alkaline radioactive liquid waste using NiS-PMMA (polymethyl methacrylate) composite beads loaded in a column and found the  $K_d$  value of about 8000–9000 (Fig. 2.4). 30 % NiS loading on PMMA beads was determined to be optimum for the effective removal of more than 95 % of  $^{106}\text{Ru}$ .

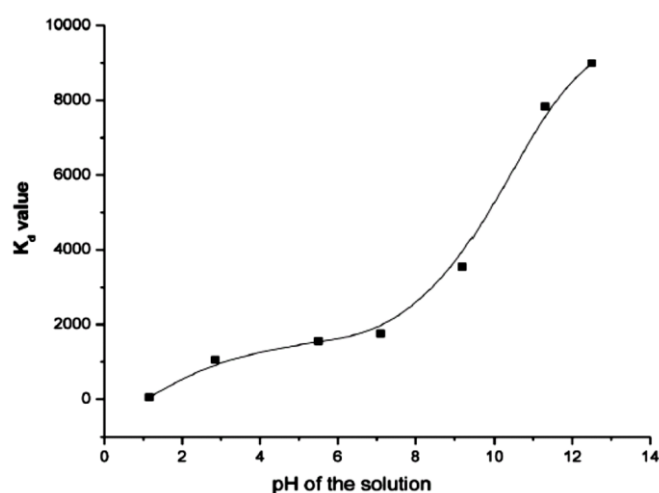


**Fig. 2.4** Effect of pH on the  $K_d$  value of Ru in NiS-PMMA composite material [76]

## 2.4 SORPTION

Sorption methods are suitable for the separation and preconcentration of ultra trace amounts of noble metals from solutions containing large excess of non-noble metals, e.g. Cu, Fe, Ni, Co, Al, Mg and Ca. Inorganic and organic complex forming sorbents are most often considered in separation procedures. Polystyrene-divinylbenzene (8%) resin with thiosemicarbazide as functional group effectively sorbed Ru from 1.5 M HCl [77]. Akatsu et al. [78] studied the properties and adsorption behaviour of sodium tetranitro nitrosyl ruthenate,  $\text{Na}[\text{RuNO}(\text{NO}_2)_4\text{OH}]_2\text{H}_2\text{O}$ , the most stable species among nitro and nitrate complexes of nitrosyl ruthenium on activated charcoal and found better adsorption behaviour of ruthenate on the activated charcoal of Tsurumicoal HC-30 (8–28 mesh). It was difficult to desorb the adsorbed ruthenate with water. Hence, this method can be deployed in the treatment of the effluent from reprocessing plants for the removal of tetranitronitrosyl ruthenate. The sorption behaviour of thioacetamide based Amberlite IRC-50 in separating Ru from PMG at pH 7 was investigated by Dey et al. [79].

Radio-active Ru can be separated by passing the liquid waste in a column packed with an adsorbent comprising 1:0.01:1 mixture of activated carbon, Zn and Pd powders and regenerating the deactivated adsorbent by washing with aqueous  $\text{HNO}_3$  or  $\text{H}_2\text{O}$  [80]. Pd in the mixture of zinc powder and activated carbon extends the optimum pH range to not only acidic but also to neutral and alkaline regions and has higher efficiency for  $^{106}\text{Ru}$  removal. This method utilizes both the adsorbing action of activated carbon and electrochemical action that occurs between carbon and palladium electrode and zinc electrode in the liquid electrolyte (liquid waste).

Tikhomirova et al. [81] studied the sorption of Ru(IV) and Os(VIII) by silica and silica with chemically grafted sulpho groups from solutions containing 1,10-phenanthroline and found that the rate of complex formation on the surface of the sorbents considerably

exceeded the rate of formation of the corresponding complexes in solution, probably due to the catalytic action on the sorbent surface. Ru as nitrate and nitroso-nitrate complexes can be sorbed with hydrous oxide type sorbents like pyrolusite and haematite [82].  $^{106}\text{Ru}$  can be removed from the effluents of irradiated nuclear fuel processing plants by bringing the effluent into contact with finely divided iron at a pH of 6. But along with ruthenium,  $^{90}\text{Sr}$ ,  $^{144}\text{Ce}$ ,  $^{95}\text{Zr}$  and  $^{137}\text{Cs}$  were also adsorbed [83]. Granulated and dried silica alumina-gel was used as an adsorbent for trapping  $\text{RuO}_4$  from radioactive wastes [84]. Ruthenium was recovered from a spent catalyst containing ruthenium particles and hydrophobic or water insoluble particles by sorption with ( $C \geq 5$ )  $\alpha$ -olefin. One gram Ru particles ( $\approx 313 \text{ K}$ ) and 10 g  $\text{ZrO}_2$  powder were hydrogenated with an aromatic hydrocarbon in aqueous 4 %  $\text{ZnSO}_4$  to obtain a dispersion, which was autoclaved along with 30 ml 1-pentene under nitrogen blanketing at 393 K for 1 h. Floated ruthenium powder was recovered with 98 % yield [85]. Pankaj et al. [86] removed Pd(II) and Ru(III) from an aqueous waste by sorption using mica minerals and zeolites. The uptake of Pd(II) and Ru(III) increased with increase in the weight of exchanger as it provided more number of sites for the exchange of metal ions. Foos et al. [87] invented a process for trapping gaseous Ru on polyvinylpyridine, particularly for recovering radio-active Ru from irradiated nuclear fuels. The aqueous effluent containing the fission products was heated to 373–423 K, in the presence of sodium hypochlorite and  $\text{RuO}_4$  formed was trapped on the adsorbent poly-4-vinyl pyridine, crosslinked by divinyl benzene or tetra ethylene glycol dimethacrylate. These adsorbents are stable up to 533 K at atmospheric pressure, not sensitive to irradiation and are resistant to the action of reducing and oxidizing agents.

## 2.5 ELECTROCHEMICAL METHOD

According to Lietzke and Griess Jr [88] a complete electro-deposition of radio-ruthenium is possible from acid solutions containing moderately low concentrations ( $5 \times 10^{-3} - 5 \times 10^{-5} \text{ M}$ )

of ruthenium nitroso salts. The anode and the reference electrode, Saturated Calomel Electrode (SCE) were placed in a separate vessel and connected to the electrolysis cell by means of salt bridge to prevent the possible oxidation of Ru to volatile  $\text{RuO}_4$  and/deposition of the dioxide on the anode. When ruthenium nitroso salt was in either  $\text{H}_2\text{SO}_4$  or  $\text{HCl}$ , complete plating was possible at the cathode potential as low as  $-0.45$  V versus SCE. If  $\text{HNO}_3$  used in the preparation of the nitroso compound was not completely removed, or if the supporting electrolyte was  $\text{HNO}_3$ , not more than 80 % of Ru could be deposited at the cathode potential of  $-1.0$  V against SCE. Kobayashi et al. [89] electro-deposited Ru from  $^{106}\text{Ru}$ -labeled  $\text{RuCl}_3$  and  $\text{Ru}(\text{NO})\text{Cl}_3$  and extended this technique for the separation of radioactive Ru from other fission products in  $0.1$  M  $\text{HCl}$  using a cylindrical cell (Fig. 2.5) and  $\text{Ag}/\text{AgCl}$  (SSE) reference electrode. About 97 % of Ru was deposited over Pt plate cathode in one hour of electrolysis from  $0.1$  M  $\text{HCl}$  solution of  $\text{RuCl}_3$  or  $\text{Ru}(\text{NO})\text{Cl}_3$  containing  $\text{H}_2\text{PtCl}_6$  (carrier Pt) at the cathodic potential of  $-0.5$  V (vs SCE). From  $\text{Ru}(\text{NO})(\text{NO}_3)_3$  solution in  $0.1$  M  $\text{HNO}_3$  the deposition of Ru was about 36 % at the cathode potential of  $-0.5$  V, whereas under similar conditions about 69 % was deposited from  $0.1$  M  $\text{HCl}$

solution. Ruthenium oxidation using cerium(IV) nitrate was investigated by Motojima [8]; the disadvantage in this process was that when Ru in  $\text{HNO}_3$  was present as sodium hydroxotetranitrosyl ruthenate (Ru-yellow), a large amount of oxidant was necessary thereby increasing the final waste content. Hence, Motojima [90] introduced electrolytic method for the oxidation of Ru to  $\text{RuO}_4$  from  $3$  M  $\text{HNO}_3$  solution and extracted it with n-paraffin oil. For effective removal of Ru, a small amount of cerous nitrate ( $0.001$  M) was added which readily got oxidized to Ce(IV) under an electric potential, and in turn oxidized Ru. Electrolysis of HLLW at a constant potential using a three electrode system facilitated the removal of Ru by vapourizing it from the liquid waste, and bringing the vapourized Ru into contact with an aqueous solution of formic acid to precipitate ruthenium oxide and separating the precipitate

to recover Ru [91]. Palladium had to be removed from HLLW using the same electrolytic apparatus prior to the vaporization of Ru as it will hinder the recovery of Ru. By applying a constant potential of 1.85 V/SSE about 90 % of Ru was separated and recovered after 27 h of electrolysis at 323 K.

Electrochemical oxidation of Ru to RuO<sub>4</sub> and separation from the spent fuel dissolution solution in nitric acid indicated the significant effect of Ag(II) redox mediator and concentration of HNO<sub>3</sub> on the yield during the electro-volatilization of RuO<sub>2</sub> solution in comparison to [RuNO]<sup>3+</sup> synthetic solution [92]. The electrolytic cell used in this case consisted of two coaxial cylindrical compartments separated by a porous ceramic tube. RuO<sub>4</sub> formed was removed from the electrolytic solution by flowing N<sub>2</sub> and trapped in alkaline solution (1 M NaOH), where it dissolves as a mixture of ruthenate (RuO<sub>4</sub><sup>2-</sup>) and perruthenate (RuO<sub>4</sub><sup>-</sup>). Electrolysis was performed in two different ways: (i) By direct electrolysis in which the Ru solution was oxidized to volatile RuO<sub>4</sub> and (ii) electrolysis in which an electro-generated Ag(II) redox mediator was used.

In the electrolytic deposition of metal ions, room temperature ionic liquids (RTIL) can be used as the electrolytic medium instead of aqueous solutions. RTILs are salts comprised entirely of ions, molten at temperatures lower than 373 K. The major advantage of using RTILs as electrolytic medium during electro-deposition is that since these are non aqueous solutions, there is negligible hydrogen evolution. Electrochemical behaviour of the ternary and binary solutions of Ru(III), Rh(III) and Pd(II) in 1-butyl-3-methylimidazolium chloride (bmimCl) at different working electrodes and at 373 K by cyclic voltammetry and chronoamperometry was investigated by Jayakumar et al. [93]. The cyclic voltammogram of Ru(III) in bmimCl recorded with glassy carbon electrode consisted of several redox waves due to the complex nature of Ru which exists in several oxidation states. Ruthenium could be deposited using bmimPF<sub>6</sub> and bmimNTf<sub>2</sub> RTILs at -0.8 V (vs Pd). The structures of these

two room temperature ionic liquids are shown in Fig. 2.6. Cyclic voltammetry results revealed that presence of Pd(II) in bmimCl favours underpotential deposition of ruthenium metal.

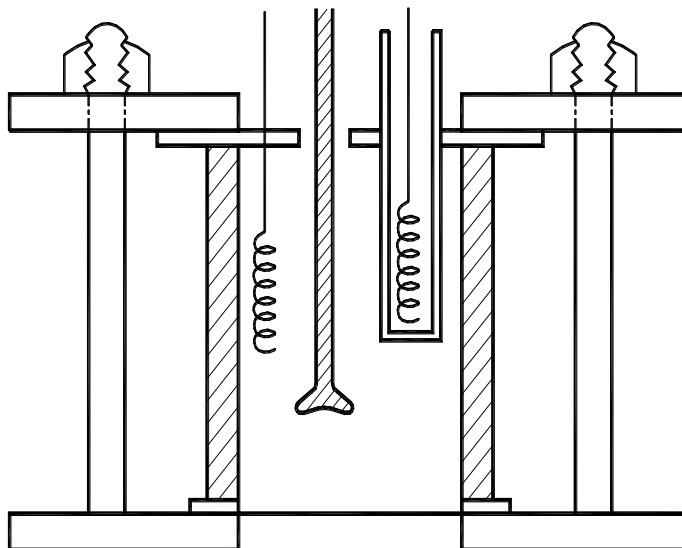


**Fig. 2.5** Cylindrical glass cell for the electro-deposition of Ru [89]

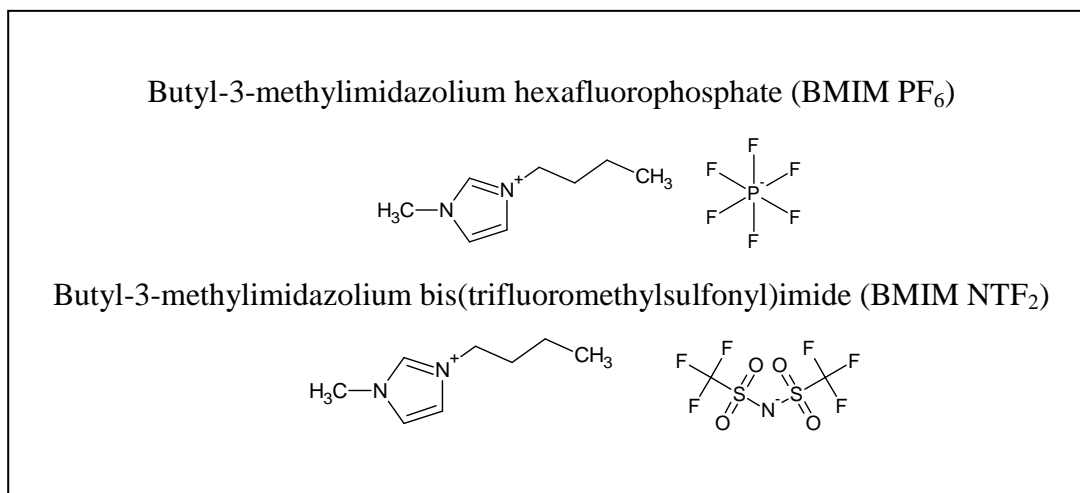


**Fig. 2.6** Structures of room temperature ionic liquids (RTILs)

## 2.6 CONCLUSIONS

The chemistry of ruthenium is extremely complex due to its various oxidation states ranging from 0 to +8. In nitric acid medium ruthenium forms more than 100 complexes depending on

the concentration of nitric acid. Several methods reported in literature for the separation of Ru have been discussed in this Chapter. In the volatilization method, ruthenium is oxidized by a strong oxidant to volatile  $\text{RuO}_4$  and subsequently recovered in NaOH, HCl and also in the presence of reducing agents. Separation of ruthenium by precipitation method is not attractive due to lack of selective reagents and in the case of nuclear industry it may not be applicable owing to external addition of foreign elements which will complicate reprocessing as well as waste management processes. Pyrochemical method of separation with lead metal can be employed for the separation of ruthenium from undissolved residue formed during the dissolution of nuclear spent fuel, which contains significant amount of platinoids. Solvent extraction is one of the industrially applicable methods of separation in which most of the extractants successfully separate Ru from nitric acid medium; however, many of the sulphur or phosphorous based extractants cannot be considered for use in nuclear industry owing to corrosion related issues. Among the ion exchange techniques and sorbents available in the literature for the separation of ruthenium, most of them are applicable to pH level solutions, in addition to their very low radiation resistance. Activated charcoal appears to be a promising sorbent for the separation of ruthenium from radioactive waste solutions. As electrochemical method does not require the addition of external reagents, it can be employed for the separation of Ru from HLLW either by depositing as Ru metal at the cathode or by oxidizing it to  $\text{RuO}_4$  at the anode. Quantitative separation of ruthenium by deposition from nitric acid solution is not possible, whereas it is possible to oxidise in the presence of a redox mediator. Among the redox mediators available, cerium will be the promising one since it is one of the fission products. Absorbing volatile ruthenium tetroxide in paraffin oil after oxidizing with ACN appears to be a promising and easy method for the separation of Ru from liquid waste. For the present thesis, systematic parametric studies have been carried out for

the separation of Ru by chemical volatilization using ACN as oxidizing agent and electro-oxidation method with and without redox mediator.

Though separation and recovery of Ru from the nuclear waste appears to be promising, challenges do exist in recovery and usage of recovered PGMs. As the flowsheets of PUREX and other processes in Back end fuel cycle are well established, introducing any new process and modifying the existing flowsheet must be supported with well-documented laboratory, pilot and industrial scale research and development. Another major challenge is the extremely complex solution chemistry of ruthenium in HLLW. These challenges need to be addressed for the successful development and implementation of any method or process aimed at the recovery of fission produced ruthenium.

## 2.7 REFERENCES

1. Ache, H.J., Baestle, L.H., Bush, R.P., Nechaev, A.F., Popik, V.P., Ying, Y., Feasibility study of separation and utilization of Ru, Rh and Pd from high level waste. Technical Reports Series - No. 308, IAEA, Vienna, **1989**
2. Holgye, Z., *J. Radioanal. Nucl. Chem. Lett.*, 117 (**1987**) 353
3. Holgye, Z., Krivanek, M., *J. Radioanal. Chem.*, 42 (**1978**) 133
4. Holgye, Z., *Radiochem. Radioanal. Lett.*, 37 (**1979**) 101
5. Ayabe, T., Tatsugae, R., *Chem. Abstr.*, 110, No.143304c, **1989**
6. Kobayashi, T., *Chem. Abstr.*, 110, No. 103732j, **1989**
7. Ayabe, T., Tatsugae, R., *Chem. Abstr.*, 110, No.139105W, **1989**
8. Motojima, K., *J. Nucl. Sci. Technol.*, 26 (**1989**) 358
9. Grehl, M., Meyer, H., Schafer, D., U S Patent, No. 6475448B2, **2002**
10. Haas, M., Weuta, P., Wolf, A., Schlueter, OF-K., U S Patent, No. 0287282A1, **2008**

11. Meyer, H., Grehl, M., Nowotny, C., Stettner, M., Kralik, J., U.S. Patent, No. 0191107A1, **2009**.
12. Isa, I., Takahashi, T., U S Patent, No. 4,002,470, **1977**
13. DePablo, R.S., Harrington, D.E., Bramstedt, W.R., U S Patent, No. 4132569, **1979**
14. Singh, K., Sonar N.L., Valsala, T.P., Kulkarni, Y., Vincent, T., Kumar, A., Proc. DAE-BRNS biennial Internatl. Symp. on 'Emerging trends in separation science and technology (SESTEC-2012)', Mumbai (**2012**) 116
15. Bogl, W., Bachmann, K., *Radiochem. Radioanal. Lett.*, 17 (**1974**) 239
16. Bogl, W., Buttner, K., Bachmann, K., *Radiochem. Radioanal. Lett.*, 18 (**1974**) 315
17. Tatschob, V., Bachmann, K., *J. Inorg. Nucl. Chem.*, 41 (**1979**) 141
18. Clark, W. E., Godbee, H.W., U S Patent, No. 3120493, **1964**
19. Sato, T. *J. Radioanal. Nucl. Chem.*, 129 (**1989**) 77
20. Kubota, K., Yamana, H., Takeda, S., U S Patent, No. 4526658, **1985**
21. Wallace, R.M., Aiken, S.C., U S Patent, No. 3208819, **1965**
22. Beamish, F.E., *Talanta*, 13 (**1966**) 773
23. Moore, R.L., *J. Inorg. Nucl. Chem.*, 14 (**1960**) 38
24. Gandon, R., Boust, D., Bedue, O., *Radiochim. Acta*, 61 (**1993**) 41
25. Samanta, S.K., Theyyanni, T.K., Report BARC-E/012, **1994**
26. Kore, S.G., Prasad, V., Singh, U.S., Yeotikar, R.G., Mishra, A., Ali, S.S., 12th Annual Conf. Ind. Nucl. Soc. (INSAC-2001), Indore, **2001**
27. Sonar, N.L., Mishra, P.K., Kore, S.G., Sonavane, M.S., Kulkarni, Y., Raj, K., Manchanda, V.K., *Sep. Sci. Technol.*, 44 (**2009**) 506

28. Thiers, R., Graydon, W., Beamish, F.E, *Anal. Chem.*, 20 (1948) 831
29. Allan, W.J., Beamish, F.E., *Anal. Chem.*, 24 (1952) 1569
30. Diamantatos, A., *Anal. Chim. Acta*, 91 (1997) 281
31. Naito, K., Matsui, T., Tanaka, Y., *J. Nucl. Sci. Technol.*, 23 (1986) 540
32. Jensen, G.A., *Nucl. Technol.*, 65 (1984) 305
33. Matsui, T., Hoshikawa, T., Naito, K., *Solid State Ionics*, 40 (1990) 993
34. Matsui, T., Naito, K., *J. Nucl. Sci. Technol.*, 26 (1989) 1102
35. Naito, K., Matsui, T., Nakahira, H., Kitagawa, M., Okada, H., *J. Nucl. Mater.*, 184 (1991) 30
36. Arai, K., Ayabe, M., Hatta, M., Myochin, M., Wada, Y., Takahashi, T., *Prog. Nucl. Energy*, 29 (1995) 235
37. Hyman, H.H., Leader, G.R., U S Patent, No. 2894816, 1959
38. Fitoussi, R., Lours, S., Musikas, C., U S Patent, No. 4282112, 1981
39. Weng, F., Qiyuan, C., Huiping, H., Chunlin, N., Qinqin, Z., *Sep. Purif. Technol.*, 80 (2011) 52
40. Valenzuela, F., Fonseca, C., Basualto, C., Correa, O., Tapia, C., Sapag, J., *Miner. Eng.*, 18 (2005) 33
41. Kiba, T., Miura, A., Sugioka, Y., *Bull. Chem. Soc. Jpn.*, 36 (1963) 663
42. Fieberg, M.M., Edwards, R.I., U S Patent, No. 4105442, 1978
43. Lingen, J., Shiyan, L., Cheng, L.G., Jingxuan, S., Manchang, R., *Solvent Extract. Ion Exchange*, 7 (1989) 613

44. Dhami, P.S., Naik, P. W., Jagasia, P., Thomas, G., Tripathi, S. C., Gandhi, P. M., Janardan, P., Proc. DAE-BRNS biennial Internatl. Symp. on 'Emerging trends in separation science and technology (SESTEC-2012)', Mumbai (2012) 97
45. Gaikwad, A. P., Mahamuni, S. V., Pawar, B. G., Mandhare, A. M., Mane, C. P., Kolekar, S. S., Anise, M. A., Proc. DAE-BRNS biennial Internatl. Symp. on 'Emerging trends in separation science and technology (SESTEC-2012)', Mumbai (2012) 133
46. Healy, T.V., U S Patent, No. 3326811, 1967
47. Grummitt, W.E., Hardwick, W.H., U S Patent, No. 2967209, 1961
48. Epperson, C.E., Landolt, R.R., Kessler, W.V., *Anal. Chem.*, 48 (1976) 979
49. Marczenko, Z., Balcerzak, M., *Anal. Chim. Acta.*, 109 (1979) 123
50. Jaya, S., Ramakrishna, T.V., *Bull. Chem. Soc. Jpn.*, 57 (1984) 267
51. Al – Bazi, S.J., Chow, A., *Anal. Chem. Acta.*, 157 (1984) 83
52. Al – Bazi, S.J., Chow, A., *Talanta*, 31 (1984) 189
53. Tagashira, S., Murakami, Y., Nishiyama, M., Harada, N., Sasaki, Y., *Bull. Chem. Soc. Jpn.*, 69 (1996) 3195
54. Shetty, S.S., Turel, Z.R., *J. Radioanal. Nucl. Chem. Lett.*, 135 (1989) 51
55. Bahrainwala, T.M., Turel, Z.R., *J. Radioanal. Nucl. Chem.*, 237 (1998) 175
56. Mhaske, A., Dhadke, P., *Hydrometall.*, 63 (2002) 207
57. Dskovic, V., Vojkovic, V., Antonic, T., *Croat Chem. Acta*, 78 (2005) 617
58. Kedari, C.S., Coll, M.T., Fortuny, A., Goralska, E., Sastre, A.M., *Sep. Sci. Technol.*, 40 (2005) 1927

59. Panigrahi, S., Dash, T., Sarangi, K., Nathsarma, K.C., Chemical engineering in nuclear technology series-1, Natl. Seminar on solvent extraction (CHEMENT-2009), Kalpakkam (2009) C-5
60. Kedari, C.S., Coll, M.T., Fortuny, A., Goralska, E., Sastre, A.M., *Hydrometall.*, 82 (2006) 40
61. Goralska, E., Coll, M.T., Fortuny, A., Kedari, C.S., Sastre, A.M., *Solvent Extract. Ion Exchange*, 25 (2007) 65.
62. Kartil, J., Menel, J., Moravec, A., *Chem. Abstr.*, 80, 90008n, 1974
63. Wasey, W., Bansal, R.K., Satake, M., Puri, B.K., *Bull. Chem. Soc. Jpn.*, 56 (1983) 3603
64. Sharma, R.K., *Bull. Chem. Soc. Jpn.*, 66 (1996) 1084
65. El-Shahawi, M.S., Almebdi, M., *J. Chromatogr. A*, 697 (1995) 185
66. Polak, P., *Radiochim. Acta*, 24 (1977) 193
67. Lee, S.H., Chung, H., *Sep. Sci. Technol.*, 38 (2003) 3459
68. Liu, Q.P., Wang, Y.C., Liu, J.C., Cheng, J.K., *Anal. Sci.*, 9 (1993) 523
69. Zhang, X.S., Shi, L., Zhang, L., You, L.F., Lin, C.S., *J. Chromatogr. A*, 789 (1997) 485
70. Singh, N., Mehrotra, M., Rastogi, K., Srivastava, T.N., *Analyst*, 110 (1985) 71
71. Floreancig, A., Nicolas, F., U S Patent, No. 5219540, 1993
72. Mimura, H., Ohta, H., Akiba, K., Onodera, Y., *J. Nucl. Sci. Technol.*, 38 (2001) 342.
73. Mimura, H., Ohta, H., Akiba, K., Onodera, Y., *J. Nucl. Sci. Technol.*, 39 (2002) 655
74. Schmuckler, G., U S Patent, No. 4885143, 1988

75. Grant, R.A., U S Patent, No. 7163570B2, **2007**
76. Sonar, N.L., Sonavane, M.S., Valsala, T.P., Kulkarni, Y., Raj, K., Manchanda, V.K.,  
*Sep. Sci. Technol.*, 44 (**2009**) 3753
77. Siddhanta, S., Das, H.R., *Talanta*, 32 (**1985**) 457
78. Akatsu, E., Yonezawa, C., Motojima, K., *J. Nucl. Energy*, 6 (**1979**) 399
79. Dey, P., Bag, M., Basu, S., Proc. DAE-BRNS biennial Internatl. Symp. on 'Emerging trends in separation science and technology (SESTEC-2012)', Mumbai (**2012**) 45
80. Motoki, R., Motoishi, S., Izumo, M., Onoma, K., Sato, T., U S Patent, No. 4622176, **1986**
81. Tikhomirova, T.I., Fadeeva, V.I., Kudryavtsev, G.V., *Anal. Chim. Acta*, 257 (**1992**) 109
82. Berak, L., Uher, E., Marhol, M., *Atomic Energy Rev.*, 13 (**1975**) 325
83. Blum, J.M., Jaumier, J.J., Verot, J.L., *Chem. Abstr.*, 79, No. 1395393g, **1973**
84. Yoshio, K., Shozo, I., *Chem. Abstr.*, 111, No. 63499a, **1989**
85. Hajima, N., Teruhiko, I., *Chem. Abstr.*, 111, No. 10602x, **1989**
86. Pankaj, S., Bhardwaj, D., Renu, T., Radha, T., *J. Radioanal. Nucl. Chem.*, 274 (**2007**) 281
87. Foos, J., Lemaire, M., Guy, A., Draye, M., Chomel, R., Deloge, A., U S Patent, No. 5417942, **1995**
88. Lietzke, M.H., Griess, J.C. Jr, *J. Electrochem. Soc.*, 100 (**1953**) 434
89. Kobayashi, Y., Yamatera, H., Okuno, H., *Bull. Chem. Soc. Jpn.*, 38 (**1965**) 1911
90. Motojima, K., *J. Nucl. Sci. Technol.*, 27 (**1990**) 262

91. Yoneya, M., Kawamura, K., Torata, S.I., Takahashi, T., U S Patent, No. 5437847,  
**1995**
92. Mousset, F., Bedioui, F., Eysseric, C., *Electrochem. Commun.*, 6 (**2004**) 351
93. Jayakumar, M., Venkatesan, K.A., Srinivasan, T.G., Vasudeva, Rao, P.R.,  
*Electrochim. Acta*, 54 (**2009**) 6747

---

## 3. EXPERIMENTAL

---

This Chapter briefly describes the methods, materials and other experimental techniques used to generate data for the thesis work. The principles involved in electroanalytical techniques such as cyclic voltammetry, chronoamperometry and chronopotentiometry have been discussed. The spectroscopic techniques UV-Visible spectrophotometry and inductively coupled plasma – optical emission spectroscopy (ICP-OES) used for quantitative determination of ruthenium are described. Other experimental techniques such as X-ray photoelectron spectroscopy (XPS), X-ray diffraction (XRD), Fourier transform infrared spectroscopy (FTIR) and Transmission electron microscopy (TEM) are briefly discussed.

### 3.1 MATERIALS AND CHEMICALS

#### 3.1.1 Chemicals

All the chemicals used for experimental work were of analytical grade and procured from the following companies:

**M/s. Arora Matthey, Kolkata:** Ruthenium(III) chloride ( $\text{RuCl}_3 \cdot 3\text{H}_2\text{O}$ ) powder, Ruthenium nitrosyl nitrate (1.7% W/V) in 9 M nitric acid and Silver nitrate.

**M/s. Loba Chemie, Mumbai:** Ammonium ceric nitrate ( $(\text{NH}_4)_2\text{Ce}(\text{NO}_3)_6$ , Assay: 98 %); Hydrogen peroxide( $\text{H}_2\text{O}_2$ ), Assay 30%

**M/s. SD fine chem. Ltd, Mumbai:** Cerium (III) nitrate hexahydrate, Assay: 90%

**Merk, Germany:** 1 10-phenanthroline, Assay: 99.5%, Water content: 8.5-10%; Hydroxylammoniumchloride, Assay: 99%, Water content: 5%

**Jiangsu Huaxi International Trade Co. Ltd. China:** Ethanol, Assay: 99.9%

**Hi-Pure fine chem. Industries, Chennai:** Sodium Hydroxide, Assay: 99%

All other nitrate salts and oxides used for the preparation of simulated high level liquid waste (SHLLW) were procured from M/s. Alfa Aesar, UK, Merck, Germany, Sigma Aldrich, USA, and Strem Chemicals, USA. Nitric acid (AR Grade; Assay: 69 %) used throughout this study was supplied by M/s. Fischer Chemicals Ltd, Chennai.

### **3.1.2 Materials**

Platinum, Glassy carbon and Gold working electrodes and Ag/AgCl reference electrode were procured from M/s. Metrohm India Pvt Ltd, Chennai. Platinum mesh electrodes of different surface area used for electro-oxidation experiments were supplied by M/s. Ravindra Heraeus Ltd, Udaipur. One end closed, reaction bonded silicon nitride (RBSN) diaphragm tube used in electro-oxidation study was fabricated by CGCRI, Kolkata.

## **3.2 INSTRUMENTATION AND FACILITIES**

### **3.2.1 Electrochemical System**

The electrochemical studies cyclic voltammetry, chronocoulometry and chrono amperometry were carried out using Autolab (PGSTAT- 030; procured from M/s. Eco-Chemie, the Netherlands) equipped with an IF 030 interface. General Purpose Electrochemical (GPES) System Version 4.9 installed in a personal computer was used for data acquisition and analysis. Electro-oxidation studies with two electrode system were performed by applying either constant current or constant potential using regulated DC power supply DSC20-50E (supplied by M/s. AMKET, USA).

### **3.2.2 UV-Visible Spectrophotometer**

Quantitative analysis of pure ruthenium containing solutions in nitric acid media was carried out from the absorption spectra recorded using Chemito Instruments Pvt Ltd - UV 2600 double beam Spectrophotometer with the wave length range 190 -1100 nm. Quartz cuvettes of path length 1 cm were used for all analysis. Ruthenium concentration in pure  $\text{Ru}(\text{NO}_3)_3$

and  $[\text{RuNO}]^{3+}$  solution was estimated spectrophotometrically using 1-10, Phenanthroline as chromogenic reagent [1]. However this method of analysis of ruthenium was not applicable in case of SHLLW solution due to interference of other metal. Speciation of various  $[\text{RuNO}]^{3+}$  complexes was carried out using this technique.

### 3.2.3 XRD

X-ray diffraction (XRD) analysis was carried out using INEX-XRG-3000 diffractometer with a curved position sensitive detector using  $\text{Cu K}\alpha 1$  (0.15406 nm) radiation with grazing angle ( $\omega$ ) as  $5^\circ$ .

### 3.2.4 XPS

X-ray photo electron spectroscopic (XPS) measurements were carried out using SPECS make (Germany) spectrometer.  $\text{Al K}\alpha$  was used as the X-ray source at 1486.71 eV. The anode was operated at a voltage of 13 kV and source power level was set to 300 W. An  $\text{Ar}^+$  ion source is also provided for sputter-etch cleaning of specimens. It was operated at 5 kV and 10  $\mu\text{A}$ . The system sputters approximately at the rate of  $10\text{\AA}^2/\text{min}$  for standard silver sample. Spectra were collected using the PHOIBOS 150 MCD-9 analyzer with a resolution of 0.6 eV at the pass energy of 10 eV. The spectrometer was calibrated using a standard silver sample for the  $\text{Ag 3d } 5/2$  peak at 368.3 eV. Data were processed by Specslab2 software. The binding energy of C 1s transition from adventitious C at 285 eV was used as the reference to account for any charging of the sample and the peak positions were compared with standard values for identification of different elements and their oxidation states.

### 3.2.5 TEM

Microstructural analysis was carried out with LIBRA 200FE, a high resolution transmission electron microscope (HRTEM) operated at 200 kV with a field emission electron source and equipped with high angle annular dark field detector and in-column Omega filter for

spectroscopic analysis. Specimen for TEM analysis was prepared by the standard method for powder TEM specimen preparation; ultrasonication of the sample powder in ethanol, followed by a drop placed on carbon coated Cu TEM grid and dried for evaporating the solvent. Electron energy loss spectra (EELS) were acquired using the in-column Omega filter in the TEM (Libra 200FE) and the energy resolution of EELS was 0.7 eV.

### **3.2.6 FTIR**

In the thesis work, Fourier Transform – Infra red spectra were recorded from 4000  $\text{cm}^{-1}$  to 500  $\text{cm}^{-1}$  using the FTIR spectrometer (ABB make model) MB3000 with a DTGS (deuterated triglycine sulphate) detector. Liquid samples were analysed using horizontal ATR (Attenuated Total Reflectance) accessory. Horizon MB Software was employed to analyze the spectra. All measurements were made using 32 scans and 4  $\text{cm}^{-1}$  resolution, proper baseline was selected for each peak.

### **3.2.7 ICP-OES**

The amount of ruthenium in acidic aqueous phase was determined by Optical emission spectroscopic analysis using the ICP-OES (Jobin Yvon, France) and the standards were produced by MBH analytical limited.

Atomic spectrometry is the commonly used technique for the determination of trace concentrations of elements in the sample. Elements in solution can be detected and quantified by means of optical emission spectrometry with inductively coupled plasma (ICP-OES). Because of its high sensitivity, ability to perform rapid and simultaneous multi-element analysis, low detection limit and free from chemical interference, optical emission spectroscopy is the principal tool of analysis at trace levels [2]. The solution under analysis is nebulised and the aerosol thus formed is transported to a high-frequency plasma (8,000–10,000°C) in which the constituents of the sample solution are atomized, ionized and excited

to higher energy states to produce characteristic optical emissions. The characteristic emission lines of the atoms and ions are dispersed by a monochromator or polychromator and the intensity of the lines is recorded in a photo multiplier tube (PMT) detector. The block diagram of a typical ICP-OES instrument is shown in Fig. 3.1[3]. The intensity of the spectral lines is proportional to the concentrations of analytes in the aqueous sample; i.e. quantification by means of external calibration with a linear regression line is possible. The highest concentration of the standard for a calibration should be greater than the lowest concentration by a factor of 10-20. The linearity within the working range should be verified. The coefficient of correlation 'r' should be  $> 0.995$ . The wavelengths are selected in accordance with the required limit of detection and the possibility of interference by other elements present in the sample solution. In determining the concentration of Ru, the wavelength of spectral line selected was 245.66 nm and the lowest point of calibration graph was 0.4 ppm since at this concentration the confidence level was more. Standard solutions prepared for generating calibration graph were single element standard for pure ruthenium solution and multi-element standard for SHLLW solution. 1000 ppm of MBH standard solution of Ru was diluted with required volume to prepare each 10 ml of 0.4, 1, 2, 4, 10 and 20 ppm of standard solutions for calibration. Experiments were initiated by generating calibration graphs by plotting intensity against known concentration Ru standard and stored in the computer. A typical calibration graph for Ru in nitric acid medium, showing a linear relationship between the intensity (as detector count) and concentration is given in Fig. 3.2. Using this calibration graph the unknown concentrations of Ru in test samples were determined. The software used for analysis was Jobin Yvon HORIBA – ICP ANALYST version 5.2. All experiments were carried out as per the operating conditions listed in Table 3.1.

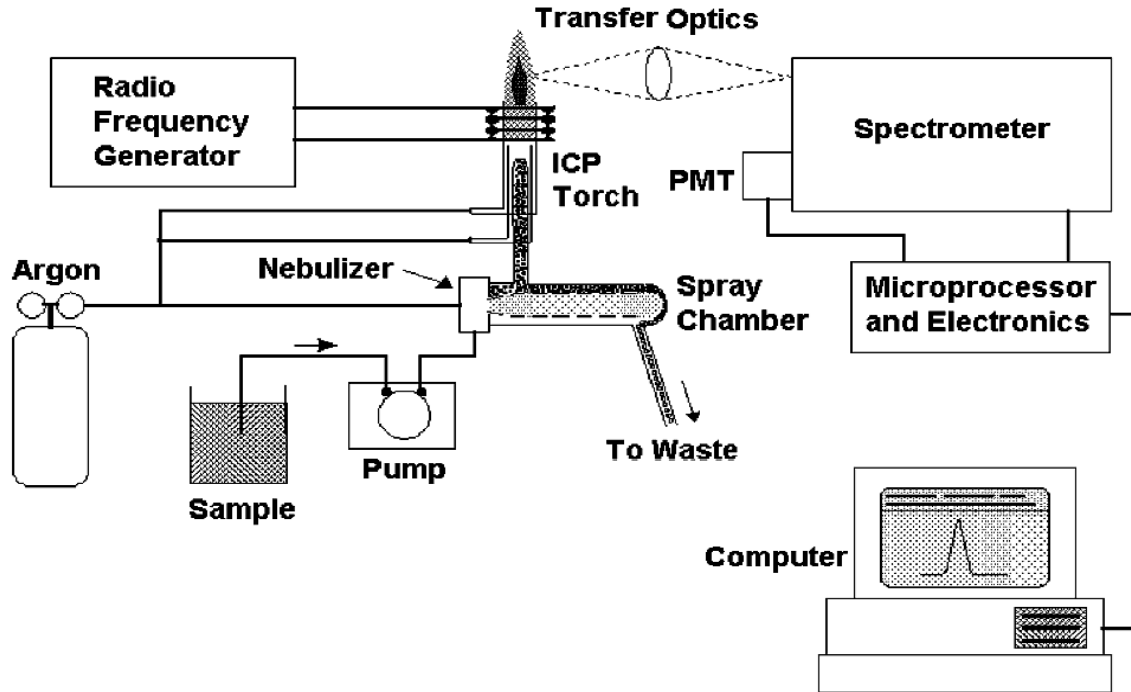


Fig. 3.1 Block diagram of a typical ICP – OES instrument [2]

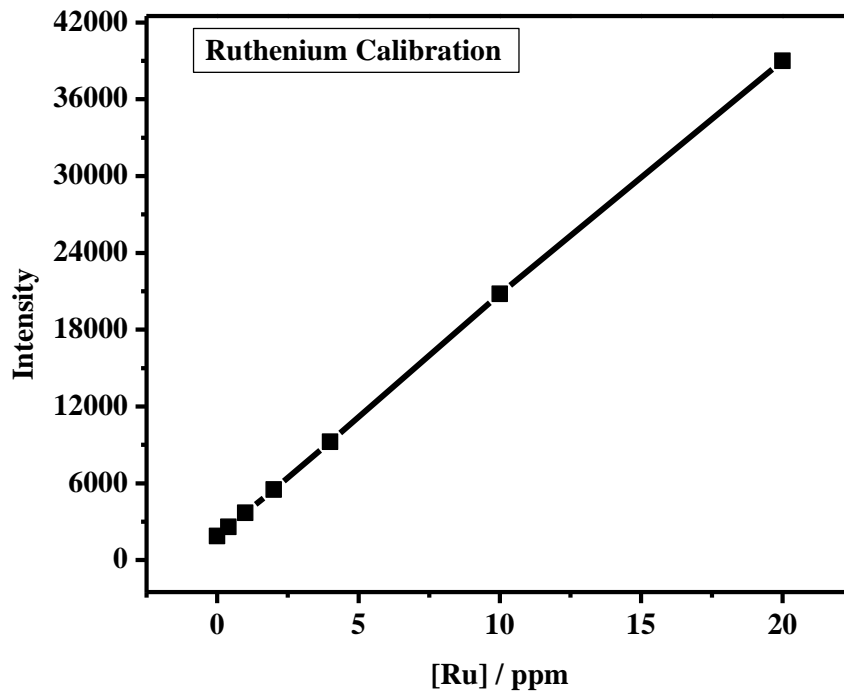


Fig. 3.2 Calibration graph for Ruthenium

**Table 3. 1** Operating conditions and description of ICP-OES instrument

RF generator	40.68 MHz
RF incident power	1000 W
Inner dia of torch alumina injector	2 mm
Nebulizer argon gas flow rate	1 litre/min
Argon gas flow rate	12 litre/min (plasma)
Signal measurement mode	Peak jump
Spray chamber	Cyclonic
Nebulizer type	Pneumatic
Pump	Peristaltic, three channel
Sample uptake flow rate	1 ml/min
Polychromator	Paschen-Runge system
Resolution	0.003 nm
Detector	Photomultiplier tube

### 3.3 PREPARATION OF SOLUTIONS

#### 3.3.1 Ruthenium Nitrosyl Solution

Stock solutions of different concentrations of ruthenium nitrosyl nitrate in nitric acid were prepared by dissolving the required quantity of ruthenium nitrosyl nitrate stock in appropriate nitric acid concentrations.

#### 3.3.2 Simulated HLLW Solution

A 27 component, synthetic high level liquid waste solution simulated with fission and corrosion product elements in 4 M nitric acid was prepared by mimicking the reprocessed waste of FBTR fuel with a burn-up of 150 GWd/ton and after a cooling period of 1 year. The chemical form of the elements and their concentration in the simulated waste solution are listed in Table 3.2. The prepared waste solution was diluted to 6.62 times to bring down the concentration of ruthenium to 160 ppm (the concentration of Ru envisaged in the first cycle raffinate) and used throughout the experiments at various concentrations of HNO<sub>3</sub> ranging from 4 to 1 M.

**Table. 3.2** The chemical composition of fission and corrosion product elements in simulated waste solution in 4M HNO<sub>3</sub>

Element	Concentration of element (g/L)	Chemical form used	Quantity (g/L)
Ag <sup>a</sup>	0.097	AgNO <sub>3</sub>	0.153
Ba	0.485	Ba(NO <sub>3</sub> ) <sub>2</sub>	0.922
Cd	0.046	Cd(NO <sub>3</sub> ) <sub>2</sub>	0.097
Ce	0.769	Ce(NO <sub>3</sub> ) <sub>3</sub> ·6H <sub>2</sub> O	2.383
Cs	1.405	CsNO <sub>3</sub>	2.061
Dy	0.0009	Dy(NO <sub>3</sub> ) <sub>3</sub> ·5H <sub>2</sub> O	0.0024
Eu	0.051	Eu(NO <sub>3</sub> ) <sub>3</sub> ·6H <sub>2</sub> O	0.151
Gd	0.032	Gd(NO <sub>3</sub> ) <sub>3</sub> ·6H <sub>2</sub> O	0.091
In	0.0042	In(NO <sub>3</sub> ) <sub>3</sub> ·6H <sub>2</sub> O	0.012
La	0.418	La(NO <sub>3</sub> ) <sub>3</sub> ·6H <sub>2</sub> O	1.300
Mo	1.115	(NH <sub>4</sub> ) <sub>6</sub> Mo <sub>7</sub> O <sub>27</sub> ·6H <sub>2</sub> O	2.052
Nb	0.0006	Nb <sub>2</sub> O <sub>5</sub>	0.001
Nd	1.186	Nd <sub>2</sub> O <sub>3</sub>	1.383
Pd	1.070	Pd(NO <sub>3</sub> ) <sub>2</sub>	2.317
Pr	0.410	Pr <sub>2</sub> O <sub>3</sub>	0.479
Rb	0.070	RbNO <sub>3</sub>	0.121
Ru	1.086	RuNO(NO <sub>3</sub> ) <sub>3</sub> ·(H <sub>2</sub> O) <sub>2</sub>	63.88 ml (1.7 % Ru)
Sb	0.017	Sb <sub>2</sub> O <sub>3</sub>	0.0204
Sm	0.342	Sm(NO <sub>3</sub> ) <sub>3</sub> ·6H <sub>2</sub> O	1.010
Sr	0.146	Sr(NO <sub>3</sub> ) <sub>2</sub>	0.352
Te	0.160	TeH <sub>6</sub> O <sub>3</sub>	0.287
Y	0.084	Y(NO <sub>3</sub> ) <sub>3</sub> ·6H <sub>2</sub> O	0.364
Zr	0.900	ZrO(NO <sub>3</sub> ) <sub>3</sub> ·9H <sub>2</sub> O	2.28
Fe	0.084	Fe powder	0.084
Ca	0.637	Ca(NO <sub>3</sub> ) <sub>2</sub> ·4 H <sub>2</sub> O	3.69
Ni	0.026	Ni(NO <sub>3</sub> ) <sub>2</sub> ·6H <sub>2</sub> O	0.129
Al	0.062	Al(NO <sub>3</sub> ) <sub>3</sub> ·9H <sub>2</sub> O	0.862

<sup>a</sup>Though Ag is not a fission product, it is included in the simulated waste as it serves as a mediated redox catalyst in the electro-oxidative dissolution of Pu-rich oxide fuels

### 3.3.3 Ammonium Cerium Nitrate Solution

Ammonium cerium nitrate solution (1M) was prepared by dissolving the salt in appropriate concentrations of nitric acid and diluting to required concentrations after standardizing the prepared solution by conducting potentiometric titration against standard ferrous sulphate.

### 3.3.4 Nitric Acid Solutions

Nitric acid of different concentrations were prepared by diluting the concentrated acid with millipore water and the concentrations were estimated by titrimetry against sodium hydroxide base in the presence of phenolphthalein indicator.

## 3.4 THEORY OF ELECTROANALYTICAL TECHNIQUES

Electroanalytical techniques are unique tools to investigate several chemical, physical and biological systems by measuring the potential and/or current in an electrochemical cell and detailed discussions on the fundamental aspects and applications of these techniques are covered in standard textbooks [4-9]. A brief summary of the electroanalytical techniques with relevance to the present study is discussed below.

The species that responds to the applied potential or current is known as electroactive species. Electrochemical response of an electroactive species is dependent on the mode of mass transport. The three types of mass transport are (1) diffusion, (2) migration and (3) convection. Conducting the experiments under quiescent conditions eliminate the convection mode of transport. Adding large excess of an inert supporting electrolyte eliminates the migration mode of transport. Thus, the essential mode of mass transfer is made to occur only by diffusion of electroactive species. The kinetic rate of an electrochemical reaction is controlled by three processes, namely (a) Diffusion rates of the oxidized and reduced species, (b) The rate of heterogeneous charge transfer across the electrode/electrolyte interface and (c) The rates of chemical reactions coupled with charge transfer [9]. These processes dictate the

shape of the electrochemical response for a particular electrochemical system or cell under investigation.

The electroanalytical techniques are classified into three categories: potentiometry (where the difference in electrode potentials is measured), coulometry (cell's current is measured over time) and voltammetry (the cell's current is measured while actively altering the potential). Voltammetric techniques are among the most commonly used electrochemical transient techniques to study the behaviour of the analyte at an electrode-electrolyte interface. The voltammetric techniques are broadly classified as potentiostatic and galvanostatic techniques. In potentiostatic technique the potential of the system is controlled and the response in the form of current is measured and in galvanostatic technique the current of the system is controlled and the potential response is measured. The potential of the system (working electrode against a standard reference electrode) can be varied linearly with time (scan or sweep methods) or it can be varied step wise incremental with time (step method). Voltammetric methods such as cyclic voltammetry and linear sweep voltammetry are sweep techniques (Section 3.4.1) and chronomethods (Section 3.4.2) are step techniques.

### **3.4.1 Cyclic Voltammetry**

Cyclic voltammetry (CV), although one of the more complex electrochemical techniques, is very frequently used because it offers a wealth of experimental information and insight into both the kinetic and thermodynamic details of many chemical systems [4] It is the most versatile electroanalytical technique for the study of electroactive species [10].

CV is one of the most widely used forms and it is useful to obtain information about the redox potential and electrochemical reaction (e.g. the chemical rate constant) of analyte solutions. The voltage is swept between two values at a fixed rate and when the voltage reaches  $V_2$  the scan is reversed and the voltage is swept back to  $V_1$ , as illustrated in Fig. 3.3.

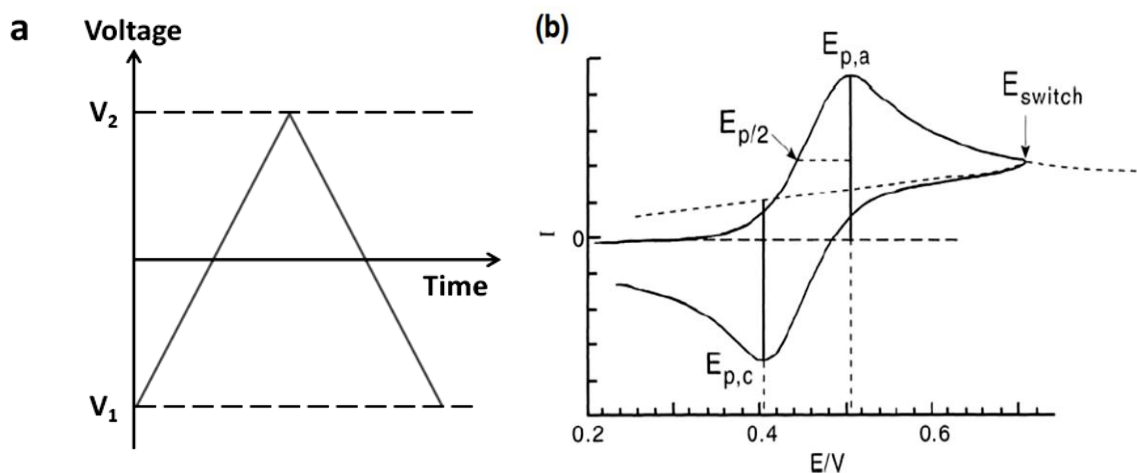


**Fig. 3.3** (a): Cyclic voltammetry waveform and (b): Typical cyclic voltammogram;  $E_{p,c}$  and  $E_{p,a}$  are cathodic and anodic peak potentials respectively.

Voltammogram is the plot of measured current against voltage. The parameters in a cyclic voltammogram include cathodic ( $E_{p,c}$ ) and anodic ( $E_{p,a}$ ) peak potentials, cathodic ( $i_{p,c}$ ) and anodic ( $i_{p,a}$ ) peak currents and half-peak potential,  $E_{p/2}$ . The convention followed in this thesis is, cathodic current is negative and anodic current is positive and plotted to the left and right, respectively.

In an electrochemical redox system, two parameters controlling the overall rate of the reaction are the charge transfer at the electrode/electrolyte interface and the mass transfer from the bulk of the solution to the electrode surface. Based on these parameters, redox systems are broadly classified into reversible, irreversible and quasi-reversible processes. Comprehensive analysis of the cyclic voltammetric results reveal the reversibility of the electrochemical processes and the details are discussed below [8, 11-12].

(i) *Reversible System*: This system obeys Nernst's equation and rate of the electrochemical process is controlled by diffusion (mass transfer) and not by charge transfer kinetics; hence, diffusion is the rate controlling step. The key criterion for a reversible charge transfer process is that  $E_p$  is independent of scan rate ( $\nu$ ) and the difference between  $E_{p,c}$  and  $E_{p,a}$  is close to

the value of  $2.3 RT/nF$  and is also independent of scan rate. The ratio of  $i_{p,a}$  and  $i_{p,c}$  is unity and is independent of  $\nu$ ; the wave shape is also independent of scan rate. In a reversible system, if both the reactant and product are soluble-soluble, then the relation between the peak current and the scan rate is given by *Randles-Sevick* equation (Eq. 3.1).

$$i_p = 0.4463 nFC_0 A \nu^{1/2} D_0^{1/2} \left( \frac{nF}{RT} \right)^{1/2} \quad (3.1)$$

$$\left| E_p - E_{p/2} \right| = 2.2 \frac{RT}{nF} \quad (3.2)$$

where,  $n$  is the number of electrons involved in the charge transfer reaction,  $F$  is the Faraday constant,  $A$  is area of the electrode ( $\text{cm}^2$ ),  $C_0$  is the bulk concentration of electroactive species ( $\text{mol.cm}^{-3}$ ),  $R$  is the gas constant,  $T$  is the absolute temperature (K),  $\nu$  is the scan rate ( $\text{V.s}^{-1}$ ) and  $D_0$  is the diffusion coefficient ( $\text{cm}^2.\text{s}^{-1}$ ) of the electroactive substance.

(ii) *Irreversible System*: In this system, a non-Nernstian path is totally followed and the rate of the electrochemical process is controlled mostly by charge transfer kinetics. The main criterion of the irreversible charge transfer kinetics is the shift in the peak potential with scan rate. For instance, the cathodic peak potential shifts towards more negative potentials with increase in scan rate. The relation between the peak current and diffusion coefficient for an irreversible system is given by *Delahay* equation (Eq. 3.3).

$$i_{p,c} = 0.4958 nFAC_0 \left( \frac{\alpha nFD_0}{RT} \right)^{1/2} \quad (3.3)$$

$$\Delta E_{p,c} = \frac{1.15RT}{\alpha n_\alpha F} \quad (3.4)$$

where  $\Delta E_p^c$  is the shift in peak potential ( $E_p^c$ ) for increase in scan rate by 10 times.

In irreversible process, the peak separation ( $E_p^c - E_p^a$ ) is very large and sometimes the reverse peak (oxidation peak) cannot be seen in the scan reversal of the cyclic voltammogram and also the wave shape is determined by  $\alpha$  and is independent of scan rate. For the irreversible process the following equations can be used to deduce the important parameters using cyclic voltammetry

$$\left| E_p^c - E_p^a \right| = \frac{1.857RT}{\alpha n_\alpha F} \quad (3.5)$$

$\alpha$  - the charge transfer coefficient, is the measure of the symmetry of the energy barrier and its value  $0.1 \geq \alpha \leq 0.9$ .

(iii) *Quasi-reversible System*: In quasi-reversible processes the rate of the electrochemical reaction is a mixed control of both diffusion and charge transfer kinetics. In cyclic voltammetry, the peak potential shifts with scan rate and the peak shape visually broadens as scan rate is increased. If the difference between the cathodic and anodic peak potentials ( $\Delta E_p$ ) increases with scan rate and the average of the peak potentials ( $(E_{p,a} + E_{p,c}) / 2$ ) is constant at different scan rates, then the process could be quasi-reversible.

The heterogeneous charge transfer coefficient,  $k_s$ , can be obtained by using Eq. (3.6), which was proposed by Klingler and Kochi [8, 13].

$$k_S = 2.18 \left[ D_0 (\alpha n_\alpha) \frac{vF}{RT} \right]^{1/2} \exp \left[ \frac{\alpha^2 nF}{RT} (E_{p,c} - E_{p,a}) \right] \quad (3.6)$$

The value of  $k_s$  can also be obtained by Nicholson's method using the following equation:

$$\psi = \frac{k_s \left( \frac{D_0}{D_R} \right)^{1/2}}{\left[ \pi D_0 \left( \frac{nF}{RT} \right) v \right]^{1/2}} \quad (3.7)$$

Depending upon the magnitude of  $k_s$ , the electrode reaction can be classified [7] as reversible when  $k_s \geq 0.3v^{1/2}$  cm.s<sup>-1</sup>, quasi-reversible when  $0.3v^{1/2} \geq k_s \geq 2 \times 10^{-5}v^{1/2}$  cm.s<sup>-1</sup> and irreversible when  $k_s \leq 2 \times 10^{-5}v^{1/2}$  cm.s<sup>-1</sup>.

### 3.4.2 Chronopotentiometry (Controlled Current Technique)

Chronopotentiometry (CP) is one of the well known voltammetric techniques, extensively used to study the electrochemical behaviour. In this technique, the controlled current will be applied between the working and counter electrodes using a galvanostat and the potential of the working electrode versus reference electrode will be monitored/measured simultaneously. The potential against time will be plotted as response and the plot is called as chronopotentiogram. Different types of controlled current techniques are available based on the type of current function applied [5, 14]. These include constant current chronopotentiometry, chronopotentiometry with linearly increasing current, current reversal chronopotentiometry and cyclic chronopotentiometry.

When the constant current is applied between the working and counter electrodes, the concentration of the analyte ion decreases and the potential of the working electrode changes. This process continues until the concentration of the analyte ion at the electrode becomes zero. Since the concentration of the analyte ion changes with time, obviously, the potential of the electrode also changes. The duration of this potential change or the concentration change of the analyte ion is called as the transition time and is denoted by  $\tau$  [15]. The transition time can also be defined as the time, when the potential transition occurs after application of the constant current [8]. The relation between the applied current and transition time was first derived by H. J. S. Sand and is given in Eq. (3.8) [8, 11].

$$i\tau^{1/2} = \frac{nFA(D_0\pi)^{1/2}C_0}{2} \quad (3.8)$$

The diffusion coefficient ( $D_0$ ) can be calculated from the experimentally determined value of  $\tau$  at a particular current, using Sand's equation.

### 3.4.3 Electro-oxidation

Electro-oxidation is an electrochemical technique wherein the species of interest is oxidized at the anode and it can be performed either by galvanostatic or potentiostatic mode. While electroanalytical techniques deal with small surface area and transient time intervals, electro-oxidation is carried out with larger electrode area for fairly longer time intervals and the electrolyte solution is mechanically mixed to enhance the mass transport of the electroactive species from the bulk of the solution to the electrode. The amount of species oxidized is governed by Faraday's First law: i.e. the amount of material evolved or deposited during electrolysis is directly proportional to the quantity of the electricity passing through the solution. The passage of 1 faraday (1F) or 96485 coulomb of electricity results in the oxidation of 1 equivalent of material (1 mole of metal in an one-electron transfer) [8]. Therefore, it is possible to estimate the amount of oxidized material using Eq. (3.9).

$$\Delta m = \frac{i\Delta t}{nF} = \frac{C}{nF} \quad (3.9)$$

where  $\Delta m$  is the number of moles of material oxidized,  $i$  is the current in ampere,  $\Delta t$  is the time in second,  $C$  is the charge passed in coulomb,  $n$  is the number of electrons transferred and  $F$  is the Faraday's constant. Equation (3.9) is obeyed only under the ideal condition, where the faradaic or current efficiency,  $\eta$  is 100 %. In most of the cases, this value is less than 100 %. Faradaic efficiency is defined by the relation,

$$\eta = \frac{\Delta m}{\Delta m^0} \times 100 \quad (3.10)$$

where  $\Delta m$  is the metal which is practically oxidized and  $\Delta m^0$  is the amount of oxidized metal predicted by Faraday's law for the passage of the Coulombic charge. Faraday's laws govern

the relationship between the coulombic charge and electrode-oxidized materials. Another important aspect of electro-oxidation is the separation percentage of the material.

$$\text{Separation \%} = \frac{[\text{Metal}]_{\text{Initial}} - [\text{Metal}]_{\text{Final}}}{[\text{Metal}]_{\text{Initial}}} \times 100 \quad (3.11)$$

In a particular electro-oxidation process, if the overall separation and the rate of oxidation are very low, the process becomes practically fruitless even if the value of  $\eta$  is  $\sim 100\%$ .

### 3.5 REFERENCES

1. Banks, C. V., O'Laughlin, J. W., *Anal. Chem.*, 29 (1957) 1412
2. Moore, G.L., Introduction to Inductively Coupled Plasma – Atomic Emission spectroscopy, Elsevier Science, Amsterdam, The Netherlands, 3<sup>rd</sup> Edition, pp. 121, 1988
3. Boss, C.B., Fredeen, K.J., Concepts, instrumentation and techniques in inductively coupled plasma optical emission spectrometry, Perkin Elmer, 2<sup>nd</sup> Edition, pp.36, 1997
4. Scholz, F., Electroanalytical methods: Guide to experiments and applications, 1<sup>st</sup> Edition, Springer, Berlin, 2005
5. MacDonald, D.D., Transient techniques in electrochemistry, Plenum Press, New York, 1977
6. Galus, Z., Chalmers, R.A., Bryce, W.A.J., Fundamentals of electrochemical analysis, 2<sup>nd</sup> Edition, Ellis Horwood, New York, 1994
7. Kissinger, P.T., Heineman, W.R., Laboratory techniques in electro-analytical chemistry, 2<sup>nd</sup> Edition, Marcell Dekker, New York, 1996
8. Bard, A.J., Faulkner, L.R., Electrochemical methods - Fundamentals and applications, 2<sup>nd</sup> Edition, Wiley, New York, 2001
9. Rossiter, B.W., Hamilton, J.F., Physical methods of chemistry: Electrochemicals methods, Vol. II, Wiley, New York, 1986

10. Kissinger, P.T., Heineman, W.R., *J. Chem. Ed.*, 60 (**1983**) 702
11. Brown, E.R., Sandifer, J.R., Physical methods of chemistry- Volume II, Electrochemical methods, Wiley, New York, **1986**
12. Bamford, C.H., Compton, R.G., Electrode kinetics – principles and methods, Volume 26, In Chemical Kinetics, Elsevier, Netherlands, **1986**
13. Klingler, R.J., Kochi, J.K., *J. Phys. Chem.*, 85 (**1981**) 1731
14. Delahay, P., New instrumental methods in electrochemistry: Theory, instrumentation and application to analytical and physical chemistry, Interscience, New York, **1954**
15. Paunovic, M., *J. Electroanal. Chem.*, 14 (**1967**) 447

---

## 4. SEPARATION OF RUTHENIUM FROM SIMULATED NUCLEAR WASTE USING NORMAL PARAFFIN HYDROCARBON

---

### 4.1 INTRODUCTION

Various techniques reported in the literature for the removal of ruthenium from high level liquid waste (HLLW) are volatilization, precipitation, solvent extraction, chromatography, sorption and electrochemical methods. A simple method for the removal of ruthenium is by making use of the high volatility of  $\text{RuO}_4$ . The principle involved in the volatilization method for the separation of Ru consists of oxidizing the ruthenium species to  $\text{RuO}_4$  vapour using strong oxidizing agents such as  $\text{KMnO}_4$ ,  $\text{K}_2\text{Cr}_2\text{O}_7$ , Ozone,  $\text{AgO}$  or by electro-oxidation and subsequently, removing the  $\text{RuO}_4$  formed as  $\text{RuO}_2$  or Ru in the presence of reducing agents like hydrazine, formaldehyde and  $\text{SO}_2$  gas. Ruthenium can also be separated as  $\text{RuO}_4^-$  or  $\text{RuO}_4^{2-}$  ions by contacting with an absorbent like NaOH and as  $\text{RuCl}_3$  in HCl medium [1-5]. Motojima [6] adopted the volatilization method for the separation of ruthenium using ammonium ceric nitrate (ACN) as the oxidizing agent. The  $\text{RuO}_4$  vapour evolved owing to the oxidation of Ru species in the aqueous phase was trapped by paraffin oil and the black coloured precipitate formed was filtered off using cellulose fiber filter paper. As Ce is one of the fission products, its use as the oxidizing agent will not make any significant change in the vitrification process. Adopting this method, complete separation of ruthenium was possible from ruthenium nitrate in 4M nitric acid in the present study and the separation was more effective with lower concentration of nitric acid and higher concentration of ACN. Motojima reported that depending on the various chemical forms of Ru present in nitric acid solutions, the percentage of removal of Ru varied and a low percentage of ruthenium was removed in the case of ruthenium nitrosyl  $[\text{RuNO}]^{3+}$  solution in 4 M nitric acid. He also observed that

addition of H<sub>2</sub>O<sub>2</sub> and subsequent heating of the ruthenium solution for longer duration enhanced the removal of ruthenium from [RuNO]<sup>3+</sup> solution. However, implementing this process in the actual plant is practically difficult.

The present Chapter deals with the attempts made to improve the separation percentage of ruthenium from [RuNO]<sup>3+</sup> solution by optimizing the process parameters in a systematic way in the oxidation of Ru species using ACN and without adding H<sub>2</sub>O<sub>2</sub>. Since ruthenium is expected to be present as ruthenium nitrosyl complex of the general formula [RuNO(NO<sub>3</sub>)<sub>x</sub>(NO<sub>2</sub>)<sub>y</sub>(OH)<sub>z</sub>(H<sub>2</sub>O)<sub>5-x-y-z</sub>]<sup>3-x-y-z</sup> in the actual HLLW [7], experiments were conducted with pure [RuNO]<sup>3+</sup> solution as well as with a synthetic non-radioactive waste solution simulated with all fission product elements to investigate the effect of different concentrations of nitric acid and ammonium ceric nitrate, temperature and ageing of the ruthenium bearing solutions on the separation of ruthenium. The black ruthenium oxide suspension formed at the interface between the organic and aqueous phases during the recovery of Ru was characterized by XRD, TEM, EELS and XPS techniques. The organic phase, normal paraffin hydrocarbon (NPH) which had been used to trap RuO<sub>4</sub> was characterized by FTIR spectroscopy before and after the separation.

## 4.2 EXPERIMENTAL

### 4.2.1 Chemicals

Standard solutions of ruthenium nitrosyl, [RuNO]<sup>3+</sup> in 0.5, 1, 2, 3 and 4 M nitric acid (ruthenium content: 160 ppm) were prepared by diluting the commercially available ruthenium nitrosyl nitrate (supplied by M/s. Arora Matthey Ltd, 1.7 % ruthenium by weight in 9 M nitric acid). Nitric acid supplied by M/s. Fischer Chemicals Ltd, Chennai (AR grade; Min. Assay: 69 – 71 %) was used in the experiments. Ruthenium nitrate solution was prepared by dissolving hydrated RuCl<sub>3</sub> (supplied by M/s. Arora Matthey Ltd) in millipore

water, adding excess (than the required ratio) of  $\text{AgNO}_3$  and filtering out the  $\text{AgCl}$  precipitate. The concentrations of Ru in ruthenium nitrate filtrate and in ruthenium nitrosyl solutions were adjusted to be 160 ppm in 4 M  $\text{HNO}_3$  since the quantity of Ru in HLLW is estimated to be about 160 ppm in the case of the waste generated from the mixed carbide fuel of FBTR at the burn-up of 150 GWd/ton and reprocessed after a cooling period of one year [8]. A solution of 1 M ammonium ceric nitrate (M/s. Loba Chemie, Assay: 98%) was prepared in nitric acid. The NPH used for the experiments had the composition of n- $\text{C}_{10}$ : 0.04 %; n- $\text{C}_{11}$ : 0.23 %; n- $\text{C}_{12}$ : 57.92 % and n- $\text{C}_{13}$ : 41.81 %.

A synthetic HLLW solution (SHLLW) simulated with fission and corrosion product elements envisaged in the reprocessed waste of the mixed carbide fuel of FBTR was prepared in 4 M  $\text{HNO}_3$ . The chemical form of the elements and their concentration used for the preparation of simulated waste solution are reported elsewhere [8] and the details are also listed in Table 3.2 of Chapter 3. The simulated waste solution prepared was diluted suitably to adjust the concentration of ruthenium to 160 ppm in 4, 3, 2 and 1 M  $\text{HNO}_3$ .

#### **4.2.2 Equipment**

Separation studies were carried out in a 15 ml centrifuge tube and the aqueous and organic phases were mixed using a vortex mixer. The amount of ruthenium in the aqueous phase before and after mixing was determined by Inductively Coupled Plasma assisted Optical Emission Spectroscopic (ICP-OES) analysis. Cellulose extraction thimble of dimensions 25×80 mm was used for filtering the black coloured ruthenium oxide suspension formed at the organic and aqueous interface. X-ray powder diffraction (XRD) analysis was carried out for phase identification of the black ruthenium based suspension formed after mixing. Infrared spectra of the organic (NPH) phase, before and after the separation experiments were recorded over the range 4000 - 650  $\text{cm}^{-1}$  using a BOMEM MB 100 FTIR spectrometer, at the

resolution of  $4 \text{ cm}^{-1}$  to find out the structural modification of NPH caused by the reaction of NPH with the strong oxidizing agent,  $\text{RuO}_4$ , produced from Ru bearing test solutions.

Analysis of the microstructure of ruthenium oxide suspension was carried out using a high resolution transmission electron microscope (HRTEM; Model: LIBRA 200FE), operated at 200 kV with a field emission electron source and equipped with high angle annular dark field detector and in-column Omega filter for spectroscopic analysis. Specimen for TEM analysis was prepared by the standard powder TEM specimen preparation method, which involved ultrasonication of the sample powder in ethanol followed by a drop placed on carbon coated Cu TEM grid and dried for evaporating the solvent. Electron energy loss spectrum (EELS) was acquired by using the in-column Omega filter in the TEM and energy resolution of the EELS spectrometer was 0.7 eV.

Using SPECS make spectrometer, X-ray photoelectron spectroscopic (XPS) measurements were carried out. Al  $K\alpha$  was used as the X-ray target at 1486.71 eV. The anode was operated at the voltage of 13 kV and source power level was set to 300 W. An (Ar+) ion source provided sputter-etch cleaning of specimens. It was operated at 5 kV and 10  $\mu\text{A}$ . The system sputters at the rate of  $10 \text{ \AA} \text{ min}^{-1}$  for standard silver sample. Spectra were collected using the PHOIBOS 150 MCD-9 analyzer with a resolution of 0.6 eV at the pass energy of 10 eV. The spectrometer was calibrated using a standard silver sample for the Ag  $3d_{5/2}$  peak at 368.3 eV. Data were processed by Specslab2 software.

### **4.2.3 Procedure for Separating Ru**

#### **4.2.3.1 Effect of the concentration of Ce(IV)**

Separation of Ru from pure  $\text{Ru}(\text{NO}_3)_3$ ,  $[\text{RuNO}]^{3+}$  and SHLLW solutions was carried out to determine the optimum concentration of ACN required for the removal of Ru. To 5 ml of the Ru bearing solutions in a definite concentration (1-4 M) of nitric acid and 5 ml of NPH,

various concentrations of ACN (0.01-0.1 M) were added. The mixture was shaken well for 5 minutes at room temperature using a vortex mixer and allowed to settle for 10 minutes for complete separation of organic and aqueous phases. To 3 ml of the aqueous sample, 30% H<sub>2</sub>O<sub>2</sub> (the quantity of which was just sufficient to reduce the unreacted Ce(IV) in the sample to Ce(III)) was added for the purpose of preventing further oxidation of Ru in the sample to RuO<sub>4</sub> by Ce(IV). Concentration of Ru in the sample was analysed by ICP-OES technique. Ruthenium tetroxide, produced by the oxidation of Ru in the aqueous phase by Ce(IV) is highly volatile even at room temperature [9] and due to the presence of NPH over the aqueous phase, the RuO<sub>4</sub> vapour was trapped from escaping out of the centrifuge tube. In the organic phase, the trapped RuO<sub>4</sub>, which is unstable and a powerful oxidizing agent, oxidised NPH to alcohol/ketone and a black coloured hydrophobic suspension of ruthenium oxide was formed at the interface between organic and aqueous phases (Fig. 4.1).

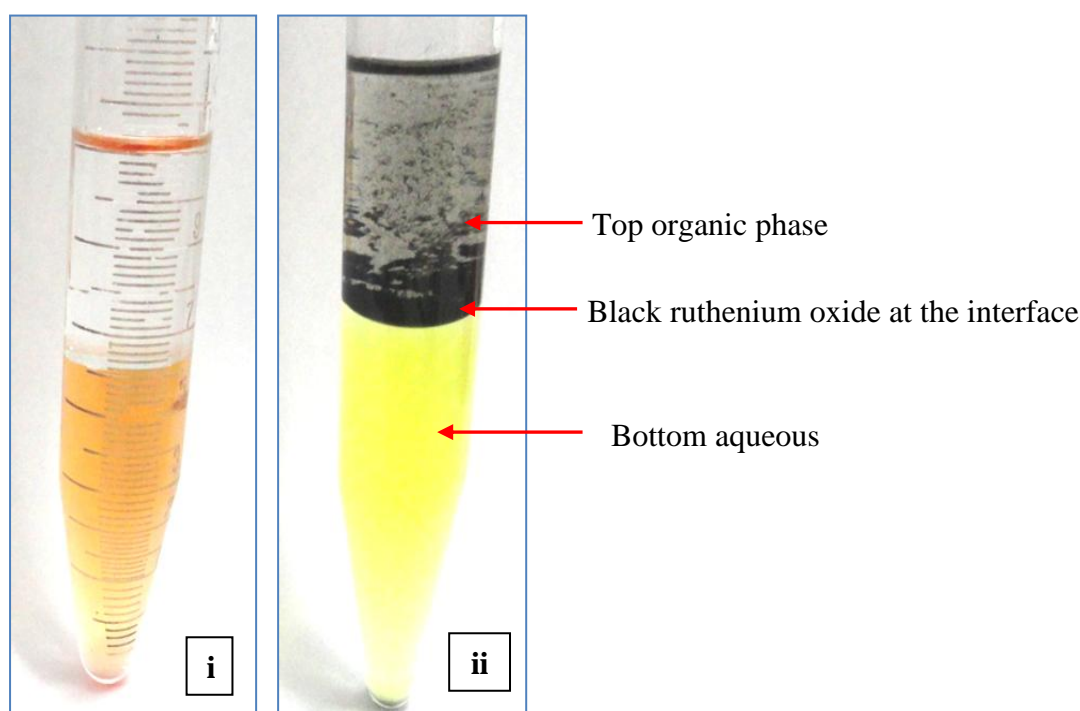


**Fig. 4.1** Black Ru suspension at the organic and aqueous interface: (i) before adding ACN and (ii) after adding ACN

After separating the aqueous phase using a separating funnel, the organic phase along with the black coloured Ru suspension was filtered off by means of a cellulose extraction thimble, which allowed the organic phase to pass through, leaving behind the black suspension on it. The extraction thimble containing Ru suspension was dried with a hot air blower and the black solid mass obtained was subjected to characterisation of phase by XRD technique. The IR spectra of NPH were recorded before and after separating ruthenium to ascertain structural modifications, if any, due to its oxidation by  $\text{RuO}_4$  vapour.

#### **4.2.3.2 Effect of acid concentration, temperature and mixing time**

Experiments conducted initially for the separation of Ru using different concentrations of Ce(IV) in the range 0.01-0.1M revealed that about 0.02–0.04 M of Ce(IV) was adequate for the complete oxidation of 160 ppm of Ru present in the simulated waste as well as in pure ruthenium nitrosyl solution. Subsequently, all experiments were conducted using ACN as the oxidizing agent in the concentration range 0.02–0.04 M for the purpose of investigating the effect of nitric acid concentration, temperature and mixing time on the separation of ruthenium. Separation experiments were carried out in 0.5, 1, 2, 3 or 4 M nitric acid media. Maximum concentration of nitric acid was chosen as 4 M, since the HLLW generated from the aqueous reprocessing of spent fuel of fast breeder test reactor contains all fission products in 4 M nitric acid. The influence of temperature on the separation was evaluated at 300, 313 and 333 K. To examine the effect of mixing time, separation experiments were carried out with the mixing time of 5 and 10 minutes.

#### **4.2.3.3 Effect of ageing of ruthenium bearing solutions**

As inter-conversion of ruthenium complexes in nitric acid medium with ageing is reported in the literature [10], the effect of ageing of the test solutions on the separation of Ru was studied in batch mode using simulated HLLW as well as  $[\text{RuNO}]^{3+}$  solution in 1 M nitric acid

medium at 300 K. The ageing effect was also examined using n-dodecane as the organic phase.

### 4.3 RESULTS AND DISCUSSION

#### 4.3.1 Separation of Ruthenium from $[\text{RuNO}]^{3+}$ Solution and SHLLW Containing $[\text{RuNO}]^{3+}$ Complexes

##### 4.3.1.1 Effect of Ce(IV) concentration

Experiments were conducted to separate Ru from pure nitrosyl nitrate and SHLLW solutions using NPH after oxidizing Ru to  $\text{RuO}_4$  by ACN in the concentration range 0.01-0.1 M. The separation percentage of ruthenium ( $\{([\text{Ru}]_{\text{initial}} - [\text{Ru}]_{\text{final}})/[\text{Ru}]_{\text{initial}}\} \times 100$ ) increased with increasing concentration of ACN. Maximum separation of 33 % was obtained in the concentration range of 0.02-0.04 M CAN in 4 M nitric acid, beyond which, the separation percentage remained constant in the case of  $[\text{RuNO}]^{3+}$  solution. Figure 4.2 shows the variation in the separation percentage of ruthenium by NPH from  $[\text{RuNO}]^{3+}$  and simulated HLLW solutions in 1 and 4 M nitric acid at 300 K. The amount of Ru separated from SHLLW solution in 4 M nitric acid was only 22 % in the entire concentration range of Ce(IV). When the concentration of nitric acid was decreased to 1 M, the separation of Ru from  $[\text{RuNO}]^{3+}$  solution increased to more than 80 % using 0.025 M ACN. Further increase in the concentration of ACN did not increase the separation yield of Ru. In the case of SHLLW in 1 M acidity, separation percentage of Ru reached a constant value of about 85 % with 0.04 M ACN. Ruthenium forms nitrato ruthenium nitrosyl complexes in 1 M nitric acid which can be readily oxidized (as discussed in the following Section 4.3.1.2) and hence, the separation percentage of Ru in 1 M nitric acid was higher than that in 4 M acid within the precision of  $\pm 5\%$ , in the presence of the oxidizing agent, Ce(IV).

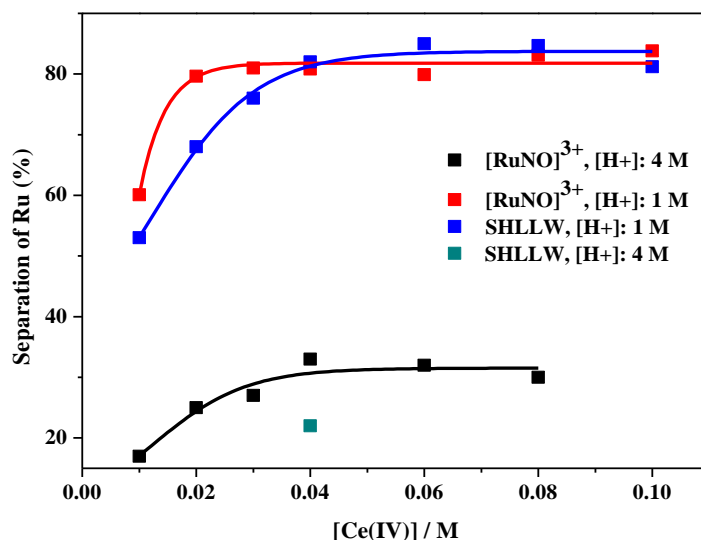


**Fig. 4.2** Separation of Ru from  $[\text{RuNO}]^{3+}$  and simulated HLLW solutions using Ce(IV) in 1 and 4 M nitric acid at 300 K; mixing time: 5 min.

#### 4.3.1.2 Effect of nitric acid concentration and temperature on the separation of ruthenium

The effect of temperature on the separation of Ru at different concentrations of nitric acid (0.5–4 M) in the case of pure  $[\text{RuNO}]^{3+}$  and simulated HLLW solutions are shown in Figs. 4.3 and 4.4 respectively. Three different temperatures employed were 300, 313 and 333 K. Mixing time for each experiment was 5 min and 0.025 M Ce(IV) was used as the oxidant. Figures 4.3 and 4.4 reveal that the separation percentage of Ru increased with decrease in acid concentration and increase in temperature. The separation percentage of Ru from  $[\text{RuNO}]^{3+}$  solution and from simulated HLLW in 4 M nitric acid were about 25 and 12 % respectively at 300 K, which increases to 54 and 48 % respectively at 333 K. The separation percentage at 300 K increased gradually with decreasing acid concentration from 4 to 0.5 M. Increasing the temperature from 300 to 313 and 333 K did not show any improvement in the separation percentage, when nitric acid concentration was reduced from 1 to 0.5 M. 91 and 88 % of ruthenium could be separated from ruthenium nitrosyl and simulated HLLW solutions

respectively in 1 M nitric acid medium in the presence of 0.025 M Ce(IV) at 333 K. The stability constant for ruthenium trinitrato complex is reported to decrease from 0.147 to 0.096 and 0.0853 with increase in temperature from 283 to 293 and 303 K respectively at 0.95 M acidity [11]. With increase in temperature the stability constant for the formation of trinitrato complex decreases and facilitates the formation of lower nitrato complexes which are easily oxidisable than trinitrato complex; hence, separation of ruthenium increases with increase in temperature.

The decrease in the separation of Ru with increase in nitric acid concentration could also be due to the formation of various ruthenium nitrosyl complexes at different concentrations of acid. According to Siczek and Steindler [11], the proportion of nitrous acid to nitric acid increases with increasing acid concentration and owing to increasing nitrous acid concentration, the weakly bound  $\text{NO}_3^-$  groups are replaced by the more nucleophilic  $\text{NO}_2^-$  groups.



Boswell and Soentono [10] reported that the proportion of nitrato nitro complexes increases with increasing nitric acid concentration and the RuNO mono nitro complex has its maximum concentration of 50 % in 4 M acid solution. It is known from the spectrochemical series that  $\text{NO}_2^-$  is a strong field ligand compared to  $\text{NO}_3^-$  and  $\text{H}_2\text{O}$  ligands and the crystal field stabilization energy will be higher for nitrito ( $\text{NO}_2^-$ ) complex than that for nitrato ( $\text{NO}_3^-$ ) and aqua ( $\text{H}_2\text{O}$ ) analogues. Since the nitrito complex is more stable than the other ligands, it is difficult to oxidize the metal to  $\text{RuO}_4$ . Yet another reason given by Mousset et al. [12] for the decrease in the separation percentage of ruthenium with increasing nitric acid concentration was due to the stabilization of  $\text{RuO}_4$  as  $\text{HRuO}_4$  in higher concentration of nitric acid.

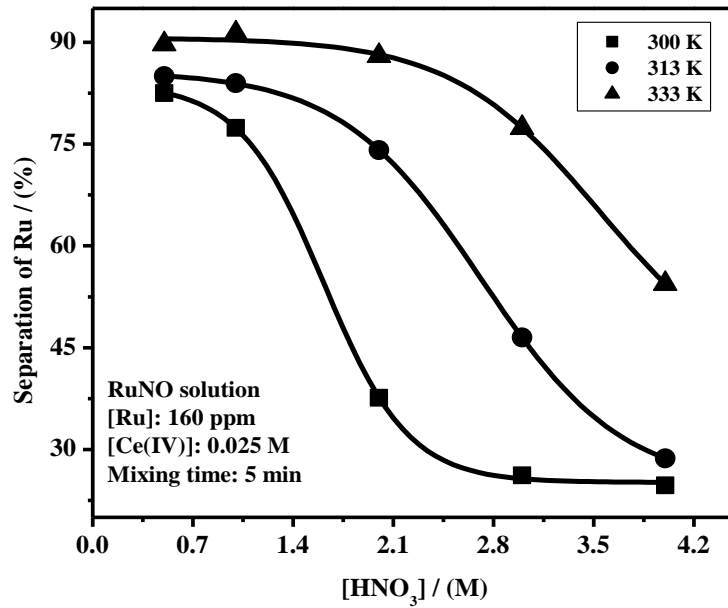


**Fig. 4.3** Effect of temperature on the separation of Ru from  $[\text{RuNO}]^{3+}$  solution in different concentrations of nitric acid

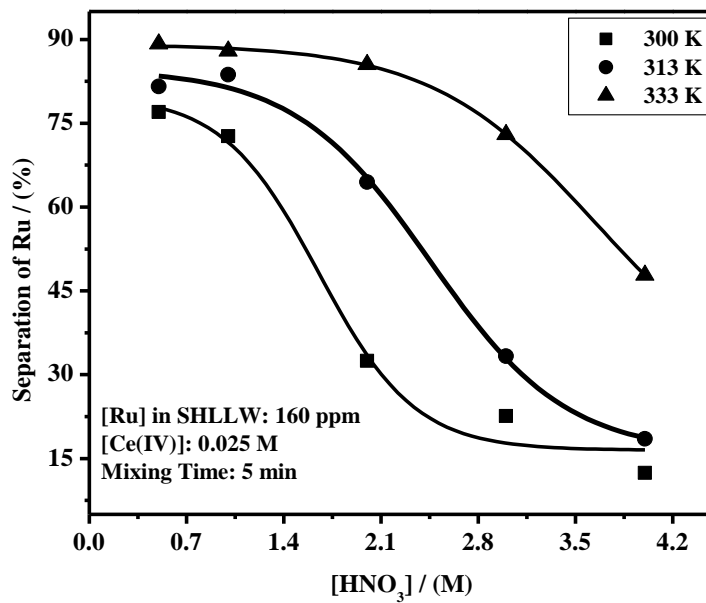


**Fig. 4.4** Separation of Ru from simulated HLLW at different temperatures and acid concentrations

#### 4.3.1.3 Ageing effect of ruthenium solution on its separation

The role of ageing of Ru bearing solutions on its separation in 1 M nitric acid medium was investigated by conducting separation experiments after 1 h, 1, 2, 4, 7, 10 and 30 days using a freshly prepared stock solution and the results are shown in Fig. 4.5. The separation percentage of Ru was found to increase with ageing and after about 10 days the ageing effect was insignificant. Ruthenium in nitric acid medium can exist in cationic, anionic or neutral form of octahedral arrangements (Fig. 4.6) with 1, 2, 3 and 4 stable positions and labile 5th position. The rate of exchange of the ligand in position 5 is more rapid than the ligands in the positions 1-4 [11]. Ruthenium can also form about hundreds of nitrosyl complexes in nitric acid and these complexes have the ability to exchange ligands. The composition of the solution containing a mixture of ruthenium nitrosyl complexes depends on the concentration of acid, temperature, ruthenium species present initially and the time elapsed since its formation because of inter-conversion of different nitrosyl complexes with different half times [10]. In the present work, the effect of ageing on the distribution of Ru in 1 M nitric acid, which was prepared by diluting commercial ruthenium nitrosyl nitrate solution in 9 M nitric acid was studied. During the dilution of ruthenium bearing solution, nitro and nitrate ligands in the ruthenium nitrosyl complexes are replaced by aqua ligands and the “inter-conversion half times” are different for different complexes ranging from a few h to days. The increase in separation percentage observed with ageing might be due to the inter-conversion of less easily oxidized ruthenium complexes (i.e. trinitrato, nitro ruthenium nitrosyl complexes) to more easily oxidized complexes (i.e. lower nitrate, nitro ruthenium complexes formed due to replacement of nitrate and nitro ligands by aqua ligands). Hence, the separation percentage was less for freshly diluted solution, which increased with ageing and had reached the steady state value after 12 days of dilution; this time period might be the inter-conversion half times required for the replacement of ligands.

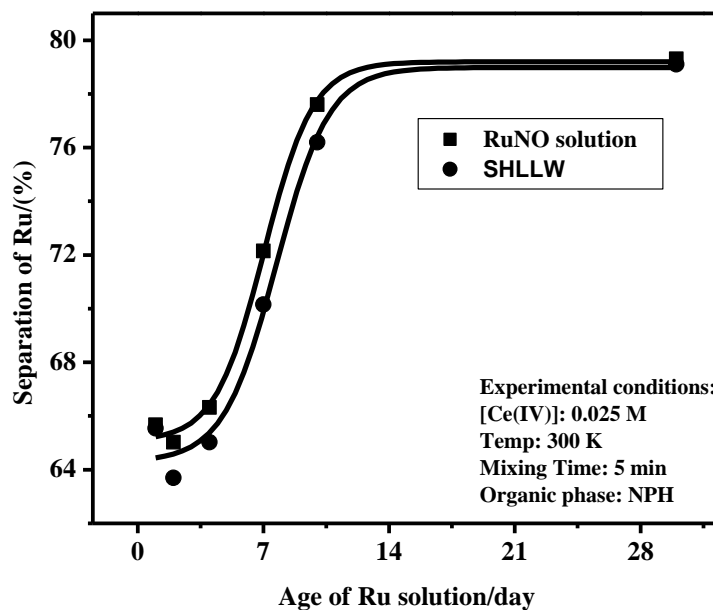


**Fig. 4.5** Effect of ageing on the separation of Ru

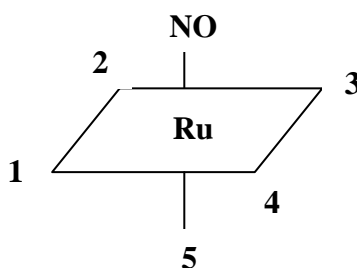


**Fig. 4.6** The octahedral structure of ruthenium nitrosyl complex

A marginal increase could be observed in the separation percentage of ruthenium when n- dodecane was used as the organic phase instead of NPH, while the other experimental conditions remained identical. The results obtained with NPH and n-dodecane as the organic phases for the separation of Ru are compared in Table 4.1.

**Table 4.1** Separation of Ru using the organic phases NPH and n-dodecane at different ageing periods; [Ce(IV)]: 0.025 M; Mixing time: 5 min; Temperature: 300 K; [HNO<sub>3</sub>]: 1 M

Ageing period of Ru Solution	Separation (%) using NPH		Separation (%) using n-dodecane	
	RuNO soln.	SHLLW	RuNO soln.	SHLLW
1 h	45.0	58.7	51.6	58.5
1 day	65.6	65.5	67.7	68.1
10 days	77.6	76.2	79.1	79.5
30 days	79.3	79.1	81.1	80.0

### 4.3.2 Separation of Ruthenium from Nitrate Solutions

The percentage of ruthenium separated from Ru(NO<sub>3</sub>)<sub>3</sub> and SHLLW containing ruthenium in the form of Ru(NO<sub>3</sub>)<sub>3</sub> at 300 and 333 K are given in Table 4.2. The separation percentage of ruthenium was found to be higher in the case of SHLLW than that of pure Ru(NO<sub>3</sub>)<sub>3</sub>. Removal of 81 and 96 % of Ru in 4 M nitric acid and in the presence of 0.04 M ACN (oxidizing agent) was possible from Ru(NO<sub>3</sub>)<sub>3</sub> and SHLLW solutions respectively. Motojima [6] estimated the separation percentage of Ru from a Ru(NO<sub>3</sub>)<sub>3</sub> solution containing 20 ppm of Ru at various concentrations of nitric acid and reported that the separation percentage increased as 72, 75, 81 and 87 % when the acid concentration decreased from 4 to 3, 2 and 1 M respectively, in the presence of 0.01 M ACN. He could separate Ru almost completely from Ru(NO<sub>3</sub>)<sub>3</sub> solution containing 100 ppm of Ru in 3 M HNO<sub>3</sub>, when the concentration of Ce(IV) was increased to 0.02 M. In the present work, 81 % was obtained for the separation of Ru from a 160 ppm Ru(NO<sub>3</sub>)<sub>3</sub> solution in 4 M HNO<sub>3</sub> containing 0.04 M ACN. This value is in reasonable agreement with that reported by Motojima [6], considering the higher concentration of 4 M nitric acid in the present study compared to 3 M acid used by Motojima, though the initial concentration of Ru and ACN were different in the two studies.

The effect of temperature was observed to be insignificant in the separation of ruthenium from nitrate solutions. Separation of Ru was more in the case of Ru(NO<sub>3</sub>)<sub>3</sub> when

compared to  $[\text{RuNO}]^{3+}$  solution. The reason is that in the latter case, the Ru-NO bond is exceedingly difficult to break by substitution or oxidation reaction due to the extraordinary stability of the species  $[\text{RuNO}]^{3+}$  in ruthenium nitrosyl complexes. The NO group in  $[\text{RuNO}]^{3+}$  is reported to bond as  $\text{NO}^+$  and donate an electron to Ru(III) and hence, RuNO becomes a bivalent Ru(II) complex containing  $\text{NO}^+$ . The Ru-N distance in  $[\text{RuNO}]^{3+}$  complexes varies from 1.7 to 2.0 Å depending on the structure of the complex, and it is sufficiently short for the formation of the bonding  $\text{Ru}=\text{N}^+=\text{O}$  [11].

Separation of Ru from  $\text{Ru}(\text{NO}_3)_3$  prepared in 4 M  $\text{HNO}_3$  was also studied using 30 % tributyl phosphate (TBP) in NPH as the organic phase to trap  $\text{RuO}_4$  vapour after oxidising  $\text{Ru}(\text{NO}_3)_3$  with 0.04 M ACN. Unlike the behaviour of pure NPH, the separation % of Ru increased from 11 to 15 % only from pure  $\text{Ru}(\text{NO}_3)_3$  and from 20 to 25 % in the case of SHLLW containing  $\text{Ru}(\text{NO}_3)_3$  with increase in temperature from 300 to 333 K, respectively (Table 4.2). The very low separation of 25 % from SHLLW using 30 % TBP as against the value of 97 % when NPH was used as the organic phase for separation, is attributed to the unavailability of Ce(IV) in the aqueous phase for oxidising Ru, since Ce(IV) was observed to be extracted by 30 % TBP immediately.

**Table 4.2** Separation of Ru from ruthenium nitrate solutions;  $[\text{HNO}_3]$ : 4 M and  $[\text{Ce}(\text{IV})]$ : 0.04 M

Organic phase	Aqueous phase	Temperature (K)	Separation (%) of Ru <sup>a</sup>
NPH	Pure $\text{Ru}(\text{NO}_3)_3$	300	81
		333	82
	SHLLW containing $\text{Ru}(\text{NO}_3)_3$	300	96
		333	97
30 % TBP in NPH	Pure $\text{Ru}(\text{NO}_3)_3$	300	11
		333	15
	SHLLW containing $\text{Ru}(\text{NO}_3)_3$	300	20
		333	25

$$^a\text{Ru in percentage} = \left( \frac{[\text{Ru}]_{\text{initial}} - [\text{Ru}]_{\text{final}}}{[\text{Ru}]_{\text{initial}}} \right) \times 100$$

### 4.3.3 Characterisation of Black Ruthenium Suspension

The black coloured ruthenium based suspension formed at the organic and aqueous interface during the separation of ruthenium was filtered off, dried and subjected to powder XRD characterization. The XRD pattern revealed the black Ru based powder to be an amorphous phase (Fig. 4.7), which was further confirmed from the TEM image and electron diffraction pattern (Fig. 4.8). Hence, phase identification was not possible by both the techniques. However, the presence of ruthenium and oxygen was confirmed by Electron Energy Loss Spectroscopic (EELS) technique. As the M45 edge of Ru was coinciding with the K-edge of carbon, and since the sample was prepared on amorphous carbon coated grid, it was difficult to estimate the charge state of the black powder.

To obtain information regarding the oxidation state and stoichiometry of the black ruthenium oxide, the powder was compacted into a pellet of dimensions 3 mm thickness and 5 mm diameter and XPS measurements were performed. The binding energy of C 1s transition from adventitious C at 285 eV was used as the reference to account for any charging of the sample and the peak positions were compared with standard values for identifying different elements and their oxidation states. The data were collected only over the surface for the analysis. The Ru-3d core level spectrum presented in Fig. 4.9 shows two doublets at 282.0 and 282.95 eV corresponding to the 3d<sub>5/2</sub> region and suggesting RuO<sub>2</sub> species. The other peaks at higher binding energies of 286.4 and 287.35 eV correspond to the 3d<sub>3/2</sub> region of ruthenium species. The 3d<sub>5/2</sub> and the 3d<sub>3/2</sub> levels reveal the same information except for the energy shift and the intensity. The ratio of the areas under the curves of the 3d<sub>5/2</sub> and 3d<sub>3/2</sub> levels is 3:2, which would arise from the number of possible sub-states, (2J+1) for each level guided by quantum mechanics. In spin-orbit coupling, the orbital angular momentum number, 'l' and the spin quantum number, 's' interact with each other giving rise to the total angular momentum number, 'J' which splits as (l+s) and (l-s). 'l' = 2 for d-orbital and 's' = 1/2 for the electron implies J = 5/2 (l+s) and 3/2 (l-s). Therefore, (2J+1) = 2 x 5/2 + 1 = 6 for l+s and 2 x 3/2 + 1 = 4 for l-s; hence, the ratio of the areas under the curves of the 3d<sub>5/2</sub> and 3d<sub>3/2</sub> levels is 6:4 i.e. 3:2.

Some researchers [13-15] are of the opinion that the low and high binding energy of Ru 3d<sub>5/2</sub> core level peaks are due to the presence of two distinct oxidation states (Ru(IV) and Ru(VI)), the latter one being present in the near-surface region of RuO<sub>2</sub>. According to Cox et al. [16], the dominant, low-binding energy peak corresponding to the doublet of RuO<sub>2</sub> was due to screened final-state and the other doublet was due to unscreened final-state. This interpretation is consistent with the fact that (i) RuO<sub>3</sub> is not known to be a very stable phase and (ii) non-metallic Ru(IV) oxide has a typical Ru 3d binding energy of 282.2 eV. Figure 4.9 shows three peaks at the binding energies 284.6, 286.35 and 288.4 eV corresponding to C 1s. The lowest binding energy peak corresponds to the adventitious C-C peak, which is used as the reference, while the other two higher energies correspond to C-N and C-O bonds respectively. The O 1s spectrum is presented in Fig. 4.10. This spectrum shows four peaks at 530.1, 531.45, 532.3 and 533.75 eV, corresponding to the bonds of O\*-Ru-OH, RuO<sub>2</sub>, O-Ru-O\*H and C-O and/or adsorbed H<sub>2</sub>O respectively [17, 18]. To confirm the stoichiometry of the chemical (Ru) species, the atomic ratios (concentrations) of each of the states was calculated. This was done by taking into account of the Relative Sensitive Factor (RSF) for individual element since the area under the curve does not directly give the atomic ratio. The RSF of O, N, C and Ru were 2.93, 1.80, 1.0 and 12.5 respectively for the instrument. The O/Ru atomic ratio of the ruthenium oxide under investigation was much higher than the value of 2 expected from the stoichiometry of the compound. Hygroscopic nature of the oxide surface and the highly porous structure with a very large electrochemically active surface area in RuO<sub>2</sub> are responsible for the observed departure of the O/Ru surface concentration ratio from its expected value of 2. From the foregoing discussion on the XPS spectra of Ru 3d and O 1s, it is concluded that the Ru species in the suspension at the interface between the organic and aqueous phases was in +4 oxidation state, corresponding to RuO<sub>2</sub> and to a certain extent oxyhydroxide species of Ru(IV).

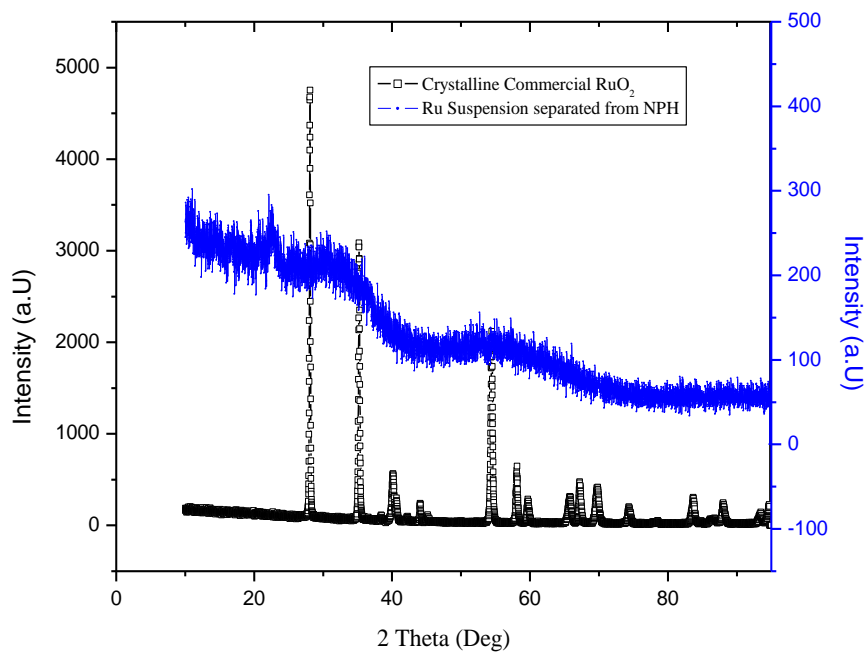


**Fig. 4.7** XRD pattern of commercial (crystalline) RuO<sub>2</sub> and the black Ru suspension generated during the separation of Ru by NPH

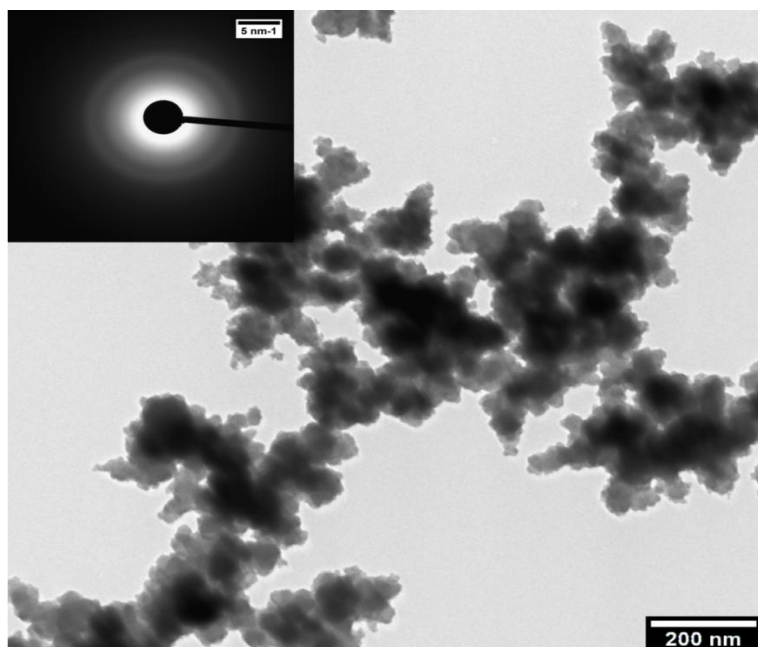


**Fig. 4.8** TEM image and electron diffraction pattern of amorphous ruthenium oxide suspension

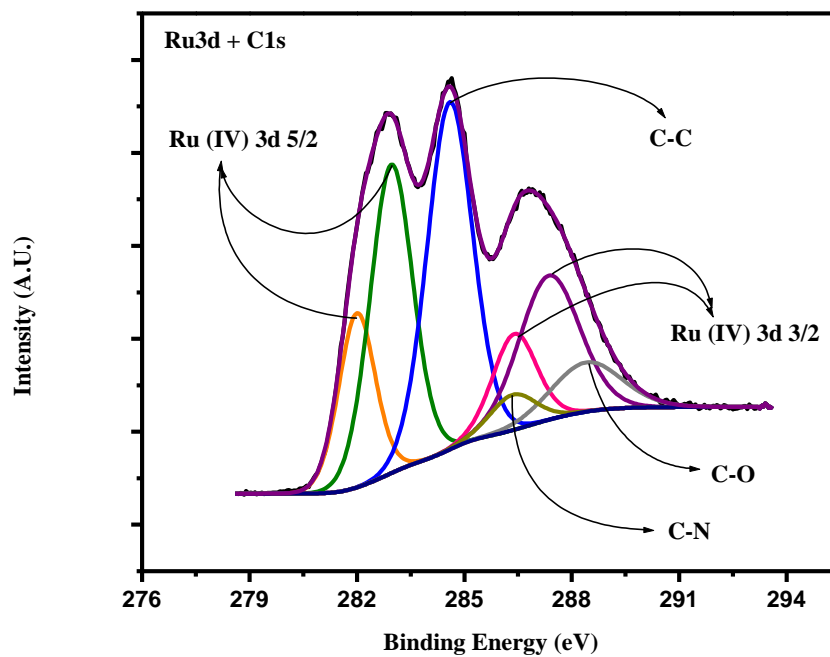


Fig. 4.9 XPS spectra of Ru 3d core level lines on ruthenium species

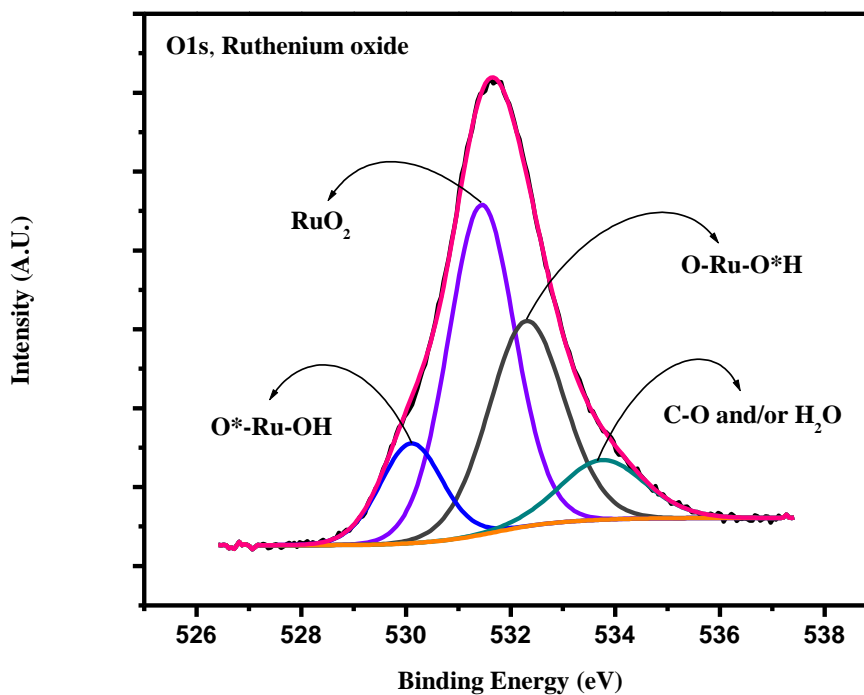


Fig. 4.10 XPS spectra of O 1s on ruthenium bearing species

#### 4.3.4 Characterisation of NPH Before and After Ruthenium Separation

The organic phase, NPH over the aqueous phase had trapped the escaping volatile  $\text{RuO}_4$  vapour (formed during the oxidation of Ru by ACN) and converted it to black solid suspension. Motojima [6] reported that the escaping  $\text{RuO}_4$  vapour oxidized NPH to a ketonic group, during which reaction  $\text{RuO}_4$  was reduced to black  $\text{RuO}_2$  solid. This  $\text{RuO}_2(\text{s})$  formed a black coloured suspension at the interface of organic and aqueous layers. To confirm the oxidation of NPH by  $\text{RuO}_4$ , FTIR spectra of NPH were recorded before and after the separation experiments. Figure 4.11 shows the IR spectra of pure NPH. A strong absorption band centered between  $2850\text{--}3000\text{ cm}^{-1}$ , owing to the C-H stretching of both methyl and methylene groups and three other bands centered between  $1450\text{--}1470$ ,  $1370\text{--}1380$  and  $720\text{--}725\text{ cm}^{-1}$ , owing to the C – H bending motions could be observed in Fig. 4.11. These bands correspond to the typical IR absorption bands for saturated hydrocarbons. The IR spectra of NPH recorded after separation of 65 ml of ruthenium bearing solution ( $[\text{Ru}]$ : 1870 ppm;  $[\text{HNO}_3]$ : 1M) by 30 ml of NPH, is shown in Fig. 4.12. This figure shows an absorption band at  $1722\text{ cm}^{-1}$  with very low intensity, which is characteristic of C = O stretching. The presence of this band ascertains the conversion of the hydrocarbon, NPH to a ketone and not aldehyde, since the doublet between  $2830\text{--}2695\text{ cm}^{-1}$  which is characteristic of aldehydic C – H stretching was absent. Literature reports are available on the oxidation of alkanes to alcohol and ketones by the strong oxidizing agent,  $\text{RuO}_4$  [19 – 21]. The oxidation of alkane by  $\text{RuO}_4$  is a concerted (3+2) addition reaction which was supported with kinetic data [22]. Since HLLW contains very low concentration of Ru, the NPH used for separating Ru can be reused several times for the separation experiments without purifying it to remove the ketone produced.

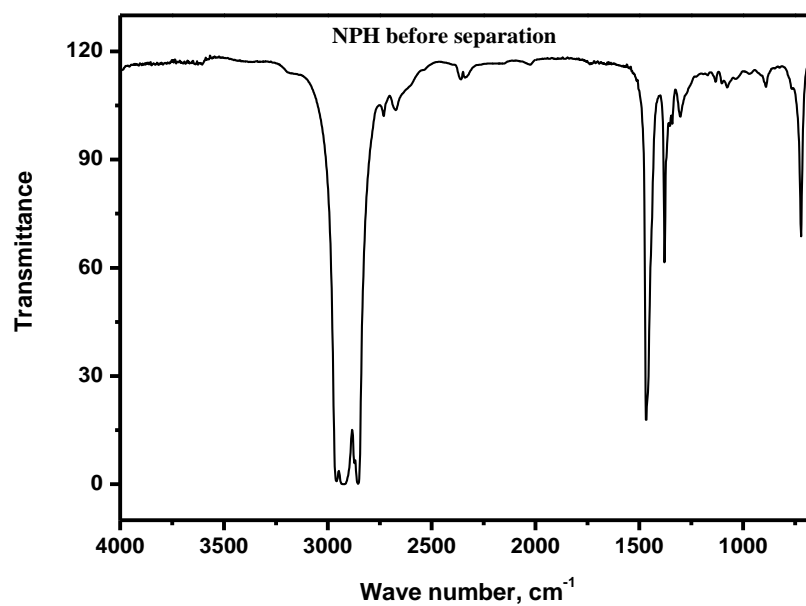


Fig. 4.11 IR spectra of NPH recorded before the separation experiment

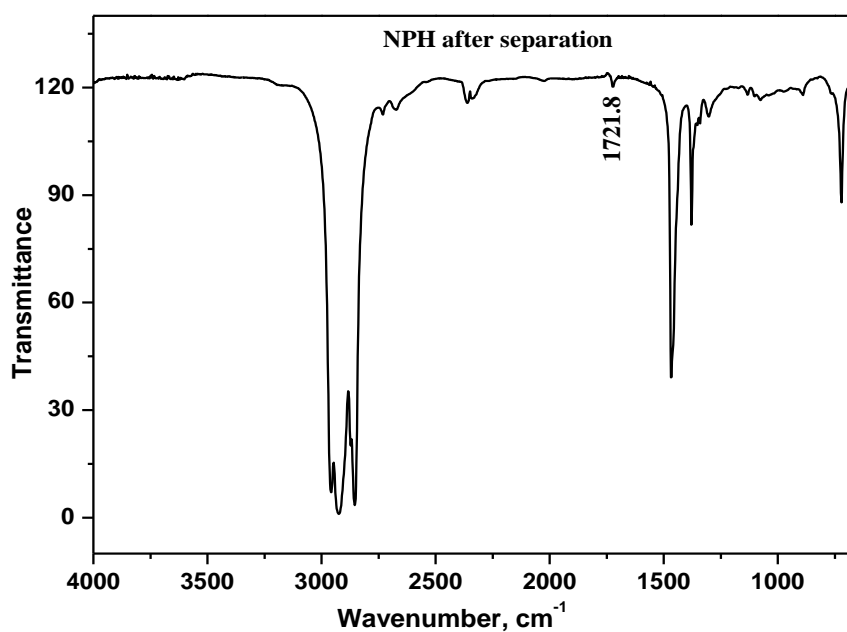


Fig. 4.12 IR Spectra of NPH recorded after Ru separation

#### 4.4 CONCLUSIONS

The volatilisation behaviour of ruthenium tetroxide was made use of in the separation of ruthenium, for its removal from the high level liquid waste generated during the aqueous reprocessing of spent plutonium-rich nuclear fuels. Separation experiments conducted by mixing Ru bearing nitrate, nitrosyl nitrate or SHLLW solutions with NPH in the presence of ACN as oxidizing agent for Ru, revealed that separation of about 80-90 % Ru from  $\text{Ru}(\text{NO}_3)_3$  and SHLLW (containing Ru in the form of  $\text{Ru}(\text{NO}_3)_3$ ) solutions was possible with 0.04 M ACN in 4 M nitric acid. About 80 % of Ru could be separated from nitrosyl nitrate solutions, at low concentration of nitric acid in the range 0.5–1 M using 0.02–0.04 M Ce(IV) as the oxidizing agent and at ambient temperature. The black Ru suspension formed at the interface between the aqueous and organic phases was characterized by XRD, TEM and XPS techniques. XRD and TEM results revealed the Ru based powder to be amorphous phase and the presence of Ru and O in the powder was confirmed from EELS. The XPS results showed the Ru species present in the black suspension to be in +4 oxidation state corresponding to  $\text{RuO}_2$  and oxy-hydroxide species of Ru(IV) to some extent over the surface. The efficiency of n-dodecane for the separation of Ru was marginally higher than that of NPH. The ketonic group formed in the used NPH upheld the reduction of  $\text{RuO}_4$  to  $\text{RuO}_2$  by the alkane. As cerium is one of the fission products, addition of Ce(IV) as the oxidizing agent in the separation of Ru is not expected to significantly increase the burden of waste fixing. The procedure involved in the separation of Ru by volatilization after oxidation and absorption by NPH is simple, less time consuming and cost effective process. Hence, this method is suitable for deployment in the reprocessing plant for the separation and recovery of the troublesome fission product, ruthenium. However, this systematic parametric study recommends the separation of Ru from waste solutions with nitric acid concentration in the range 0.5-1 M and ACN in the range 0.02-0.04 M at ambient temperature for improved separation efficiency,

since in the PUREX process waste, Ru exists mainly in the form of nitrosyl nitrate complexes.

#### 4.5 REFERENCES

1. Ayabe, T., Tatsugae, R., *Chem. Abstr.*, 110, No. 143304c, **1989**
2. Ayabe, T., Tatsugae, R., *Chem. Abstr.*, 110, No. 139105W, **1989**.
3. Kobayashi, T., *Chem. Abstr.*, 110, No. 103732j, **1989**
4. Grehl, M., Meyer, H., Schafer, D., U S Patent, No. 6475448, **2002**
5. Haas, M., Weuta, P., Wolf, A., Schlueter, O.F-K, U S Patent, No. 0287282A1, **2008**
6. Motojima, K., *J. Nucl. Sci. Technol.*, 26 (**1989**) 358
7. Scargill, D., Lyon, C.E., Large, N.R., Fletcher, J.M., *J. Inorg. Nucl. Chem.*, 27 (**1965**)  
161
8. Satyabrata, M., Falix, L., Sreenivasan, R., Pandey, N.K., Mallika, C., Koganti, S.B.,  
Kamachi Mudali, U., *J. Radioanal. Nucl. Chem.*, 285 (**2010**) 687
9. Seddon, E.A., Seddon, K.R., *The Chemistry of Ruthenium*, Monograph, 19, Elsevier,  
Amsterdam, **1984**
10. Boswell, G.G.J., Soentono, S., *J. Inorg. Nucl. Chem.*, 43 (**1981**) 1625
11. Siczek, A.A., Steindler, M.J., *Atomic Energy Rev.*, 16 (**1978**) 575
12. Mousset, M., Bedioui, F., Eysseric, C., *Electrochem. Commun.*, 6 (**2004**) 351
13. Kim, K.S., Winograd, N., *J. Catal.*, 35 (**1972**) 66
14. Lewerenz, H.J., Stucki, S., Kotz, R., *Surf. Sci.*, 126 (**1983**) 463
15. Kotz, R., Lewerenz, H.J., Stucki, S., *J. Electrochem. Soc.*, 130 (**1983**) 825

16. Cox, P.A., Goodenough, J.B., Tavener, P.J., Telles, D., Egdell, R.G., *J. Solid State Chem.*, 62 (1986) 360
17. Rochefort, D., Dabo, P., Guay, D., Sherwood, P.M.A., *Electrochim. Acta*, 48 (2003) 4245
18. Mun, C., Ehrhardt, J.J., Lambert, J., Madic, C., *Appl. Surface Sci.*, 253 (2007) 7613
19. Bakke, J.M., Frohaug, A.E., *Acta Chem. Scandinavica*, 48 (1994) 160
20. Griffith, W.P., Ruthenium oxidation complexes-Their uses as homogenous organic catalysts. Springer, Dordrecht, pp.215, 2011
21. Drees, M., Strassner, T., *J. Org. Chem.*, 71 (2006) 1755
22. Tenaglia, A., Terranova, E., Waegell, B., *J. Org. Chem.*, 57 (1992) 5523

---

## 5. SEPARATION AND RECOVERY OF RUTHENIUM BY ELECTRO-OXIDATION

---

### 5.1 INTRODUCTION

Electrochemical methods are promising techniques for various applications in the back end of nuclear fuel cycle and these techniques are employed in the dissolution of  $\text{PuO}_2$ , valency adjustment of Pu, destruction of acids and organics in the waste, etc. [1]. Various methods reported in the literature for the removal of ruthenium from high level liquid waste (HLLW) include volatilization, precipitation, solvent extraction, chromatography, sorption and electro-oxidation/reduction. The electrochemical method for the removal of ruthenium from nitric acid medium is one of the easiest, inherently safe and promising techniques due to its simplicity; congeniality for scaling-up operations and this method does not demand the addition of external reagents to the feed, which is indeed desirable for the treatment and disposal of HLLW. In the electrochemical method, Ru can be separated either by deposition as metal on the cathode [2-6] or by electro-oxidation to  $\text{RuO}_4$  at the anode [7-9]. Separation of Ru using electro-oxidation was carried out by Motojima [7] and Mousset et al. [9] in constant current mode using Pt anode. Motojima used cerium ion as the redox mediator in an undivided electrolytic cell whereas, Mousset et al. had employed a porous ceramic diaphragm to separate the anode and cathode compartments and Ag was used as the redox catalyst. Since cerium is one of the fission products, its use as the redox catalyst will neither make any change in the vitrification process nor would add significantly to the waste volume as the quantities added are not very high.

In the present Chapter, the separation of ruthenium from ruthenium nitrosyl,  $[\text{RuNO}]^{3+}$  solution as well as from simulated high level liquid waste (SHLLW) in nitric acid medium by electro-oxidation of Ru to volatile  $\text{RuO}_4$  in constant current mode using cerium as the redox

mediator in undivided and divided electrolytic cell configurations is described. The amount of RuO<sub>4</sub> collected in 8 M nitric acid as well as in alkaline trap was compared under different experimental conditions. A divided cell fabricated using borosilicate glass frit as the separating membrane was employed for separating Ru from SHLLW without adding metal ions as the redox catalyst. The influence of process parameters like concentration of nitric acid, current density, temperature and concentration of the redox catalyst cerium, on the separation of Ru was investigated. Cyclic voltammetric (CV) studies were also performed to understand the oxidation behaviour of ruthenium nitrosyl complexes with different working electrodes and at different concentrations of nitric acid.

## 5.2 MATERIALS AND METHOD

### 5.2.1 Chemicals

Standard ruthenium nitrosyl, [RuNO]<sup>3+</sup> solutions with the concentration of Ru as 160 ppm in 1, 2 and 4 M nitric acid were prepared by diluting commercially available ruthenium nitrosyl nitrate solution (1.7 % Ru in 9 M nitric acid; supplied by M/s. Arora Matthey Ltd, Kolkata). Nitric acid supplied by M/s. Fischer Chemicals Ltd, Chennai (AR grade, 69–71 %) was used throughout the experiments. Cerium(III) nitrate hexa hydrate (AR grade, Min. assay: 99 %) procured from M/s. SDFCL, Mumbai was used as the redox mediator during electrolysis.

A synthetic HLLW solution simulated with fission and corrosion product elements envisaged in the reprocessed waste of the spent mixed carbide fuel of fast breeder test reactor (FBTR) at Kalpakkam, was prepared in 4 M HNO<sub>3</sub>. The chemical form of the elements and their concentration in the simulated waste solution (Table 3.2, Chapter 3) are reported elsewhere [10]. The waste solution thus prepared was diluted suitably to adjust the concentration of ruthenium to be 160 ppm (expected concentration of Ru in the actual HLLW) in 4 M HNO<sub>3</sub>.

## 5.2.2 Electrolytic Cell Assembly

### 5.2.2.1 Undivided cell

The schematic diagram of the leak tight, undivided electrolytic cell is shown in Fig. 5.1a. Platinum electroplated Ti mesh (surface area: 150 cm<sup>2</sup>) and Pt plated Ti gauze (surface area: 20 cm<sup>2</sup>) were used as anode and cathode respectively. The required current/potential was applied through a Switch Mode DC Power Supply (M/s. Aplab Ltd, Chennai). Diaphragm type vacuum pump was used for the suction of gases evolved in the cell. A magnetic stirrer cum heater facilitated gentle mixing of the electrolyte in the cell at a fixed temperature. The electrolytic cell was connected in series to gas wash bottles containing trap solution for trapping RuO<sub>4</sub> and NO<sub>x</sub> gas liberated from the cell.

500 ml of ruthenium nitrosyl or SHLLW solution containing 160 ppm of Ru in 1, 2 or 4 M HNO<sub>3</sub> was taken in the cell and electrolysis was performed with the anodic current density ( $J_a$ ) of 10 or 20 mA/cm<sup>2</sup> at the temperatures 313 and 333 K, with and without Ce(III)/Ce(IV) redox couple. Concentration of cerous nitrate ranging from 0.001 to 0.04 M was added to the electrolyte. The RuO<sub>4</sub> gas generated owing to oxidation of ruthenium at anode was absorbed in the gas wash bottles containing 8 M HNO<sub>3</sub> / 0.5 M NaOH solution. The absorption of RuO<sub>4</sub> in the trap solution could be visualised from the change in the colourless trap solutions to reddish brown and to orange colour in 8 M HNO<sub>3</sub> and 0.5 M NaOH respectively. During electrolysis, samples of the anolyte and the trap solution were analysed at regular intervals of time to determine the concentration of Ru. One drop of 30 % H<sub>2</sub>O<sub>2</sub> was added to the electrolyte test sample (for analysis) to prevent the loss of Ru as RuO<sub>4</sub>. Hydrogen peroxide reduces Ce(IV) (orange colour) present in the sample to colourless Ce(III), thereby preventing further oxidation of Ru to RuO<sub>4</sub> gas. As H<sub>2</sub>O<sub>2</sub> is a weak oxidizing agent, it will decompose in nitric acid medium and will not oxidize ruthenium further in the electrolyte sample. Estimation of Ru was carried out by Inductively Coupled Plasma Optical

Emission Spectroscopic (ICP-OES, Jobin Yvon, France) analysis and the standards were supplied by M/s. MBH Analytical Ltd, UK. Spectrophotometric measurements were performed with a Chemito double beam UV-Vis spectrophotometer (Thermo Scientific; Model: UV 2600). Polymer materials like teflon, parafilm, polyvinyl chloride and polypropylene tubes within the cell assembly and also in the line to gas wash bottles should be avoided, since  $\text{RuO}_4$  evolved during electrolysis was observed to get reduced to  $\text{RuO}_2$  solid instantaneously and deposit as black coloured particles on polymer substrates; which hinders the quantitative recovery of ruthenium. The cell assembly was therefore, fabricated with smooth glass material and the lid of the electrolytic cell was heated by IR lamp to avoid the decomposition of  $\text{RuO}_4$  to  $\text{RuO}_2$  and its deposition over the colder regions of the glass vessel.

#### **5.2.2.2 Divided cell with glass frit as diaphragm**

In the divided cell assembly shown in Fig. 5.1b, a glass frit served as the diaphragm to isolate the catholyte from the anolyte (it should be noted that polymer membranes like Nafion cannot be used in the cell to separate anolyte and catholyte, owing to the high radioactivity envisaged in plant). Platinum mesh (surface area: 38 or 84  $\text{cm}^2$ ) and Pt wire (surface area: 4 or 9  $\text{cm}^2$ ) were used as anode and cathode respectively. The other components of the cell were similar to those used in the case of undivided electrolytic cell. Catholyte was taken inside the glass frit which was fused to a glass tube suspended in the cell from the centre of the lid and anolyte was taken outside the glass frit in the cell vessel. Electrolysis was performed with the  $J_a$  value as 20  $\text{mA/cm}^2$  at the temperature  $313 \pm 2$  K. Initially, electro-oxidation of Ru bearing solutions was conducted in a cell which could accommodate only 50 ml of anolyte. Since complete separation of Ru was possible in this divided cell, cell assemblies were fabricated to hold higher volume of electrolyte (220 and 440 ml of anolyte

and correspondingly 44 and 88 ml of catholyte) and electrolysis was conducted with the same 20 mA/cm<sup>2</sup> as  $J_a$ .

### 5.2.3 Cyclic Voltammetric Measurements

Solutions of [RuNO]<sup>3+</sup> (containing 5, 20 and 40 mM of Ru) in different concentrations of nitric acid were prepared for performing cyclic voltammetric (CV) measurements in order to understand the electrochemical oxidation behaviour of [RuNO]<sup>3+</sup> in acidic medium. CV runs were carried out at 298 K in a standard three-electrode cell comprising a Pt wire (surface area: 0.42 cm<sup>2</sup>) or Au wire (surface area: 0.2 cm<sup>2</sup>) as working electrode, Pt mesh as counter electrode and standard Ag/AgCl reference (SSE) electrode using Comprehensive Autolab Model PGSTAT-30 (M/s. Eco-Chemie, Netherlands) electrochemical system equipped with General Purpose Electrochemical Software. Cyclic voltammograms were recorded at the potential scan rate of 100 mV/s, starting with the anodic scan and reversal of the scan at the anodic switching potential in the range 0-1.6 V (vs SSE). De-oxygenation of the test solution prior to the scans was done by flushing with argon and the results were analysed after IR compensation.

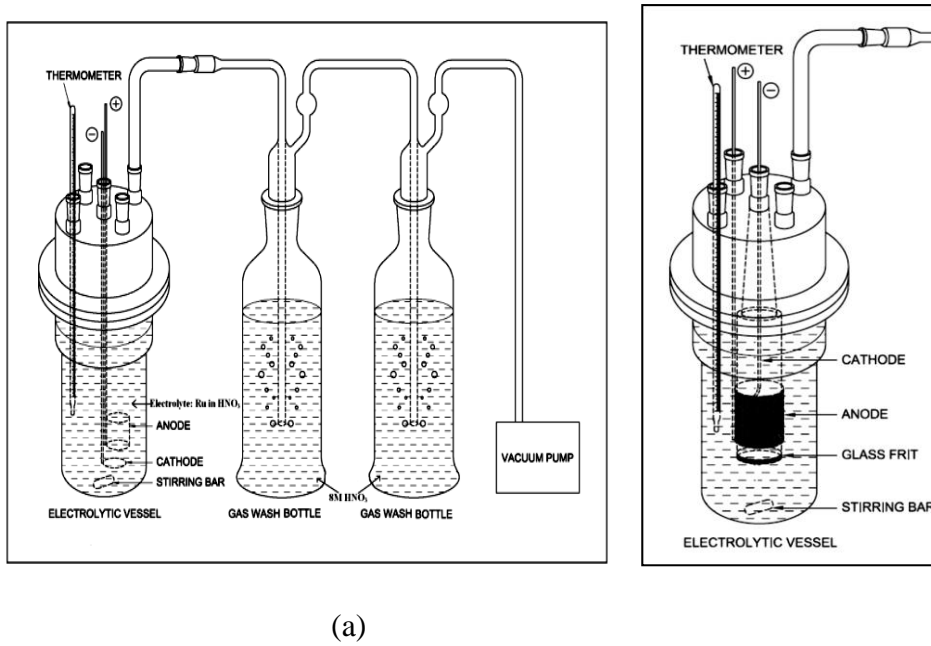
## 5.3 RESULTS AND DISCUSSION

### 5.3.1 Separation of Ruthenium Using Undivided Cell

#### 5.3.1.1 Effect of concentration of nitric acid

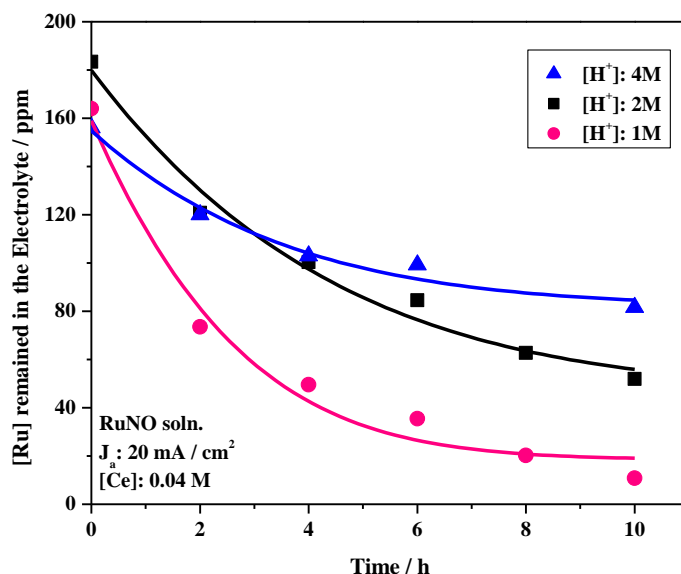
Prior to the electro-oxidation runs in undivided cell, separation of Ru was attempted in a divided cell, using a one end closed porous ceramic diaphragm tube to divide the anode and cathode compartments. Though oxidation of Ru species was effective, recovering Ru by trapping the vapour of RuO<sub>4</sub> was not successful due to its rapid decomposition and deposition as RuO<sub>2</sub> solid on the colder regions of the cell assembly and on the outer surface of the diaphragm tube just above the solution level. Preliminary experiments on the separation of Ru by electrolyzing [RuNO]<sup>3+</sup> solution in 4 M HNO<sub>3</sub> using the cell configuration shown in

Fig.5.1a at the  $J_a$  value of  $10 \text{ mA/cm}^2$ , without cerous ions and in the presence of 0.001 and 0.01 M  $\text{Ce}(\text{NO}_3)_3$  revealed the amount of Ru oxidized to be insignificant even at 333 K and after 6 h of electrolysis, whereas substantial quantity of Ru could be separated in the presence of 0.02 and 0.04M  $\text{Ce}(\text{NO}_3)_3$ . The separation percentage of Ru  $\{([\text{Ru}]_{\text{initial}} - [\text{Ru}]_{\text{final}})/[\text{Ru}]_{\text{initial}}\} \times 100$  from 500 ml of  $[\text{RuNO}]^{3+}$  solution in 4 M  $\text{HNO}_3$  was determined to be only 24 and 36 % after 6 h of electrolysis at 333 K in the presence of 0.04 M  $\text{Ce}(\text{NO}_3)_3$  and using the anodic  $J$  of 10 and 20  $\text{mA/cm}^2$  respectively. According to Motojima [7], complete removal of Ru was possible from 300 ml of 3 M nitric acid solution containing 333 ppm Ru, when electrolysis was performed for 6 h, using the anodic current density  $7 \text{ mA/cm}^2$  at 333 K and in the presence of 0.001M cerium in an undivided cell. The volume and concentration of nitric acid in the present study are higher than those reported by Motojima. Though the concentration of the redox catalyst and the current density used in the present work are higher than the values employed in Motojima's report, separation percentage could not be improved. The low separation yield is attributed to the high concentration of nitric acid in the solution, since separation of ruthenium is favoured at low concentrations of acid, and is corroborated by the observation that separation percentage of ruthenium was increasing with decrease in nitric acid concentration in the presence of Ag as redox catalyst [9]. Further, Motojima [7] did not mention the nature of the Ru species present in the solution. The increase in the separation percentage of Ru with decrease in nitric acid concentration is due to the formation of easily oxidizable ruthenium nitrosyl complexes in lower nitric acid solution which had been discussed in detail in Chapter 4 of this thesis.



**Fig. 5.1** (a): Schematic diagram of the undivided electrolytic cell; (b): Divided electrolytic cell.

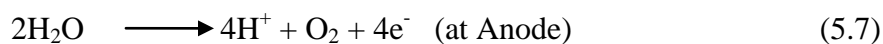
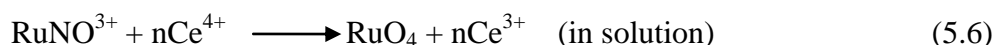
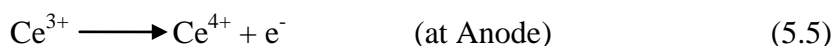
Figure 5.2 shows the results of electro-oxidation experiments conducted subsequently, at lower concentrations of nitric acid for longer duration for the purpose of obtaining better separation yield. In the presence of 0.04 M cerous ions, after 10 h of electrolysis with 20 mA/cm<sup>2</sup> as  $J_a$ , separation of Ru increased from 48 to 72 and 93 % when the nitric acid concentration decreased from 4 to 2 and 1 M respectively. As the initial concentration of Ru in 2 M nitric acid was 182 ppm when compared to 160 ppm in 1 and 4 M acid solutions, Fig. 5.2 indicates the concentration of Ru in the electrolyte with acidity as 2 M to be higher than that for the electrolyte in 4 M nitric acid up to about 3 h of electrolysis. Beyond 3 h, [Ru] remained in 4 M acid solution was higher than the amount of Ru in the electrolyte whose acidity was 2 M.



**Fig. 5.2** Dependence of acidity on the separation of Ru

### 5.3.1.2 Effect of anodic current density, cerium concentration and temperature

The separation percentage of Ru increased with increase in the anodic  $J$  and temperature. Increase in the rate of oxidation of Ru in the presence of Ce was because of the instantaneous oxidation of Ce(III) to Ce(IV) at the anode which in turn oxidized Ru to  $\text{RuO}_4$ , since Ce(IV) is a powerful oxidant with the Ce(IV)-Ce(III) potential of 1.71 V in nitric acid medium at ambient temperature [11]. As Ce is a fission product, its use as the redox catalyst will not complicate the separation process while oxidising the actual nuclear waste solution. The reactions which occur at the anode and cathode are listed below:



Separation of Ru from pure  $[\text{RuNO}]^{3+}$  solution in 1 M nitric acid solution was investigated to determine the effect of cerium concentration,  $J_a$  and temperature. As evidenced from Fig. 5.3, the separation of Ru increased with increase in  $J_a$ ,  $[\text{Ce}]$  and temperature, when electro-oxidation was continued for 10 h. The experimental conditions and the separation percentage of Ru from  $[\text{RuNO}]^{3+}$  solution in 1 M acid are listed in Table 5.1. It is observed that the separation of Ru increased from 81 to 93 % by increasing  $J$  from 10 to 20  $\text{mA}/\text{cm}^2$  and temperature from 313 to 318 K, in the presence of 0.04M cerous nitrate. Nevertheless, the same amount of Ru could be separated with 0.02 M Ce also under identical experimental conditions. Maximum separation could also be accomplished with a lower concentration of Ce and at low  $J_a$  by conducting electro-oxidation at marginally higher temperatures.

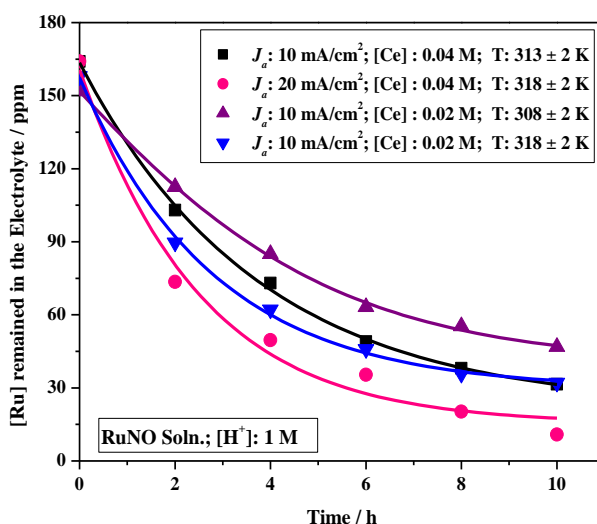


**Fig. 5.3** Variation in the separation of Ru with respect to anodic  $J$ , temperature and  $[\text{Ce}]$

**Table 5.1** The separation percentage of ruthenium from  $[\text{RuNO}]^{3+}$  solution of acidity 1 M

$J_a$ ( $\text{mA}/\text{cm}^2$ )	T (K)	$[\text{Ce}]$ (M)	Separation (%) after 10 h
10	$313 \pm 2$	0.04	81
20	$318 \pm 2$	0.04	93
10	$308 \pm 2$	0.02	69
10	$318 \pm 2$	0.02	80
20	$318 \pm 2$	0.02	95

### 5.3.1.3 Separation of Ru from simulated HLLW

Separation of Ru from SHLLW in 4 and 1 M nitric acid solutions by electro-oxidation was carried out with different experimental conditions. Separation of about 21 % only was possible after 10 h of electrolysis from SHLLW in 4 M HNO<sub>3</sub> at the anodic  $J$  of 10 mA/cm<sup>2</sup> in the presence of 0.04 M of Ce and this value increased to 47 % when the acid concentration was reduced to 1 M under identical experimental conditions. Increasing  $J$  to 20 mA/cm<sup>2</sup> could enhance the separation of Ru from SHLLW in 1 M nitric acid to about 54 % in the presence of 0.04 M cerium at 318 K. Compared to the near quantitative separation of 95 % of Ru from [RuNO]<sup>3+</sup> solution, the value of 54 % (listed in Table 5.2) obtained from the simulated liquid waste is very low. No reliable explanation could be offered for the lower separation percentage of Ru from SHLLW at this stage, without analyzing the chemical state of Ru bearing species in nitric acid medium in the presence of other metallic ions. Apparently, the large amount of nitrite ions in the waste also could have contributed to the low separation yield of Ru. To minimize the interference of nitrite ions produced at the cathode (Eq. 5.1) during the oxidation reaction of Ru at the anode, a divided cell with glass frit as the diaphragm was fabricated and employed for further studies.

**Table 5.2** The separation percentage of Ru from simulated HLLW

Acidity (M)	[Ce] (M)	Current Density (mA/cm <sup>2</sup> )	Separation of Ru
4	0.04	10	21 %
1	0.04	10	47 %
1	0.04	20	54 %

### 5.3.2 Divided Cell with Glass Frit as Diaphragm

To improve the efficiency in the separation of Ru from SHLLW, another set of electro-oxidation experiments were carried out using a divided cell with glass frit as diaphragm (Fig. 5.1b). Initially, 50 ml of the anolyte ( $[\text{RuNO}]^{3+}$  solution or SHLLW prepared in 4 M  $\text{HNO}_3$ ) was electrolysed with  $20 \text{ mA/cm}^2$  as  $J_a$  at 313 K (anode and cathode: Pt mesh and a Pt wire of surface area 38 and  $4 \text{ cm}^2$  respectively). Under these experimental conditions the separation of Ru was 92 and 94 % from  $[\text{RuNO}]^{3+}$  solution and SHLLW respectively after electrolysis for 6 h without any redox mediator. The migration of nitrous acid (produced at the cathode owing to the reduction of nitric acid) towards the anode was restricted by the glass frit diaphragm. Thus, its concentration in the anolyte was not sufficient to suppress the oxidation of Ru species and hence, high separation yield of Ru could be obtained even from SHLLW in the cell with glass frit.

### 5.3.2.1 Effect of volume, concentration of redox catalyst and acid

Electro-oxidation runs were conducted under similar experimental conditions as stated above (Section 5.3.2) with higher volume of electrolyte in the divided cell assembly using glass frit to separate anolyte and catholyte; the electrodes were Pt mesh anode of surface area  $84 \text{ cm}^2$  and Pt wire cathode of area  $9 \text{ cm}^2$ . As expected the separation percentage of Ru decreased with increase in the volume of anolyte. The separation from pure  $[\text{RuNO}]^{3+}$  solution decreased from 92 to 81 and to 57 % respectively when 110, 220 and 440 ml of the anolyte were oxidized for 6 h.

To improve the separation percentage for higher volume of the anolyte, electrolysis was performed in the presence of the redox catalyst Ce and also with low acid concentration. The variation in the separation of Ru with respect to time during the electrolysis of 440 ml of pure  $[\text{RuNO}]^{3+}$  solution and SHLLW ( $[\text{HNO}_3]$ : 4 M) using  $20 \text{ mA/cm}^2$  as the anodic current density at  $313 \pm 2 \text{ K}$  with and without Ce is shown in Fig. 5.4. About 75 and 80 % of Ru could be separated without Ce and 74 and 83 % of Ru were separated in the presence of 0.02

M Ce from pure  $[\text{RuNO}]^{3+}$  solution and SHLLW respectively after electrolyzing for 10 h. These results revealed that the redox catalyst Ce did not influence the separation of Ru in the cell with glass frit as diaphragm.

For the purpose of comparing the efficiency of the oxidation process using divided and undivided cell assemblies, yet another set of experiments were carried out after removing the glass frit in the divided cell. The results under identical experimental conditions plotted in Fig. 5.5 indicated a different trend when compared to the results obtained with divided cell. Electrolysis of 440 ml of pure  $[\text{RuNO}]^{3+}$  solution and SHLLW ( $[\text{HNO}_3]$ : 4 M) with 20  $\text{mA}/\text{cm}^2$  as  $J_a$  at  $313 \pm 2$  K yielded about 5 and 16 % Ru without Ce and about 74 and 48 % with 0.02 M Ce respectively after 10 h of electrolysis. It is evident from Fig. 5.5 that separation of Ru is efficient only in divided cell. The behaviour of SHLLW in the undivided cell requires to be investigated, by conducting more experiments with different process parameters and evaluating the influence of interfering metal ions on the electro-oxidation of Ru. The separation percentage of Ru increased marginally from 74 to 83 % (Fig. 5.6) after 10 h of electrolysis of 440 ml of  $[\text{RuNO}]^{3+}$  solution in a divided cell with 20  $\text{mA}/\text{cm}^2$  as the anodic current density and at  $313 \pm 2$  K, when the concentration of nitric acid was decreased from 4 to 1 M.

### 5.3.2.2 Constant potential experiments

The average potential measured during the electro-oxidation of Ru from pure  $[\text{RuNO}]^{3+}$  solution in constant current mode in the divided cell was 3.6 V. The results obtained in the separation of Ru by conducting experimental runs with constant potentials of 2 and 3 V instead of constant current have been tabulated in Table 5.3. About 30 and 77 % of Ru could be separated after 10 h of electrolysis of 440 ml of anolyte. At potentials below 2 V, the separation yield was very low; whereas at potentials higher than 3 V, the temperature of the cell could not be controlled owing to IR heating. Significant variation could not be observed

in the separation of Ru by electro-oxidation in constant current and constant potential modes. The results presented in Section 5.3.2 clearly depict that near quantitative separation of Ru from SHLLW in 4 M HNO<sub>3</sub> is possible in a divided cell with glass frit as the diaphragm and without any redox catalyst.

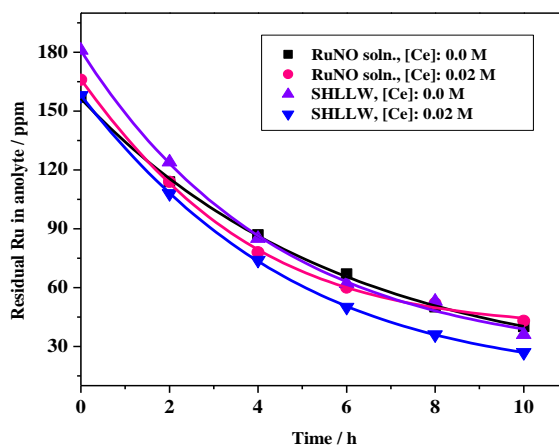


**Fig. 5.4** Variation in the separation of Ru from pure [RuNO]<sup>3+</sup> solution and SHLLW during electrolysis in the cell with glass frit as diaphragm; Volume of anolyte: 440 ml;  $J_a$ : 20 mA/cm<sup>2</sup>; T: 313 K; [H<sup>+</sup>]: 4 M

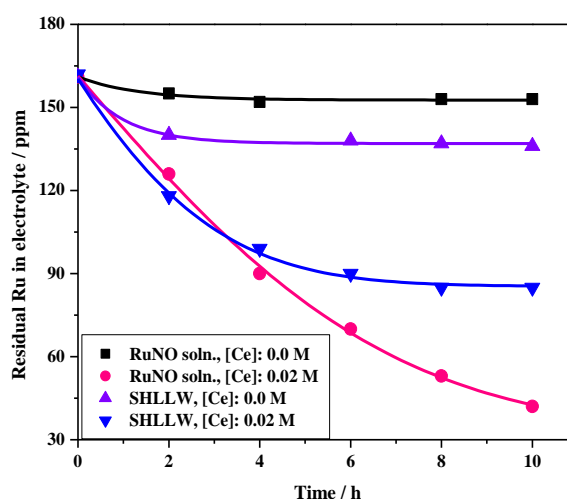


**Fig. 5.5** Separation of Ru from [RuNO]<sup>3+</sup> solution and SHLLW in undivided cell (without glass frit); Volume of anolyte: 440 ml;  $J_a$ : 20 mA/cm<sup>2</sup>; T: 313 K; [H<sup>+</sup>]: 4 M

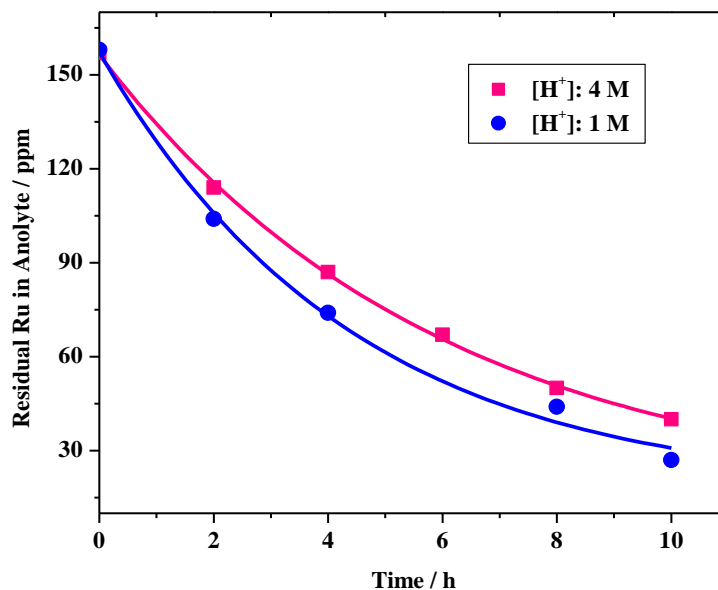


**Fig. 5.6** Comparison of separation yield of Ru from pure  $[\text{RuNO}]^{3+}$  solution at 4 and 1 M acidity in the divided cell; Volume of anolyte: 440 ml;  $J_a$ : 20 mA/cm<sup>2</sup>; T: 313 K

**Table 5.3** Percentage separation of Ru from  $[\text{RuNO}]^{3+}$  solution of acidity 4 M in the divided cell by constant potential electrolysis; Volume of anolyte: 440 ml; Anode: Pt mesh of surface area 84 cm<sup>2</sup>; Cathode: Pt wire of surface area 9 cm<sup>2</sup>

$[\text{H}^+]$ (M)	Potential (V)	Temperature (K)	Current (A)	Separation (%)
4	2	303	0.09 - 0.1	30
4	3	306	0.7 - 0.8	77

### 5.3.3 Cyclic Voltammetric Analysis

Section 5.3.2 dealt with the separation of ruthenium from nitric acid media by electro-oxidation method involving a two electrode system in either constant current or potential mode. Though good separation percentage was accomplished, the energy efficiency in this process was not appreciable due to the competing side reactions like water oxidation, in addition to the formation of intermediates during the oxidation of  $[\text{RuNO}]^{3+}$  ions. Hence, to

understand the oxidation behaviour of Ru bearing solutions in nitric acid during electrolysis, cyclic voltammetric studies were carried out employing Au and Pt as working electrodes.

Figure 5.7 portrays the cyclic voltammogram recorded with the scan rate of 100 mV/s for  $[\text{RuNO}]^{3+}$  solution (containing 5 mM Ru in 0.15 M  $\text{HNO}_3$ ) using Au working electrode. The anodic peak (peak  $I_a$ ) during the positive direction of scanning (0.0 to + 1.6 V vs Ag/AgCl reference) probably corresponds to water oxidation and/or oxidation of  $[\text{RuNO}]^{3+}$  and thereafter a surge in anodic current was observed at the potential of + 1.28 V (vs Ag/AgCl) culminating into a small hump around + 1.49 V (vs Ag/AgCl). Perhaps, the simultaneous oxidation of  $[\text{RuNO}]^{3+}$  to higher oxidation states of Ru (up to  $\text{Ru}^{8+}$ ) could have taken place in the potential range from 1.28 to 1.49 V [9]. During the negative scan, a cathodic peak ( $I_c$ ) appeared at 0.86 V (vs Ag/AgCl). The cyclic voltammogram of  $[\text{RuNO}]^{3+}$  solutions in 1 M acid (containing 5, 20 and 40 mM of Ru) at Pt as working electrode are shown in Fig. 5.8. During the anodic scan, a surge in the anodic current occurred at about 1.25 V and the current increased with increase in the concentration of Ru from 5 to 40 mM, which could be due to oxidation of Ru to  $\text{RuO}_4$ . The formation of  $\text{RuO}_4$  at this potential range (1.25–1.6 V) was confirmed directly by chronocoulometry at 1.25 and 1.5 V (vs Ag/AgCl). Controlled potential electrolysis of  $[\text{RuNO}]^{3+}$  solution ([Ru]: 160 ppm and  $[\text{HNO}_3]$ : 1 M) carried out in a divided cell with glass frit as diaphragm ascertained the formation of  $\text{RuO}_4$  as black deposition of  $\text{RuO}_2$  (produced by the instantaneous reduction of the unstable  $\text{RuO}_4$  vapour over the stem of the electrode surface). Formation of  $\text{RuO}_4$  was also confirmed from the UV-Vis spectra of the anolyte recorded during electrolysis (Fig. 5.9), in which, the absorbance recorded in the wave length region of 360-400 nm corresponded to ruthenium tetroxide [12].

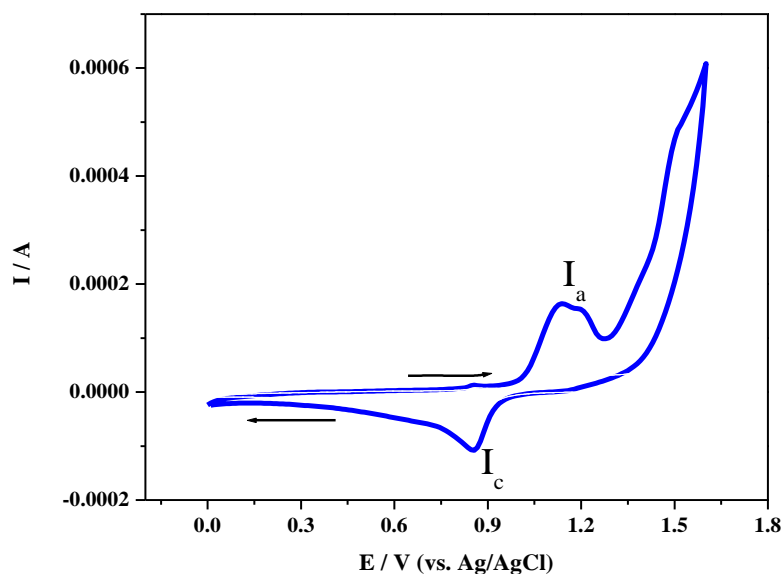


**Fig. 5.7** Cyclic voltammogram of 5 mM  $[\text{RuNO}]^{3+}$  solution ( $[\text{H}^+]$ : 0.15 M) recorded with Au working electrode; CE: Pt; Reference: Ag/AgCl; Scan rate: 100 mV/s; T: 298 K

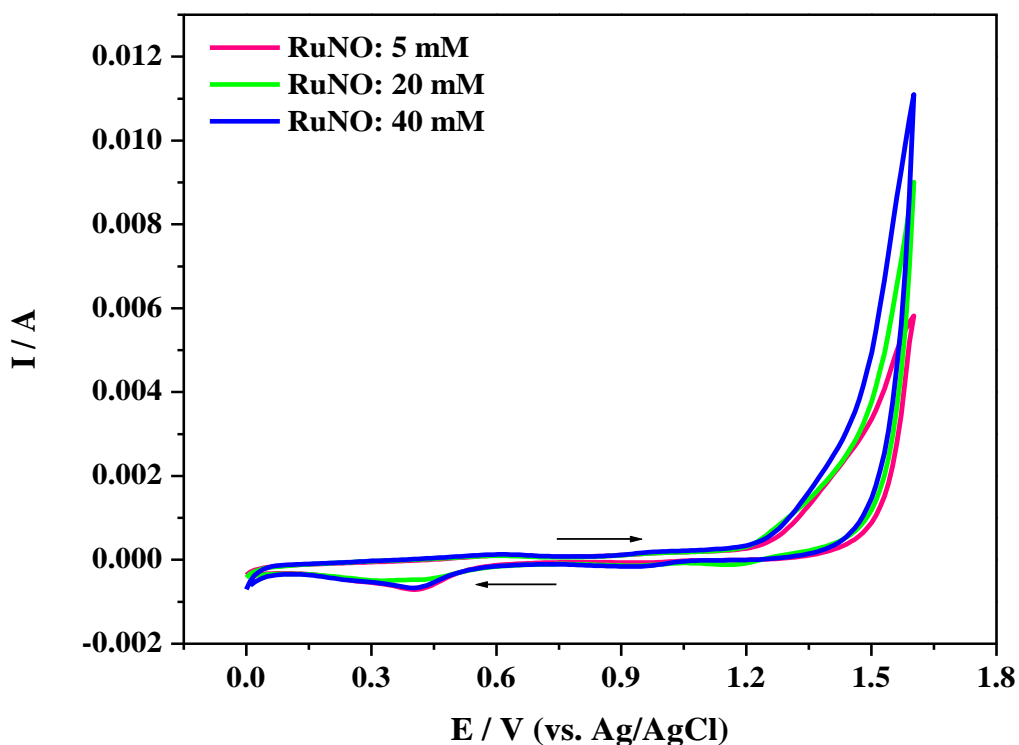


**Fig. 5.8** Cyclic voltammograms of 5, 20 and 40 mM  $[\text{RuNO}]^{3+}$  solutions ( $[\text{H}^+]$ : 1 M) recorded with Pt working electrode; CE: Pt; RE: Ag/AgCl; Scan Rate: 100 mV/s; T: 298 K

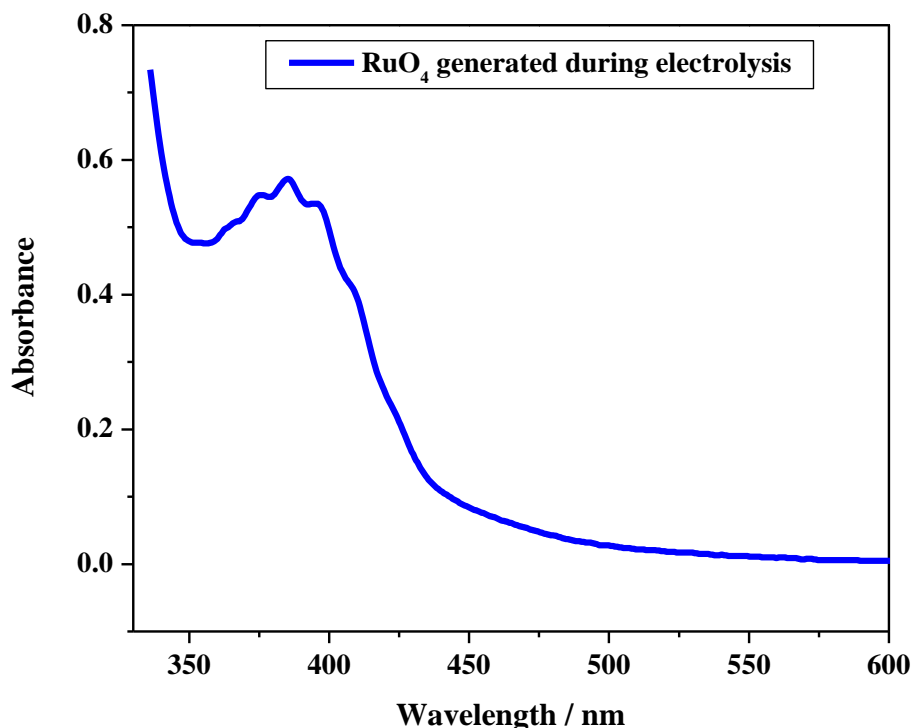


**Fig. 5.9** The UV-Visible spectra of RuO<sub>4</sub> formed during chronocoulometric study

A detailed investigation of the CV runs with different acid concentrations and Ru content at different scan rates, including the analysis of the species in the electrolyte just after the oxidation/reduction reaction is warranted to interpret the CV results. This exercise of identifying the oxidation and reduction peaks in the cyclic voltammograms is discussed in Chapter 6.

### 5.3.4 Recovery of Ruthenium

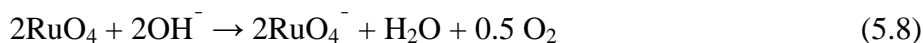
The NO<sub>x</sub> and RuO<sub>4</sub> vapour generated during the electro-oxidation of Ru bearing species were trapped together in 8 M HNO<sub>3</sub>. The idea of trapping RuO<sub>4</sub> and NO<sub>x</sub> in nitric acid is that NO<sub>x</sub> gas facilitates the transformation of RuO<sub>4</sub> to stable nitrosyl ruthenium complex [13-15] and thus, it is possible to regenerate the ruthenium nitrosyl based solution and also to estimate the Ru recovered accurately. During the electrolysis of ruthenium solution in 4 M nitric acid, the NO<sub>x</sub> gas generated was found to be sufficient for converting RuO<sub>4</sub> to [RuNO]<sup>3+</sup> complex, which could be ascertained from the reddish brown colour of trap solution.

Separation of ruthenium was maximum in the electrolysis of Ru bearing solutions in 1 M nitric acid medium; however, the amount of  $\text{NO}_x$  generated at cathode in this case, was not adequate to convert the  $\text{RuO}_4$  vapour into  $[\text{RuNO}]^{3+}$  complex and hence, pale green colour (colour of  $\text{RuO}_4$ ) in the trap solution was visible unlike the reddish brown colour of trap solution when electrolysis of ruthenium solution was conducted in 4 M nitric acid. Therefore, a fraction of  $\text{RuO}_4$  was converted to ruthenium nitrosyl complex and back diffusion of the remaining portion occurred from the trap. The back diffused  $\text{RuO}_4$  was observed to decompose to lower black oxide ( $\text{RuO}_2$ ) and deposit over the inner wall of the glass electrolytic vessel just above the electrolyte solution as well as on the glass tube which connected the electrolytic vessel and gas wash bottle (Fig. 5.10). The back diffusion and deposition of ruthenium oxide vapour decreased the percentage recovery of Ru. Therefore, for complete conversion of the trapped  $\text{RuO}_4$  vapour generated from lower acidities into ruthenium nitrosyl complex,  $\text{NO}_x$  gas had to be admitted externally into the trap until the colour of the solution changed from pale green to reddish brown.

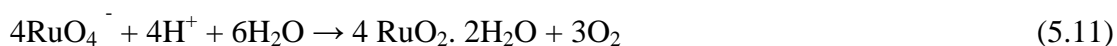
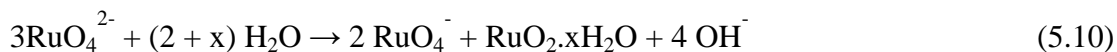
Mun et al. [16] reported that decomposition of  $\text{RuO}_4$  occurs in the gas phase and presence of steam as well as already deposited ruthenium dioxide play a catalytic role in the decomposition and the rate of decomposition increases with increasing temperature. The half life times of  $\text{RuO}_4$  in the presence of steam were found to be 9 and 5 h at 313 and 363 K respectively. These authors had proposed a mechanism for the decomposition of  $\text{RuO}_4$  with and without steam and indicated the formation of the end product,  $\text{RuO}_2$  via the intermediates  $\text{RuO}_3$ , diruthenium pentoxide ( $\text{Ru}_2\text{O}_5$ ) and hyperruthenic acid ( $\text{H}_2\text{RuO}_5$ ). Sakurai et al. [17] claimed that the deposited material was a peroxy – bonded polymeric  $(\text{RuO}_4)_n$  and other reports [18, 19] suggested oxyhydroxides of Ru(IV),  $\text{RuO}(\text{OH})_2$  and also hydrous or anhydrous non-volatile  $\text{RuO}_2$  species in the deposit.

In an electro-oxidation experiment of pure  $[\text{RuNO}]^{3+}$  solution in 1 M nitric acid, performed with  $10 \text{ mA/cm}^2$  as  $J_a$  in the presence of 0.02 M cerium ions as the redox catalyst, the initial quantity of Ru in the electrolyte was 75.9 mg and after electrolysis for 10 h, the amount of Ru remained was 23.4 mg, accounting for the total conversion of 52.5 mg of Ru to  $\text{RuO}_4$ . The amount of Ru collected in the nitric acid trap was 44.3 mg, which accounted for the recovery of 84 % of ruthenium in the acidic trap; the rest would have got deposited as lower oxide of ruthenium.

Basic trap of 0.5 M NaOH solution was also tried in some of the experiments since  $\text{RuO}_4$  forms stable ruthenate ( $\text{RuO}_4^{2-}$ ) and perruthenate ( $\text{RuO}_4^-$ ) complexes [20] in the basic medium.



Matrix interference of Na created difficulty in the estimation of ruthenium by ICP-OES analysis; nevertheless, the interference could be minimised by diluting the alkali solution to required concentration, since the concentration of ruthenium separated in the present study was high. Yet another difficulty which restricted the accurate determination of ruthenium is the decomposition of ruthenate and perruthenate to hydrated ruthenium dioxide in the trap solution [21, 22].



Thus, the concentration of ruthenium in the trap solution started to decrease over a period of time, which was confirmed by the UV-Visible spectra of trap solution recorded at different times (Fig.5.11) and thereby, preventing the accurate estimation of Ru. Since the amount of  $\text{RuO}_2 \cdot \text{H}_2\text{O}$  formed in the trap was not significant, collection of it and determination of Ru concentration was difficult.

In nuclear industry, in order to avoid the spread of contamination all over the equipment owing to  $\text{RuO}_4$  vapour and its decomposition over the wall of equipment as solid lower oxide, it is essential to trap  $\text{RuO}_4$  immediately after its formation. For the purpose of completely restricting the  $\text{RuO}_4$  vapour escaping from the anolyte solution and subsequently getting deposited over the wall of the electrolytic vessel, the organic phase, n-paraffin hydrocarbon (NPH) was kept over the electrolyte as was done by Motojima [7]. NPH facilitated the instantaneous reduction of  $\text{RuO}_4$  formed during electrolysis to black solid  $\text{RuO}_2$  and hence, there was no black deposit of Ru over the wall of glass vessel (Fig. 5.12). Ruthenium dioxide could be filtered off from NPH using cellulose filter paper.

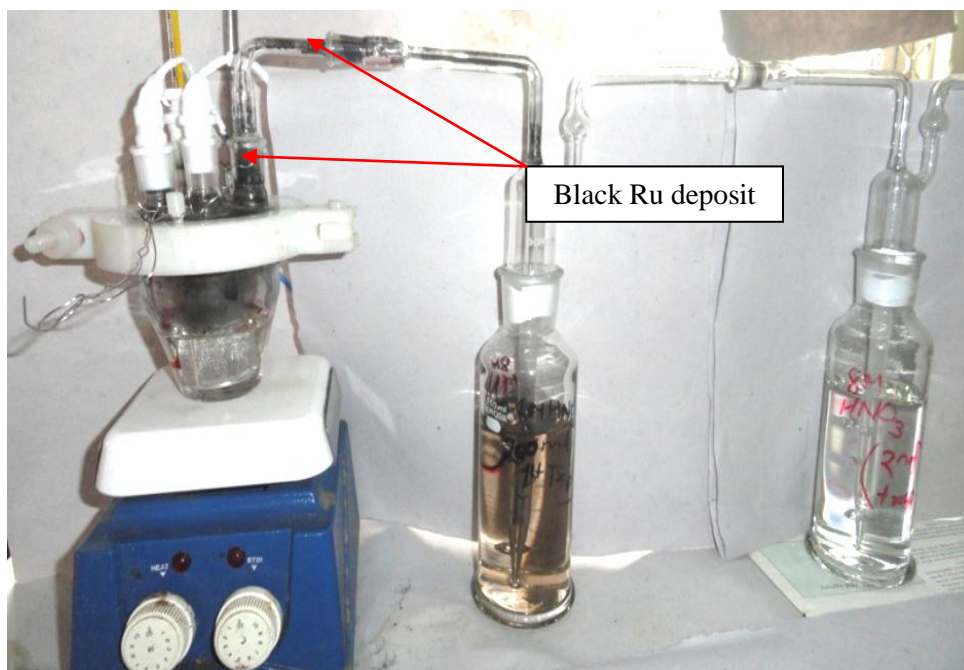


**Fig. 5.10** Decomposition of  $\text{RuO}_4$  and deposition as black lower oxide of Ru over the inner wall of electrolytic vessel

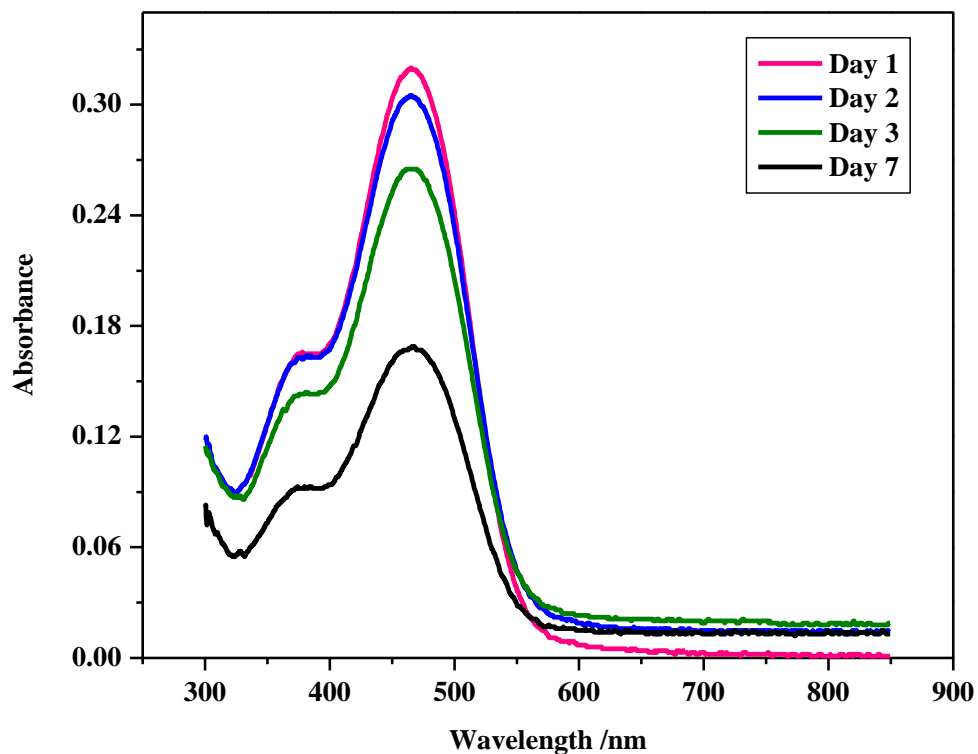


**Fig. 5.11** UV-Vis spectra of ruthenate and perruthenate in NaOH trap solution

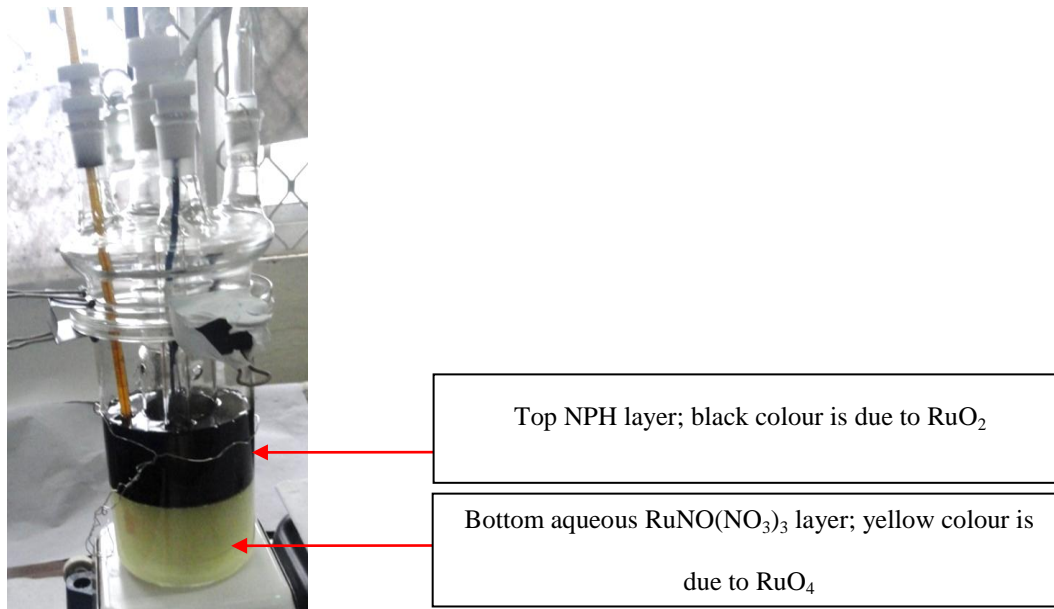


**Fig. 5.12** Trapping of  $\text{RuO}_4$  by n- paraffin hydrocarbon

## 5.4 CONCLUSIONS

A simple and inherently safe electrochemical process for the separation of Ru from the simulated waste solution is demonstrated for the purpose of eliminating the spreading of

contamination during vitrification of high level liquid waste. Separation up to 95 % Ru could be achieved from ruthenium nitrosyl nitrate solution in 1 M nitric acid when electrolysis was conducted for 10 h with the anodic current density as  $20 \text{ mA/cm}^2$  at 318 K and with 0.02 M cerous ions. Under identical conditions, the amount of Ru separated from SHLLW was only 54 %, due to the interference of nitrite ions present in the waste. A divided cell with glass frit as diaphragm eliminated the interference caused by nitrite ions. In the divided cell 74 and 80 % of Ru was separated from pure  $[\text{RuNO}]^{3+}$  solution and SHLLW respectively in 4 M  $\text{HNO}_3$  solution after electrolyzing for 10 h at  $20 \text{ mA/cm}^2$  anodic current density, without any redox mediator. n-paraffin oil above the electrolyte served as a better trap for gaseous  $\text{RuO}_4$ , thereby, preventing the deposition of  $\text{RuO}_2$  on the wall of the vessel. Oxidation of Ru to  $\text{RuO}_4$  in the potential range 1.28-1.49 V (vs Ag/AgCl) on the surface of gold electrode was ascertained from cyclic voltammetric investigations. Modification in the design of the electrolytic cell with glass frit as diaphragm to prevent the deposition of  $\text{RuO}_2(\text{s})$  within the cell and estimating the energy efficiency of the process in proto-type cell assembly are required prior to implementing the electro-oxidation process in the plant for the separation and recovery of radioactive Ru. However, this systematic parametric study recommends the separation of Ru from waste solutions in higher concentration of acid, using the divided cell assembly without any redox catalyst for improved separation efficiency, since in the PUREX process waste, Ru exists in the form of nitrosyl nitrate complexes in 4 M nitric acid.

## 5.5 REFERENCES

1. Kosyakov, V.N., Marchenko, V.I., *Radiochem.*, 50 (2008) 333
2. Griess, J.C. Jr., *J. Electrochem. Soc.*, 100 (1953) 429
3. Lietzke, M.H., Griess, J.C. Jr., *J. Electrochem. Soc.*, 100 (1953) 434
4. Kobayashi, Y., Yamatera, H., Okuno, H., *Bull. Chem. Soc. Japan*, 38 (1965) 1911

5. Ozawa, M., Suzuki, T., Koyama, S., Fujii, Y., *Prog. Nucl. Energy*, 47 (2005) 462
6. Jayakumar, M., Venkatesan, K.A., Srinivasan, T.G., *J. Radioanal. Nucl. Chem.*, 284 (2005) 79
7. Motojima, K., *J. Nucl. Sci. Technol.*, 27 (1990) 262
8. Yoneya, M., Kawamura, K., Torata, S.I., Takahashi, T., U S Patent, No. 5437847, 1995
9. Mousset, F., Bedioui, F., Eysseric, C., *Electrochem. Commun.*, 6 (2004) 351
10. Satyabrata, M., Falix, L., Srinivasan, R., Pandey, N.K., Mallika, C., Koganti, S.B., Kamachi Mudali, U., *J. Radioanal. Nucl. Chem.*, 285 (2010) 687
11. Sini, K., Mishra, S., Falix, L., Mallika, C., Koganti, S.B., *Radiochim. Acta*, 99 (2011) 23
12. Aswegen, W.V., The kinetics and associated reactions of ruthenium (VIII). Dissertation (MS). Nelson Mandela Metropolitan University, 2009
13. Boswell, G.G.J., Soentono, S., *J. Inorg. Nucl. Chem.*, 43 (1981) 1625
14. Igarashi, H., Kato, K., Takahashi, T., *Radiochim. Acta*, 57 (1992) 51
15. Fletcher, J.M., Jenkins, I.L., Lever, F.M., Martin, F.S., Powell, A.R., Todd, R., *J. Inorg. Nucl. Chem.*, 1 (1955) 378
16. Mun, C., Cantrel, L., Madic, C., *Radiochim. Acta*, 95 (2007) 643
17. Sakurai, T., Hinatsu, Y., Takahashi, A., Fujisawa, G., *J. Phys. Chem.*, 89 (1985) 1892
18. Mun, C., Ehrhardt, J.J., Lambert, J., Madic, C., *Appl. Surface Sci.*, 253 (2007) 7613
19. Holm, J., Glanneskog, H., Ekberg, C., *J. Nucl. Mater.*, 392 (2009) 55
20. Seddon, E.A., Seddon, K.R., The Chemistry of Ruthenium, Monograph 19, Elsevier, Amsterdam, pp. 51, 1984
21. Connick, R.E., Hurley, C.R., *J. Am. Chem. Soc.*, 74 (1952) 5012
22. Mun, C., Cantrel, L., Madic, C., *Nucl. Technol.*, 156 (2006) 332

---

## 6. CONSTANT POTENTIAL ELECTRO-OXIDATION AND REDUCTION BEHAVIOUR OF $[\text{RuNO}]^{3+}$ IN NITRIC ACID

---

### 6.1 INTRODUCTION

Among the various methods available for the separation of Ru, one of the promising techniques in nuclear industry is the electro-oxidation method, since in this method addition of external reagents to the feed is not involved, which is preferred for the treatment and disposal of the high level liquid waste (HLLW). Separation of Ru as volatile  $\text{RuO}_4$  by electrolytic oxidation and as metal by electrolytic reduction has been widely attempted by many researchers [1-5]. The separation yield of Ru is very less in the electro-deposition process and a large portion of Ru remains in the electrolyte solution; however, quantitative removal of Ru can be accomplished by the electro-oxidation method. Separation of Ru by electro-oxidation was performed by Motojima [1] and Mousset et al. [3] in constant current mode using Ce and Ag as redox mediators respectively, in divided and undivided cell assemblies. Parametric studies conducted for the separation of Ru from ruthenium nitrosyl  $[\text{RuNO}]^{3+}$  solution as well as from simulated high level liquid waste (SHLLW) by electro-oxidation in constant current mode in the presence of Ce as the redox mediator using divided and undivided electrolytic cells, for the present thesis has been discussed in Chapter 5. Though good separation percentage of Ru was accomplished in constant current electro-oxidation, the energy efficiency in this process was not appreciable due to the competing side reactions like water oxidation. Hence, to understand the oxidation behaviour of Ru bearing solutions in nitric acid during electrolysis, cyclic voltammetric (CV) studies were carried out, employing Au and Pt as working electrodes (Chapter 5). A fundamental study on the constant potential electro-oxidation of Ru under various experimental conditions i.e. temperature and promoter element, Ce was carried out by Sato et al. [6] to improve the efficiency and rate of

oxidation of Ru at lower potentials. Yoneya et al. [2] separated Ru quantitatively from HLLW by applying a constant potential of 1.85 V/SSE to Pt working electrode using a divided electrolytic cell. In order to obtain good separation percentage as well as better energy efficiency of the process, separation of ruthenium was carried out in the present study by constant potential electro-oxidation using the process parameters derived from cyclic voltammetric studies.

As discussed in Chapter 1, the chemistry of Ru is very complex due to large range of oxidation states (from 0 to +8 and also -2). In nitric acid medium, ruthenium forms hundreds of  $[\text{RuNO}]^{3+}$  complexes with the general formula  $[\text{RuNO}(\text{NO}_3)_x(\text{NO}_2)_y(\text{OH})_z(\text{H}_2\text{O})_{5-x-y-z}]^{3-x-y-z}$  [7-12]. Since these complexes have the ability to exchange ligands, the composition of the solution containing a mixture of ruthenium nitrosyl complexes depends on the concentration of nitric acid, temperature, ruthenium species present initially and the time elapsed since its formation because of inter-conversion of different nitrosyl complexes with different half times [13]. During the aqueous reprocessing of spent nuclear fuels by PUREX process, some of the complexes of Ru, mainly trinitrato ruthenium nitrosyl complexes,  $[(\text{RuNO})^{3+}(\text{NO}_3)_3(\text{H}_2\text{O})_2]$  get extracted to the organic phase, 30 % TBP along with U and Pu and contaminate the product stream. Investigating the behaviour of the reduced species of  $[\text{RuNO}]^{3+}$  complexes namely,  $[\text{RuNO}]^{2+}$  is desirable, since conversion of  $[\text{RuNO}]^{3+}$  complexes to lower oxidation state would provide a means for separating Ru from U and Pu during PUREX process. The electrolytic reduction of ruthenium nitrosyl complexes was studied by many researchers in different acid media [14-19]; however, no reliable study has been in nitric acid medium except for a single study on the oxidation of ruthenium nitrosyl complexes in nitric acid medium [20].

The first half of the present Chapter deals with the separation of Ru from pure  $[\text{RuNO}]^{3+}$  solution and from simulated HLLW (SHLLW) by performing constant potential

electro-oxidation at various applied potentials, nitric acid concentration, temperature and in the presence of redox mediator, Ce. The efficiency of separation of Ru under these experimental conditions has been discussed, in addition to the determination of rate constant and activation energy for the oxidation of Ru.

The second part of this Chapter describes the study of the electrolytic reduction of ruthenium nitrosyl complex  $[\text{Ru}^{\text{II}}\text{-NO}^+]^{3+}$  and its electrochemical behaviour in nitric acid medium using the potentiostatic electrolysis techniques, cyclic voltammetry (CV) and chronopotentiometry (CP) at Pt and glassy carbon working electrodes and Ag/AgCl reference electrode.

## **6.2 EXPERIMENTAL**

### **6.2.1 Chemicals**

Standard solutions of ruthenium nitrosyl nitrate with the concentration of Ru as 160 ppm in 1, 2 and 4 M nitric acid were prepared by diluting commercially available ruthenium nitrosyl nitrate solution (1.7 % Ru in 9 M nitric acid, supplied by M/s. Arora Matthey Ltd, Kolkata). Cerium(III) nitrate hexa hydrate (AR grade, Min. assay: 99 %) procured from M/s. SDFCL, Mumbai was used as the redox mediator during electrolysis. For performing cyclic voltammetric and chronopotentiometric measurements, standard solutions of ruthenium nitrosyl containing 40 mM of Ru in 1 M nitric acid was prepared. A synthetic HLLW solution simulated with fission and corrosion product elements envisaged in the reprocessed waste of the spent mixed carbide fuel of fast breeder test reactor (FBTR) at Kalpakkam was prepared in 4 M  $\text{HNO}_3$ . The chemical form of the elements and their concentration in the simulated waste solution (Table 3.2, Chapter 3) are reported elsewhere [21]. The waste solution thus prepared was diluted suitably to adjust the concentration of ruthenium to be 160 ppm (which is the concentration of Ru in the actual waste) in 4 M  $\text{HNO}_3$ .

### 6.2.2 Electro-volatilization Cell

Separation of Ru by electro-oxidation was conducted at platinum mesh (surface area:  $34 \text{ cm}^2$ ) working electrode (WE), with platinum mesh (SA:  $20 \text{ cm}^2$ ) as the counter electrode (CE) and double junction Ag/AgCl as reference electrode (supplied by M/s. Metrohm India Ltd, Chennai) using a divided cell with glass frit as diaphragm (the schematic of which is shown as Fig. 1a in Chapter 5). The electro-oxidation studies were performed by chronoamperometric method at various applied potentials, temperatures and in the presence of redox mediator Ce. Catholyte (10 ml) and cathode were taken inside the glass frit which was fused to a glass tube suspended into the cell from the centre of the lid. Anolyte (50 ml) and Pt mesh working electrode along with Ag/AgCl reference electrode were placed outside the glass frit in the cell vessel. The  $\text{RuO}_4$  gas generated owing to oxidation of ruthenium at anode was absorbed in the gas wash bottles containing 0.5 M NaOH solution. During electrolysis, samples of the anolyte were taken out at regular intervals of time for analyzing the concentration of Ru. Estimation of ruthenium was by Inductively Coupled Plasma-Optical Emission Spectroscopic (ICP-AES, Jobin Yvon, France) analysis and the standards were produced by MBH Analytical Ltd, UK.

### 6.2.3 Electrochemical Measurements

Solutions of  $[\text{RuNO}]^{3+}$  (containing 5, 20 and 40 mM of Ru) in different concentrations of nitric acid were prepared for performing cyclic voltammetric measurements in order to understand the electrochemical oxidation behaviour of  $[\text{RuNO}]^{3+}$  in acidic medium. CV runs were carried out at 298 K in a standard three-electrode cell comprising a Pt wire (surface area:  $0.42 \text{ cm}^2$ ) or Au wire (surface area:  $0.2 \text{ cm}^2$ ) as WE, Pt mesh as CE and standard Ag/AgCl (SSE) reference electrode (RE). Cyclic voltammograms were recorded at the potential scan rate of 50 mV/s, starting with the anodic scan and reversal of the scan at the anodic switching potential in the range 0-1.8 V (vs SSE). Electrochemical studies on the

reduction of ruthenium nitrosyl complex were conducted in the cell configuration shown in Fig.6.1, in which a Pt foil (SA:  $1.2 \text{ cm}^2$ ) and Ag/AgCl were used as the CE and RE respectively. Platinum and Glassy carbon working electrodes were used separately. 25 ml of ruthenium nitrosyl solution containing 5, 20 and 40 mM ruthenium in 1M nitric acid were taken as the electrolyte. The voltammograms were recorded at different scan rates in the range  $0.01 - 0.1 \text{ Vs}^{-1}$ . De-oxygenation of the test solutions prior to the scans was done by flushing with argon and the results were analysed after IR compensation. Similar to CV, chronopotentiograms were recorded by applying very small increments of current to the system. Reduction of the ruthenium nitrosyl complex,  $[\text{RuNO}]^{3+}$  was carried out by chronoamperometry and the reduced Ru species generated was characterized by UV-Visible spectrophotometry. Chemito Spectroscan, UV 2600 double beam UV Vis spectrophotometer was used for recording the spectra. Bulk electrolysis was carried out in a divided electrolytic cell with glass frit as the diaphragm. Pt mesh of SA:  $34 \text{ cm}^2$  and SA:  $\sim 20 \text{ cm}^2$  were used as working and counter electrodes respectively along with the reference electrode. The potentiostatic and constant potential electro-oxidation studies were carried out using Comprehensive Autolab (Model PGSTAT-30; Eco-Chemie, the Netherlands) electrochemical system equipped with General Purpose Electrochemical Software.

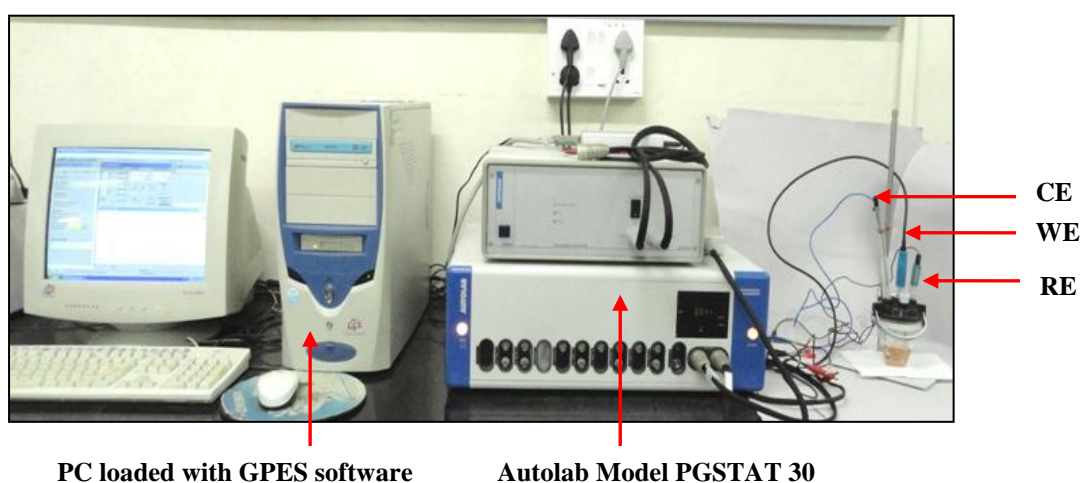


**Fig. 6.1** Cell assembly for electrochemical studies

## 6.3 RESULTS AND DISCUSSION

### 6.3.1 Separation of Ruthenium by Constant Potential Electro-oxidation

The separation percentage of Ru by anodic oxidation was calculated using the following equation,

$$\text{Separation \%} = \frac{[\text{Ru}]_{\text{Initial}} - [\text{Ru}]_{\text{Final}}}{[\text{Ru}]_{\text{Initial}}} \times 100 \quad (6.1)$$

Faradaic efficiency is defined by the relation,

$$\eta = \frac{\Delta m}{\Delta m^0} \times 100 \quad (6.2)$$

where,  $\Delta m$  is the number of moles of ruthenium oxidized in the experiment and  $\Delta m^0$  is the number of moles of ruthenium which would be oxidized theoretically, as per Faraday's law, for the passage of the Coulombic charge.

$\Delta m$  can be calculated from Faraday's 1<sup>st</sup> law as follows:

$$\Delta m = \frac{i \Delta t}{nF} = \frac{C}{nF} \quad (6.3)$$

where,  $\Delta m$  is the number of moles of material oxidized,  $i$  is the current in ampere,  $\Delta t$  is the time in second,  $C$  is the charge passed in coulomb,  $n$  is the number of electrons transferred and  $F$  is the Faraday's constant.

#### 6.3.1.1 Oxidation potential and cyclic voltammetry of ruthenium

The CV of  $[\text{RuNO}]^{3+}$  solution of (a) various Ru concentrations in 1 M nitric acid and (b) 20 mM Ru in various nitric acid concentrations and (c) at different temperatures, recorded at platinum electrode at the potential sweeping rate of 50 mV/s in order to understand the oxidation behavior of  $[\text{RuNO}]^{3+}$  ion in acidic solution are shown in Figs. 6.2 (A, B and C) respectively.

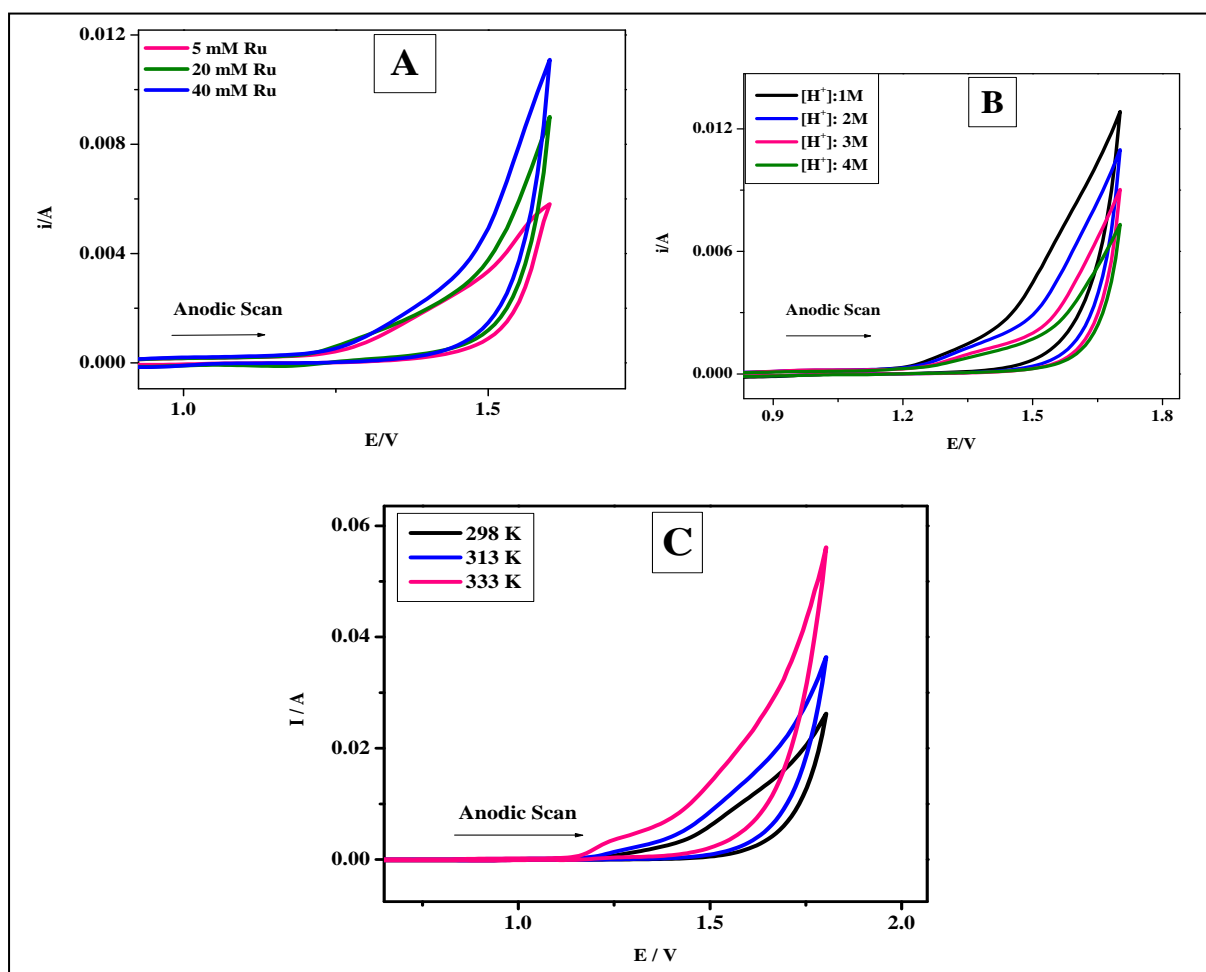


**Fig. 6.2** Cyclic voltammetric studies with  $[\text{RuNO}]^{3+}$  solution: **A.** In 1M nitric acid with different Ru content; **B.** 20 mM of Ru in different acid concentrations and **C.** At different temperatures; CVs were recorded at Pt WE, Pt plate CE and Ag/AgCl RE; Scan rate: 50 mV/s

During anodic scan (0 to 1.8 V vs Ag/AgCl) there was a surge in anodic current at the potential 1.25 V (vs Ag/AgCl), which corresponds to the oxidation of both water and Ru to  $\text{RuO}_4$  and the anodic current was observed to increase with increase in the concentration of Ru, temperature and with decrease in nitric acid concentration. For the electro-oxidative separation of Ru, the following three different potentials: 1.25 V (the onset potential), 1.45 V and 1.65 V were employed.

### 6.3.1.2 Separation of Ru from $[\text{RuNO}]^{3+}$ solution by electro-oxidation

#### *(i) Effect of applied potential and nitric acid concentration*

The experimental conditions and the results of the electro-oxidation of Ru from  $[\text{RuNO}]^{3+}$  solution are listed in Table 6.1. The separation percentage of Ru was observed to increase with increase in applied potential and decrease in nitric acid concentration as expected (Viz. Chapter 5). For the same applied potential of 1.25 V (vs Ag/AgCl), the separation percentage of ruthenium increased from 17 to 23 and 35 % with decrease in nitric acid concentration from 4 to 2 and 1 M respectively after 10 h of electrolysis owing to the formation of easily oxidizable Ru complexes at lower acidity (as explained already in the Section 4.3.1 of Chapter 4). When the applied potential was 1.45 V (vs Ag/AgCl), the separation percentage of ruthenium increased from 24 to 46 and 60 % and at the applied potential of 1.65 V (vs Ag/AgCl), the separation percentage of ruthenium increased from 29 to 48 and 74 % with decrease in concentration of nitric acid from 4 to 2 and 1 M respectively after 10 h of electrolysis. However, in the separation of Ru from  $[\text{RuNO}]^{3+}$  solution prepared in 1 M nitric acid, the faradaic efficiency decreased from 63 to 29 and 11 % with increase in applied potential from 1.25 to 1.45 and 1.65 V (vs Ag/AgCl).

Figures 6.3 and 6.4 show the plot of coulombic charge against time for the electrolysis of  $[\text{RuNO}]^{3+}$  solution at the three different applied potentials and nitric acid concentrations respectively. It was observed that the number of coulombs passed against time increased with increase in applied potential and decrease in the nitric acid concentration. Though the number of coulombs passed increased with increase in time and applied potential, the efficiency in separating Ru declined, which is attributed to the increase in the rate of water oxidation – a side reaction occurring simultaneously along with Ru oxidation.

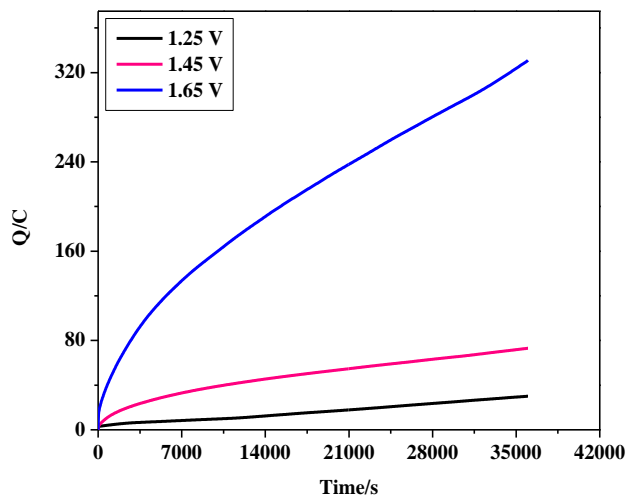


**Fig. 6.3** Plot of coulombic charge passed into the solution against time for the electro-oxidation of Ru from  $[\text{RuNO}]^{3+}$  solution in 1M nitric acid at different applied potentials

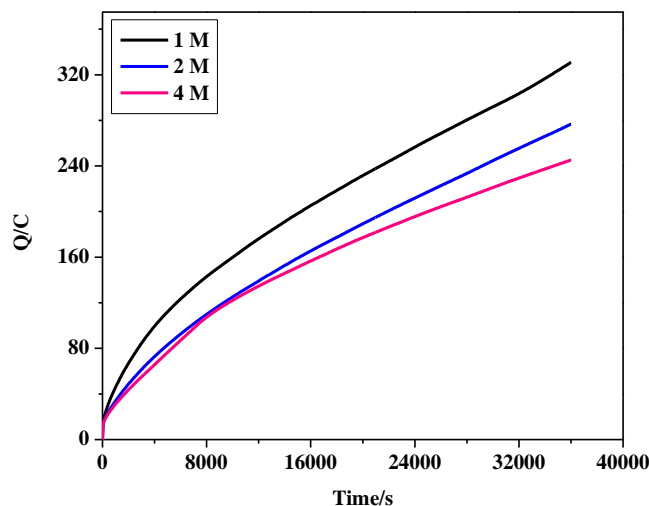


**Fig. 6.4** Plot of coulombic charge passed into the solution against time for the electro-oxidation of Ru from  $[\text{RuNO}]^{3+}$  solution at three different  $[\text{HNO}_3]$  and at the fixed potential of 1.65 V

*(ii) Effect of temperature*

As the faradaic efficiency for the separation of Ru was maximum at the applied potential of 1.25 V (vs Ag/AgCl) in 1 M nitric acid medium in spite of the low separation percentage,

electrolysis was carried out at higher temperatures (without changing the other experimental conditions) to obtain better separation of Ru. The results of the electrolysis experiments performed with  $[\text{RuNO}]^{3+}$  solution in 1 M nitric acid at 300, 313 and 333 K by applying the constant potential of 1.25 V (vs. Ag/AgCl) are shown in Fig. 6.5. The separation percentage of Ru increased from 35 to 65 and 68 % with increase in temperature from 300 to 313 and 333 K respectively after 10 h of electrolysis. Figure 6.6 indicates that the coulombic charge passed as a function of time increased with increase in temperature. It was also observed that during the electrolysis of Ru solution at 333 K there was an abrupt increase in the passage of coulombic charge in the first 2 h of electrolysis, followed by a gradual increase in coulombic charge; this observation implies that oxidation of significant amount of Ru would have occurred during this abrupt increase in the passage of coulombic charge; i.e. separation of 63 % Ru after 2 h, followed by 65, 67, 67 and 68 % after 4, 6, 8 and 10 h of electrolysis respectively. When the temperature was 313 K, the separation percentage increased from 38 to 64 and 65 % after 4, 8 and 10 h of electrolysis respectively. At 300 K, the separation of Ru increased gradually from 17 to 30 and 35 % after 4, 8 and 10 h of electrolysis.

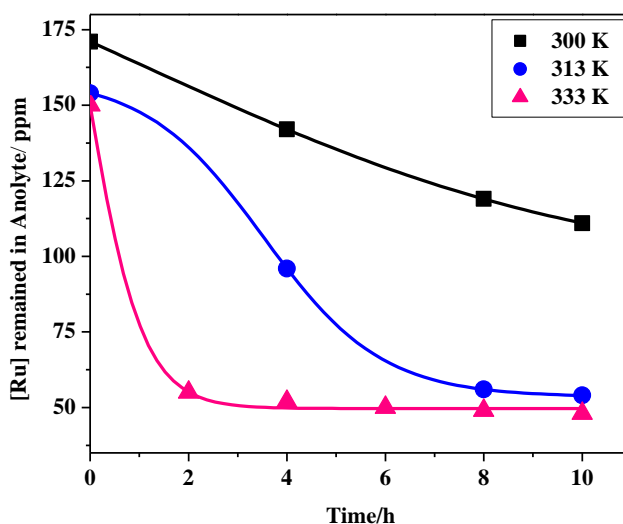


**Fig. 6.5** Variation in the separation of Ru from  $[\text{RuNO}]^{3+}$  solution in 1M nitric acid during electrolysis at different temperatures with the applied potential of 1.25 V

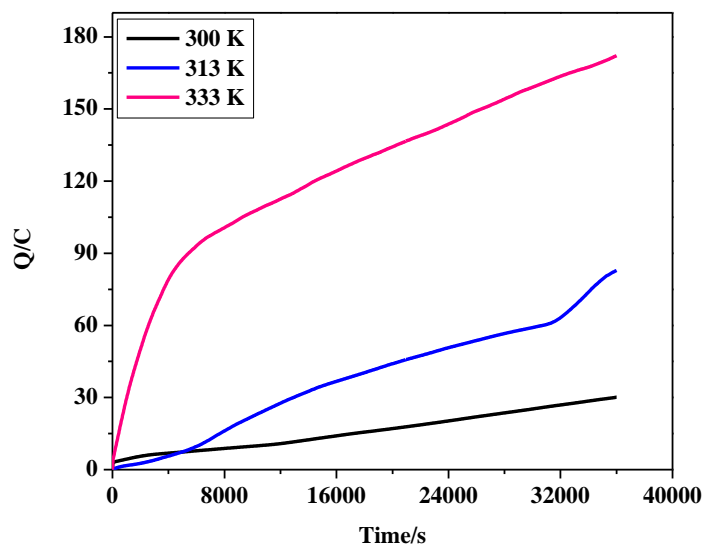


**Fig. 6.6** Plot of coulombic charge passed into the solution against time in the electro-oxidation of Ru from  $[\text{RuNO}]^{3+}$  solution in 1M nitric acid at different temperatures with 1.25 V as the applied potential

*(iii) Effect of the redox mediator, cerium*

To improve the separation efficiency of Ru, the influence of the redox mediator, Ce on the oxidation of Ru was investigated during electrolysis. In the presence of 0.04 M Ce and at different nitric acid concentrations, the experiments performed at the applied potentials 1.25, 1.45 and 1.65 V (vs Ag/AgCl) indicated that the separation of ruthenium was only 29 % with cerium in 1 M nitric acid at the potential of 1.25 V, whereas without cerium the separation was about 35 % under the same experimental conditions; as the oxidation of Ce(III) to Ce(IV) occurs only above 1.4 V, the presence of Ce(III) was ineffective in the oxidation of ruthenium below 1.4 V. Table 6.1 shows the separation percentage of Ru and Faradaic efficiency during the electrolysis of  $[\text{RuNO}]^{3+}$  solution prepared in 1, 2 and 4 M nitric acid at various applied potentials after 10 h of electrolysis. With decrease in the nitric acid concentration of  $[\text{RuNO}]^{3+}$  solution from 4 to 2 and 1 M, the separation percentage increased from 43 to 87 and 89 % respectively after 10 h of electrolysis at the applied potential of 1.45

V (vs Ag/AgCl) and the current efficiency after 10 h was found to be increasing from 6.4 to 12.1 and 17.2 % with decrease in acidity from 4 to 2 and 1 M respectively. Figure 6.7 shows the coulombic charge vs time plot for the electrolysis of  $[\text{RuNO}]^{3+}$  solution in the presence of 0.04 M Ce at different acid concentrations and at the applied potential of 1.45 V (vs Ag/AgCl). In this experiment, the passage of coulombic charge was found to be higher with 4 M acid than that with 2 and 1 M, because of the increase in the rate of oxidation of Ce(III) with increase in nitric acid concentration, which is the dominating reaction in this process [22].

During the electrolysis of  $[\text{RuNO}]^{3+}$  solution in 1 M nitric acid in the presence of 0.04 M Ce, the separation percentage of Ru increased from 89 to 97 % with increase in the applied potential from 1.45 to 1.65 V (vs Ag/AgCl); however, the Faradaic efficiency decreased from 17 to 7 % respectively after 10 h of electrolysis, which value is even lower than that for the electro-oxidation without Ce (Table 6.1). Figures 6.8 and 6.9 show the variation in the number of coulombs passed and the concentration of Ru in the anolyte against time respectively, for the electrolysis of  $[\text{RuNO}]^{3+}$  solution prepared in 1 M nitric acid in the presence of 0.04 M Ce at 1.45 and 1.65 V applied potentials. It is observed from Fig 6.8 that during electrolysis with 1.45 V potential, the number of coulombs passed increased gradually, whereas at the potential of 1.65 V, it increased abruptly for one hour, followed by gradual increase with the time of electrolysis. Figure 6.9 revealed that when the applied potential was 1.65 V, the rate of separation of Ru was rapid during the first hour of electrolysis and it decreased gradually up to 6 h of electrolysis and subsequently, steady state had reached. In the electrolysis with 1.45 V (vs Ag/AgCl), the rate of separation of Ru decreased gradually up to 6 h and reached saturation afterwards.

**Table 6.1** Comparison of separation percentage of Ru and Faradaic efficiency after 10 h of electrolysis at various applied potentials and concentration of nitric acid, with and without cerium

[HNO <sub>3</sub> ]/(M)	Applied Potential V/(vs Ag/AgCl)	Separation of Ru after 10 h of electrolysis/(%)		Faradaic efficiency after 10 h of electrolysis/(%)	
		Without Ce	With Ce	Without Ce	With Ce
1	1.25	35		63	
	1.45	60	89	29	17
	1.65	74	97	11	7
2	1.25	23		48	
	1.45	46	87	29	12
	1.65	48		8	
4	1.25	17		32	
	1.45	24	43	24	6
	1.65	29		6.2	

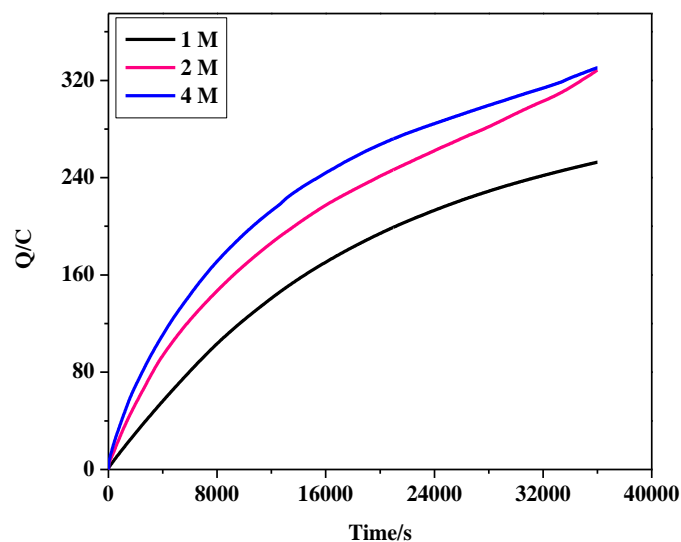


**Fig. 6.7** Plot of coulombic charge passed into the solution against time for the electro-oxidation of Ru from  $[\text{RuNO}]^{3+}$  solution in the presence of 0.04 M Ce at various acidities and at 1.45 V (vs Ag/AgCl) as the applied potential

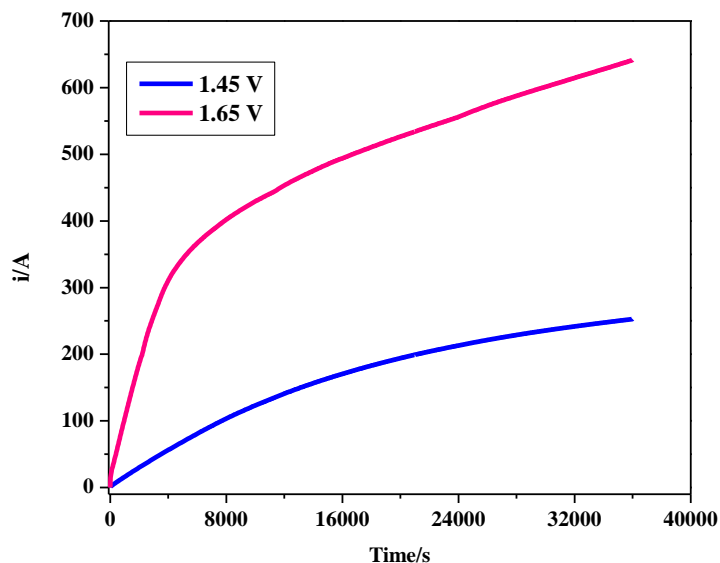


**Fig. 6.8** Plot of coulombic charge passed into the solution against time for the electro-oxidation of Ru from  $[\text{RuNO}]^{3+}$  solution prepared in 1 M nitric acid in the presence of 0.04 M Ce at the applied potentials of 1.45 and 1.65 V (vs Ag/AgCl)

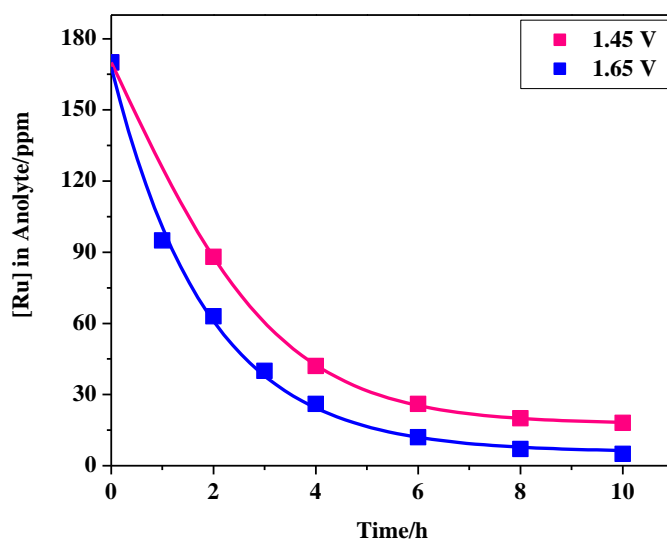
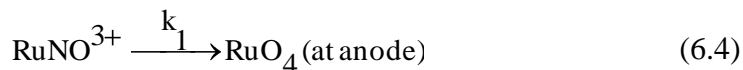


**Fig. 6.9** Variation of [Ru] in the anolyte against time during the electrolysis of  $[\text{RuNO}]^{3+}$  solution in 1 M nitric acid in the presence of 0.04 M Ce at the applied potentials 1.45 and 1.65 V

### 6.3.1.3 Determination of kinetic parameters in the electrochemical oxidation of Ru

During the electrolysis of pure  $[\text{RuNO}]^{3+}$  solution, the Ru ions are oxidized and the rate oxidation follows first order kinetics [6], which is given as follows:



$$-\frac{d(\text{RuNO}^{3+})}{dt} = k_1[\text{RuNO}^{3+}] \quad (6.5)$$

$$\frac{[\text{Ru}]_t}{[\text{Ru}]_0} = \exp(-k_1 t) \quad (6.6)$$

where  $[\text{Ru}]_t$  is the concentration of Ru (mg/L) at time  $t$ ,  $[\text{Ru}]_0$  is the initial concentration of Ru (mg/L),  $k_1$  is the rate constant and  $t$  is the electrolysis time (h). The value of  $k_1$  was determined from the regression analysis of experimental data.

#### (i) Effect of nitric acid concentration and applied potential on the rate of oxidation of Ru

Figures 6.10 to 6.12 show the decrease in the ratio of concentration of Ru in the anolyte i.e.  $[\text{Ru}]_t/[\text{Ru}]_0$  with the time of electrolysis of pure  $[\text{RuNO}]^{3+}$  solution prepared in 4, 2 and 1 M nitric acid respectively at various applied potentials. It is observed that the rate of oxidation of Ru was rapid in the case of 1 M acid solution and it increased with increase in the applied potential. The rate constant,  $k_1$  (from Eq. 6.6) for each condition was determined by least squares method and are listed in Table 6.2.

**Table 6.2** Reaction rate constant,  $k_1$  for the electrochemical oxidation of Ru at different nitric acid concentrations and applied potentials

[HNO <sub>3</sub> ] / M	Rate constant ( $k_1$ ) / h <sup>-1</sup>		
	1.25 V	1.45 V	1.65 V
4	0.019	0.027	0.034
2	0.026	0.061	0.065
1	0.046	0.09	0.135

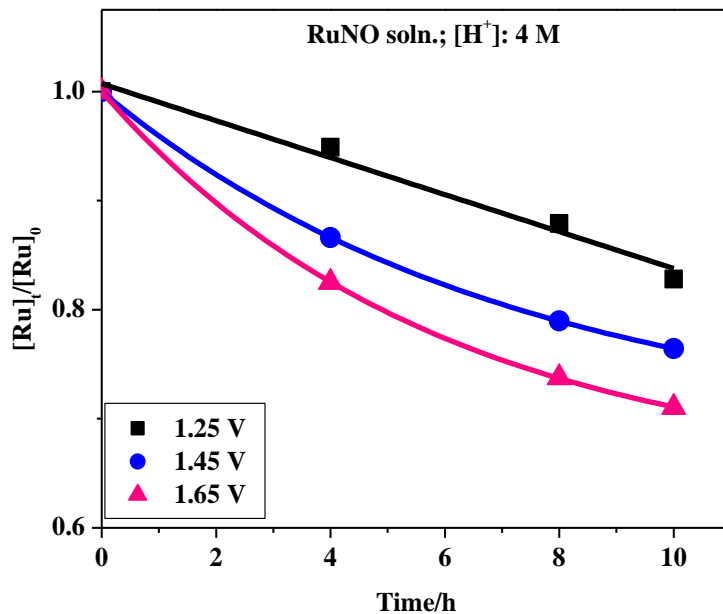


**Fig. 6.10** Variation in the ratio of Ru concentration in anolyte ( $[\text{Ru}]_t/[\text{Ru}]_0$ ) with time during the electrolysis of  $[\text{RuNO}]^{3+}$  solution prepared in 4 M nitric acid at various applied potentials

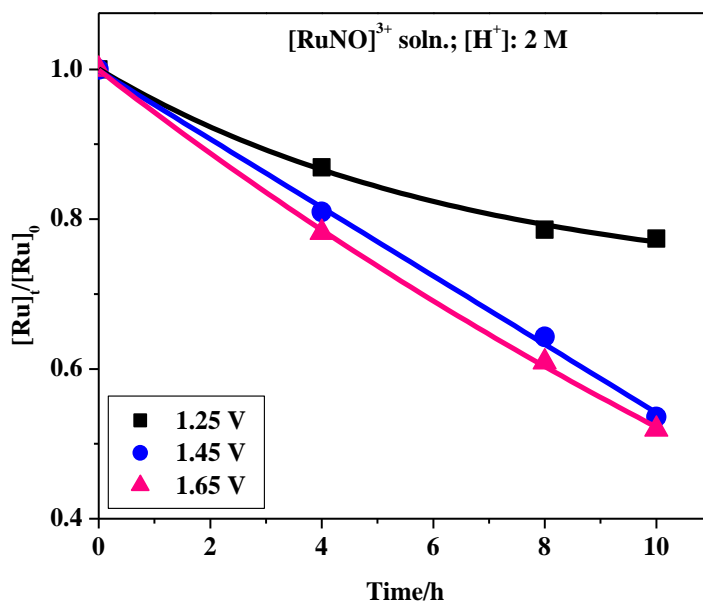


**Fig. 6.11** Variation in the ratio of Ru concentration in anolyte ( $[\text{Ru}]_t/[\text{Ru}]_0$ ) with time during the electrolysis of  $[\text{RuNO}]^{3+}$  solution prepared in 2 M nitric acid at various applied potentials

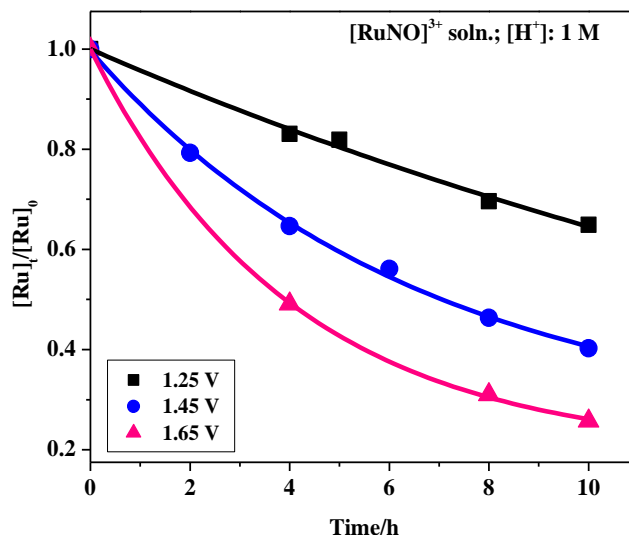


**Fig. 6.12** Ratio of Ru concentration in anolyte ( $[\text{Ru}]_t/[\text{Ru}]_0$ ) with time during the electrolysis of  $[\text{RuNO}]^{3+}$  solution prepared in 1 M nitric acid at various applied potentials

(ii) *Effect of temperature on the rate of oxidation of Ru*

Temperature plays a vital role in the determination of the rate constant of slow reactions. Since Ru oxidation is a reasonably slow reaction, temperature had significant effect on the rate of oxidation when it was increased from 300 to 333 K, as evident from Fig. 6.13 and Table 6.3. The rate constants calculated for the temperatures 300, 313, 323 and 333 K were 0.046, 0.114, 0.593 and 0.72  $\text{h}^{-1}$  respectively. The temperature dependence of the reaction rate is governed by the Arrhenius equation:

$$\ln(k_1) = \ln(A) - (E_a/RT) \quad (6.7)$$

where A is the frequency factor,  $E_a$  is the activation energy, R is the gas constant and T is the experimental temperature. The plot of  $\ln(k_1)$  against  $1/T$  (Fig. 6.14) gives a straight line with the slope equal to  $(-E_a/R)$ , from which the activation energy was calculated to be 18.09 kCal/mol.

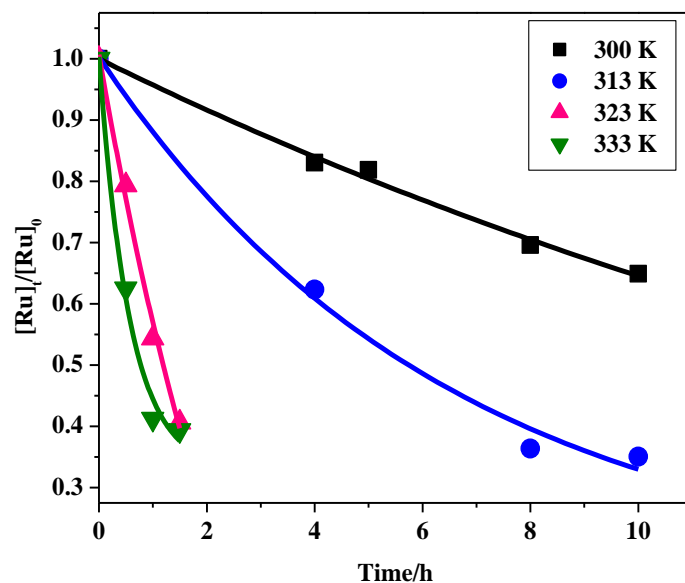


**Fig. 6.13** Ratio of Ru concentration in the anolyte ( $[\text{Ru}]_t/[\text{Ru}]_0$ ) with time during the electrolysis of  $[\text{RuNO}]^{3+}$  solution prepared in 1 M nitric acid at the applied potential of 1.25 V and different temperatures

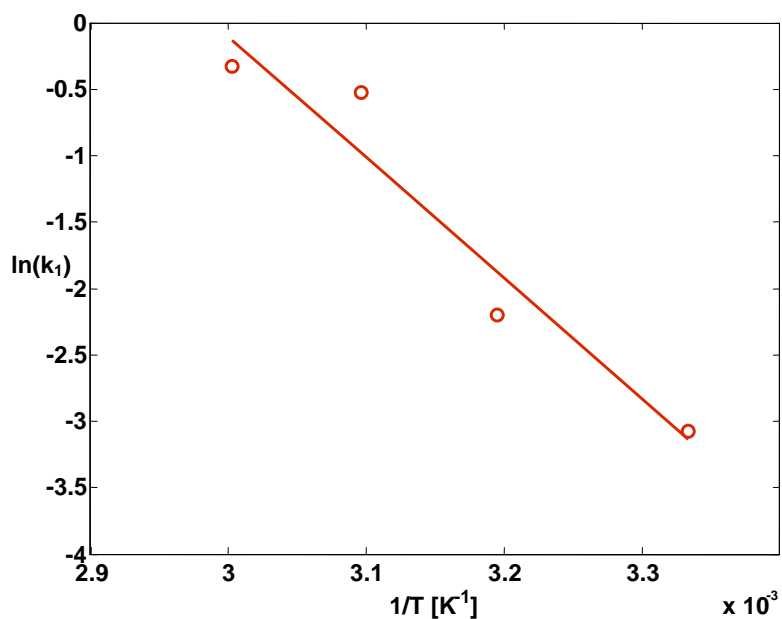


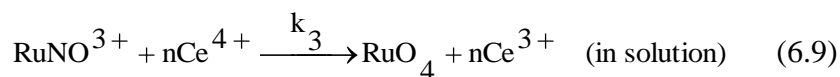
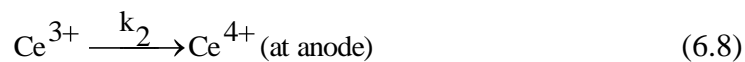
**Fig. 6.14** Rate constant against inverse temperature for the oxidation of ruthenium

**Table 6.3** Reaction rate constant ‘ $k_1$ ’ for the electro-oxidation of Ru from  $[\text{RuNO}]^{3+}$  solution prepared in 1 M nitric acid at different temperatures; applied potential: 1.25 V

$[\text{HNO}_3] / \text{M}$	Temperature / K	Rate constant ( $k_1$ ) / $\text{h}^{-1}$
1	300	0.046
	313	0.114
	323	0.593
	333	0.72

*(iii) Effect of redox mediator Ce on the rate of oxidation of Ru*

The possible electrochemical and chemical reactions during the electrolysis of  $[\text{RuNO}]^{3+}$  solution prepared in 1, 2 and 4 M nitric acid and carried out with constant potentials of 1.45 and 1.65 V (vs Ag/AgCl) in the presence of 0.04 M Ce are given as follows:



Therefore, the rate of the oxidation of Ru becomes

$$-\frac{d(\text{RuNO}^{3+})}{dt} = k_1[\text{RuNO}^{3+}] + k_3[\text{RuNO}^{3+}][\text{Ce}^{4+}]^n \quad (6.10)$$

$$= (k_1 + k_3[\text{Ce}^{4+}]^n)[\text{RuNO}^{3+}] \quad (6.11)$$

$$= (k_1 + k_3')[\text{RuNO}^{3+}] \quad (6.12)$$

where  $k_3' = k_3[\text{Ce}^{4+}]^n$ . It is assumed that  $[\text{Ce}^{4+}]$  is constant during electrolysis as it is in large excess when compared to the concentration of Ru. Hence, Eq. (6.12) takes the form

$$-\frac{d(\text{RuNO}^{3+})}{dt} = k \cdot [\text{RuNO}^{3+}] \quad (6.13)$$

where  $k = k_1 + k_3'$

Integration of Eq. (6.13) gives

$$\frac{[\text{Ru}]_t}{[\text{Ru}]_0} = \exp(-k \cdot t) \quad (6.14)$$

The rate constants,  $k$  and  $k_3'$  for each condition were determined with by least-square method and are listed in Table 6.4. Presence of the redox mediator Ce is found to be effective in increasing the oxidation rate of Ru when compared to the electrolysis without Ce.

**Table 6.4** Rate constants  $k$  and  $k_3'$  for the electrochemical oxidation of Ru from  $[\text{RuNO}]^{3+}$  solution in the presence of 0.04 M Ce at various nitric acid concentration and applied potentials

$[\text{HNO}_3]/\text{M}$	Applied Potential/V (vs Ag/AgCl)	$(k) / \text{h}^{-1}$	$(k_3') / \text{h}^{-1}$
4	1.45	0.062	0.035
2	1.45	0.205	0.144
1	1.45	0.263	0.173
1	1.65	0.396	0.261

#### 6.3.1.4. Separation of Ru from SHLLW at various applied potentials in the presence of Ce

From the foregoing discussions, it is evident that the separation percentage of Ru is maximum from  $[\text{RuNO}]^{3+}$  solutions in 1 M nitric acid and hence, electrolysis of a SHLLW solution prepared in 1 M nitric acid was performed at the applied potentials 1.25, 1.45 and 1.65 V (vs Ag/AgCl) with and without the redox catalyst, Ce and the results are shown in Fig. 6.15. The separation percentage of Ru was observed to increase from 18 to 32.5 and 39

% by increasing the applied potential from 1.25 to 1.45 and 1.65 V (vs Ag/AgCl). Similar to the behaviour exhibited in the case of  $[\text{RuNO}]^{3+}$  solution, the Faradaic efficiency decreased from 35.7 to 19.7 and 5.3 respectively with increase in the applied potentials. Compared to the separation of 74.3 % Ru from  $[\text{RuNO}]^{3+}$  solution, the value of 39 % (listed in Table.6.5) obtained for the separation of Ru from SHLLW is very low and this could be attributed to the simultaneous oxidation of Pd present in the solution [1, 2]. Hence, it is essential to remove Pd from the waste solution prior to the separation of Ru for increasing the separation percentage.

In order to obtain still better separation yield of Ru from SHLLW, electrolysis was carried out in the presence of 0.04 M Ce and by applying the potential of 1.45 and 1.65 V (vs Ag/AgCl) and the separation percentage was found to increase marginally from 57 to 58 % and the Faradaic efficiency decreased from 24.8 to 10.2 %. The decrease in Faradaic efficiency with increase in the applied potential, in the presence of Ce is more than that without the redox mediator. In the case of SHLLW, the Faradaic efficiency increased in the presence of redox mediator Ce, whereas it was found to decrease in the separation of Ru from  $[\text{RuNO}]^{3+}$  solution in the presence of Ce.

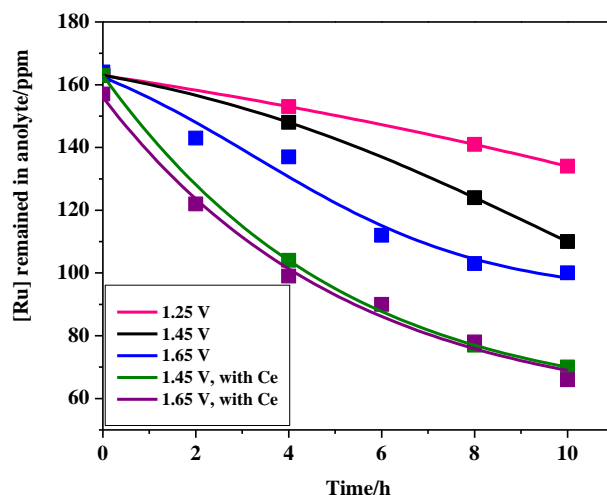


**Fig. 6.15** Variation of [Ru] in the anolyte against time during the electrolysis of SHLLW in 1 M nitric acid (with and without 0.04M Ce) at different applied potentials

**Table 6.5** Comparison of separation percentage of Ru and Faradaic efficiency during the electrolysis of SHLLW

Acidity/(M)	Applied potential /V (vs Ag/AgCl)	[Ce]/(M)	Separation of Ru after 10 h of electrolysis/(%)	Faradaic efficiency after 10 h of electrolysis/(%)
1	1.25	0.00	17.8	35.7
	1.45	0.00	32.5	19.7
	1.65	0.00	39.0	5.3
	1.45	0.04	57.0	24.8
	1.65	0.04	58.0	10.2

### 6.3.2 Reduction Behaviour of $[\text{RuNO}]^{3+}$ Solution in Nitric Acid Medium

#### 6.3.2.1 Reduction potential and cyclic voltammograms of $[\text{RuNO}]^{3+}$ complex in nitric acid

The cyclic voltammograms of 40 mM of  $[\text{RuNO}]^{3+}$  solution in 1 M nitric acid recorded at the scan rate of 0.05 V/s at platinum working electrode, at 298 K are shown in Fig. 6.16. The voltammograms were recorded starting with cathodic scan over the potential range 1.0 to -0.3 V against Ag/AgCl reference electrode. One distinct reduction peak ( $I_c$ ) at about 0.4 V and one oxidation peak ( $I_a$ ) at about 0.6 V (vs Ag/AgCl) were observed and these could be due to the redox couple  $[\text{RuNO}]^{3+} / [\text{RuNO}]^{2+}$ . In addition to this peak, during the cathodic scan there was a surge in the cathodic current at 0.04 V culminating into a small hump at about -0.156 V which could be due to the reduction of  $[\text{RuNO}]^{2+}$  to Ru. Another oxidation peak observed at 0.95 V when the CV was recorded at Pt over the potential region 1.2 V to 0.0 V (vs Ag/AgCl) is shown in Fig. 6.17. This oxidation peak might be due to the oxidation of  $[\text{RuNO}]^{3+}$  to  $[\text{RuNO}]^{4+}$ . In order to understand the redox behaviour of  $[\text{RuNO}]^{3+}$  complexes, cyclic voltammograms of 5, 20 and 40 mM of  $[\text{RuNO}]^{3+}$  solution in 1 M  $\text{HNO}_3$  were

recorded with 0.05 V/s scan rate and the reduction peak current was observed to increase with increase in the concentration of Ru as could be seen in Fig. 6.17.

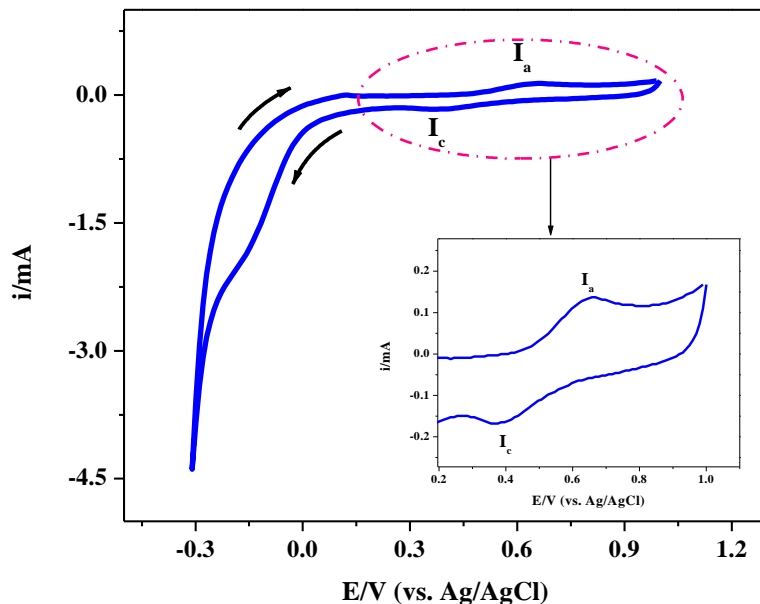


**Fig. 6.16** Cyclic voltammogram of 40 mM ruthenium nitrosyl ( $[\text{RuNO}]^{3+}$ ) solution in 1 M  $\text{HNO}_3$  recorded with 0.05 V/s scan rate at platinum working electrode and at 298 K

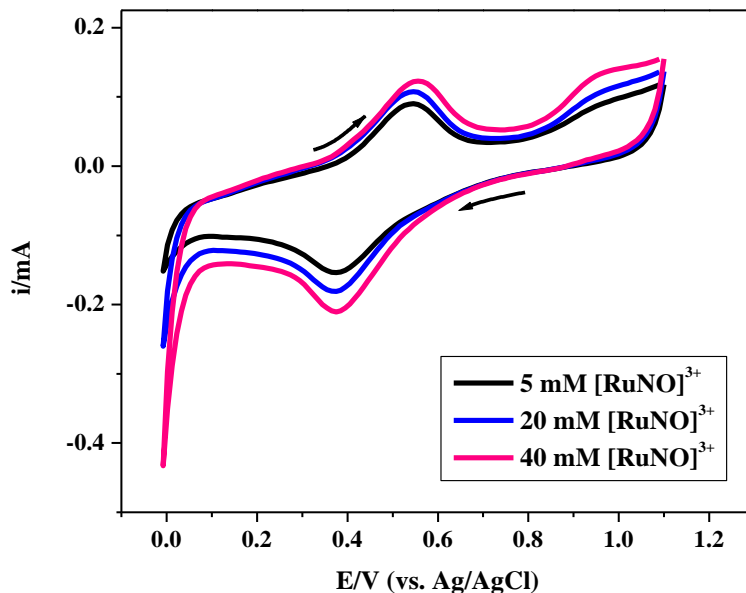
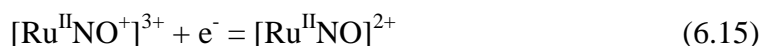


**Fig. 6.17** Cyclic voltammograms of 5, 20 and 40 mM  $[\text{RuNO}]^{3+}$  solution in 1 M  $\text{HNO}_3$  recorded at 0.05 V/s scan rate at Pt working electrode at 298 K

It is well known that in nitric acid medium Ru forms hundreds of RuNO complexes depending on the acidity, temperature and ageing of the solution. The general formula given for the complex is  $[\text{RuNO}(\text{NO}_3)_x(\text{NO}_2)_y(\text{OH})_z(\text{H}_2\text{O})_{5-x-y-z}]^{3-x-y-z}$  and depending on the value of x, y and z, it can be cationic, anionic or neutral complex. In the RuNO complex, NO ligand is considered to bond formally as  $\text{NO}^+$  by donating an electron to Ru(III). The diamagnetism exhibited by RuNO complexes ascertain this; hence, the complex is equivalent to a bivalent Ru(II) containing  $\text{NO}^+$  and the most probable description for the moiety would be  $[\text{Ru}^{\text{II}}\text{NO}^+]^{3+}$  [23, 24]. The bonding electrons are partially donated from the filled metal d-orbitals to the empty ligand NO  $\pi^*$  orbital (the process is known as metal-to-ligand  $\pi$ -bonding or back-bonding). The six coordinated ruthenium complexes are extremely stable because  $\text{Ru}^{2+}$  with the  $d^6$  configuration, obeys the 18-electron rule when octahedrally coordinated and additionally stabilized by  $\pi$ -bonding ligands. Based on molecular orbital (MO) analysis using the density functional theory (DFT) and from the reduction product analysis, it has been reported that during the electrochemical reduction of ruthenium nitrosyl complexes the first site of reduction was assigned to the  $\text{NO}^+$  to NO at the coordinated  $\text{NO}^+$  (Eq. 6.15) [25] and further reduction may occur at the ruthenium centre with the possible reduction is  $\text{Ru}^{2+}$  to Ru metal (i.e.  $\text{Ru}^{2+} + 2e^- = \text{Ru}^0$ ). It is also reported that the reduction potential for  $\text{NO}^+/\text{NO}$  in Ru nitrosyl complexes is sensitive to the nature of trans ligand. As the  $\pi$  acidity of ligand increases, more nitrosonium character is imposed in the NO ligand and, thus, its reduction is easier [14-17, 25]. In the present work, the reduction wave ( $I_c$ ) and the corresponding oxidation wave ( $I_a$ ) are assigned to the reduction of  $[\text{Ru}^{\text{II}}\text{NO}^+]^{3+}$  to  $[\text{Ru}^{\text{II}}\text{NO}]^{2+}$ .



Gomes et al. [17] reported that the  $\text{NO}^+/\text{NO}$  reduction process in some ruthenium nitrosyl complexes is reversible in the time scale of experiments, suggesting the reasonable stability

of some of the reduced complexes whereas Doro et al. [26] observed that this reduction process for some complexes is irreversible and it depends on the experimental conditions such as scan rate and temperature.

The peak corresponding to the reduction of ruthenium nitrosyl complex was validated by carrying out a controlled potential electrolysis of a solution containing 160 ppm of Ru in 1 M nitric acid at 0.4 V and the behaviour of current against time is shown Fig.6.18. The UV-Visible spectra of the electrolyte solutions recorded before and after electrolysis are reproduced in Fig.6.19. Tfouni et al. [25] observed the spectra of ruthenium nitrosyl complexes to display a broad absorption in the range 400-500 nm which they attributed it to metal - to - ligand charge transfer (MLCT)  $\text{Ru}^{\text{II}} \rightarrow \text{NO}$  transition; another higher absorption peak with high intensity in the range 300-350 nm recorded by them was ascribed to d-d transition. In the present study also similar observations were recorded. With increase in the duration of electrolysis, the intensity of characteristic absorption band owing to MLCT transition at 473 nm was found to decrease, which might be due to destabilization of metal centre caused by the decrease in back bonding because of  $\text{NO}^+$  reduction [27]. Increase in the intensity of the absorption band at about 340 nm and generation of new shoulders at 387, 370 and 358 nm were also observed as electrolysis proceeded.

### **6.3.2.2. Estimation of kinetic parameters for the reduction of ruthenium nitrosyl complexes**

If the rate of an electrochemical process is controlled by diffusion (mass transfer) and not by charge transfer kinetics, then the process is called as reversible process. In a reversible process, the charge transfer is rapid and the slow mass transfer is the rate determining step. The key criterion for a reversible charge transfer process is that  $E_p$  is independent of scan rate ( $v$ ) and

$$E_{p,c} - E_{p,a} = 2.29 \text{ RT/nF} \quad (6.16)$$

The reversibility of the electrode process corresponding to the peaks  $I_c$  and  $I_a$  in Fig. 6.16 was checked by evaluating the effect of scan rates on the current-potential behaviour in the electro-reduction of ruthenium nitrosyl ions. Figure 6.20 represents all the scans from 0.01 to 0.1 V/s for the reduction of 40 mM of  $[\text{RuNO}]^{3+}$  solution in 1 M nitric acid within the selective potential window of 0.15 to 0.85 V at 298 K. This figure reveals that the cathodic peak potential,  $I_{p,c}$  shifted significantly from 0.457 to 0.387 V (vs Ag/AgCl) as the scan rate was increased from 0.01 to 0.1 V/s, which is not the characteristics of a reversible reaction. The peak parameters measured from the cyclic voltammograms in Fig. 6.20 are tabulated in Table 6.6.

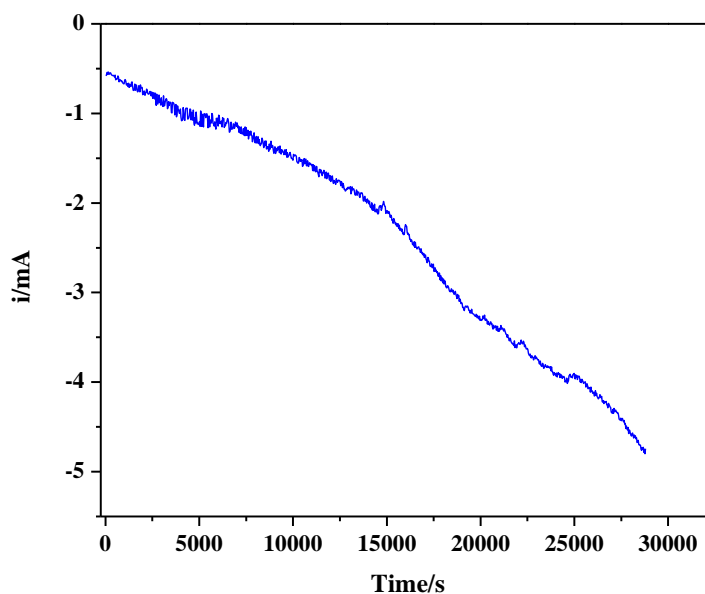


**Fig. 6.18** Current vs time plot for the electrolysis of 160 ppm of ruthenium nitrosyl solution in 1 M  $\text{HNO}_3$ ; WE: Pt mesh, CE: Pt mesh, RE: Ag/AgCl

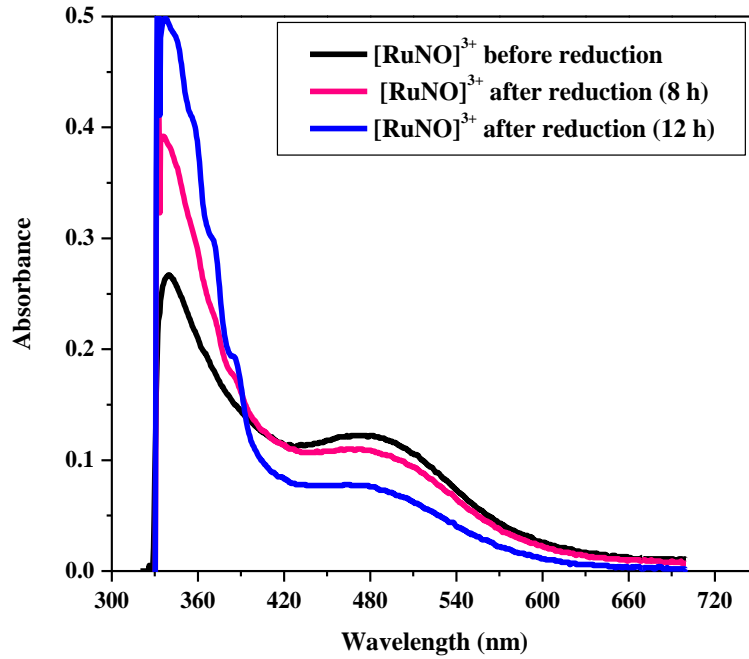


**Fig. 6.19** UV-Visible spectra of  $[\text{RuNO}]^{3+}$  solution in 1 M  $\text{HNO}_3$  before and after electrolysis

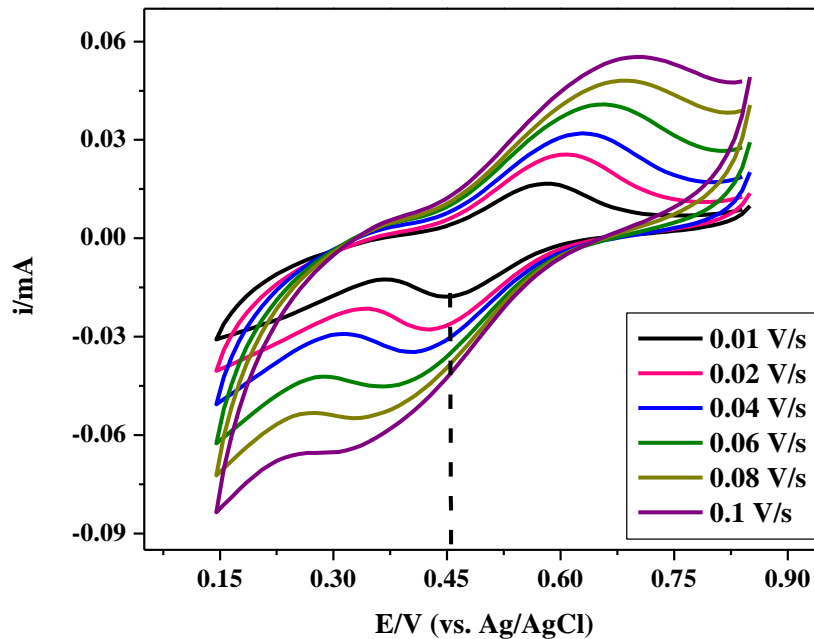


**Fig. 6.20** Cyclic voltammograms of 40 mM of ruthenium nitrosyl solution in 1 M  $\text{HNO}_3$  recorded at Pt electrode with different scan rates; T: 298 K

**Table 6.6** Peak parameters obtained from the CVs for 40 mM  $[\text{RuNO}]^{3+}$  solution in 1M  $\text{HNO}_3$  recorded with Pt working electrode

Scan Rate/( $\text{V}\cdot\text{s}^{-1}$ )	$E_{p,c}/\text{V}$	$i_{p,c}/\text{A}$	$E_{p,a}/\text{V}$	$(E_{p,a} - E_{p,c})/\text{V}$	$[1/2(E_{p,c} + E_{p,a})]/\text{V}$
0.01	0.457	-9.35E-06	0.578	0.121	0.52
0.02	0.436	-1.24E-05	0.599	0.163	0.52
0.04	0.428	-1.35E-05	0.618	0.19	0.52
0.06	0.407	-1.47E-05	0.637	0.23	0.52
0.08	0.395	-1.61E-05	0.659	0.264	0.53
0.1	0.387	-1.67E-05	0.675	0.288	0.53

If the electrochemical process is controlled mainly by charge transfer kinetics, then the process is called as irreversible process. The important criterion for the irreversible charge transfer kinetics is the shift in the peak potential with scan rate. A relation between the cathodic diffusion peak current,  $i_{p,c}$  and the scan rate given by Bard and Faulkner [28] is

$$i_{p,c} = 0.496nFAC_0 \sqrt{\frac{D_0(\alpha n \alpha)Fv}{RT}} \quad (6.17)$$

where  $n$  is the number of electrons involved in the charge transfer reaction,  $F$  is the Faraday constant,  $A$  is area of the electrode (in  $\text{cm}^2$ ),  $C_0$  is the bulk concentration of electro-active substance ( $\text{mol}\cdot\text{cm}^{-3}$ ),  $R$  is Gas constant,  $T$  is the absolute temperature (K),  $v$  is the scan rate ( $\text{V}/\text{s}$ ),  $D_0$  is the diffusion coefficient ( $\text{cm}^2/\text{s}$ ) and  $\alpha$  is charge transfer coefficient.

The value of diffusion coefficient of  $[\text{RuNO}]^{3+}$  ion calculated using Eq. 6.17 and from slope of the plot of  $i_{p,c}$  vs square root of scan rate (Fig.6.21) was  $2.95 \times 10^{-8} \text{ cm}^2\text{s}^{-1}$ .

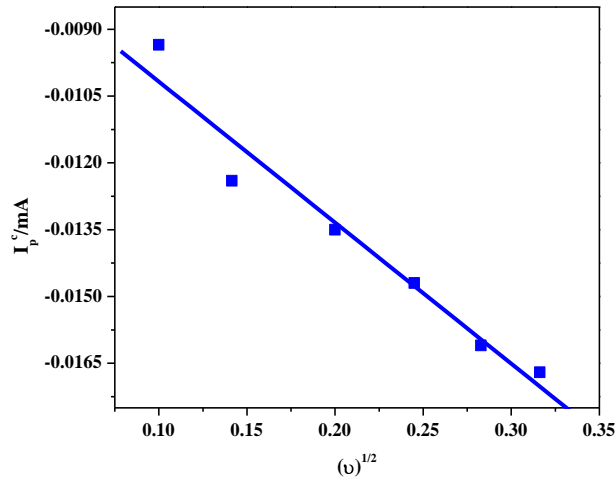


**Fig. 6.21** Plot of peak current vs square root of scan rate for the reduction of 40 mM of  $[\text{RuNO}]^{3+}$  in 1 M  $\text{HNO}_3$

For the reduction of  $[\text{RuNO}]^{3+}$  ions in 1 M nitric acid medium, peak potential shift and broadening of peak shape with scan rate were observed in cyclic voltammetric runs. The difference between the cathodic and anodic peak potentials ( $\Delta E_p$ ) increased with scan rate and the average of the peak potentials  $1/2(E_{p,c} + E_{p,a})$  was almost constant at different scan rates indicating that the process is quasi-reversible [29, 30].

The heterogeneous electron transfer rate constant,  $k_s$  can be calculated using the following equation which was proposed by Klinger and Kochi [31] based on peak separation.

$$k_s = 2.18 \left[ D_0 (\alpha n_\alpha) \frac{\nu F}{RT} \right]^{1/2} \exp \left[ \frac{\alpha^2 n F}{RT} (E_{p,c} - E_{p,a}) \right] \quad (6.18)$$

According to Eq. (6.18), if  $[k_s / (\nu)^{1/2}] > 0.11$ , the process is reversible. If  $0.11 > [k_s / (\nu)^{1/2}] > 3.7 \times 10^{-6}$ , then it is quasi-reversible. If  $3.7 \times 10^{-6} > [k_s / (\nu)^{1/2}]$ , the process is irreversible.

The value of  $k_s$  calculated at the scan rate of  $0.01 \text{ V.s}^{-1}$  using  $D_0 = 2.95 \times 10^{-8} \text{ cm}^2 \text{ s}^{-1}$  was found to be  $2.06 \times 10^{-5} \text{ cm.s}^{-1}$  and the value of  $[k_s / (\nu)^{1/2}]$  obtained for the same scan rate was

$2.06 \times 10^{-4} \text{ cm}\cdot\text{s}^{(-1/2)}\cdot\text{V}^{(-1/2)}$ . These values indicate that the reduction of  $[\text{RuNO}]^{3+}$  ions is quasi-reversible.

### 6.3.2.3 Chronopotentiometric study on the reduction of ruthenium

The chronopotentiograms of 40 mM  $[\text{RuNO}]^{3+}$  solution in 1 M  $\text{HNO}_3$  recorded at Pt electrode at various applied constant current are shown in Fig. 6.22. The transient time ( $\tau$ ) in the chronopotentiogram is a measure of time elapsed between the attainment of constant potential and the time at which the concentration of electro-active species (resulting from diffusion) reaches zero at the electrode. A relation between the applied current and transition time is given by Sand's equation [28], which enables the determination of diffusion coefficient.

$$i\tau^{1/2} = \frac{nFA(D_0\pi)^{1/2}}{2} C_0 \quad (6.19)$$

The  $D_0$  value of  $1.1 \times 10^{-8} \text{ cm}^2\text{s}^{-1}$  derived using Eq. (6.19) at room temperature is in reasonably good agreement with the value of diffusion coefficient calculated from cyclic voltammetric results.

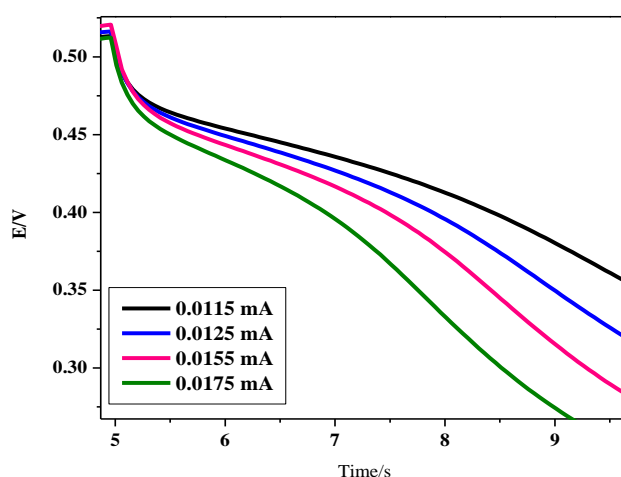


**Fig. 6.22** Chronopotentiograms of 40 mM of  $[\text{RuNO}]^{3+}$  in 1 M  $\text{HNO}_3$  recorded with Pt electrode at different applied currents; WE: Pt, CE: Pt, RE: Ag/AgCl

### 6.3.2.4 Reduction of $[\text{RuNO}]^{3+}$ moiety using glassy carbon (GC) working electrode

The cyclic voltammograms recorded with a solution of  $[\text{RuNO}]^{3+}$  containing 40 mM Ru in 1 M  $\text{HNO}_3$  at different scan rates using glassy carbon as the working electrode at 298 K are shown in Fig. 6.23. The redox behaviour exhibited by  $[\text{RuNO}]^{3+}$  in 1 M  $\text{HNO}_3$  at GC electrode was similar to that of Pt electrode. However, the reduction wave for  $[\text{RuNO}]^{3+}$  complex was observed to occur at lower cathodic potentials (0.9 V vs. Ag/AgCl) with GC working electrode when compared to 0.45 V vs Ag/AgCl with Pt WE at  $0.01 \text{ V}\cdot\text{s}^{-1}$  as the scan rate. The peak parameters measured from the cyclic voltammograms using GC as the working electrode are listed in Table 6.7.

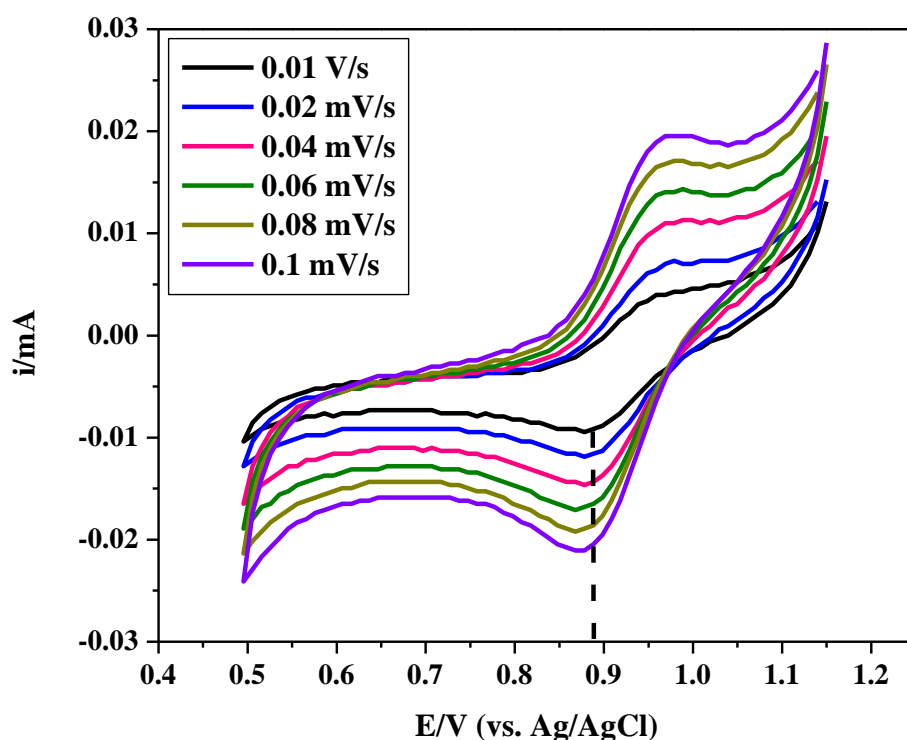


**Fig. 6.23** Cyclic voltammograms of 40 mM  $[\text{RuNO}]^{3+}$  solution in 1 M nitric acid recorded using glassy carbon electrode with different scan rates at 298 K; CE: Pt, RE: Ag/AgCl

**Table 6.7** Peak parameters obtained for 40 mM  $[\text{RuNO}]^{3+}$  solution in 1 M  $\text{HNO}_3$  from the CVs recorded with GC working electrode

Scan Rate/( $\text{V}\cdot\text{s}^{-1}$ )	$E_{p,c}/\text{V}$	$i_{p,c}/\text{A}$	$E_{p,a}/\text{V}$	$(E_{p,a} - E_{p,c})/\text{V}$	$[1/2(E_{p,c} + E_{p,a})]/\text{V}$
0.01	0.892	-5.91E-06	0.959	0.067	0.93
0.02	0.885	-6.68E-06	0.969	0.084	0.93
0.04	0.879	-1.08E-05	0.975	0.096	0.93
0.06	0.869	-1.24E-05	0.981	0.112	0.93
0.08	0.864	-1.42E-05	0.984	0.12	0.92
0.1	0.86	-1.50E-05	0.989	0.129	0.92

Similar to the behaviour of the CVs at Pt electrode, peak potential shift and broadening of peak shape with scan rate in cyclic voltammetry were observed with GC electrode also. The difference between the cathodic and anodic peak potentials ( $\Delta E_p$ ) increased with scan rate and the average of the peak potentials  $1/2 (E_{p,c} + E_{p,a})$  was almost constant at different scan rates which suggests that the process could be quasi-reversible.

The value of diffusion coefficient calculated on the basis of Eq. (6.17) is  $1.65 \times 10^{-8} \text{ cm}^2 \text{ s}^{-1}$  for the reduction of  $[\text{RuNO}]^{3+}$  moiety at GC electrode, which is in good agreement with the value of  $2.95 \times 10^{-8} \text{ cm}^2 \text{ s}^{-1}$  obtained at Pt electrode.

The potential versus time transients for the reduction of  $[\text{RuNO}]^{3+}$  at GC electrode is shown in Fig. 6.24. Using Eq. (6.19),  $D_0$  of  $[\text{RuNO}]^{3+}$  at GC electrode was determined to be  $1.57 \times 10^{-8} \text{ cm}^2 \text{ s}^{-1}$  which is in excellent agreement with the value obtained at GC electrode using Eq. (6.17). The heterogeneous electron transfer rate constant,  $k_s$  ( $6.73 \times 10^{-5} \text{ cm}\cdot\text{s}^{-1}$ ) obtained at GC electrode also indicate the reduction of  $[\text{RuNO}]^{3+}$  in 1 M nitric acid to be quasi-reversible.

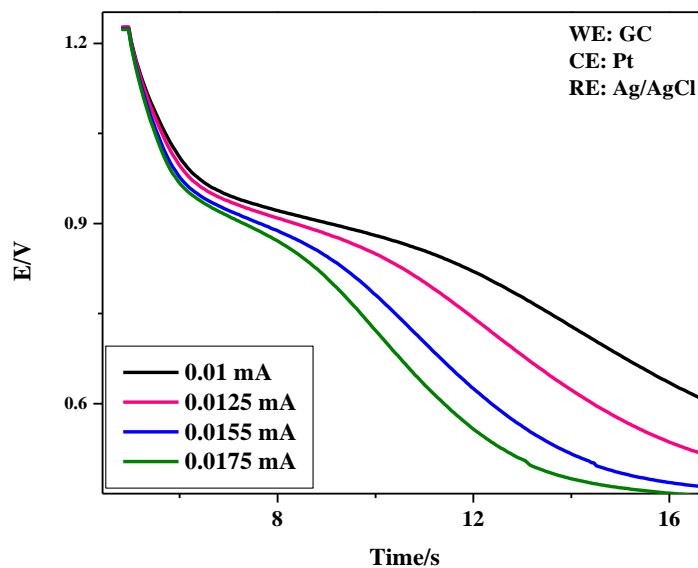


**Fig.6.24** Chronopotentiogram of 40 mM  $[\text{RuNO}]^{3+}$  solution in 1 M  $\text{HNO}_3$  recorded at GC electrode with different applied currents

### 6.3.2.5 Comparison of the kinetic parameters obtained with different working electrodes

The value of heterogeneous electron transfer rate constant ( $k_s$ ) which was estimated using Klingler and Kochi equation and the diffusion coefficient values determined from the results of cyclic voltammetry and chronopotentiometry for reduction of  $[\text{RuNO}]^{3+}$  species in 1 M  $\text{HNO}_3$  are compared in Table 6.8. The data in Table 6.8 reveal that the redox behaviour of  $[\text{RuNO}]^{3+}$  solution in 1 M  $\text{HNO}_3$  to be the same with both the electrodes.

**Table 6.8** Comparison of kinetic parameters derived for reduction of  $[\text{RuNO}]^{3+}$  species in 1 M  $\text{HNO}_3$  at different working electrodes

Kinetic parameters	40 mM $[\text{RuNO}]^{3+}$ solution in 1 M $\text{HNO}_3$	
	Platinum electrode	Glassy carbon electrode
$D_0$ ( $\text{cm}^2 \cdot \text{s}^{-1}$ )/CV expt.	$2.95 \times 10^{-8}$	$1.65 \times 10^{-8}$
$D_0$ ( $\text{cm}^2 \cdot \text{s}^{-1}$ )/CP expt.	$1.1 \times 10^{-8}$	$1.57 \times 10^{-8}$
$K_s$ ( $\text{cm} \cdot \text{s}^{-1}$ )/ Eq. (6.18)	$2.06 \times 10^{-5}$	$6.73 \times 10^{-5}$

### 6.3 CONCLUSIONS

Ruthenium was separated from  $[\text{RuNO}]^{3+}$  solution and SHLLW by constant potential electro-oxidation at different applied potentials based on the cyclic voltammetric study. The cyclic voltammograms of  $[\text{RuNO}]^{3+}$  solution recorded using Pt working electrode and Ag/AgCl reference electrode revealed that oxidation of both Ru to  $\text{RuO}_4$  and water is occurred simultaneously after 1.25 V (vs Ag/AgCl). The separation percentage of Ru increased with increase in applied potential and temperature and decrease in nitric acid concentration; however, the Faradaic efficiency was found to decrease with increase in applied potential, temperature and nitric acid concentration. Maximum separation of Ru from  $[\text{RuNO}]^{3+}$  solution was achieved at the applied potential of 1.65 V (vs Ag/AgCl) and in 1 M nitric acid solution whereas, the Faradaic efficiency decreased from 63 to 29 and 11 % with increase in applied potential from 1.25 to 1.45 and 1.65 V (vs Ag/AgCl). The decrease in Faradaic efficiency at higher potentials and temperatures might be due to the rapid and predominant oxidation of water (side reaction) than Ru oxidation under these experimental conditions. Presence of the redox mediator, cerium enhanced the separation of Ru by way of chemical oxidation of Ru species by the electro-generated Ce(IV) ions, whereas Faradaic efficiency with Ce was found to be lower than that without Ce under identical experimental conditions. About 97 % Ru could be separated from  $[\text{RuNO}]^{3+}$  solution using 0.04 M Ce at the applied potential of 1.65 V (vs Ag/AgCl). Nevertheless, the separation percentage of Ru from SHLLW was about 58 % only under similar experimental conditions which might be due to the simultaneous oxidation of Pd present in the waste solution.

Rate constant for the oxidation of Ru from  $[\text{RuNO}]^{3+}$  solution was calculated from the analysis of the overall rate data. The oxidation reaction of Ru was fast at higher applied potential in 1 M acid and also in the presence of Ce catalyst. The rate of oxidation of Ru was more at higher temperatures (323 and 333 K) compared to that in the presence of the redox

mediator, Ce. The activation energy calculated from the temperature effect on the oxidation of Ru from  $[\text{RuNO}]^{3+}$  solution in 1 M nitric acid at the applied potential of 1.25 V (vs Ag/AgCl) was 18.09 kCal/mol.

The redox behaviour of  $[\text{RuNO}]^{3+}$  species in nitric acid medium was investigated by cyclic voltammetry and chronopotentiometry with Pt as well as GC working electrodes. Quasi-reversible one electron reduction of  $[\text{RuNO}]^{3+}$  was observed at both GC and Pt electrodes. The diffusion coefficient ( $D_0$ ) of  $[\text{RuNO}]^{3+}$  species estimated by CV and CP techniques was in the order of  $10^{-8} \text{ cm}^2 \cdot \text{s}^{-1}$  and the heterogeneous electron transfer rate constant ( $k_s$ ) for the reduction of  $[\text{RuNO}]^{3+}$  was estimated to be in the order of  $10^{-5} \text{ cm} \cdot \text{s}^{-1}$  using Klingler and Kochi equation with Pt and GC working electrodes.

#### 6.4 REFERENCES

1. Motojima, K., *J. Nucl. Sci. Technol.*, 27 (1990) 262
2. Yoneya, M., Kawamura, K., Torata, S.I., Takahashi, T., U S Patent, No.5437847, 1995
3. Mousset, F., Bedioui, F., Eysseric, C., *Electrochem. Commun.*, 6 (2004) 351
4. Ozawa, M., Suzuki, T., Koyama, S., Fujii, Y., *Prog. Nucl. Energy*, 47 (2005) 462
5. Jayakumar, M., Venkatesan, K.A., Srinivasan, T.G., *J. Radioanal. Nucl. Chem.*, 284 (2005) 79
6. Sato, S., Endo, N., Fukuda, K., Morita, Y., *J. Nucl. Sci. Technol.*, 49 (2012) 182
7. Fletcher, J. M., Jenkins, T. L., Lever, F. M., Martin, F. S., Powell, A. R., Todd, R. J., *J. Inorg. Nucl. Chem.*, 1 (1955) 378
8. Brown, P.B.M., *J. Inorg. Nucl. Chem.*, 13 (1960) 73
9. Wallace, R.M., *J. Inorg. Nucl. Chem.*, 20 (1961) 283
10. Balcerzak, M., *Critical Rev. Anal. Chem.*, 32 (2002) 181

11. Scargill, D., Lyon, C.E., Large, N.R., Fletcher, J.M., *J. Inorg. Nucl. Chem.*, 27 (1965) 161
12. Szczek, A.A., Steindler, M., *J. Atomic Energy Rev.*, 16 (1978) 4
13. Boswell, G.G.J., Soentono, S., *J. Inorg. Nucl. Chem.*, 43 (1981) 1625
14. Toledo Jr., J.C., da Silva, L.P., Franco, D.W., *J. Inorg. Biochem.*, 89 (2002) 267
15. Borges, S.S.S., Davanzo, C.V., Castellano, E.E., Schpector, J.Z., Silva, S. C., Franco, D.W., *Inorg. Chem.*, 37 (1998) 2670
16. Lang, L., Davis, J., Lopes, L.G.F., Ferro, A.A., Vasconcellos, L.C.G., Prock, A., Franco, D.W., Tfouni, E., Wierasko, A., Clarke, M., J., *Inorg. Chem.*, 39 (2000) 2394
17. Gomes, M.G., Davanzo, C.V., da Silva, S.C., Lopes, L.G.F., Santos, P.S., Franco, D.W., *J. Chem. Soc. Dalton Trans.*, (1998) 601
18. Lopes, L.G.F., Gomes, M.G., Borges, S.S.S., Franco, D.W., *Aust. J. Chem.*, 51 (1998) 865
19. McGarvey, B.R., Ferro, A.A., Tfouni, E., Bezerra, C.W., Bagatin, I., Franco, D.W., *Inorg. Chem.*, 39 (2000) 3577
20. Leon M., *J. Inorg. Nucl. Chem.*, 41 (1979) 67
21. Mishra, S., Falix, L., Sreenivasan, R., Pandey, N.K., Mallika, C., Koganti, S.B., Kamachi Mudali, U., *J. Radioanal. Nucl. Chem.*, 285 (2010) 687
22. Wei, Y., Fang, B., Arai, T., Kumagai, M., *J. Appl. Electrochem.*, 35 (2005) 561
23. Bailar, J. C., Emeleus, H. J., Nyholm, R., Trotman-Dickenson, A. F., *Comprehensive Inorganic Chemistry*, Pergamon Press, Oxford, 1973
24. Cotton, S.A., Hart, F.A., *The Heavy Transition Elements*, Wiley, New York, rights controlled by Macmillan, London and Bosingstoke, 1975.

25. Tfouni, E., Krieger, M., McGarvey, B.R., Franco, D.W., *Coordination Chem. Rev.*, 236 (2003) 57
26. Doro, F.G., Rodrigues-Filho, U. P., Tfouni, E., *J. Colloid Interface Sci.*, 307 (2007) 405
27. Duchovnay, A., Comparative electrochemistry, electronic absorption spectroscopy and spectroelectrochemistry of the monometallic ruthenium polypyridyl complexes, Dissertation (MS), Virginia Polytechnic Institute and State University, 2011
28. Bard, A.J., Faulkner, L.R., *Electrochemical Methods - Fundamentals and Applications*, 2<sup>nd</sup> Edition, Wiley, New York, 2001
29. Jagadeeswara Rao, Ch., Venkatesan, K.A., Nagarajan, K., Srinivasan, T.G., Vasudeva Rao, P.R., *Electrochim. Acta*, 54 (2009) 4718
30. Jagadeeswara Rao, Ch., Venkatesan, K.A., Nagarajan, K., Srinivasan, T.G., Vasudeva Rao, P.R., *J. Nucl. Mater.*, 399 (2010) 81
31. Klingler, R.J., Kochi, J.K., *J. Phys. Chem.*, 85 (1981) 1731

---

## 7. SUMMARY AND SCOPE FOR FUTURE WORK

---

### 7.1 SUMMARY

Ruthenium (Ru) is a rare transition metal element belonging to the platinum group of the periodic table. It is produced as a fission product in nuclear reactors in large quantity due to the fission of uranium and plutonium and is one of the most troublesome fission products creates problems during nuclear fuel reprocessing and waste management processes due to its complex chemistry and formation of highly volatile radiotoxic ruthenium tetro-oxide ( $\text{RuO}_4$ ). Ruthenium is having wide industrial application whereas it is scarce in nature. Since significant quantity of Ru is produced as fission product and most of them are nonradioactive it can be separated and recovered after eliminating the radioactivity associated by cooling the fuel for 10-20 years then spent nuclear fuel can be recognized as an alternate source of Ru. In order to solve the problems both in nuclear fuel reprocessing and waste management and also for industrial applications there is increased interest on the separation and recovery of ruthenium. The work presented in this thesis deals with the development of chemical and electrochemical methods for separation and recovery of Ru from high level liquid waste. A summary of the results is given below.

Removal of Ru from high level liquid waste was carried out by chemical volatilization method using ammonium ceric nitrate oxidizing agent in presence of n-paraffin oil. Separation of ruthenium by electrochemical oxidation in a constant current mode was studied using undivided and divided electrolytic cell in presence of redox mediator cerium. Feasibility of separation of ruthenium from high level liquid waste by constant potential electro-oxidation was carried out. The reduction behavior of  $[\text{RuNO}]^{3+}$  in nitric acid medium was studied by various electroanalytical techniques.

### 7.1.1 Separation of ruthenium by n-paraffin hydrocarbon

The volatilisation behaviour of ruthenium tetroxide was made use of in the removal of ruthenium from the high level liquid waste. Separation experiments was conducted by mixing Ru bearing nitrate, nitrosyl nitrate or SHLLW solutions with NPH in the presence of ACN as oxidizing agent for Ru, revealed that separation of about 80-90% Ru from  $\text{Ru}(\text{NO}_3)_3$  and SHLLW (containing Ru in the form of  $\text{Ru}(\text{NO}_3)_3$ ) solutions was possible with 0.04 M ACN in 4M nitric acid. About 80% of Ru could be separated from ruthenium nitrosyl ( $\text{RuNO}$ ) solutions, at low concentration of nitric acid in the range 0.5–1M using 0.02–0.04M  $\text{Ce}(\text{IV})$  as the oxidizing agent and at ambient temperature. The black ruthenium powder removed during this study was characterized by XRD, TEM and XPS techniques and is found to be amorphous  $\text{RuO}_2$  and oxy-hydroxide species of  $\text{Ru}(\text{IV})$ . The ketonic group formed in the used NPH upheld the reduction of  $\text{RuO}_4$  to  $\text{RuO}_2$  by the alkane.

### 7.1.2 Separation of ruthenium by electro-oxidation

Separation of Ru was carried out by anodically oxidizing Ru to volatile  $\text{RuO}_4$  using undivided and divided electrolytic cell. Separation up to 95% Ru could be achieved from ruthenium nitrosyl ( $\text{RuNO}$ ) solution in 1M nitric acid when electrolysis was conducted for 10 h with the anodic current density as  $20 \text{ mA/cm}^2$  at 318 K and with 0.02 M cerous ions using undivided electrolytic cell. Under identical conditions, the amount of Ru separated from SHLLW was only 54 %, due to the interference of nitrite ions present in the waste. A divided cell with glass frit as diaphragm eliminated the interference caused by nitrite ions. In the divided cell 74 and 80 % of Ru was separated from pure  $\text{RuNO}$  solution and SHLLW respectively in 4M  $\text{HNO}_3$  solution after electrolyzing for 10 h at  $20 \text{ mA/cm}^2$  anodic current density, without any redox mediator. Compared to nitric acid and sodium hydroxide, n-paraffin oil above the electrolyte

served as a better trap for gaseous  $\text{RuO}_4$ , thereby preventing the deposition of  $\text{RuO}_2$  on the wall of the vessel. In the present method of separation of Ru by applying constant current quantitative separation of was possible both from  $[\text{RuNO}]^{3+}$  solution as well as SHLLW, however the current efficiency of the system was very low.

### **7.1.3 Feasibility study on the separation of ruthenium by constant potential electro-oxidation**

From cyclic voltammograms of  $[\text{RuNO}]^{3+}$  solution recorded at Pt working electrode and Ag/AgCl reference electrode it was revealed that oxidation of both Ru to  $\text{RuO}_4$  and water is occurring simultaneously after 1.25 V(vs. Ag/AgCl). The separation % of Ru was increased with increase in applied potential, increase in temperature and decrease in nitric acid concentration, however the faradaic efficiency was found to decrease with increase in applied potential, temperature and nitric acid concentration. Maximum % of Ru from RuNO solution was achieved at a applied potential of 1.65 V (vs. Ag/AgCl) and 1M nitric acid solution whereas the Faradaic efficiency decreased from 63% to 29% and 11% with increase in applied potential from 1.25 V to 1.45 V and 1.65 V (vs. Ag/AgCl). The decrease in faradaic efficiency at higher potential and temperature might be due to faster and predominant oxidation of water than Ru under these experimental conditions. The presence of redox mediator cerium increases the separation of Ru whereas Faradaic efficiency was found to be lower than that without Ce under same experimental conditions. Maximum of about 97 % Ru was separated from RuNO solution in presence of 0.04M Ce at 1.65 V(vs. Ag/AgCl) applied potential however in case of SHLLW it was about 58 % under same experimental conditions which might be due to simultaneous oxidation of Pd present in it.

Rate constants for oxidation of Ru from RuNO solution were calculated from the analysis of overall rate data. The rate of oxidation of Ru was faster at higher applied potential and 1M in acidity and also in presence of redox mediator Ce. Compared to the presence of redox mediator Ce the rate of oxidation of Ru was still faster at higher temperatures (i.e. 323 and 333 K). The activation energy was calculated from the temperature effect on the oxidation of Ru from RuNO solution in 1M nitric acid at 1.25 V(vs. Ag/AgCl) applied potential and was found to be 18.09 kcal/mol.

#### **7.1.4 Electroanalytical studies on the reduction of $[\text{RuNO}]^{3+}$ in nitric acid**

The redox behavior of  $[\text{RuNO}]^{3+}$  species in nitric acid medium were investigated by cyclic voltammetry and chronopotentiometry at both Pt and GC working electrodes. A quasi-reversible one electron reduction of  $[\text{RuNO}]^{3+}$  was observed at both GC and Pt. The diffusion coefficient ( $D_0$ ) of  $[\text{RuNO}]^{3+}$  species in the order of  $10^{-8} \text{ cm}^2 \cdot \text{s}^{-1}$  was estimated by CV and CP techniques and the heterogeneous electron transfer rate constant ( $k_s$ ) for reduction of  $[\text{RuNO}]^{3+}$  in the order of  $10^{-5} \text{ cm} \cdot \text{s}^{-1}$  was estimated using Klingler and Kochi equation using Pt and GC working electrode.

### **7.2 SCOPE FOR FUTURE STUDIES**

The parametric studies conducted for the separation of Ru chemical and electrochemical volatilization method can be implemented in the plant for the removal of Ru from the actual HLLW. Presently only batch processes for chemical and electrochemical method of separation have been carried out, continuous processes have to be designed, optimized and operated. Although quantitative separation of ruthenium was possible by electrochemical method, the energy efficiency of the method was less in case of SHLLW hence studies ought to be carried out to enhance the efficiency of the method by altering factors such as anode material, additives

etc. Further studies on the electrolytic reduction and oxidation of ruthenium nitrosyl complexes in nitric acid medium since very less data available due to its complex chemistry. Designing suitable electrolytic cells and demonstrating the performance of these cells in separating Ru from simulated HLLW are also within the scope of future work.